

Vitomir Šunjić
Michael J. Parnham

Signposts to Chiral Drugs

Organic Synthesis in Action

 Springer

Signposts to Chiral Drugs

Vitomir Šunjić • Michael J. Parnham

Signposts to Chiral Drugs

Organic Synthesis in Action

 Springer

Prof. Dr. Vitomir Šunjić
University of Zagreb
Faculty of Natural Sciences and
Mathematics
Department of Organic Chemistry
Horvatovac 102A
HR-10000 Zagreb
Croatia
vitomir.sunjic@chirallica.hr

Prof. Dr. Michael J. Parnham
Research and Clinical Immunology
Departments
University Hospital for Infectious Diseases
“Dr. Fran Mihaljevic”
Mirogojska cesta 8
HR-10000 Zagreb, Croatia
mike.j.parnham@gmail.com

ISBN 978-3-0348-0124-9 e-ISBN 978-3-0348-0125-6
DOI 10.1007/978-3-0348-0125-6

Library of Congress Control Number: 2011928235

© Springer Basel AG 2011

This work is subject to copyright. All rights are reserved, whether the whole or part of the material is concerned, specifically the rights of translation, reprinting, re-use of illustrations, recitation, broadcasting, reproduction on microfilms or in other ways, and storage in data banks. For any kind of use, permission of the copyright owner must be obtained.

The use of general descriptive names, registered names, trademarks, etc. in this publication does not imply, even in the absence of a specific statement, that such names are exempt from the relevant protective laws and regulations and therefore free for general use.

Product liability: The publishers cannot guarantee the accuracy of any information about dosage and application contained in this book. In every individual case the user must check such information by consulting the relevant literature.

Cover design: eStudio Calamar, Berlin/Figueres

Printed on acid-free paper

Springer Basel AG is part of Springer Science + Business Media (www.springer.com)

Preface

Describing the intrinsic attraction of basic research in organic synthesis, Elias J. Corey, Nobel Laureate in 1990, wrote in 1988: “The appeal of a problem in synthesis and its attractiveness can be expected to reach a level out of all proportion to practical considerations, whenever it presents a clear challenge to the creativity, originality and imagination of the expert in synthesis” [1].

A few years earlier, Vladimir Prelog, Nobel Laureate in 1975, had expressed a similar opinion in his typical laconic way: “Any problem of organic chemistry is a scientific challenge if observed by scientific eyes” (According to notes made by V. Šunjić after a conversation at the Burgenstock Conference on Stereochemistry, 1972). Creativity and scientific challenge in synthetic organic chemistry, in particular, because of its frequent broad application, are repeatedly recognized by many others, organic and other chemists and even scientists from the other disciplines.

During 25 years of teaching an undergraduate course on “Synthetic Methods in Organic Chemistry” and a graduate (Ph.D.) course on “Stereoselective (previously asymmetric) Synthesis and Catalysis in Organic Chemistry”, at the Faculty of Natural Sciences and Mathematics, University of Zagreb, one of us (VŠ) encountered an interesting phenomenon. The undergraduate course, mostly based on retrosynthetic analysis using the problem-solving approach introduced by Warren [2, 3] and elaborated by others [4–7], differed in its pragmatic approach from the graduate course, which was based on the discussion of exciting chemistry in original papers and monographies [8–14]. There was a notably different response of the students during these two courses. While the undergraduates participated intensively in discussions of possible retrosynthetic paths and proposed new syntheses, the graduates, in spite of the inclusion of up-to-date, exciting examples of non-catalytic, catalytic and biocatalytic stereoselective transformations, were less inclined to interact. Obviously, the future “experts in synthesis” (Corey) greatly preferred lectures in which target structures were well defined, and the complex synthetic problem was clearly defined. This is the basic premise of the current monograph.

The concept of this book was born out of our joint experience in teaching and research in academic institutions on the one hand, and our combined, more than 40 years participation in research projects in small and large pharmaceutical companies on the other. The volume collects together exciting achievements in synthetic organic chemistry, as they appeared during the development of target molecules, mostly chiral, enantiopure drugs. Fifteen target structures are selected to demonstrate these synthetic achievements, some of them are established drugs, the others are candidates for drugs under clinical research, one a natural product with broad application and one a library of lead molecules. In the introduction, we describe the various stages of research towards a new drug entity (NDE), as organized within the innovative pharmaceutical industry. The search for hits, improvement of biological properties from hits to leads and selection of clinical candidates are outlined, followed by the various phases of clinical research.

The sequence of chapters is roughly based on the (potential) clinical indications, but each chapter is complete in itself. The chapter abstracts are structured to enable the interested reader to easily identify the synthetic achievements and biological profile of the specific compound or structural class presented. These include mechanistic and stereochemical aspects of enantioselective transformations, new methodologies such as click chemistry, multi-component syntheses and green chemistry criteria, as well as brief information on the biological targets, mechanisms of action and biological and therapeutic profiles of target structures. Presentation of synthetic chemistry in each chapter is guided by the concept inherent in modern organic chemistry, that mechanistic organization ties together synthesis, reactivity and stereoelectronic structures of the key reagents or intermediates [15].

In the chemical schemes in this book, all specific, defined compounds or chemical entities are consecutively designated with Arabic numbers, while general formulae are listed with Roman numbers.

We are very grateful to the support and assistance provided by the publisher, Springer, particularly that from Dr. Hans-Detlef Klueber and Dr. Andrea Schlitzberger. Finally, we hope you, the reader, will find much to interest and inform you as you browse through the book, both initially and as a subsequent reference text.

Zagreb, Croatia
February 2011

Vitimir Šunjić
Michael J. Parnham

References

1. Corey EJ (1998) *Chem Soc Rev* 17:111–133
2. Warren S (1989) *Design organic synthesis: a programmed introduction to the synthon approach*. Wiley, New York
3. Warren S (1989) *Workbook for organic synthesis: the disconnection approach*. Wiley, New York
4. Fuhrhopf J, Penzlin G (1994) *Organic chemistry, concepts, methods, starting materials*. Wiley-VCH, Weinheim

5. Smith M (1994) *Organic synthesis*. McGraw-Hill, New York
6. Serratos F, Xicart J (1996) *Organic chemistry in action: the design of organic synthesis*. Elsevier, Amsterdam
7. Chiron C, Tomas RJ (1997) *Exercises in synthetic organic chemistry*. Oxford University Press, Oxford
8. Drauz K, Waldmann H (1995) *Enzyme catalysis in organic synthesis: a comprehensive handbook*. Wiley-VCH, Weinheim
9. Cornelis B, Hermann WA (eds) (1996) *Applied homogeneous catalysis with organometallic compounds*, vols 1 and 2. Wiley-VCH, Weinheim
10. Collins AN, Sheldrake GN, Crosby J (eds) (1998) *Chirality in industry: the commercial manufacture and application of optically active compounds*. Wiley, Chichester
11. Beller M, Bolm C (eds) (1998) *Transition metals for organic synthesis*, vols 1 and 2. Wiley-VCH, Weinheim
12. Tsuji J (2000) *Transition metal reagents and catalysts*. Wiley, New York
13. Berkessel A, Groger H (2005) *Asymmetric organocatalysis*. Wiley-VCH, Weinheim, pp 349–352
14. Etherington K, Irving E, Scheinmann F, Wakefield B (2006) *Synthesis of homochiral compounds: a small company's role*. *Handbook of chiral chemicals*, 2nd edn. CRC, Boca Raton, pp 559–571
15. Yurkanis-Bruice P (2007) *Organic chemistry*, 6th edn. Prentice Hall, New Jersey

Contents

1	Organic Synthesis in Drug Discovery and Development	1
1.1	Introduction	1
1.2	Synthetic Organic Chemistry in Pharmaceutical R&D	2
1.3	New Concepts in the Drug Discovery Process	5
1.3.1	The Impact of Natural Products on Modern Drug Discovery	6
1.3.2	Biologically Orientated Synthesis in Drug Discovery	8
1.3.3	Incorporation of Genomics and DNA-templated Synthesis into Drug Discovery	9
1.4	Conclusion	11
	References	11
2	Aliskiren Fumarate	13
2.1	Introduction	13
2.2	Renin and the Mechanism of Action of Aliskiren	14
2.3	Structural Characteristics and Synthetic Approaches to Aliskiren	16
2.3.1	Strategy Based on Visual Imagery, Starting from Nature's Chiral Pool: A Dali-Like Presentation of Objects	18
2.3.2	Fine-Tuning of the Chiral Ligand for the Rh Complex: Hydrogenation of the Selected Substrate with Extreme Enantioselectivities	21
2.4	Conclusion	26
	References	26
3	(R)-K-13675	29
3.1	Introduction	29
3.2	Peroxisome Proliferator-Activated Receptor α Agonists	29
3.2.1	β -Phenylpropionic Acids	30
3.2.2	α -Alkoxy- β -Arylpropionic Acids	31
3.2.3	α -Aryloxy- β -Phenyl Propionic Acids	33
3.2.4	Oxybenzoylglycine Derivatives	34
3.3	Non-hydrolytic Anomalous Lactone Ring-Opening	35

3.4 Mitsunobu Reaction in the Ether Bond Formation	38
3.5 Conclusion.....	42
References.....	42
4 Sitagliptin Phosphate Monohydrate	45
4.1 Introduction.....	45
4.2 Endogenous Glucoregulatory Peptide Hormones and Dipeptidyl Peptidase IV (DPP4) Inhibitors	46
4.3 Synthesis with C-acyl Meldrum's Acid as the <i>N</i> -Acyating Agent	47
4.4 Highly Enantioselective Hydrogenation of Unprotected β -Enamino Amides and the Use of Josiphos-Ligands.....	50
4.5 Ammonium Chloride, an Effective Promoter of Catalytic Enantioselective Hydrogenation	52
4.6 Conclusion.....	53
References.....	53
5 Biaryl Units in Valsartan and Vancomycin	55
5.1 Introduction.....	55
5.2 Angiotensin AT1 Receptor, a G-Protein-Coupled Receptor	56
5.3 Cu-Promoted Catalytic Decarboxylative Biaryl Synthesis, a Biomimetic Type Aerobic Decarboxylation	59
5.4 Stereoselective Approach to the Axially Chiral Biaryl System; the Case of Vancomycin	63
5.5 Conclusion.....	67
References.....	67
6 3-Amino-1,4-Benzodiazepines	69
6.1 Introduction.....	69
6.2 3-Amino-1,4-Benzodiazepine Derivatives as γ -Secretase Inhibitors...	70
6.3 Configurational Stability: Racemization and Enantiomerization.....	71
6.4 Crystallization Induced Asymmetric Transformation	73
6.5 Asymmetric Ireland–Claisen Rearrangement.....	74
6.6 Hydroboration of the Terminal C=C Bond: Anti-Markovnikov Hydratation	76
6.7 Crystallization-Induced Asymmetric Transformation in the Synthesis of L-768,673.....	79
6.8 Conclusion.....	81
References.....	81
7 Sertraline	83
7.1 Introduction	83
7.2 Synaptosomal Serotonin Uptake and Its Selective Inhibitors (SSRI)	84
7.3 Action of Sertraline and Its Protein Target.....	85

7.4	General Synthetic Route	86
7.5	Stereoselective Reduction of Ketones and Imines Under Kinetic and Thermodynamic Control	87
7.5.1	Diastereoselectivity of Hydrogenation of rac-tetralone-Methylimine: The Old (MeNH ₂ /TiCl ₄ /Toluene) Method Is Improved by Using MeNH ₂ /EtOH-Pd/CaCO ₃ , 60–65°C in a Telescoped Process	87
7.5.2	Kinetic Resolution of Racemic Methylamine: Hydrosilylation by (R,R)-(EBTHI)TiF ₂ /PhSiH ₃ Catalytic System	88
7.5.3	Catalytic Epimerization of the <i>Trans</i> - to the <i>Cis</i> -Isomer of Sertraline	90
7.5.4	Stereoselective Reduction of Tetralone by Chiral Diphenyloxazaborolidine.....	91
7.6	Desymmetrization of Oxabenzonorbornadiene, Suzuki Coupling of Arylboronic Acids and Vinyl Halides	92
7.7	Pd-Catalyzed (Tsuji-Trost) Coupling of Arylboronic Acids and Allylic Esters	94
7.8	Simulated Moving Bed in the Commercial Production of Sertraline	97
7.9	Conclusion	101
	References.....	101
8	1,2-Dihydroquinolines	103
8.1	Introduction.....	103
8.2	Glucocorticoid Receptor	104
8.3	Asymmetric Organocatalysis: Introducing a Thiourea Catalyst for the Petasis Reaction	105
8.3.1	General Consideration of the Petasis Reaction	106
8.3.2	Catalytic, Enantioselective Petasis Reaction.....	109
8.4	Multi-component Reactions: General Concept and Examples	112
8.4.1	General Concept of Multi-component Reactions.....	112
8.4.2	Efficient, Isocyanide-Based Ugi Multi-component Reactions ...	113
8.5	Conclusion.....	115
	References.....	115
9	(–)-Menthol	117
9.1	Introduction.....	117
9.2	Natural Sources and First Technological Production of (–)-Menthol	118
9.3	Enantioselective Allylic Amine–Enamine–Imine Rearrangement, Catalysed by Rh(I)-(–)-BINAP Complex	119
9.4	Production Scale Synthesis of Both Enantiomers	122
9.5	Conclusion.....	123
	References.....	123

10 Fexofenadine Hydrochloride	125
10.1 Introduction	125
10.2 Histamine Receptors as Biological Targets for Anti-allergy Drugs	126
10.3 Absolute Configuration and “Racemic Switch”	127
10.4 Retrosynthetic Analysis of Fexofenadine	129
10.4.1 ZnBr ₂ -Catalyzed Rearrangement of α -Haloketones to Terminal Carboxylic Acids	131
10.4.2 Microbial Oxidation of Non-activated C–H Bond	135
10.4.3 Bioisosterism: Silicon Switch of Fexofenadine to Sila-Fexofenadine	137
10.5 Conclusion	139
References	139
11 Montelukast Sodium	141
11.1 Introduction	141
11.2 Leukotriene D ₄ Receptor (LTD ₄), CysLT-1 Receptor Antagonists	142
11.3 Hydroboration of Ketones with Boranes from α -Pinenes and the Non-linear Effect in Asymmetric Reactions	144
11.4 Ru(II) Catalyzed Enantioselective Hydrogen Transfer	148
11.5 Biocatalytic Reduction with Ketoreductase KRED (KetoREDuctase)	150
11.6 CeCl ₃ -THF Solvate as a Promoter of the Grignard Reaction: Phase Transfer Catalysis	150
11.7 Conclusion	152
References	153
12 Thiolactone Peptides as Antibacterial Peptidomimetics	155
12.1 Introduction	155
12.2 Virulence and Quorum-Sensing System of <i>Staphylococcus</i> <i>aureus</i>	156
12.3 Development of Chemical Ligation in Peptide Synthesis	158
12.4 Development of Native Chemical Ligation; Chemoselectivity in Peptide Synthesis	160
12.5 Development of NCL in Thiolactone Peptide Synthesis	163
12.6 Conclusion	167
References	167
13 Efavirenz	169
13.1 Introduction	169
13.2 HIV-1 Reverse Transcriptase Inhibitors	170
13.2.1 Steric Interactions at the Active Site	171

13.3 Asymmetric Addition of Alkyne Anion to C=O Bond with Formation of Chiral Li ⁺ Aggregates.....	173
13.3.1 Mechanism of the Chirality Transfer.....	173
13.3.2 Equilibration of Lithium Aggregates and the Effect of Their Relative Stability on Enantioselectivity.....	175
13.4 Scale-up of Alkynylation Promoted by the Use of Et ₂ Zn.....	176
13.5 Conclusion	177
References.....	177
14 Paclitaxel	179
14.1 Introduction	179
14.2 Disturbed Dynamics of Cellular Microtubules by Binding to β -Tubulin.....	180
14.3 Three Selected Synthetic Transformations on the Pathway to Paclitaxel	181
14.3.1 Intramolecular Heck Reaction on the Synthetic Route to Baccatin III.....	182
14.3.2 Trifunctional Catalyst for Biomimetic Synthesis of Chiral Diols: Synthesis of the Paclitaxel Side-Chain....	185
14.3.3 Zr-Complex Catalysis in the Reductive N-deacylation of Taxanes to the Primary Amine, the Key Precursor of Paclitaxel	192
14.4 Conclusion	194
References.....	194
15 Neoglycoconjugate	197
15.1 Introduction	197
15.2 Human α -1,3-Fucosyltransferase IV (Fuc-T).....	198
15.3 Click Chemistry: Energetically Preferred Reactions	200
15.4 Target-Guided Synthesis or Freeze-Frame Click Chemistry.....	202
15.5 Application of Click Chemistry to the Synthesis of Neoglycoconjugate 1.....	205
15.6 Conclusion	207
References.....	207
16 12-Aza-Epothilones	209
16.1 Introduction	209
16.2 Epothilones: Mechanism of Action and Structure–Activity Relationships.....	210
16.3 Extensive vs. Peripheral Structural Modifications of Natural Products	212
16.4 Ring Closure Metathesis: An Efficient Approach to Macrocyclic “Non-natural Natural Products”	213

16.5 Diimide Reduction of the Allylic C=C Bond	220
16.6 Conclusion	222
References.....	222
Synthetic Methods and Concepts Discussed in the Chapters	225
Index	229

Abbreviations and Acronyms

A

A β	Amyloid-beta-peptide
AChE	Acetylcholine esterase
ACL	Assisted chemical ligation
Ac ₂ O	Acetic anhydride
AD	Alzheimer's disease
ACE	Angiotensin-converting enzyme
ADME	Absorption–distribution–metabolism–excretion
agr	Accessory gene regulator
agrA (B,C,D)	Accessory gene regulator A (B,C,D)
AIDS	Acquired immunodeficiency syndrome
AIPs	Autoinducing peptides
Amberlyst 15	Sulphonic acid-based cationic ion exchange resin
4-AMS	Molecular sieves of 4Å
API	Active pharmaceutical ingredient
APP	Amyloid precursor protein
AT1	Angiotensin II type 1 receptor
AUC	Area under the curve

B

BINA	2,2'- <i>bis</i> (Diphenylphosphino)-1,1'-binaphthyl
Bioisosters	Substituents or groups with similar physical or chemical properties that impart similar biological properties to a parent compound
Boc	Butoxycarbonyl
BOP-Cl	<i>bis</i> -(2-Oxo-3-oxazolidinyl)phosphonic chloride

C

CBS-QB3	Complete basis set-quantum B3
CC	Clinical candidate
CD	Candidate drug

CL	Chemical ligation
Click chemistry	Reliable chemical transformations that generate collections of test compounds
CNS	Central nervous system
COD	1,5-Cyclooctadiene
Cp	Cyclopentadienyl
Cp ₂ TiH	Titanium(<i>bis</i> -cyclopentadienyl)hydride
CSA	Camphor sulphonic acid
CSP	Chiral stationary phase
CYP 3A4	Cytochrome P450
CYP/hERG	Cytochrome P450/human <i>ether-à-go go</i> related gene (potassium ion channel) drug–drug interaction screening assay

D

DEAD	Diethylazidodicarboxylate
DBU	1,8-Diazabicyclo[5,4,0]undec-7-ene, strong crowded base
DCC	Dicyclohexylcarbodiimide
DCE	Dichloroethane
DCM	Dichloromethane
DHP	Dihydropyrane
DHQ	Dihydroquinine
DHQD	Dihydroquinidine
DHQ-PHN	Dihydroquinyl phenanthroline
DHQ-MeQ	Dihydroquinyl 4'-methyl-2'-quinolyl dihydroquinine
(DHQ) ₂ -PHAL	<i>bis</i> -Dihydroquinyl phthalazine
(DHQD) ₂ -PHAL	<i>bis</i> -Dihydroquinidyl phthalazine
DIA	Diethylamine
DIAD	Diisopropylazidodicarboxylate
DIBAL-H	Diisobutylaluminium hydride
DIEA	Diisopropylethylamine
DMAP	4-Dimethylaminopyridine
DMSO	Dimethylsulphoxide
DMF	Dimethylformamide
DOS	Diversity-oriented synthesis
DPPA	Diphenylphosphorylazide
DPP-4	Dipeptidyl peptidase 4
DTS	DNA-templated organic synthesis
DuPHOS	Chiral, bidentate phosphine ligand developed by DuPont company

E

EBTHI	Ethylene- <i>bis</i> (eta ₅ -tetrahydroindenyl)
EC ₅₀	Effective concentration producing 50% of maximal response
EDG	Electron-donating group

e.e.	Enantiomeric excess
ESM	Electrospray mass spectrometry
EtOAc	Ethylacetate
EWG	Electron-withdrawing group

F

Fc	Ferrocene
FDA	Food and Drug Administration (USA)
FGI	Functional group interconversion
Fmoc	Fluorenylmethyloxycarbonyl
Fuc-T	alpha-1,3-Fucosyl transferase

G

GABA	Gamma-aminobutyric acid
GCR	Glucocorticoid receptor
GDP-fucose	Guanidine diphosphate-beta-L-fucose
GIP	Gastric inhibitory peptide
GLP1	Glucagon-like peptide 1
GMP	Guanosine monophosphate
GPCR	G-protein-coupled receptors
G3MP3	Gaussian method for very accurate calculation of energies

H

HAART	Highly active antiretroviral therapy
HBTU	<i>O</i> -Benzotriazole- <i>N,N,N',N'</i> -tetramethyl-uronium-hexafluorophosphate
HBP	Halogen-binding pocket
HDL	High-density lipoprotein
HIV	Human immunodeficiency virus
HTS	High-throughput synthesis (or screen)
Hunig's base	<i>N,N</i> -diisopropylethylamine
5-HT	5-Hydroxytryptamine

I

IC ₅₀	Concentration at which 50% inhibition of maximum response is achieved
Iosiphos	Ferrocene-based, chiral bidentate phosphine ligands
IPEA	Isopropylethyl amine
(Ipc) ₂ BCl	Chlorodiisopinocampheyl borane

L

LacNAC	<i>N</i> -acetyllactosamine
LBD	Ligand-binding domain
LC/MS	Liquid chromatography/mass spectrometry
LDA	Li-diisopropylamide

LDH	Layered double hydroxide
LDL	Low-density lipoprotein
LiHMDS	Lithium hexamethyldisilazane
Log P	Logarithm of the ratio of the concentrations of the unionized solute in two solvents
LPPS	Liquid phase protein synthesis
L-Selectride	Lithium tri- <i>sec</i> -butyl(hydrido)borate
LTC ₄ , LTD ₄ , LTE ₄	Leukotrienes C ₄ , D ₄ , E ₄

M

MAO	Monoamine oxidase
MCR	Multicomponent reaction
MDR	Multidrug resistance
Mesylate	Methanesulphonic ester moiety
MeQ	4'-Methyl-2'-quinolyl dihydroquinine
MsCl	Methanesulphonic acid chloride

N

N-Boc	<i>N</i> -Benzyloxycarbonyl
NBS	<i>N</i> -Bromosuccinimide
NCE	New chemical entity
NCL	Native chemical ligation
NDE	New drug entity
NLE	Non-linear effect
NME	New molecular entity
NMO	4-Methyl-morpholine- <i>N</i> -oxide
NMP	<i>N</i> -methylpyrrolidine
NNRTI	Non-nucleoside reverse transcriptase inhibitor

O

OPMB	<i>para</i> -Methoxybenzyl
OTBS	<i>O</i> -tertiary-Butyldimethylsilyl

P

PADA	Dipotassium diazidocarboxylate
PCy ₃	Tricyclohexyl phosphine
PDC	Pyridinium chlorochromate
PEGA	Poly[acryloyl- <i>bis</i> (aminopropyl)polyethylene glycol]
Peptone	Various water-soluble protein derivatives obtained by partial hydrolysis of a protein by an acid or enzyme during digestion and used in culture media in bacteriology
PET	Positron emission tomography
P-gp	P-glycoprotein
PHAL	Phthalazine
Phen	1,10-Phenanthroline

PHN	Phenanthrenyl dihydroquinine
PK	Pharmacokinetics
PMB	<i>para</i> -Methoxybenzyl
PoC	Proof of concept
PPA	Polyphosphoric acid
PPAR α	Peroxisome proliferator-activated receptor alpha
PPTS	Pyridinium <i>para</i> -toluenesulphonate
4-PPy	4-Phenylpyridine
PSA	Polar surface area
pTsOH	<i>para</i> -Toluenesulphonic acid

Q

QSAR	Quantitative structure–activity relationship
------	--

R

RAAS	Renin–angiotensin–aldosterone system
RaNi	Raney nickel catalyst
RCM	Ring closure metathesis
R&D	Research and development
REM	Regenerative Michael receptor
RT	Reverse transcriptase

S

SAR	Structure (biological) activity relationship
SCRAM	[CpIrI ₂] ₂ (Cp = cyclopentadienyl)
SERT	Plasma membrane serotonin transporter
SMB	Simulated moving bed chromatography
SPS	Solid phase synthesis
SPPS	Solid phase protein synthesis
SRS-A	Slow-reacting substance of anaphylaxis
SRS	Slow-reacting substance
SSRI	Selective serotonin uptake inhibitor

T

TACs	Tricyclic antidepressants
TBAB	<i>tetra-n</i> -Butylammonium bromide
TBAF	<i>tetra-n</i> -Butylammonium fluoride
TBS	<i>tert</i> -Butyldimethylsilyl
TBSCl	<i>tert</i> -Butyl-dimethylsilyl-chloride
TBSOTf	<i>tert</i> -Butyl-dimethylsilyl-trifluoroacetate (triflate)
T2DM	Type 2 diabetes mellitus
TCEP	<i>tris</i> -(2-Carboxy)ethyl phosphine
TEA	Triethylamine
TEMPO	2,2,6,6-Tetramethylpiperidine-1-oxyl
TFA	Trifluoroacetic acid

TGS	Target-guided synthesis
THF	Tetrahydrofuran
THP	Tetrahydropyran
TIS	Triisopropylsilane
TM	Target molecule
TM domain	Transmembrane domain
TMS	Trimethylsilyl group
TMSCl	Trimethylsilyl chloride
TMSI	Trimethylsilyl iodide
TON	Turnover number
Tosylate	Toluenesulphonic ester moiety
TPAP	Perruthenate complex
TriFer	Ferrocene-based C ₂ -symmetric diphosphine ligand
Triflate	Trifluoromethanesulphonic moiety
Triton B	Benzyl trimethyl ammonium hydroxide
TRPM8	Transient receptor potential cation channel subfamily M member 8
TsDPEN	(1 <i>R</i> ,2 <i>R</i>)- <i>N</i> -(<i>p</i> -tolylsulphonyl)-1,2-diphenylethane
TsOH	Toluenesulphonic acid
Y	
YMS	Culture medium supplemented with soybean peptones

Chapter 1

Organic Synthesis in Drug Discovery and Development

Abstract The discovery and development of a new drug entity (NDE) to become a marketable drug is a complex, costly and time-consuming process. It is subject to increasingly stringent regulations and high attrition, which squeeze the time available both for the development and sale of the final product within the remaining window of patent coverage.

Organic synthesis of NDEs is challenged by the creation of novel, biologically active, safe and suitably targeted molecules and the improvement of lead compounds, as well as by the need to scale up compound quantities for safety and clinical studies. Even though natural and biologically derived drug molecules are *en vogue*, small synthetic molecules are preferable for oral drug administration and organic synthesis is required to modify natural compounds.

Biologically orientated synthesis can generate compounds with multiple activities. The industrial use of genomics research to identify potential target proteins and of high throughput screening to test compounds, including synthesized libraries of DNA sequence-programmed small molecules, all increase the chance of identifying totally new NDEs.

Chirality of NDEs is crucial because of the three-dimensional nature of biological target molecules and 68% of the top 200 marketed drugs are optically pure. Consequently, the stereoselective approach to drug molecules will remain important for many years to come.

1.1 Introduction

The complexity of the process leading to the marketing of a new drug entity (NDE) and its introduction to therapy is well recognized. As a matter of fact, complexity has become synonymous with high risk and frequent failure, or attrition, in searching for an NDE. Currently, innovative pharmaceutical companies that are focused on the development of NDEs are facing huge financial and organizational problems. This is related to the decreasing likelihood of being able to introduce successfully a “blockbuster”, or “\$1 billion drug” to the world market. This situation is, in part, the consequence of the ever more stringent requirements of regulatory authorities in

developed countries, primarily of the Food and Drug Administration (FDA) in the USA, concerning the required documentation for all phases of preclinical and clinical investigations of an NDE. In addition, the diseases for which new therapies are still needed are now generally complex chronic diseases, which are difficult to categorize and require long-term, safe drug treatment.

These factors also enhance the risk of investment in long-term NDE-orientated research and development (R&D) due to the prolonged period between the first patent application and the appearance of the drug on the market. Consequently, the number of new first-in-class drugs that have reached the market in the last decade has been steadily declining. As a result of new technological developments, interest and investment in biological (protein-based) drugs is increasing, partially because of their relative specificity and the expected higher price, which companies can set following their introduction to the market (see also Sect. 1.2). However, this approach too has its limitation as biologicals cannot usually be given orally and the pressure of reimbursement agencies is likely to reduce pricing in the future.

An NDE is expected to meet an unmet medical need or to improve therapy where existing drugs have proved ineffective due to lack of efficacy, development of resistance or tolerance, to unexpected toxic side-effects, or have shown incompatibility with other drugs. New pathological states or diseases are also being continuously revealed and require effective therapy.

In spite of all these incentives to the development and marketing of new drugs, the success rate is decreasing. Rapid progress in the sophistication of the technical and analytical methods used to monitor all NDE development steps has resulted in clearly safer drugs. But, at the same time, this has further contributed to the delay in the introduction of drugs to the world market. The span between the first patent claiming biological activity of the new chemical entity and its introduction to the market has been prolonged from less than 6–8 years in 1970–1990 to over 15 years today. Two economic drawbacks for innovative pharmaceutical companies have been the inevitable consequences: much higher investment is needed for the whole R&D process, and the periods available for exploration of the original drug under patent protection and for recovering this investment with drug sales are now much shorter.

In the next three sections, we briefly present some characteristics of the R&D process in the pharmaceutical industry and the specific approaches that are being taken to confront the scientific and organizational problems.

1.2 Synthetic Organic Chemistry in Pharmaceutical R&D

The discovery of a drug has always depended on creative thinking, good science and serendipity. Due to the ever more stringent criteria that need to be satisfied for the introduction of an NDE to the market, drug discovery has always had a high attrition rate. A key goal is therefore to reduce this attrition rate by transforming drug discovery into a high-throughput, rational process. This is possible at some

specific early stages during drug discovery, particularly with biological assays that identify numerous hit compounds and when the data accumulated support progress towards synthesis of a limited number of lead compounds.

To provide background information for the role of synthetic chemistry, some aspects of the R&D process in innovative pharmaceutical companies deserve comment. The complexity of the usual multidisciplinary research process in developing an NDE is presented schematically in Fig. 1.1.

The *organizational and value chain in pharmaceutical R&D* requires that a wide range of activities are interconnected, some of them loosely, the others strongly integrated. Individuals prepared to champion this progression are crucial, and they are recruited from among the scientists and physicians involved.

The importance of synthetic chemistry in the research shuttle arises from the need to access promptly the progressively increasing amounts of active substance or active pharmaceutical ingredient (API) that are required. This becomes most essential when approaching crucial activities such as safety studies (toxicology in animal species), and the development of suitable dosage forms and testing in human beings (clinical phases I–III). Lack of well-planned, timely delivery of reproducibly standardized API can result in long delays in the progression of the new product to the market, mainly by failing to arrive on time at the milestones of nomination for selection of a clinical candidate (CC) or a candidate drug (CD) [1]. The requirements for active substance at various points along the R&D shuttle process are presented in Fig. 1.2.

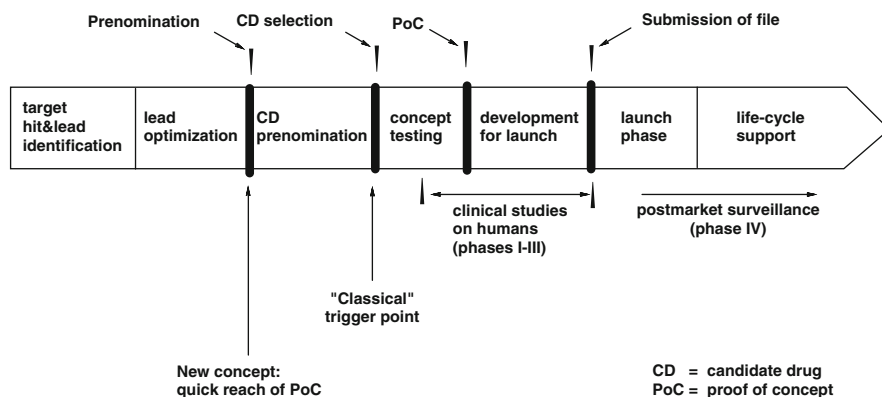


Fig. 1.1 R&D “shuttle” for delivering an NDE

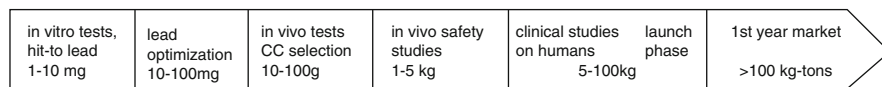


Fig. 1.2 Requirements for active compound along the R&D process

This scheme outlines the exponential requirements for the active substance over a period of approximately 10 years. The critical period for the research chemists on the project, however, lies between the selection of the lead and the clinical candidate. In this period, scale-up to kg production is undertaken for the process that was previously used for mg preparation. Besides the usual modification of the separate synthetic steps, often the complete synthetic scheme needs substantial modification to enhance efficiency, expressed as the average yield of the process, and to reach a reproducibly high level of purity of the final product. At this stage, initial consideration of the requirements for the future multi-kg production process is made. This includes planning the technological, ecological and economic aspects of the future process. The subsequent large-scale synthesis of API for clinical trials, these days, is usually contracted out to a specialized manufacturing company, for whom the research chemist will provide technical details.

Lead generation and, to a greater extent, *lead optimization* are the processes that make the most creative demands on the synthetic organic chemist. Lead generation is the process by which a series of compounds is identified that has the potential to be developed into a drug. Creativity is not only demanded in synthesizing a compound with the desired biological activity. The molecule must also have suitable physical properties for the route of administration planned, exert little or no toxicity and on administration, must be taken up efficiently into the body and distributed at adequate concentration to the desired site of action (pharmacokinetic properties).

The shuttle model in Fig. 1.2 is particularly challenged by the high attrition of the potential drug entities in the course of R&D process. Attrition of potential NDEs (termination of research projects due to their failure to satisfy the criteria set up for the different phases of the shuttle process) has various causes. Among them are toxicity in non-human tests (35%), lack of clinical efficacy (18%), unacceptable clinical safety (15%), together with unsatisfactory pharmacokinetic (PK) and bio-availability properties (9%). These data indicate that proof of concept (PoC) and clinical studies in humans are the stages at which most potential drugs fail to satisfy the criteria. Although synthetic chemistry is not directly involved in these activities, it is the basis for the unsuitable biological properties of the chemical entity. The only way to overcome the deficiencies is to design and synthesize new lead molecules.

Together with the identification of biological targets and lead optimization, the chemical synthesis of novel compounds forms one of the key steps in drug discovery (Fig. 1.1). According to Gillespie [2], the *attributes of a high-quality lead compound* are:

- Its synthetic tractability
- The patentability of the series around the lead
- Availability of chemistry space for optimization
- Acceptable solubility, permeability and protein binding
- Lack of inhibition of *cytochrome P450* (CYP; family of enzymes responsible for oxidative drug metabolism)

- Lack of inhibition of *human ether-à-go-go related gene* (hERG; a gene that codes for a potassium ion channel in the heart, inhibition of which can cause cardiac arrest)
- Acceptable *absorption–distribution–metabolism–excretion* (ADME)
- Its confirmed interaction with the biological target (e.g. by X-ray or NMR)
- Defined apparent *structure–activity relationship* (SAR)
- Its confirmed biological activity in vivo

However, natural compounds, which represent a rich source of new NDEs as discussed in Sect. 1.3.1, do not usually conform to these criteria.

Selection of the CD is shown as the “classical” trigger point in Fig. 1.1. According to the most recent concept, the CD should be moved forward as soon as possible to “prenomination” which commits the R&D organization to rapid attainment of the PoC in humans. Prenomination at such an early stage sets a new challenge to synthetic chemistry to provide the active substance in sufficient quantity and purity.

Without underestimating any step in the process of the R&D shuttle, demands on the first stages, prior to prenomination, make it increasingly important to get the concept right from the beginning and avoid costly late attrition. This depends largely on the skill and creativity of medicinal and synthetic chemists.

1.3 New Concepts in the Drug Discovery Process

Traditionally, synthetic chemistry in drug discovery has been the main source of new structural classes for biological testing of any kind. *Analogue-based drug design*, presented in a systematic manner in a recent monograph [3], was the leading concept. Since analogy plays an important role in applied research, it is not surprising that it became a crucial strategy in medicinal chemistry. According to the authors of the recent book, a specific aspect of this approach involves a search for a *structural and pharmacological analogue* (also called a *full analogue*) of an existing drug as a lead compound. It is also a pragmatic approach, since the therapeutic target has already been validated, although the project will race against unknown competitors who may start from the same scaffold at about the same time. On the other hand, it is not a simple research method, but a way of thinking that uses a combination of modern in silico and in-solution experimental methods. A number of stand-alone drugs taken as starting points for this approach are discussed in the monograph [3].

As biological targets for drugs are complex three-dimensional molecules, it is almost axiomatic that *chiral compounds may be potential drugs*, and synthetic methods leading to optically pure compounds represent the most important synthetic armamentarium. *Chiral drugs in an optically pure form* are present in 68% of the top 200 brand-name drugs, and in 62.5% of the top 200 generic drugs [4]. The importance of stereochemistry in drug development and medical application

is further illustrated by the fact that among the ten highest-selling drugs over the last decade, nine are chiral compounds, representing a \$53.5 billion market in 2004 [5]. The chiral nature of most drugs on the market and of those under development, thus, more than justifies the scope of this book. Its importance is reflected in the numerous modern, stereoselective transformations that have been invented or improved to synthesize chiral drugs. In fact, the percentage of commercially available, single-enantiomeric drugs increased from 10% before the 1990s to around 37% in 2005, when the sales of this type of pharmaceutical product amounted to US\$225 billion (2005 prices) [6].

The scientific and commercial value of synthetic organic chemistry research seems to have been underestimated in the recent decades dominated by molecular biology, genomics, products from exotic natural sources, and so on. However, it was recently stated that synthetic methods still attract most of the attention of the readership of many leading American Chemical Society (ACS) chemical journals [7]. Thus, five of the top ten most requested articles in the CAS Science Spotlight are from J Am Chem Soc and all refer to synthetic methods. The first four papers refer to reactions that are suitable for work on a large scale. The author concluded that nowadays, the fine chemicals industry and pharmaceutical industry generally rely on university research to discover new reactions, which are then adapted to industrial processes. The chapters in this book report many such examples.

In a recent feature article, authors from Roche reported the results of an exploratory interview, in which selected scientists were asked to take extreme positions and to derive two orthogonal strategic options: chemistry as the traditional mainstream science or chemistry as the central entrepreneurial science [8]. The outcome was that small molecules are still considered to be the only viable therapeutic options for oral drug delivery. Specific therapeutic opportunities were also identified for differentiated small molecules for indications in which large molecules face distribution barriers. These include targets within the central nervous system (CNS) and intracellular targets in general. So, synthetic chemistry appears to have a bright future.

1.3.1 The Impact of Natural Products on Modern Drug Discovery

Non-chemical synthetic processes, such as extraction and isolation from plants, biocatalysis, monoclonal antibody production, plant cell culture, gene modification and fermentation, also complement chemical synthesis as a source of new drug entities. In fact, synthetic organic chemistry is frequently required to modify the original natural product. The synthetic organic chemist is able to view the complexity of target molecules, whether synthetic or natural, in terms of the number of functional groups/molecule, the number of stereogenic centres with defined absolute configuration and the conformational flexibility of the molecule. This “qualitative picture” of molecular complexity has been reduced to numerical dimensions for medicinal chemists. For instance, Wenlock has deduced numerical criteria from

the percentage of marketed drugs with “drug-like” properties [9]. Emphasizing the mean values for molecular weight, flexibility, log *P* and H-bond donors and acceptors of marketed drugs, he drew the following conclusions:

- Dimension: 90% of marketed drugs have a molecular weight of 473 or less (mean 337)
- Flexibility: 90% of marketed drugs have 11 or fewer rotatable bonds (mean 5.9)
- Log *P*: 90% of marketed drugs have a log *P* < 5.5 (mean 2.5)
- H-bond donors: 90% of marketed drugs have ≤4 (mean 2.1)
- H-bond acceptors: 90% of marketed drugs have ≤8 (mean 4.9)

These principles can be applied across a wide range of chemical structures. Within the field of chemical synthesis, however, there are two main approaches to NDEs. The first and broadest approach is to target small, potentially biologically active synthetic molecules, based on structure-activity designs, as discussed in the previous section, followed by synthesis and testing. The second approach targets natural products, as the source of biologically active molecules, to synthesize molecules that often act at quite different receptors from those of the parent natural products. In this way, organic synthesis plays a crucial role in expanding the diversity of new compounds from natural product.

Although many traditional drugs were originally obtained from plants, there have been times when large pharmaceutical companies were reluctant to initiate projects based on chemical modification of natural products, because of the additional challenges of isolation and amenity to synthetic modification. Now, with the options for available active structural scaffolds becoming more complex, we have entered a period of renewed enthusiasm. Some aspects of this approach to modern drug discovery will be analyzed briefly here.

There are two important arguments in favour of synthetic modification of natural products:

- Natural products are amenable to further improvement, whether in terms of efficacy and selectivity for the biological target or the achievement of optimal pharmacokinetic properties
- Natural products address a different area of chemical space to that of synthetic molecules

This latter statement implies that significant differences exist in the molecular architecture produced by nature in comparison with the synthetic molecules of medicinal chemistry [10, 11]. Nature diversifies by taking a limited number of building blocks and partitioning them into a multitude of pathways. The synthetic chemist, on the other hand, fills the chemical space with numerous new compounds by repeating a reliable sequence of reactions over and over again, while changing the starting structures.

Whichever route one takes, the opportunities for innovation are immense. In terms of biological space, structural restrictions are provided by possible active target sites. The human genome consists of 3×10^4 genes, of which only a small fraction is targeted by current therapeutics [12, 13]. Conformational changes, mutations and

post-translational modifications all diversify the targets and this is only in terms of proteins. On the other hand, chemical space is infinite, and there are an estimated 10^{60} organic compounds with a molecular weight of <500 [14]. Our limited understanding of the areas of chemical space best suited to interact with biological space (i.e. the physico-chemical properties that enable interactions with biological receptors to occur) is the major barrier to the development of new drugs.

In this context, it is important to mention that various attempts have been made in recent years to surmount this barrier, particularly using statistical analysis to define descriptors for small-molecule, drug-like space. The most familiar approach is *Lipinski's "Rule of Five"* that predicts oral absorption on the basis of values containing 5 for log *P*, molecular weight and H-bond donors and acceptors [15]. Other approaches consider the importance of parameters such as the number of rotatable bonds and *polar surface area* (PSA) [16].

In conclusion, the main issue with synthetically modified natural compounds is that of their restricted "drug-like" properties, in particular, their limited solubility due to their dimensions, large molecular weight and high hydrophobicity (lipophilicity). Nevertheless, in the period 1981–2006, among a total of 1,184 new chemical entities (NCE) that were approved, 52% had a natural product connection, 30% were synthetic and 18% were biological [17].

1.3.2 *Biologically Orientated Synthesis in Drug Discovery*

Several new paradigms, including *biologically orientated synthesis* and *genomics*, have been incorporated recently into the drug discovery process. The novel concept of *biologically orientated synthesis*, introduced in 2005 by Waldmann et al. [18, 19], is based on the following three essential aspects:

- (a) Natural products represent pre-validated lead structures for medicinal chemistry and pharmacological activity
- (b) The recognition that only a limited number of binding-site topologies for small molecules exist across all protein families
- (c) Synthesis of target compound libraries is based on the two former premises, guided by biologically derived structural principles and the biological characteristics of the system to be investigated

This concept is illustrated schematically in Fig. 1.3 [20]. This diagram summarizes the discovery of new modulators of both cell cycle progression and viral entry. The crux of the whole concept is the observation that Nature pairs non-peptide small molecules with relevant protein receptors, and the number of binding-site topologies for small molecule ligands across all protein families is limited. Phenotypic screening of the library of enantiopure α,β -unsaturated- δ -lactones was exceptionally successful and has identified potent modulators of the two unrelated biological processes. In one case, the compounds are inhibitors of cell

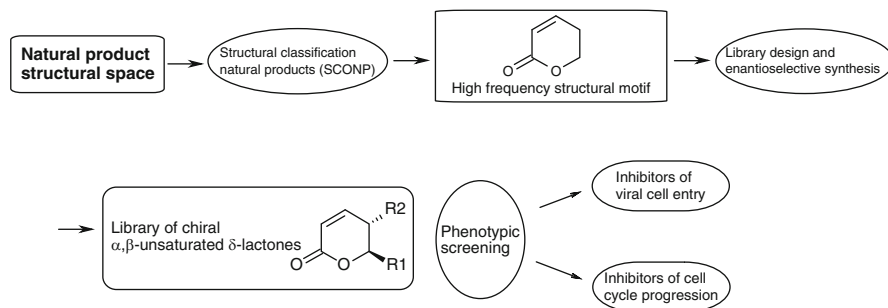


Fig. 1.3 Biologically orientated synthesis exemplified

cycle progression (potential anticancer drugs), and in the second case, inhibitors of viral cell entry (potential antiviral drugs).

This approach is expected to improve and speed up the development of NDEs in many other therapeutic fields [21].

1.3.3 Incorporation of Genomics and DNA-templated Synthesis into Drug Discovery

Another new concept is based on the premise that successful *incorporation of genomics* into the drug discovery process is critical for the long-term survival of innovative pharmaceutical companies [22, 23]. Until recently, the main approach of large companies was to identify a relatively non-specific target for medicinal chemistry that would potentially lead to a drug, which could be marketed for a wide variety of diseases and thus recover R&D investment across a broad area. Increased understanding of disease pathology, individual patient responses and the ability to target disease processes more specifically, has made the “blockbuster” approach less attractive and too expensive. Evaluation of specific gene targets allows the industry to define the role of the gene in disease at the same time as searching for a suitable drug to interact with the expression of the gene. To understand this statement, one has to take into account that innovative pharmaceutical companies worldwide can presently progress with approximately 50–100 new biological targets a year [24]. Knowledge of the detailed structure and function of the biological target, and its relevance to specific diseases, is crucial to the design of agonists or antagonists as therapeutic agents for specific pathological processes. Shortage of tractable biological targets and reliable methods for their selection are among the main obstacles in the search for new drugs. Therefore, it is clear that identification of genes relevant for specific diseases is crucial for “industrialization” of the drug discovery process [25].

The drug discovery approach based on genomics uses gene targets, discovered either by bioinformatic analysis (mining) of databases, characterization of mutant genes responsible for interesting phenotypes in animal models, or determination of disease genes by association of linkage studies in man. Figure 1.4 summarizes key components of the *genomics-based drug discovery process*.

This process is characterized by cloning of target genes followed by expression of the protein coded for by the gene and its configuration into a high-throughput screen (HTS) for interacting compounds. These steps are carried out in parallel with the generation of chemical databanks using combinatorial chemistry, and to a certain extent also parallel synthesis. The hallmark of genomic-based drug research is the use of target validation methods. This involves gene transfer and knockout studies in animals to determine its function as well as translational medicine studies to link the experimental data to the function of the gene in normal human health and disease pathology. This increases confidence in the disease relevance of the target gene.

A closely allied concept is that of DNA-templated organic synthesis (DTS) [26–28]. It is based on the translation of nucleic acid sequences into corresponding synthetic compounds, and is primarily used in the creation of libraries of DNA sequence-programmed small molecules. DTS does not require adjacent functional groups to proceed efficiently [29], can mediate sequence-programmed multistep syntheses of small molecules [30], and can enable reaction pathways that are impossible to achieve by conventional synthetic strategies [31]. This principle was shown to be particularly valuable in the selection of a library of macrocyclic compounds [32].

The final steps in Fig. 1.4 are the same as those in the non-genomic driven research in drug discovery presented in Fig. 1.1. Research is therefore currently focused on the initial steps, where opportunities for novel approaches exist. Non-chemical synthetic methodologies, such as virtual screening of virtual libraries [33], molecular modelling of receptor–ligand (agonist or antagonist) complexes [34], genomics [35], combinatorial chemistry [36], in silico target fishing [37] and proteomic approaches are regarded as particularly promising in drug discovery [38].

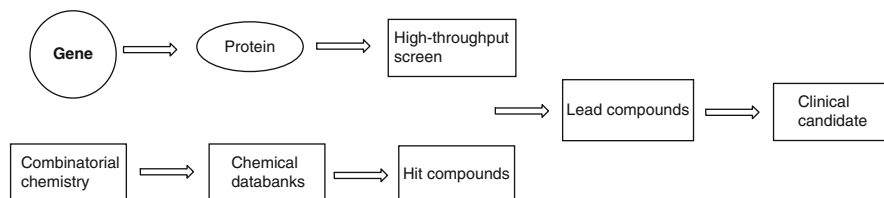


Fig. 1.4 Cloning of target genes followed by protein expression and configuration into HTS, parallels combinatorial chemistry to hit generation on the pathway to lead compound and clinical candidate

1.4 Conclusion

In spite of the highly structured nature of drug research, it has been stated repeatedly that projects in this area are less foreseeable and more risky than sending a space shuttle to a distant planet many light-years from Earth. More than in any other field, such research needs the involvement of individuals who are prepared to champion its progression.

Consequently, the economics of R&D on NDEs is under continuous challenge and re-evaluation. In 2006, only 18 *new medical entities* (NME) were approved by FDA, the same number as in 2005; the decrease in approvals is a direct result of the reduced number of new drug applications [39]. Analysis of the cost of an approved NME, by the Boston Consulting Group, yielded a figure of \$881 million, which is in good agreement with the estimate of \$802 million by DiMasi et al. [40]. With the costs of bringing a new therapeutic agent or NDE to the market now estimated at approximately \$2 billion, the drug discovery industry is under increasing pressure to improve the efficacy, selectivity, efficiency and economics of R&D [41].

The “blockbuster business model”, introduced by pharmaceutical companies a few decades ago, is orientated towards the development of high market-volume drugs. However, the potential for withdrawal of blockbuster drugs from the market for safety reasons has become a key driver for the search for alternative models [42].

Specificity, selectivity, safety and disease relevance have all increased in importance as factors in the search for the leading new drugs of the future. As we have seen, chirality has been a characteristic of selectively acting drugs for many years. The inclusion of stereoselectivity into the synthetic chemistry for complex molecules occupying novel chemical space will remain an essential attribute of research on NDEs for many years to come.

References

1. Federsel H-J (2008) *Drug News Prosp* 21:193–199
2. Gillespie P (2007) *Am Drug Disc* 2:14–17
3. Fischer J, Ganellin CR (2010) *Analogue-based drug discovery II*. Wiley-VCH, Weinheim
4. Brooks E, Brichacek M, Mc Grath N, Morton J, Batory L, Njardarson JT (2008) *Compilation of the Njardarson Group*, Cornell University
5. Sales figures from IMS Health (2004)
6. Newman DJ, Cragg GM (2007) *J Nat Prod* 70:461–47
7. Laird T (2005) *Org Proc Res Develop* 9:1
8. Hoffmann T, Bishop C (2010) *Drug Disc Today* 15:260–264
9. Wenlock MC, Austin RP, Barton P, Davis AM, Leeson PD (2003) *J Med Chem* 46:1250–1256
10. Bartlett PA, Entzeroth M (eds) (2006) *Exploiting chemical diversity for drug discovery*. RSC, Cambridge, UK
11. Grabowski K, Schneider G (2007) *Curr Chem Biol* 1:115–127
12. Russ AP, Lampert S (2005) *Drug Discov Today* 10:1607–1610
13. Overington JP, Al-Lazikani B, Hopkins AL (2006) *Nat Rev Drug Discov* 5:993–996

14. Bohacek RS, McMartin C, Guida WC (1996) *Med Res Rev* 16:3–50
15. Lipinski CA, Lombardo F, Domini BW, Feeney PJ (1997) *Adv Drug Deliv Rev* 23:3–25
16. Veber DF, Johnson SR, Cheng SR, Smith BR, Ward KW, Kopple KD (2002) *J Med Chem* 45:2615–2623
17. Newman DJ, Cragg GM (2007) *J Nat Prod* 70:461–477
18. Koch MA, Waldmann H (2005) *Drug Discov Today* 10:471–483
19. Dekker F, Koch MA, Waldmann H (2005) *Curr Opin Chem Biol* 9:232–239
20. Lessmann T, Leuenberger MG, Menninger S, Lopez-Canet M, Muller O, Hummer S, Bormann J, Korn K, Fava E, Zerial M et al (2007) *Chem Biol* 14:443–451
21. Altmann K-H (2007) *Chem Biol* 14:347–349
22. Federsel HJ (2008) *Drug News Perspect* 21:193–199
23. Federsel HJ (2005) *Pharma Chem* 4:4–9
24. CMR International 2006/2007, Pharmaceutical R&D Factbook
25. Beeley LJ, Duckworth DM, Southan C (2000) *Prog Med Chem* 37:1–37
26. Lin H, Cornich VW (2002) *Angew Chem Int Ed Engl* 41:4402–4425
27. Joyce CF (2004) *Ann Rev Biochem* 73:791–836
28. Taylor SV, Kast P, Hilvert D (2001) *Angew Chem Int Ed* 40:3310–3335
29. Gartner ZJ, Grubina R, Calderone CT, Lui DR (2003) *Angew Chem Int Ed* 42:1370–1375
30. Gartner ZJ, Kanan MW, Lui DR (2002) *J Am Chem Soc* 124:10304–10306
31. Calderone CT, Puckett JW, Gartner ZJ, Liu DR (2002) *Angew Chem Int Ed* 41:4104–4108
32. Zhou R, Huang X, Margilus CJ, Beren BJ (2004) *Science* 305:1601–1605
33. Green DVS (2004) *Prog Med Chem* 42:61–97
34. McFadeyn I, Metzger T, Subramanian G, Poda G, Jorvig E, Ferguson DM (2002) *Prog Med Chem* 40:107–135
35. Beeley LJ, Duckworth DM, Southan C (2000) *Prog Med Chem* 37:1–43
36. Floyd CD, Leblanc C, Whittaker M (2005) *Prog Med Chem* 36:91–168
37. Jenkins JL, Bender A, Davies JW (2006) *Drug Disc Today: Technologies* 3:413–421
38. Veenstra TD (2006) *Drug Disc Today: Technologies* 3:433–440
39. Owens J (2006) 2006 Drug approvals: finding a niche. *Nature Rev Drug Discov* 6:99–101
40. DiMasi JA, Hansen RW, Grabowski HG (2003) *J Health Econ* 22:151–185
41. Khanna P (2010) *Drug Disc World. Summer Suppl.* 23–24
42. Waxman HA (2005) *N Engl J Med* 352:2576–25

Chapter 2

Aliskiren Fumarate

Abstract

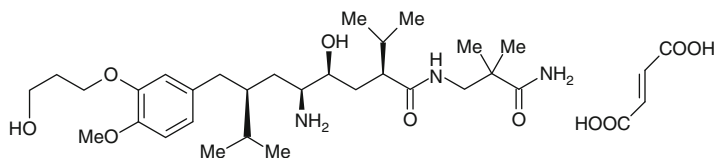
Biological target: Aliskiren is a direct inhibitor of the protease renin, secreted by the kidney, which forms angiotensin I from angiotensinogen. Further metabolism by angiotensin-converting enzyme generates angiotensin II, which is a vasoconstricting agent that also regulates adrenal cortical aldosterone production and thereby renal salt retention. This in turn regulates blood pressure.

Therapeutic profile: Aliskiren is used, either as monotherapy or in combination with other antihypertensive drugs, for the oral treatment of high blood pressure.

Synthetic highlights: Synthetic strategies are often based on visual imaging of a target structure. Using different Dali-like visual representations of a target molecule, creative retrosynthetic considerations can then lead to the selection of starting compounds from Nature’s chiral pool. In this way, imaging of the folded form of a key intermediate revealed L-pyroglytamic acid as a convenient chiral starting material in a “Daliesque synthetic route” to aliskiren. Fine-tuning of the chiral ligand for the Rh complex, which catalyses the hydrogenation of the selected substrate, resulted in extreme enantioselectivity for the critical step in aliskiren synthesis.

2.1 Introduction

Aliskiren (**1**, 2*S*,4*S*,5*S*,7*S*)-5-amino-*N*-(2-carbamoyl-2,2-dimethylethyl)-4-hydroxy-7-[[4-methoxy-3-(3-methoxypropoxy)phenyl]methyl]-8-methyl-2-(propan-2-yl)nonanamide, in the form of the fumarate salt, was approved in the US in March 2008 as a first-in-class anti-hypertensive agent (*Tektura*[®], Novartis/Speedel). It is known as *Rasilez*[®] outside the US and was approved in the EU in August 2008 [1].



1 aliskiren fumarate

The drug received FDA approval for the oral treatment of high blood pressure as monotherapy or in combination with other anti-hypertensive medications.

2.2 Renin and the Mechanism of Action of Aliskiren

The target enzyme of aliskiren is renin (EC 3.4.23.15) and the drug is the first direct inhibitor of this enzyme [2, 3], in distinction to the older ACE inhibitors, which provide incomplete suppression of the *renin–angiotensin–aldosterone* system (RAAS) (Fig. 2.1).

Renin is a protease, secreted by blood vessels in the juxtaglomerular apparatus of the kidney, under various physiological stimuli, including a decrease in renal perfusion pressure (regulated by blood pressure), thus controlling filtration of fluid through the kidney. Acting on its substrate, the plasma protein, angiotensinogen, renin forms angiotensin I, which is further converted (by angiotensin converting enzyme, ACE) to form angiotensin II. Binding to AT_1 receptors, angiotensin II stimulates growth of vascular tissue, vasoconstriction (directly and by stimulating noradrenergic nerves) and salt retention (by stimulating aldosterone release from the adrenal cortex and increasing Na^+ reabsorption by the kidney). Older anti-hypertensive agents include the ACE inhibitors and AT_1 receptor antagonists.

The inventors of aliskiren employed a combination of crystal structure analysis of renin-inhibitor complexes and computational methods to design novel renin inhibitors without the extended peptide-like backbone of previous inhibitors. In order to understand the interactions of aliskiren at the active site of renin, the

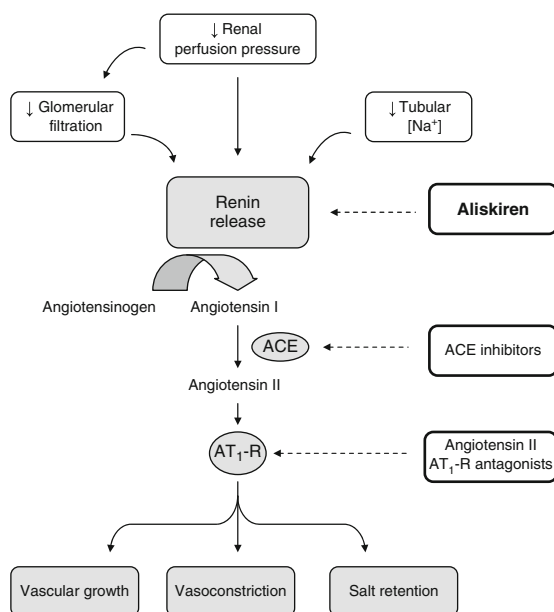
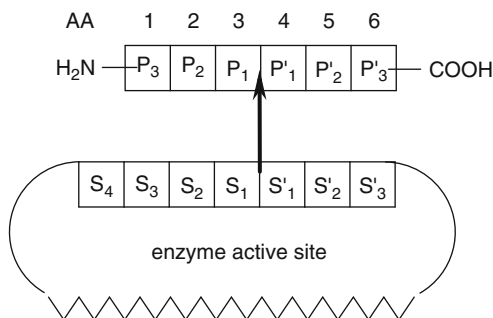


Fig. 2.1 Control of renin release and action of angiotensin II (modified from [4])

Fig. 2.2 Schematic presentation of the enzyme–substrate complex of papain with a bound hexapeptide

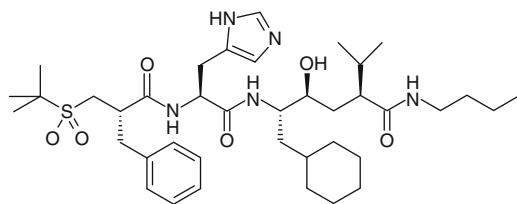


schematic presentation of enzyme–substrate complexes of peptidases introduced by Schechter [5] can be applied to renin-catalysed reactions (Fig. 2.2).

Thus, the active site of the enzyme is composed of seven sub-sites, S1–S4 and S1'–S3', located on either side of the catalytic site, indicated by the bold arrow. Substrate amino acids P are counted from the point of cleavage on both sides of the site, and thus they are numbered in the same way as the sub-sites they occupy.

Using this scheme, a molecular modelling method was developed, in order to substitute earlier peptide inhibitors with a compound lacking the P1–P4 spanning backbone that would optimally fit the hydrophobic surface of the large S3–S1 cavity of renin Fig. 2.3 [6].

Figure 2.3 shows the binding of aliskiren to renin in relation to the enzyme specificity pockets, S4–S2'. Superimposition of the peptide inhibitor CGP 38560A reveals how very different the binding interactions of aliskiren are compared to the older peptide.

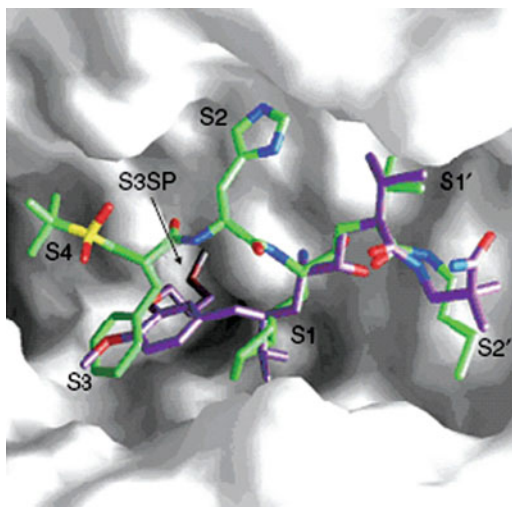


CGP 38560A

Aliskiren acts as a transition state mimetic, inhibiting renin via hydrogen bonding of both the central hydroxyl group and the amino function to the catalytic Asp32 and Asp215 residues in the S1–S3 pocket [7, 8].

Thus, one of the important interactions of aliskiren at the active site is contributed by the alkylether aromatic side-chain, which is accommodated within a distinct sub-pocket S3. This pocket is orientated perpendicularly to the substrate binding cleft of renin, which is not occupied by substrate-derived inhibitors, such as CGP 38560 [9]. The methoxypropoxy side chain in aliskiren **1** appears to be

Fig. 2.3 Superimposed binding of aliskiren (*purple*) and peptide inhibitor CGP 38560A (*green*) to the active site of human rennin (reproduced from [6], with the permission of Academic Press)

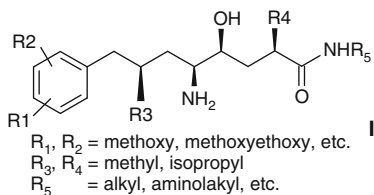


optimal with regard to length and the position of the distal ether oxygen, as the H-bond acceptor from Tyr 14 of the S3 sub-pocket.

Within the central backbone of aliskiren, the vicinal amino and hydroxyl groups at the two stereogenic centres (both in the *S*-configuration) contribute to the hydrogen bonding with the catalytic As 32 and Asp 215 residues. Extensive modification of the P2' region, the subunit on the terminal carboxylic group, led synthesis from a lipophylic *n*-butyl side chain, via a basic group, to a terminal carboxamide group and the insertion of geminal methyl groups. The terminal carboxamido group, as a consequence, became involved in the H-bonding interaction with Arg 74, while the geminal dimethyl group provided hydrophobic interactions with the S2' site of renin. As a cumulative effect of all these binding contributions, an increased affinity of aliskiren was achieved to within the sub-nanomolar range (IC_{50} 0.0006 μ M) [8].

2.3 Structural Characteristics and Synthetic Approaches to Aliskiren

Aliskiren is representative of compounds with general structure **I**, varying in the nature of the aromatic substituents, the amide moiety, and alkyl groups, representing a novel carbon backbone with unique binding affinity to renin.

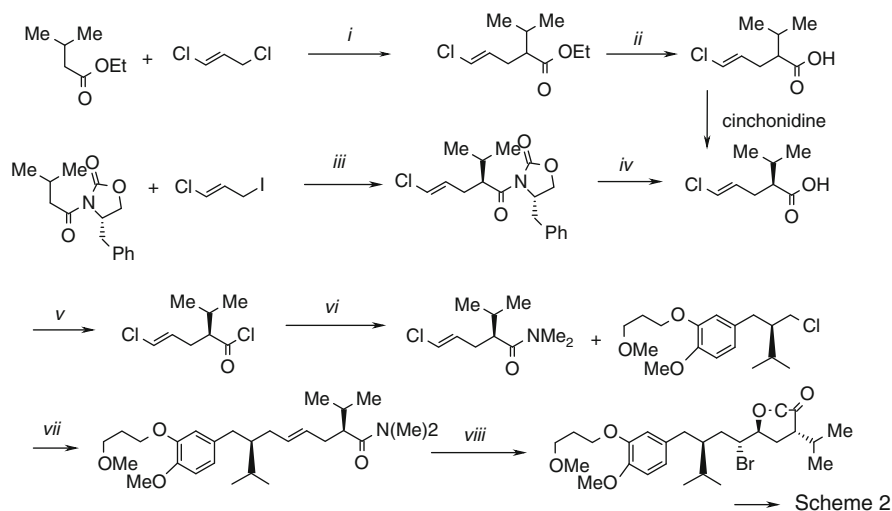


While the structure-based design of aliskiren is straightforward, synthesis of this highly flexible molecule with four stereogenic centres remains a formidable task. Synthetic approaches to aliskiren are numerous, and have been reported in a number of patents [9–12] and original papers [13–21]. Here, we present two routes to the chiral drug. Because of their conceptual and methodological differences, the two routes demonstrate instructively how a complex target molecule, such as aliskiren, offers great opportunity for creative synthetic organic chemistry.

The first strategy is characterized by imaginative retrosynthetic analysis [22] that leads to the natural chiral agent, L-pyroglutamic acid. The second strategy makes use of a chiral organometallic complex, designed for highly enantioselective hydrogenation of the strategic intermediate in the critical synthetic step. As such it represents an instructive example of the modern concept of fine-tuning of chiral ligands in organometallic catalysis. On the path to aliskiren, catalytic hydrogenation of the C=C bond in the strategic prochiral substrate is achieved using an Rh complex with a bidentate diphosphine ligand, thus creating a chiral environment constituted by the three ferrocenyl units [23].

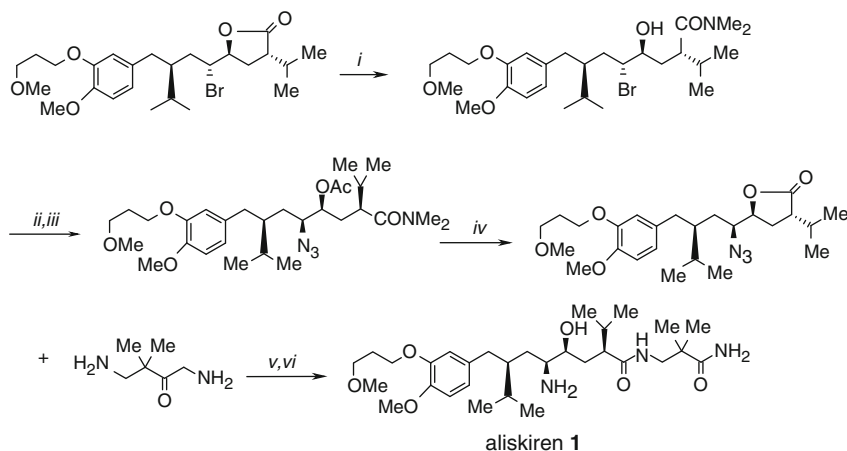
Before considering these two novel approaches in detail, Schemes 2.1 and 2.2 present the original and one of the most explored routes to aliskiren, which was developed by the originator of the active substance [9].

These schemes show how complex a synthetic project can become in order to supply a new drug. The synthetic route outlined in these two schemes is characterized by a large number of steps, a diversity of reagents and effective chirality



Reagents and conditions: *i*. N-BuLi, DIA; *ii*. NaOH, aq. EtOH; *iii*. LiHMDS/THF;
iv. Aq. LiOH; *v*. (COCl)₂; *vi*. Me₂NH, pyridine;
vii. Mg(0), THF; *viii*. H₃PO₄, NBS.

Scheme 2.1 Initial steps on the synthetic route to aliskiren



Reagents and conditions. *i.* Me₂NH, Et₂AlCl; *ii.* Ac₂O; *iii.* NaN₃; *iv.* TsOH; *v.* TEA, D; *vi.* Pd-C/H₂.

Scheme 2.2 Final synthetic steps on the route to aliskiren

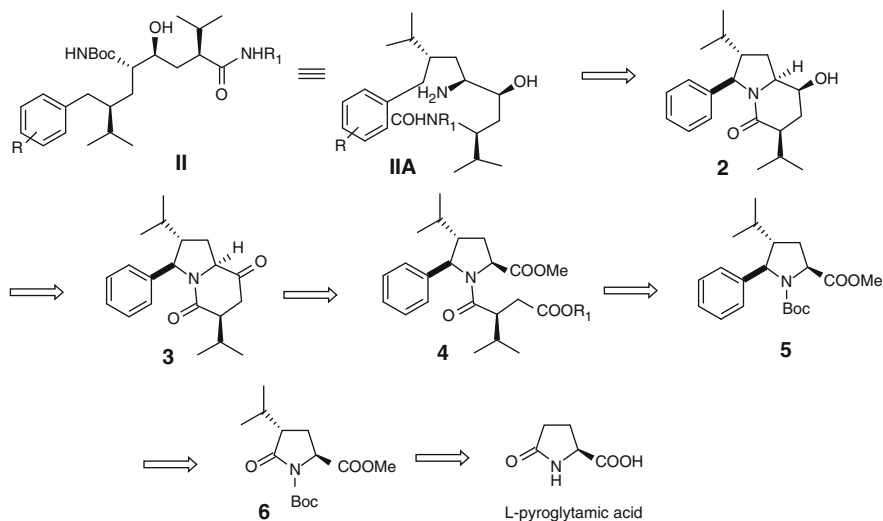
transfer. This pathway had to be scaled up to the production level, yet still meet the requirements for large quantities of active substance with high chemical and stereochemical integrity.

2.3.1 Strategy Based on Visual Imagery, Starting from Nature's Chiral Pool: A Dali-Like Presentation of Objects

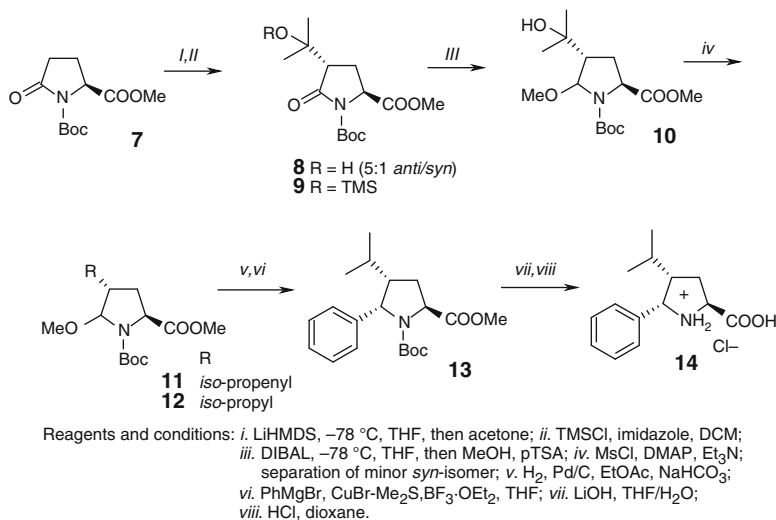
The first synthetic approach to be considered in more detail was designed and largely completed by Hanessian et al. at the University of Montreal. The authors started from retrosynthetic analysis of the generic backbone structure **1** (Scheme 2.3) [21]. They noticed that compound **II**, when presented in its “folded” form **IIA**, *visually overlaps better* with the bicyclic lactam **2**!

Further retrosynthetic steps in this Scheme led to the logical synthetic equivalents **3–6**, likely to be available in the (reverse) synthetic pathway from L-pyroglutamic acid, a chiral building block from Nature. Each synthetic step in this scheme, however, required innovative use of a specific reagent. These innovations included hydrolysis and hydrogenolysis of the two C–N bonds in **2** to obtain **1**, diastereoselective reduction of the ketone carbonyl group in **3** to obtain **2**, and arylation of the pyrrolidone **6** to obtain **5** via diastereoselective addition of a phenyl group to the intermediary iminium ion.

Once the bicyclic lactam **2** had been assembled, it was only necessary to cleave two C–N bonds to reveal the acyclic form of the target structure **II**. This situation



Scheme 2.3 Retrosynthetic analysis of the backbone structure of **1**



Scheme 2.4 L-Pyroglytamic acid as the starting point for the chiral building block **14**, with the “wrong” stereochemistry

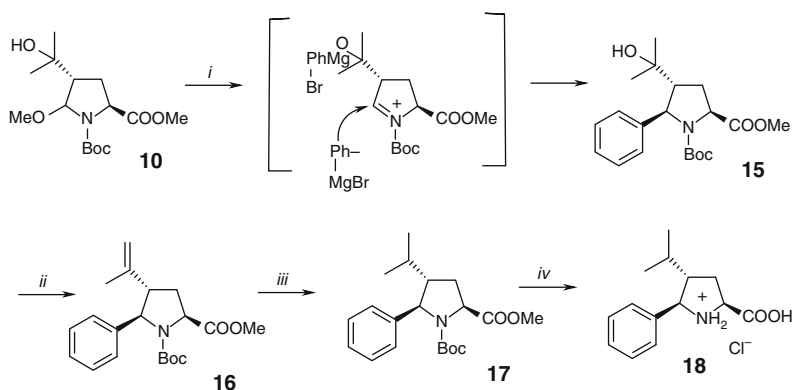
resembles the concealed imagery of some of the paintings of Salvador Dali, permitting the objects to be seen in more than one way. Therefore, the authors named this route the “Daliesque synthetic plan” [21]!

The first hurdle to be overcome in this synthetic plan was the introduction of the 2*R*-isopropyl group and 1*S*-phenyl group, with the unfavourable relative *cis*-stereochemistry, starting from suitably protected L-pyroglytamic acid (Scheme 2.4) [21].

Nearly all steps in this scheme required significant departure from the «standard» conditions or reagents! Thus, introduction of *iso*-propyl group by alkylation of Li-enolate with *iso*-PrI failed due to low reactivity of the *sec*-halide. Alkylation by acetone provided a successful detour and intermediate **8** was obtained as a 5:1 *anti/syn* mixture. On protection, as TMS ether **9**, and reduction with DIBAL-H, diastereomeric hemiaminals were obtained and, without isolation, treated with acidic methanol, thus permitting isolation of pure diastereomer **10**. En route to introduction of the isopropyl group, mesylation of **10** and conversion to the *iso*-propenyl unit in **11** was completed regioselectively. On hydrogenation to *iso*-propyl in **12**, arylation of this intermediate surprisingly afforded the undesired 4,5-*cis* product **13** with the unexpected, “wrong” diastereoselectivity. The authors concluded that this outcome was the result of nucleophilic attack from the site opposite to the 2-carbomethoxy group, which is expected to co-ordinate Grignard reagent and orientate it to the *trans*-position in relation to the *iso*-propyl group. They argued that co-ordination of an excess of Grignard reagent causes steric repulsions which counterbalance the effect of the 4-*i*-propyl group. Deprotection of N-Boc and the ester group afforded the crystalline product **14**, whose structure and “wrong” stereochemistry were ascertained by single-crystal X-ray crystallography.

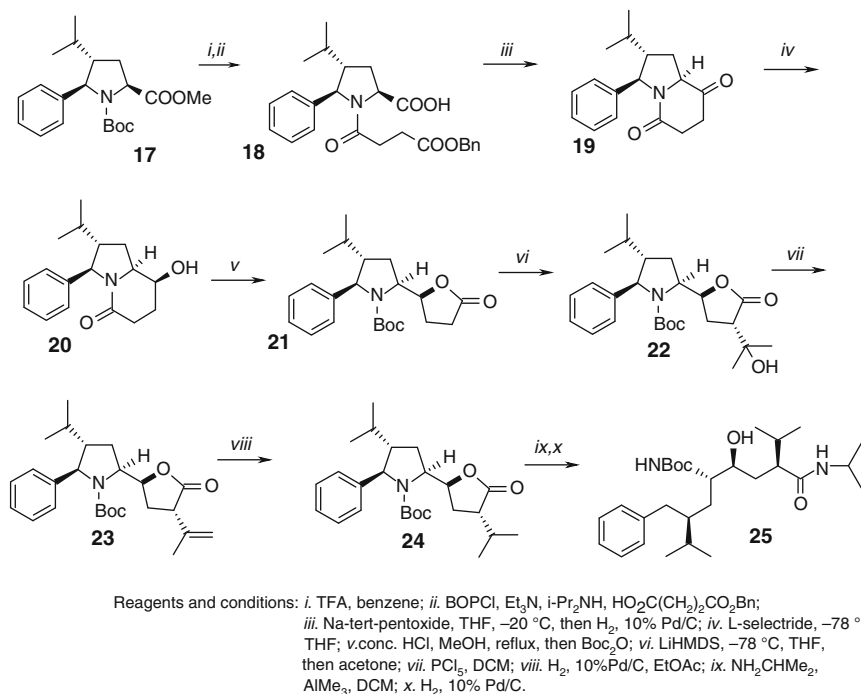
To avoid formation of the 4,5-*cis* intermediate **13**, the authors decided to introduce a phenyl group *prior* to deoxygenation of the *tert*-alcohol **10**, counting on its co-ordinating ability, as outlined in Scheme 2.5.

In this strategy, the nucleophile, phenide anion, was expected to approach the iminium ion from the side *opposite* to the bulky metal-alkoxide complex, provided excess of the reagent was used. Treatment with five equivalents of the phenylmagnesiocuprate reagent afforded 4,5-*trans*-substituted **15** with 80% diastereoseomeric excess (% d.e.). The next steps proceeded as expected. The structure and correct stereochemistry of the target compound **18**, isolated as the hydrochloride, were again confirmed by X-ray crystallography.



Reagents and conditions: *i*. PhMgBr, CuBr·Me₂S, BF₃·Et₂O, THF; *ii*. MsCl, DMAP, Et₃N, *iii*. H₂, 10% Pd/C; *iv*. LiH, MeOH/H₂O, 95%.

Scheme 2.5 “Inverted tour” to the building block **18** with “correct” stereochemistry



Scheme 2.6 Final steps leading to the aliskiren congener **25**

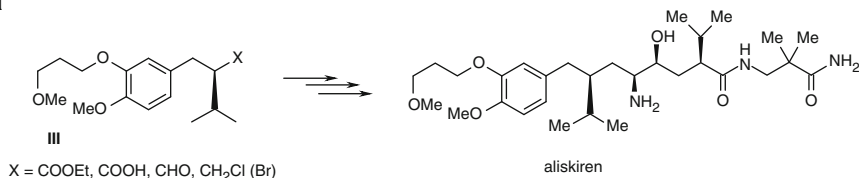
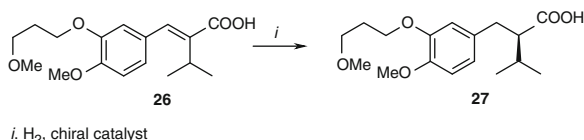
From the intermediate **17**, the aliskiren congener with an *iso*-propylamide unit, prototypical target **25**, was obtained according to Scheme 2.6 [21].

Along the pathway shown in Scheme 2.6, another departure from the original retrosynthetic concept, presented in Scheme 2.3, was required. This concerned steps *v* and *vi*, in which *trans*-cyclization of the 6-membered lactame to the 5-membered lactone was achieved, followed by alkylation of the enolate with acetone (step *vi*), analogous to the procedure in Scheme 2.4. This step proceeded with the correct diastereoselectivity, enabling completion of the synthesis of target **25**, a close structural congener of aliskiren.

2.3.2 Fine-Tuning of the Chiral Ligand for the Rh Complex: Hydrogenation of the Selected Substrate with Extreme Enantioselectivities

The intermediate structures of general formulae **III**, either racemic or in the optically pure form, are required on many routes to aliskiren (Scheme 2.7a).

Synthetic pathways to optically pure derivatives have made use of a variety of different methods: resolution of racemic acid **III** (X = COOH) [22], alkylation of

a**b**

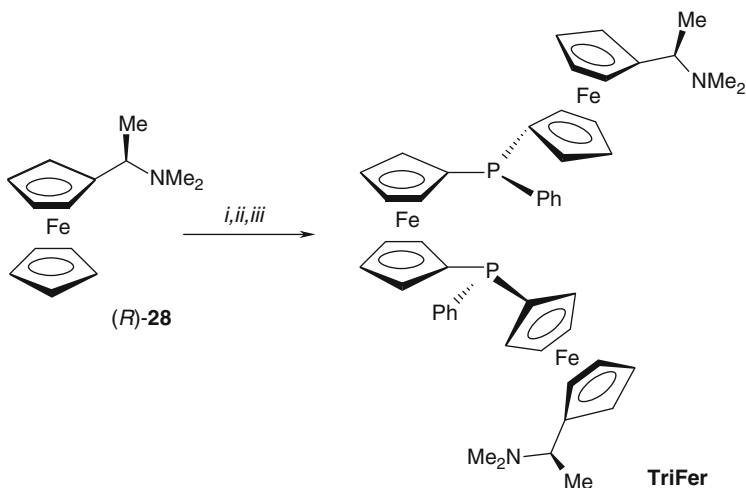
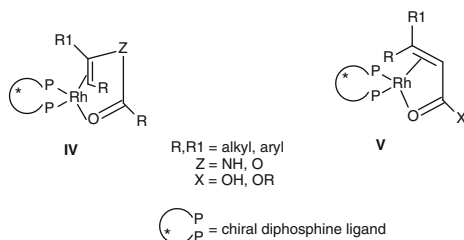
Scheme 2.7 (a) From the key intermediates **III** to aliskiren (b) Enantioselective hydrogenation leading to **27**

chiral auxiliary with bromobenzyl congener of **III** to give optically pure amide ($\text{X} = \text{CONHR}^*$) [23, 24] and enantioselective hydrogenation of unsaturated precursor ($\text{X} = \text{CH}_2\text{OH}$, $\text{C}=\text{C}$ bond in α , β -position), with Rh complexes of chiral phosphines. This last reaction proceeded with limited enantioselectivity, however, when earlier, commercially available chiral ligands were used [25, 26].

In view of the easy access to prochiral α -substituted cinnamic acids, specifically to compound **26** in Scheme 2.7b, its enantioselective hydrogenation to the chiral dihydro-derivative, (2*R*)-2-[3-(3-methoxypropoxy)-4-methoxybenzyl]-3-methylbutanoic acid **27**, represents an appealing step on the path to aliskiren. Optically pure acid **27** is a valuable intermediate in the novel routes, being a departure from those in Schemes 1.1 and 1.2. Generally, chiral α -substituted dihydrocinnamic acid derivatives, structurally related to **27**, are key intermediates in the synthesis of many bioactive compounds, including renin inhibitors [27], β -secretase inhibitors [28], enkephalinase inhibitors [29] and opioid antagonists [30]. In spite of the significant progress achieved in asymmetric hydrogenation of a wide range of substrates with an internal $\text{C}=\text{C}$ bond, enantioselective hydrogenation of α -alkyl cinnamic acids remains a challenge [31, 32]. The main reason for the low enantioselectivity in the hydrogenation of some substrates with a $\text{C}=\text{C}$ bond (achieved with Rh-complexes of most known chiral phosphines) lies with the lack of additional functionality in such substrates, preventing their co-ordination to metal as bidentate ligands. As presented in Fig. 2.4, substrates with the general formula **IV**, such as enamides ($\text{Z} = \text{NH}$) and enolacetates ($\text{Z} = \text{O}$), can co-ordinate to the metal via the n -electrons on the carbonyl oxygen and the π -electrons of the $\text{C}=\text{C}$ bond. α -Substituted cinnamic acids lack such functionality at the β -position to co-ordinate with the metal, and their small-ring chelates with the general formulae **V** are stereoelectronically unfavourable.

Based on these considerations on the existence of complexes **IV** and **V**, Chen, McCormick et al. have developed a new concept of ferrocene-based chiral ligands [33, 34]. These authors designed and completed stereoselective synthesis of the

Fig. 2.4 Two types of unsaturated substrate as bidentate ligands in Rh(I) catalytic complexes



Reagents and conditions: *i.* *t*-BuLi, Et₂O, −78 °C to r.t.; *ii.* PhPCl₂, −78 °C to r.t.
iii. 1,1'-FcLi₂, −78 °C to r.t.

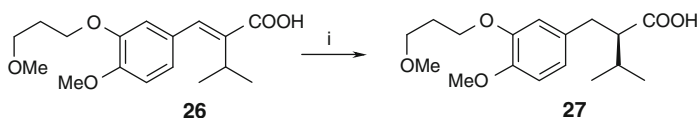
Scheme 2.8 Synthesis of bidentate P, P-ligand, TriFer

ferrocene-based *C*₂-symmetric diphosphine ligand, TriFer, characterized by the basic amino groups at the “periphery” of the ligand. They also reported on its application to the first highly enantioselective hydrogenation of α -alkyl cinnamic acids [35, 36]. Synthesis of ligand TriFer is outlined in Scheme 2.8, and starts from readily available ferrocenyl amine (*R*)-28 [35].

Ligand TriFer is the first example of a *C*₂-symmetric diphosphine that combines C-, P-central and planar chirality. Indeed, it is astonishing how straightforward and short is the synthesis of such a complex molecular assembly!

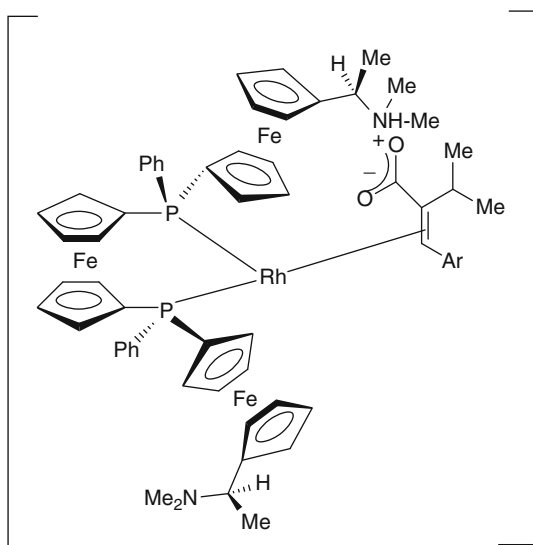
More importantly, the authors achieved unprecedented enantioselectivities in the Rh(TriFer)-catalysed asymmetric hydrogenation of **26**, a key intermediate in the syntheses of aliskiren (Scheme 2.7b). The conditions and results are given in Table 2.1.

Hydrogenation of **26** in the presence of an Rh catalyst, generated in situ from Rh(COD)₂BF₄ (0.1 mol%, COD = cycloocta-1,5-diene) and ligand TriFer in MeOH,

Table 2.1 Enantioselective hydrogenation of **26** to aliskiren intermediate **27**

i. H₂-50 barr, Rh(COD)₂BF₄/TriFer, MeOH

Entry	Substrate/catalyst	Mol of substrate	<i>t</i> (h)	e.e. (%)
1	500	0.16	13	99.6
2	500	0.16	5	99.3
3	1,000	0.55	4	98.6
4	2,000	0.55	4	98.4

Fig. 2.5 Substrate–catalyst complex in the asymmetric hydrogenation of α -alkyl cinnamic acids with Rh(TriFer) complex

gave **27** with unprecedented enantioselectivities of up to 99.6% e.e., and over 99% conversion.

To account for the extremely high enantioselectivities in the hydrogenation of an otherwise “hard” internal C=C bond with the Rh(TriFer)-complex, the authors proposed a specific secondary interaction of the ligand with the unsaturated substrate, as schematically presented in Fig. 2.5 [35].

According to the generally accepted mechanism of enantioselective hydrogenation by Rh complexes, co-ordination of the substrate to the solvated Rh complex to form the bidentate catalyst–substrate complex, outlined in Fig. 2.5, was invoked.

Unlike enamides and enol-acetates IV in Fig. 2.4, α -alkyl cinnamic acids lack such functionality at the β -position to co-ordinate with the metal. The authors proposed a dimethylamino moiety in the ligand TriFer to serve as the second interaction centre via electrostatic interaction with the carboxylate unit.

The results of this study confirmed the heuristic value of the well-known quadrant rule [36], which accounts for the origin and bias of enantioselectivity in hydrogenation with complexes of ligands with C_2 symmetry (Fig. 2.6) [35].

This rule invokes steric hindrance in the two opposite quadrants as the origin of enantioselection, as presented in Fig. 2.6 for two equatorial 2-(dimethylamino)ferrocen-1-yl groups (DMA-Fc) [35]. The configuration of the Rh(TriFer) complex, *S*- at ferrocenes and P-atoms, *R*- at C-atoms, favours the approach of the substrate so as to minimize steric interactions with the large DMA-Fc group, as in TS-1 in Fig. 2.6, yielding the *R*-enantiomer of α -alkyl- β -aryl carboxylic acid as the major product.

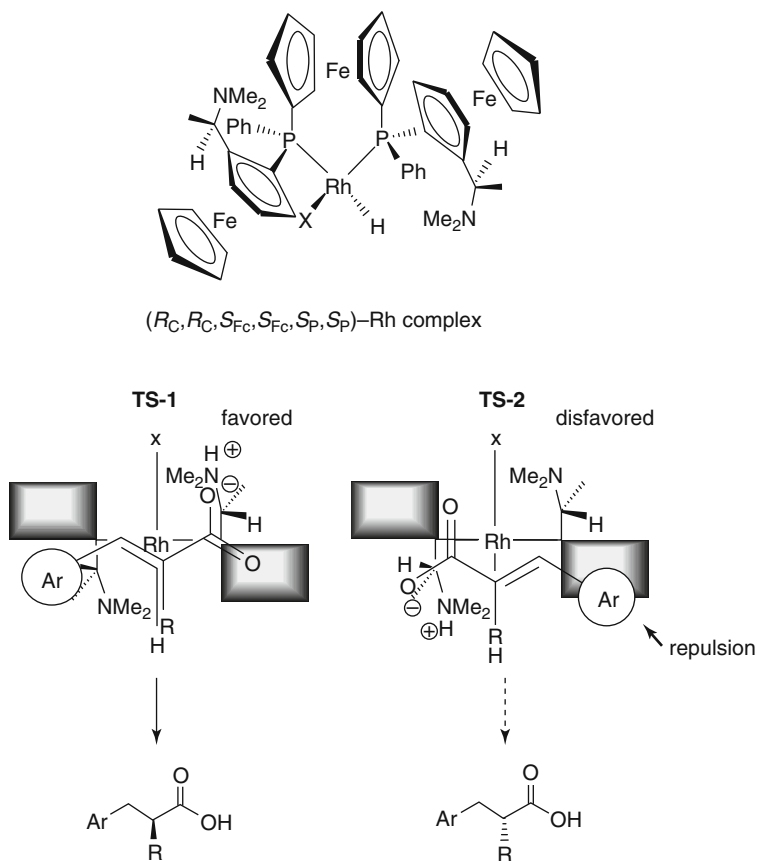


Fig. 2.6 Transition-state models for the asymmetric hydrogenation of α -substituted cinnamic acids catalysed by the (*R_C*, *R_C*, *S_{Fc}*, *S_{Fc}*, *S_P*, *S_P*)-Rh(TriFer) complex (reproduced from [35], with the permission of J. Wiley & Sons Inc.)

This second route to aliskiren elegantly demonstrates how accumulated knowledge on the topology of the catalytic complex and the existing secondary interactions promote the design of the optimal catalytic system for hydrogenation of the specific substrate. The key intermediate, prochiral carboxylic acid, is an otherwise difficult substrate to achieve high enantioselectivity. Once this conceptual synthetic problem had been solved by the use of the fine-tuned catalyst, catalytic enantioselective hydrogenation was subsequently applied successfully in the large-scale process for the commercial synthesis of aliskiren.

2.4 Conclusion

The number of synthetic methods and the way in which they can be combined to synthesize the target structure is limited only by the imagination of the chemists. The two main approaches to the construction of a complex chiral molecule with multiple stereogenic centres depend either on an original starting compound obtained from a natural source or on an initial enantioselective catalytic step. As described in this chapter, the signposts to aliskiren fumarate are based on both these approaches. The first strategy starts from L-pyroglutamic acid and is based on visual imagery in synthesis planning, akin to a Dali-like presentation of the objects. The second strategy, based on the pragmatic concept of producing a key chiral intermediate with over 99% e.e., resulted in an inventive, large-scale catalytic process with a turnover number (TON) of >5,000.

References

1. Graul AI, Prous JR, Barrienne M, Bozzo J, Castaner R, Cruces E, Revel L, Rosa E, Serradel N, Sorbera LA (2008) *Drug News Prospect* 21:10–11, 28–29
2. Oparil S, Yarows SA, Patel S, Zhang J, Satlin A (2007) *Lancet* 370(9563):1126–1127
3. Danser AH (2007) *J Cardivasc Pharmacol* 50:105–111
4. Rang HP, Dale MM, Ritter JM, Flower RJ (eds) (2007) *Rang & dale's pharmacology*. London, Churchill Livingstone, p 304
5. Schechter I, Berger A (1967) *Biochem Biophys Res Commun* 27:157–162
6. Wood JM et al (2003) *Biochem Biophys Res Commun* 308:698–705
7. Rahuel J, Rasetti V, Maibaum J, Ruger H, Goschke R, Cohen NC, Stutz S, Cumin F, Fuhrer W, Wood JM, Grutter MG (2000) *Chem Biol* 7:493–504
8. Rahuel J, Priestle JP, Grutter MG (1991) *J Struct Biol* 107:227–236
9. Goschke R et al (Novartis AG) EP 678500; EP 678503; Priority CH 116994
10. Stutz S et al (Speedel Pharma Inc.) WO 2001009079; WO 2001009083
11. Belus D, Dondoni A (Speedel Pharma Ltd.) EP 1215201; US 200208302; US 2003176717; US 6670507
12. Herold P, Stutz S (Speedel Pharma Inc.) WO 2002008172
13. Bamford MJ, Beard M, Cherry DT, Moloney MG (1995) *Tetrahedron Asymmetry* 6:337–340
14. Beard MJ, Bailey JH, Cherry DT, Moloney MG, Shim SB, Statham KA, Bamford MJ, Lamont RB (1996) *Tetrahedron* 52:3719–3740
15. Goschke R et al (1997) *Bioorg Med Chem* 7:2735–2740

16. Rüeger H, Stutz S, Göschke R, Spindler F, Maibaum J (2000) *Tetrahedron Lett* 41: 10085–10089
17. Sandham DA, Taylor RJ, Carey JS, Fässler A (2000) *Tetrahedron Lett* 41:10091–10094
18. Goschke R et al (2003) *Helv Chim Acta* 86:2848–2870
19. Dong H et al (2005) *Tetrahedron Lett* 46:6337–6340
20. Lindsay KB, Skrydstrup T (2006) *J Org Chem* 71:4766–4777
21. Hanessian S, Claridge S, Johnstone S (2002) *J Org Chem* 67:4261–4274
22. Warren S (1989) *Designing organic synthesis, a programmed introduction to the synthon approach*, 5th edn. Wiley, New York
23. Mickel SJ (Novartis AG; Novartis Pharmaceuticals UK Limited) GB 2431652
24. Goschke R et al (Novartis AG) EP 0678500; EP 0678503
25. Hopius IN, Patterson LE, Alt CA, Rizzo JR, Zhang TY, Huarez M (2005) *Org Lett* 7: 1947–1951
26. Herold P, Stutz S, Spindler F (Speedel Pharma Inc.) WO 2002002487
27. Sturm T, Weissensteiner W, Spindler F (2003) *Adv Synt Catal* 345:160–164
28. Owens AP, Nadin A, Talbot AC, Clarke EE, Harrison T, Lewis HD, Reilly M, Wrigley JDJ, Castro JL (2003) *Bioorg Med Chem Lett* 13:4143–4145
29. Monteil T, Danvy D, Sihel M, Leroux R, Plaquevent J-C (2002) *Mini Rev Med Chem* 2:209–217
30. Salo QMH, Lahtela-Kakkonen M, Gynther J, Jarvinen T, Poso A (2004) *J Med Chem* 47:3048–3057
31. Cheng X, Zhang Q, Xie J, Wang Q, Zhou Q (2005) *Angew Chem Int Ed* 44:1118–1121
32. De Vries JG, Leort L (2006) *Eur J Chem* 12:4722–4728
33. Chen W, Mbafor W, Roberts SM, Whittall J (2006) *J Am Chem Soc* 128:3922–3923
34. Chen W, Roberts SM, Whittall J, Steiner A (2006) *Chem Commun*: 2916–2918
35. Chen W, McCormack PJ, Mohammed K, Mbafor W, Roberts SM, Whittall J (2007) *Angew Chem* 119:4219–4222
36. Feldus S, Landis CR (2000) *J Am Chem Soc* 122:12714–12727

Chapter 3

(R)-K-13675

Abstract

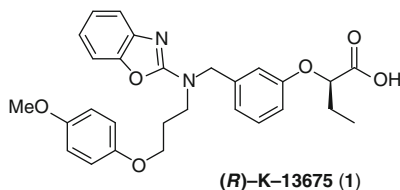
Biological target: (R)-K-13675 is a 2-aryloxy-propionic acid derivative with specific agonist activity at the peroxisome proliferator-activated receptor α (PPAR α), a transcription factor regulating lipid metabolism.

Therapeutic profile: It is a lead candidate compound for development by Kowa, Japan, as a cholesterol-lowering drug.

Synthetic highlights: A critical step in the synthesis of the compound involves non-hydrolytic anomalous lactone ring-opening by TMSI. To avoid racemization, the Mitsunobu reaction was applied in the formation of the ether bond. Optimization of the Mitsunobu reaction was finally achieved without loss of enantiomeric purity.

3.1 Introduction

Compound **(R)-K-13675** (**1**, (R)-2-[3-(benzoxazol-2-yl)[3-(4-methoxyphenoxy)propyl]amino)methyl]phenoxy]butanoic acid) is a member of the class of peroxisome *proliferator-activated receptor α* (PPAR α) agonists.



3.2 Peroxisome Proliferator-Activated Receptor α Agonists

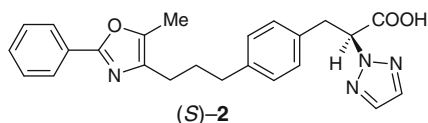
Peroxisomes are intracellular cytoplasmic organelles and the major sites for enzymatic oxidation, including that of fatty acids. The proliferation of peroxisomes is stimulated by free fatty acids and some metabolites of arachidonic acid, which are ligands for nuclear receptor proteins, the PPARs. These, in turn, are a family of

transcription factors for a wide variety of genes that regulate cellular differentiation, development and metabolism. They include PPAR α (mainly regulating lipid metabolism), PPAR β and PPAR γ (mainly involved in glucose metabolism). The members of the PPAR receptor family, therefore, represent very attractive biological targets, as they play central roles in maintaining cellular and whole-body glucose and lipid homeostasis. Their identification opened up a new approach to the treatment of altered metabolic homeostasis, as occurs in atherosclerosis, diabetes and obesity [1]. Through activation of PPAR α , pharmacological agonists lead to a decrease in triglyceride levels and an increase in *high-density lipoprotein* (HDL)-cholesterol in humans [2, 3].

3.2.1 β -Phenylpropionic Acids

One of the early approaches to the development of selective agonists for PPAR α was initiated by Casimiro-Garcia et al. [4, 5]. They observed, for the phenylpropionic acid-based class of PPAR α / γ dual agonists, that specific modifications of the linker reduced potency for binding and activation of PPAR γ , while maintaining high activity at PPAR α . Generally, these structures are characterized by the presence of a hydrophilic, carboxylic head, a central phenyl ring, a linker of specific composition and flexibility, and the lipophilic tail. Such a topology enables agonists to accommodate to the curved active site of PPARs, and to offer binding interactions with key amino acid residues. This highly schematic concept was the starting point taken by many groups for the synthesis of specific classes of agonists.

The initial researchers identified the *S*-enantiomer of compound **2** as a potent human (h) PPAR α / γ dual agonist, among a series of closely related structural analogues [5].



The high potency for binding and activation of both hPPAR subtypes, observed for **2**, was explained on the basis of numerous interactions at the ligand binding domain (LBD), that were derived from crystallographic data, presented in Fig. 3.1 [5]. The interactions between **2** and PPAR γ -LBD occur mainly between the carboxylate head group and “charge clamp” residues, His323 and Tyr327 in helix 6, His449 in helix 11, Tyr473 in helix 12 and Ser289 in helix 3, forming a network of hydrogen bonds. The phenyloxazole tail reaches into the hydrophobic pocket formed by Val339, Ile 341, Met348, Ile291 and Leu353. An important H-bonding interaction between the triazole N(2) and His440 in PPAR α was obtained from the model, in which compound **2** was superimposed onto the active site of human PPAR α , and corresponds to the interaction of triazole N(2) and His449 in PPAR γ . This latter interaction contributes to a 26-fold and 61-fold increase in potency of

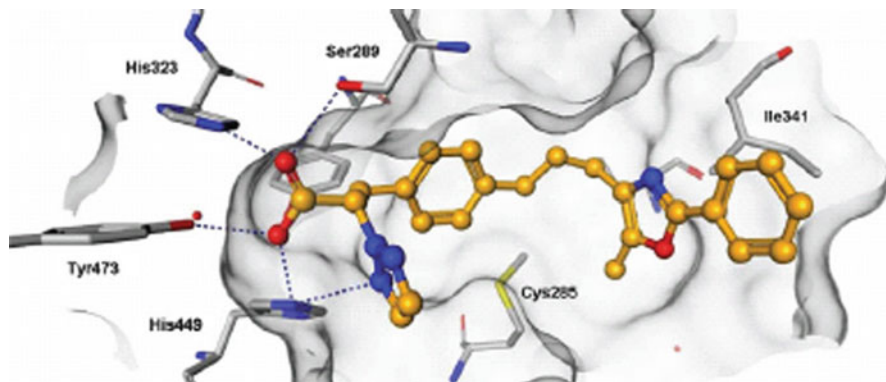
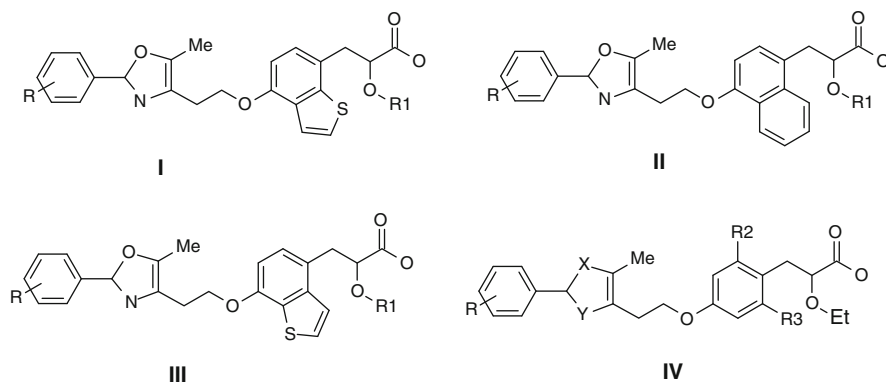


Fig. 3.1 Three-dimensional presentation of dual agonist **2** bound in the ligand binding pocket of human PPAR γ (reproduced from [5], with the permission of Elsevier Inc.)

S-2 for PPAR α and PPAR γ over its *R*-enantiomer, since only in the former is the triazole unit correctly orientated spatially towards the His449 imidazole unit.

3.2.2 α -Alkoxy- β -Arylpropionic Acids

Another group of dual hPPAR α/γ agonists is represented by α -alkoxy- β -arylpropionic acids, with the general formulae **I–IV** [6, 7].



The first three structural classes are characterized by a polycondensed aromatic ring, the fourth by an *ortho*, *ortho'*-disubstituted phenyl ring, and all four classes by a flexible linker between the 2-phenyloxazole and the O-atom in the *para*-position to the propionic acid unit.

A highly simplified model, common to the structures **I–IV**, is presented in Fig. 3.2. Importantly, the authors concluded that the linkers can be branched due to the Y-shape of the LBD in PPARs. This model led to a large number of highly

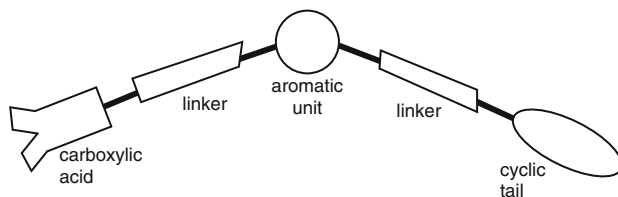


Fig. 3.2 Simplified topology of hPPAR agonists **I–IV**

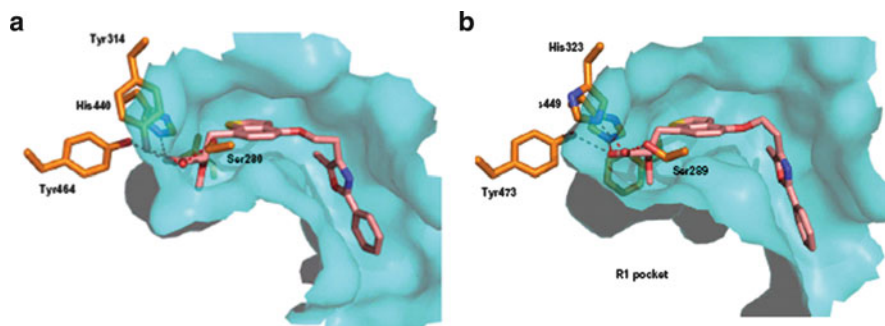
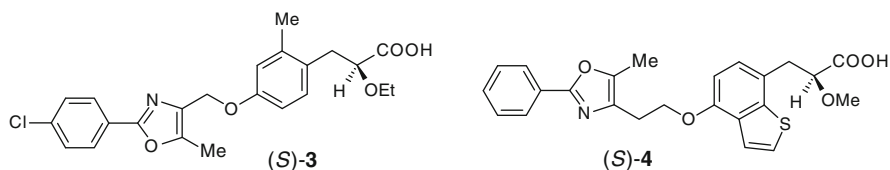


Fig. 3.3 X-Ray structures (a) of compound **3** bound to hPPAR α ; (b) bound to hPPAR γ (reproduced from [7] with the permission of Elsevier Inc.)

specific, dual hPPAR α/γ agonists. The two lead molecules, **3** and **4**, representatives of classes **I** and **IV**, respectively, together with their binding to the LBD of PPAR α and PPAR γ , are presented in Figs. 3.4 and 3.5.



In Fig. 3.3, the binding of **3** to both PPARs is shown, and in Fig. 3.4, the binding of **4** to the same couple of receptors is shown.

It can be seen that both lead molecules adopt a largely bent conformation, adapting to the curved binding pocket. However, besides this general topological characteristic of the complex, the figures indicate a number of binding interactions which engage AA residues in a similar way to that shown in Fig. 3.2. It is also interesting to note that, for compounds **2–4**, the *S*-configuration was assigned, and for compound **1**, the *R*-configuration. This was the consequence of their priority according to the Cahn–Ingold–Prelog (CIP) nomenclature [8], although all of them have the same spatial orientation of substituents on the stereogenic centre.

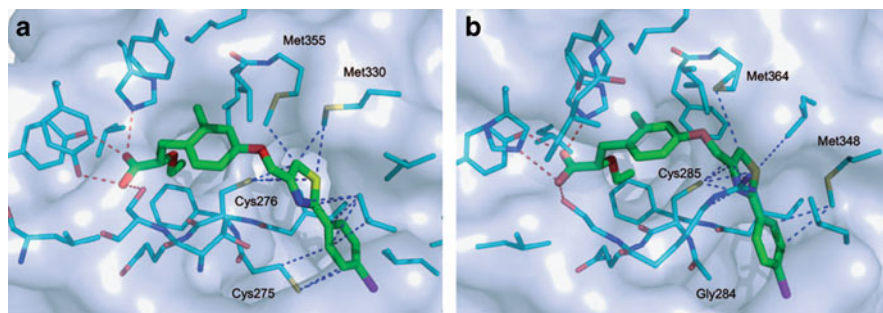
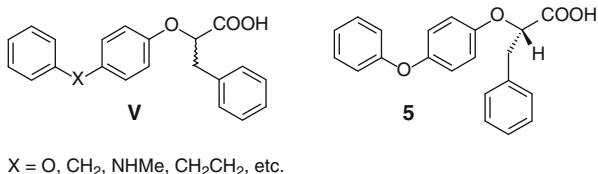


Fig. 3.4 X-Ray structures (a) of compound **4** bound to hPPAR α ; (b) bound to hPPAR γ (reproduced from [6] with the permission of Wiley-VCH Verlag GmbH & Co. KGaA)

Fig. 3.5 2-Aryloxy-3 phenyl propanoic acids **V** and lead compound (*S*)-**5**



The importance of the absolute configuration at the single stereogenic centre in **3** and **4** for their selective binding is evident from potency (EC_{50}) data. For enantiomers of **3**, EC_{50} values demonstrated that the *S*-enantiomer possesses significantly higher functional activity at α - and γ -receptors, and percentage activation data revealed that it behaves as a full agonist at both receptors [7]. The *R*-enantiomer of **4** proved to be almost inactive, as was also the case with the *R*-enantiomers of other tested compounds, thus confirming the importance of proper spatial orientation at the stereogenic centre in all agonists of this class [6].

3.2.3 α -Aryloxy- β -Phenyl Propionic Acids

Another example of dual PPAR α/γ agonists, namely, compounds with the general formula **V**, for which enantiomers with inverse spatial orientation demonstrated improved potency, is shown in Fig. 3.5.

These compounds belong to the class of α -aryloxy- β -phenyl propionic acids, the first dual PPAR inhibitors with an aryloxy group on the α -carbon in relation to the carboxylic group, represented by the lead compound, (*S*)-**5**.

The first report of the synthesis and activity of these compounds as PPAR agonists concerned the biphenyl derivative **6** (Fig. 3.6) and its congeners [9, 10]. The crystal structure and activity of the two enantiomeric forms of **6**, complexed with the ligand-binding domain (LBD) of PPAR γ , provided a molecular explanation for their different potency and efficacy. Docking of the *S*-**6** enantiomer in the PPAR γ -LBD was

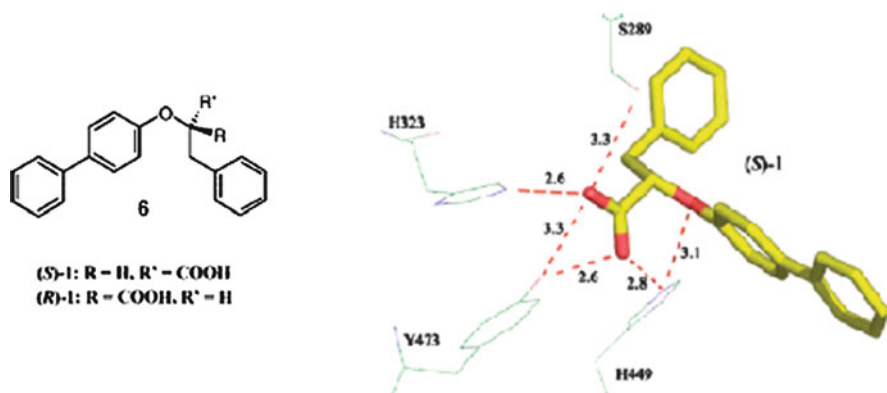


Fig. 3.6 Formula of **6**, and hydrogen bond networking of (*S*)-**6** in complex with PPAR γ (reproduced from [10], with the permission of the American Chemical Society)

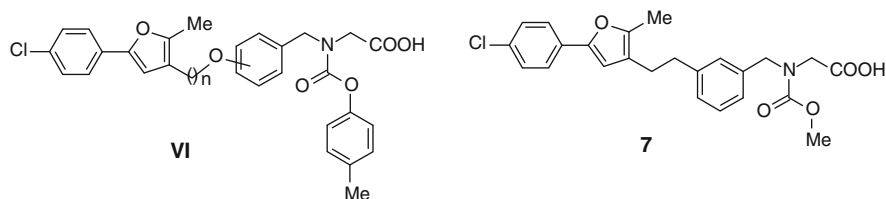
performed to examine its different sub-type pharmacological profile. Moreover, the structure of the complex with the *S*-enantiomer revealed a new binding region of the PPAR γ -LBD, not previously observed with other ligands.

The *S*-enantiomers of the 2-aryloxy derivatives **5** and **6** exhibited EC₅₀ values of 0.15 μ M and 0.22 μ M, respectively, on PPAR α , whereas in both cases, their *R*-enantiomers proved inactive at the tested concentrations [6–11].

Thus, compounds **5** and **6**, two lead molecules within the class of hPPAR 2-aryloxy-3-phenyl propionic acid agonists, exhibit opposite enantiopreference for compound **1**, the main object of our consideration in this chapter, which is also an 2-aryloxy-propionic acid derivative. Since, no details of the structure of the complex of **1** and the LBD of hPPARs were reported, it can be assumed that the absence of a phenyl group at position C(3) in **1** somehow results in inverse steric requirements for this agonist at LBD, when compared with its 3-phenyl congeners, **5** and **6**. Since, the route to enantiomerically pure (*R*)-**1** includes a number of original synthetic solutions, a detailed discussion of these is presented in later sections.

3.2.4 Oxybenzoylglycine Derivatives

Finally, a class of PPAR α selective agonists, the oxybenzoylglycine derivatives **VI**, was reported [12]. These compounds are characterized by replacement of the β -C atom, in relation to the carboxylic group, by an N-atom, and by varying the structure and position of the linker between the benzylic and heterocyclic unit.



These compounds were also studied by combining structural and molecular biological methods, and the hPPAR α selective lead compound **7** (BMS-687453) emerged from these studies. Its EC₅₀ was 10 nM for hPPAR α , and it exhibited 410-fold selectivity versus hPPAR γ . The X-ray co-crystal structure of **7**, in complex with PPAR α LBD, was also determined [12].

Intensive structural–biological activity relationship (SAR) programmes have been developed for PPAR agonists [13, 14] and (*R*)-**K-13675** (**1**) emerged as the lead from one of these projects [15]. Design of this and the related structures was based on the assumed interaction at the roughly Y-shaped binding site of PPAR α , expecting an interaction of the aromatic ring with the hydrophobic binding pocket, and of the carboxylic group with specific, basic amino acids [16].

In the next section, the synthetic highlights along the path to this lead structure and its analogues are described, in particular, non-hydrolytic, anomalous lactone ring opening, and stereo-uniform formation of the ether bond at the stereogenic centre through application of the Mitsunobu or Williamson-type reaction.

3.3 Non-hydrolytic Anomalous Lactone Ring-Opening

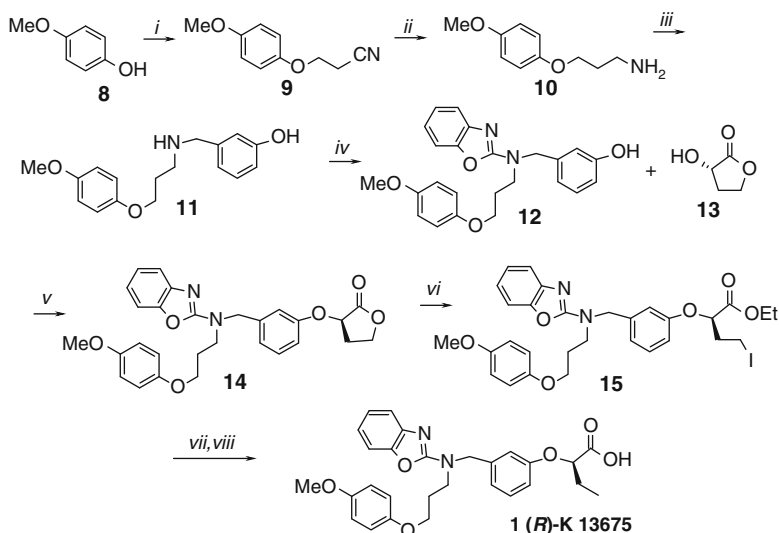
As stated in the introductory chapter, research towards a new drug entity (NDE) is a shuttle process, in which synthetic organic chemistry is often the initial step. As the research process advances, the targets and methods of synthetic organic chemistry are modified to deal with the increasing substance quantities required.

According to standard terminology, compound **1** is a *lead compound*, and following the internal company documentation system, defined by a code number. Inventive synthetic solutions leading to this target compound circumvent several obstacles posed by its specific structure. Compound **1** is characterized by the branches at the N-atom on C(2) of the benzoxazole ring and the aryl-alkyl ether bond, which links the chiral (*S*)-2-hydroxybutanoate unit at its stereogenic centre. The Y-shaped molecule of **1** has a hydrophobic aromatic unit at one end and a hydrophilic carboxylic group at the other. Reaction conditions and specific reagents for completion of the synthesis of (*R*)-**K-13675** (**1**) are presented in Scheme 3.1 [15].

The initial steps *i–iv* in Scheme 3.1 comprise standard C–O and C–N bond-forming reactions, enhancing the molecular complexity of the intermediates until Y-shaped **12** is obtained. Important synthetic events then follow these steps.

In the succeeding steps, we first encounter ether bond formation between **12** and **13**, at step *v*, which proceeds with inversion of the configuration at the stereogenic centre in the chiral building block **13**. Anomalous lactone ring opening in **14**, step *vi*, is a key step in the whole process and will be discussed in more detail. Hydrogenolysis of iodine in **15** leads to the (*S*)-2-hydroxybutanoate unit in the final product, **1**.

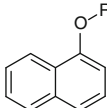
Step *vi* is particularly “obscure”. It is not apparent to the usual retrosynthetic analysis and requires the imagination of an experienced synthetic chemist. It is crucial to the synthetic direction, however, offering an elegant solution to the key



Reagents and conditions: *i*. Triton B, acrylonitrile; *ii*. BH_3 -THF, THF; *iii*. 3-hydroxybenzaldehyde, NaBH_4 , MeOH; *iv*. 2-chlorobenzoxazole, Et_3N , MeCN; *v*. DEAD, toluene, r.t.; *vi*. TMSI, EtOH, CHCl_3 ; *vii*. H_2 , 10% Pd/C, Et_3N , EtOH; *viii*. 4M NaOH, EtOH.

Scheme 3.1 Overall synthetic route to the anticholesterolemic agent **1**, (R)-K 13675

Table 3.1 Bond dissociation energies (BDE) for selected C–H, C–C and C–O bonds

BDE (C–O) ¹⁷	kcal/mol	BDE (C–H) ¹⁸	kcal/mol	BDE (O–R) ¹⁹	R	kcal/mol
$\text{CH}_3\text{O–COCH}_3$	97					
$\text{CH}_3\text{–OCH}_3$	81	H–C(OiPr, Me, Me)	93.9		–Me	61.6
$\text{CH}_3\text{–OH}$	91	H–C(COOEt, Me H)	95.6		– $\text{CH}_2\text{CH=CH}_2$	55.6
$\text{CH}_3\text{C(=O)–OH}$	106				– CH_2Ph	53.8
$\text{CH}_3\text{O–CH}_2\text{–CH}_3$	83.3					

step, the selective cleavage of the $\text{CH}_2\text{–O}$ ether bond in the presence of a C(=O)–O ester bond, generally considered to be easily cleaved.

In order to explain the rationale behind such regioselective bond cleavage, the reactivity of the two bonds under consideration must be taken into account. The reaction is governed by the inherent electronic properties of the bonds, their bond dissociation energies, and by the nature of the reacting partner. Table 3.1 summarizes the reported bond dissociation energies (BDE) for some C–H, C–C and C–O bonds relevant to this reaction.

The first set of data is taken from an earlier compilation, in which BDEs were correlated to IR stretching frequencies [17], the second set was estimated along with radical stabilization energies (RSE), determined by ESR spectroscopy [18], and the third set was determined by electrochemical reduction of naphthyl-alkyl

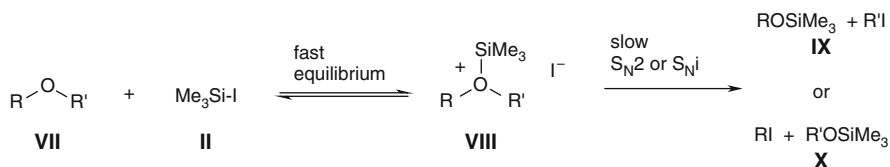
ethers [19]. They are instructive in that they reveal a high BDE for the C–O ether bond in esters and dialkyl ethers, comparable to that for the C–H bond, but significantly lower than the BDE in aryl-alkyl ethers. An additional property of the ether RCH₂–O bond is its relatively low polarization, in relation to the high polarity of the RC(=O)–O bond, due to the well-known stabilization of the acyl cation. Gas phase dissociation energies for CH₃COBr (151.1 kcal/mol^{–1}) and *tert*-BuBr (148.7 kcal/mol^{–1}) indicate that CH₃CO⁺ has comparable stability to that of the *tert*-butyl cation. Acyl cations are stabilized by a canonical form containing a triple bond R–C⁺=O ↔ R–C≡O⁺ and are linear; however, much of the positive charge is located on the carbon atom [20].

Polarization, charge distribution or atomic coefficients of the C–O bond are decisive for heterolytic bond splitting by nucleophiles [21]. Homolytic bond splitting, instead, is related to radical stability and reactivity, which in turn depends on spin density, spin polarization, delocalization of the free electron and hyperconjugation [22, 23]. Essential to all these radical reactions is the one-electron transfer from the trigger, typically under photochemical [24], (in the presence of sensitizer) [25], or electrochemical conditions [26].

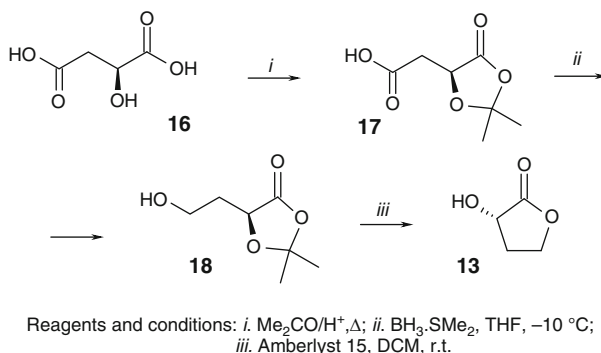
A closely similar reaction to radical-type splitting is the non-hydrolytic cleavage of the C–O ether bond in **VII**, promoted by organic molecules, such as trialkylsilyl iodides, which act as strongly oxophilic Lewis acids. Indeed, co-ordination of Lewis acids strongly polarizes ether C–O bonds, as exemplified by trimethyliodosylane (Scheme 3.2). A mixed mechanism may be operative in this reaction, whereby, after fast and reversible formation of silylated oxonium ion **VIII**, substitution by iodine anion occurs either by S_N2 or S_N1 (S_Ni) mechanisms. As a result alkyl iodides and silyl-alcohols **IX** and **X** are formed, depending on the susceptibility of the ether bond, or the nucleophilic properties of the R or R' group.

This scheme shows that specific knowledge of the preferred reactivity of the specific functionality, in the presence of the selected reaction partner, is needed in order to anticipate and design an “obscure” transformation, such as the “anomalous” splitting of the C–O bond in lactone **14**, which occurs at step *vi* in Scheme 3.1.

Since the lactone of 2-4-dihydroxybutyric acid **13** is easily available from L-malic acid **16** [27], the authors focussed on exploiting this chiral building block. In the initial phase of the project, they improved the preparation of **13**, according to Scheme 3.3, by eliminating TFA in the cyclization of **18–13** (step *iii*), which represents the major technical burden in large-scale production. The use of the



Scheme 3.2 Mechanism of non-hydrolytic cleavage of the ether C–O bond by trimethylsilyl iodide



Scheme 3.3 Large-scale production of (S)-2-hydroxybutyrolactone **13**

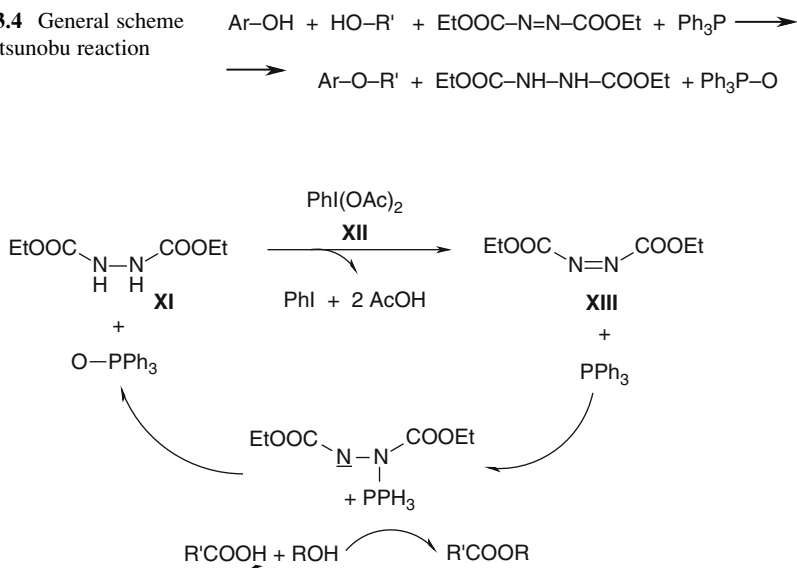
Amberlyst 15 resin in step *iii* provided lactone **13** in nearly 90% yield and >99% e.e., in other words, without loss of enantiomeric purity.

Having discussed the approach to the chiral building block **13**, we can now turn to the analysis of the overall Scheme 3.1. Whereas the steps from **8** to **12** in this scheme were achieved using standard protocols, formation of ether **14** required specific conditions. A coupling reaction between phenol **12** and derivatives of **13**, with the activated OH group as the mesylate or tosylate – one of the classic approaches to aryl-alkyl ethers [19, 28, 29] – resulted in unsatisfactory yields and significant loss of enantiomeric purity. This was due to base-catalyzed racemization, at the α-carbon relative to the lactone carbonyl group. To overcome this problem of racemization, the authors successfully applied the Mitsunobu reaction for direct coupling of phenol **12** and the non-activated alcohol **13**.

3.4 Mitsunobu Reaction in the Ether Bond Formation

The general scheme of the Mitsunobu reaction in the synthesis of aryl-alkyl ethers reveals the complexity of the reacting system (Scheme 3.4).

It illustrates the extremely low atom utilization or “atom economy”, usually expressed as the *E*-factor, of the process [30]. Quenching of 1 mol of water results in two large side-products, the hydrazodicarboxylic ester and triphenylphosphin-oxide. The Mitsunobu reaction requires two expensive reagents, a phosphine and a diazo ester. On the other hand, this is compensated for by the use of unmodified, weak nucleophiles phenol or carboxylic acid and an alcohol. The reaction product is difficult to separate from the excess of starting materials and reagents, and the reaction side-products. Despite this apparent lack of economy, the Mitsunobu reaction is popular in organic synthesis because of its scope, stereo-defined route and mild reaction conditions. Due to the large quantities of by products, the Mitsunobu reaction is also “famous for its separation headache” [31]. Numerous modified reagents and separation techniques have been developed to facilitate

Scheme 3.4 General scheme of the Mitsunobu reaction**Scheme 3.5** Organocatalytically promoted Mitsunobu-type esterification

isolation of the product. Among the most promising modifications of the Mitsunobu reaction is the use of polymeric phosphine reagents [32], and a reaction system in which both the required phosphine and azo reagents are attached to individual polymers [33].

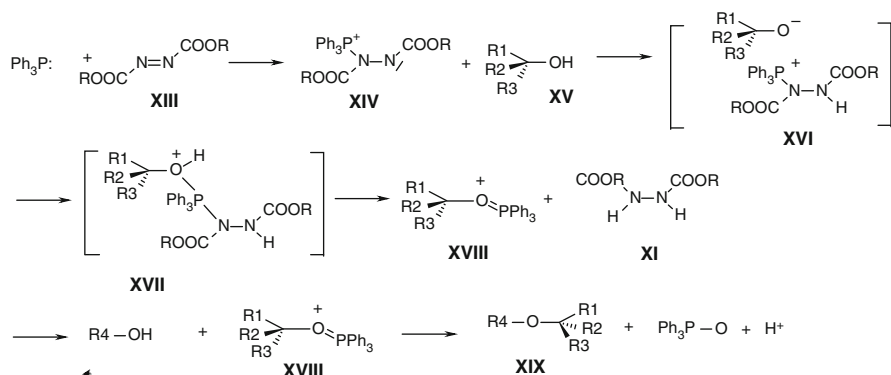
Recently, significant progress has been achieved by using an organocatalyst in the Mitsunobu-type esterification, according to the reaction cycle presented in Scheme 3.5 [34].

This reaction cycle is characterized by the use of hypervalent iodine species **XII** as the stoichiometric oxidant and a catalytic quantity, around 0.2 mol, of the oxidizing azo reagent **XIII**. The benefit of using **XII** is that the by-products, iodobenzene and acetic acid, are relatively simple to remove, while at the same time, the amount of hydrazine by-product **XI** formed is dramatically reduced. Under optimized conditions, the authors obtained aryl-carboxylic acid esters with chiral alcohols in 65% yield and with 100% e.e.

Mechanistic details and the stereochemistry of the Mitsunobu-type ether bond-forming reaction are given in Scheme 3.6.

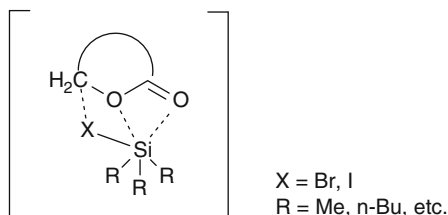
An important aspect of this unique ether-bond-forming reaction lies in the formation of the alkoxy-phosphonium cation **XVII** by the less acidic alcohol as the weak nucleophile, from which **XVIII** is obtained. In the next step, *inversion of configuration* occurs in **XVIII**, in attack on the stereogenic C-atom by alkoxide generated from the more acidic alcohol or phenol.

This mechanism also explains the *inversion of configuration* at the α -C-atom of lactone **14** in Scheme 3.1, and the formation of the open-chain intermediate **15**, with the (*R*)-configuration and 99% e.e. optical purity that is maintained in the final



Scheme 3.6 Mechanism and stereochemistry of the ether bond formation in the Mitsunobu reaction

Fig. 3.7 Schematic presentation of interactions in the $\text{R}_3\text{Si-X/lactone}$ complex

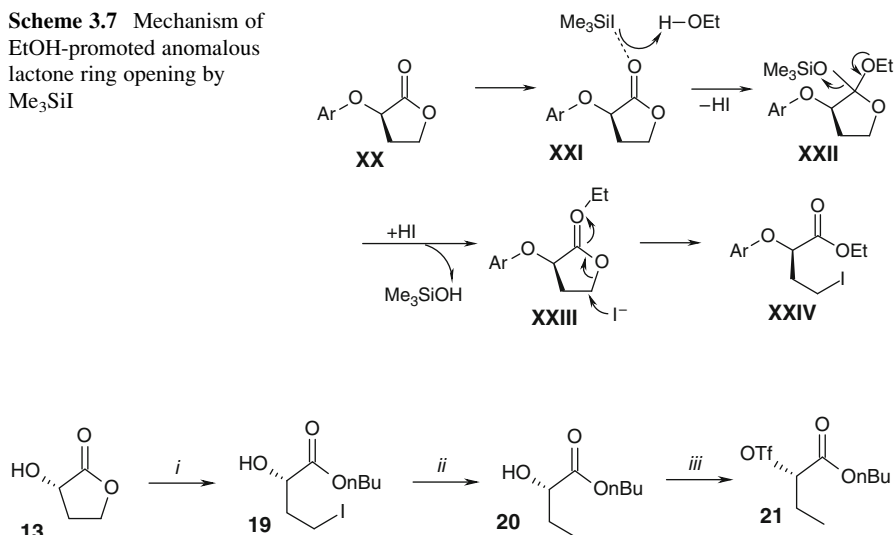


product. The authors improved the process by substituting polar solvents for toluene, keeping the reaction temperature at around 30°C , and by selecting diisopropyl azidocarboxylate (DIAD), as the coupling reagent. Under optimized conditions, 77% yield and 97% e.e. of **14** was obtained on a 0.5 kg scale. This protocol provided the key intermediate with high chemical and optical purity under controllable conditions.

In the next step, the anomalous ring opening of the lactone in **14** is achieved, more detailed discussion of which is given in Sect. 3.3. Splitting of the $\text{CH}_2\text{-O}$ bond to generate intermediate **15** was performed with iodotrimethylsilane [35]. Originally, it was assumed that this reagent effects ring opening of lactones via the cyclic transition state, in which carbonyl oxygen atom is complexed by silicon via the vacant d-orbitals (Fig. 3.7) [35].

However, using a standard protocol, the authors met with difficulties in completing this transformation, compound **15** was obtained in low yields after extended reaction times. Subsequent to a helpful discovery, the authors modified the protocol; using five equivalents of ethanol in chloroform at room temperature, significant improvement in the isolated yield of **15**, up to 97%, was achieved. Importantly, together with the ring opening of XXII, the carboxylic ester XXIV was formed, suggesting a new mechanistic path for lactone ring opening, as outlined in Scheme 3.7.

Scheme 3.7 Mechanism of EtOH-promoted anomalous lactone ring opening by Me₃SiI



Reagents and conditions: *i*. TMSI/*n*-BuOH, DCM, -20 °C, 1h, r.t., 3h; *ii*. 10% Pd/C-H₂, EtOH, r.t., 16h; *iii*. Tf₂O, 2,6-lutidine, DCM, -20 °C, 3h, 98%.

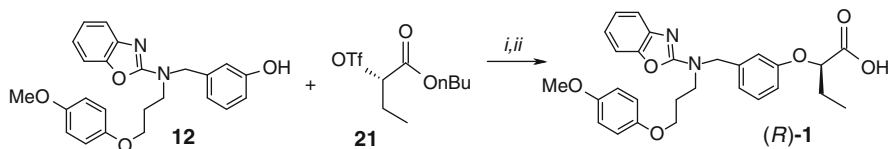
Scheme 3.8 Large-scale synthesis of triflate ester **21**

This tandem reaction proceeded at 20°C, whereas in the absence of alcohol, it required reflux conditions in acetonitrile [36].

In the penultimate step of Scheme 3.1, hydrogenolysis of **15** was carried out in the presence of triethylamine and 10% Pd/C, under hydrogen atmosphere, affording the intermediary ester in 99% yield. Since, at higher pressures, parallel hydrogenolysis of benzylic C–N bond and partial reduction of the benzoxazole unit occur, larger quantities of catalyst and *tert*-amine as the promoter were required. In the absence of *tert*-amine, hydrogenolysis of the C–I bond was hampered due to deactivation of the catalyst by the iodide ions generated. Finally, hydrolysis of the intermediary ester, under standard basic conditions, furnished target compound **1** in 90% yield, without observable racemization at the α-position and formation of the α-hydroxy carboxylic acid unit.

It is interesting to note that the inventors of (*R*)-**K-13675**, in the first reported synthetic approach, targeted the racemic compound **1**, and contracted separation of the enantiomers by preparative chiral chromatography to the expert company in this field, Diacel Chemical Industries Ltd. [37]. Continuing scale-up investigations, the authors succeeded in replacing the Mitsunobu method, in the ether bond-forming reaction, by the technically much more simple use of triflate **21**, prepared on a kg scale from (*S*)-*n*-butyl-2-hydroxybutanoate **20** (Scheme 3.8) [38].

In the final steps of the synthetic pathway, Williamson-type ether bond formation, with inversion of configuration at the stereogenic centre, followed by hydrolysis of the ester group, completed the large-scale production of (*R*)-**1** (Scheme 3.9) [38].



Reagents and conditions: *i.* $\text{K}_2\text{CO}_3/\text{MeCN}$, r.t., 22h; *ii.* 4M aq. NaOH/EtOH , r.t., 1.5 h, 75% (two steps).

Scheme 3.9 Improved large scale synthesis of (*R*)-1

3.5 Conclusion

In conclusion, the multistep synthesis of (*R*)-K-13975, presented here, is a typical example of improvement of the critical synthetic steps in new drug synthesis to provide robustness, i.e. reproducibility of the process, easy separation of the product, and the required high yield. This is always a challenge for the synthetic organic chemist when a structurally well-defined lead molecule emerges and a workable synthetic route is needed. In view of the expectation that lead compound (*R*)-1 would be required in multi-kilo quantities, the synthetic chemists developed a process, presented in this chapter, that meets many criteria for alternative scale-up.

References

1. Fruchart JC, Duriez P, Steals B (1999) *Curr Opin Lipidol* 10:245–248
2. Miyachi H (2005) *Expert Opin Ther Pat* 15:1521–1530
3. Wilson TM, Brown PJ, Sternbach DD, Henke BR (2000) *J Med Chem* 43:527–550
4. Casimiro-Garcia A, Bigge CF, Davis JA, Padalino T, Pulaski J, Ohren JF, McConnel P, Kane CD, Royer LJ, Stevens KA, Auerbach B, Collard W, McGregor C, Fakhouri S, Schaum RP, Zhou H (2008) *Bioorg Med Chem* 16:4883–4907
5. Casimiro-Garcia A, Bigge CF, Davis JA, Padalino T, Pulaski J, Ohren JF, McConnel P, Kane CD, Royer LJ, Stevens KA, Auerbach B, Collard W, McGregor C, Song K (2009) *Bioorg Med Chem* 17:7113–7125
6. Greter U, Benerdeau A, Benz J, Binggeli A, Blum D, Hilpert H, Kuhn B, Marki HP, Mayer M, Mohr P, Puntener K, Raab S, Ruf A, Schlatter D (2009) *ChemMedChem* 4:951–956
7. Benerdeau A, Benz J, Binggeli A, Blum D, Boehringer M, Greter U, Hilpert H, Kuhn B, Marki HP, Mayer M, Puntener K, Raab S, Ruf A, Schlatter D, Mohr P (2009) *Bioorg Med Chem Lett* 19:2468–2473
8. Cahn RS, Ingold CK, Prelog V (1966) Specification of molecular chirality. *Angew Chem Int Ed Engl* 5:385–415
9. Fracchiolla G, Laghezza A, Piemontese L, Tortorella P, Mazza F, Montanari R, Pochetti G, Lavecchia A, Novellino E, Pierino S, Camerino DC, Loiodice F (2009) *J Med Chem* 52:6382–6393
10. Montanari R, Saccoccia F, Scotti E, Crestani M, Godio C, Gilardi F, Loiodice F, Fracchiolla G, Laghezza A, Tortorella P, Lavecchia A, Novellino E, Mazza F, Aschi M, Pochetti G (2008) *J Med Chem* 51:7768–7776
11. Pinelli A, Godio C, Laghezza A, Mitro N, Fracchiolla G, Tortorella V, Lavecchia A, Novellino E, Fruchart JC, Staels B, Crestani M, Loiodice F (2008) *J Med Chem* 51:7768–7796

12. Li L et al (2010) *J Med Chem* 53:2854–2864
13. Brown PJ, Winegar DA, Plunket KD (1999) *J Med Chem* 42:3785–3788
14. Brown PJ, Stuart LW, Hurley KP, Lewis MC, Winegar DA, Wilson JG, Wilkison WO, Ittoop OR, Willson TM (2001) *Bioorg Med Chem Lett* 11:1225–1227
15. Yamazaki Y, Araki T, Koura M, Shibuya K (2008) *Synthesis* 7:1017–1022
16. Xy HE, Lambert MH, Montana VG, Plunket KD, Moore LB, Collins JL, Oplinger JA, Kliewer SA, Gampe RT Jr, McKee DD, Moore JT, Willson TM (2001) *Proc Natl Acad Sci USA* 98:13919–13924
17. Zavitsas AA (1987) *J Phys Chem* 91:5573–5577
18. Brocks JJ, Beckhaus H-D, Beckwith ALJ, Ruchardt C (1998) *J Org Chem* 63:1935–1943
19. Andrieux CP, Farriol M, Gallardo I, Marquet J (2002) *J Chem Soc Perkin Trans* 2:985–990
20. Katritzky AR, Burton RD, Shipkova PA, Qi M, Watson CH, Eyler JR (1998) *Perkin Trans* 2:835–840
21. Fish RH, Dupon JW (1988) *J Org Chem* 53:5230–5234
22. Ruchardt C, Beckhaus H-D (1985) *Top Curr Chem* 130:1–22
23. Tsang W (1996) In: Soames AM, Greenberg A, Liebman F (eds) *Energetics of organic free radicals*. Black Academic and Professional, London, pp 22–58
24. Pillai VNR (1987) *Organic photochemistry*, vol 9. Marcel Dekker Inc., New York
25. Pillai VNR (1980) *Synthesis*: 1–26.
26. Casado F, Pilano L, Farriol M, Gallardo I, Marguet J, Melloni G (2000) *J Org Chem* 65:322–331
27. White JD, Hrcnciar C (2000) *J Org Chem* 65:9129–9142
28. Fuhrmann E, Talbiersky J (2005) *Org Process Res Dev* 9:206–211
29. Ikunaka M (2008) *Org Process Res Dev* 12:698–709
30. Sheldon RA (2008) *Chem Commun*: 3352–3365
31. Dandapani S, Curran DP (2004) *Chem Eur J* 10:3130–3138
32. Choi MKW, Toy PH (2003) *J Org Chem* 68:9831–9834
33. Harned AM, He HS, Toy PH, Flynn DL, Hanson PR (2005) *J Am Chem Soc* 127:52–53
34. But TYS, Toy PH (2006) *J Am Chem Soc* 128:9636–9637
35. Kirsheldorf HR (1979) *Angew Chem Int Ed* 18:689–690
36. Olah GA, Narang SC, Gupta BGB, Malhotra R (1979) *J Org Chem* 44:1247–1251
37. Yamazuka Y, Abe K, Toma T, Nishikawa M, Ozawa H, Okuda A, Araki T, Oda S, Inoue K, Shibaya K, Steals B, Fruchart J-C (2007) *Bioorg Med Chem Lett* 17:4689–4693
38. Yamazaki Y, Araki T, Koura M, Shibuya K (2008) *Tetrahedron* 64:8155–8158

Chapter 4

Sitagliptin Phosphate Monohydrate

Abstract

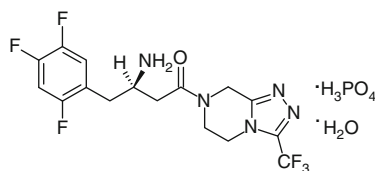
Biological target: Sitagliptin is a β -amino acid-derived inhibitor of dipeptidyl peptidase 4 (DPP4), a serine protease with membrane cell-signalling and soluble N-terminal proline peptidase activity. As a result, sitagliptin inhibits the in vivo degradation of the incretins, such as glucagon-like peptide-1 (GLP-1), which are endogenous glucoregulatory peptide hormones that regulate the production of insulin and blood glucose concentration.

Therapeutic profile: Sitagliptin is used in the treatment of type 2 diabetes mellitus.

Synthetic highlights: With C-acyl mevalonate as the *N*-acylating agent, a one-pot, three-component procedure was used for the preparation of the β -keto amide intermediate and complete stereoselectivity was achieved in conversion to the β -enamino amide. Highly enantioselective hydrogenation of the unprotected β -enamino amide was then developed using Josiphos-ligands. For large-scale production, ammonium chloride proved to be an effective promoter of catalytic enantioselective hydrogenation.

4.1 Introduction

Sitagliptin phosphate monohydrate (**1**, 7-[(3*R*)-3-amino-1-oxo-4-(2,4,5-trifluorophenyl)butyl]-5,6,7,8-tetrahydro-3-(trifluoromethyl)-1,2,4-triazolo[4,3-a]pyrazine phosphate monohydrate, *Januvia*[®]) is an oral hypoglycaemic drug, an inhibitor of the dipeptidyl peptidase-IV (DPP4) enzyme. It is widely used in the therapy of type 2 diabetes mellitus [1, 2].

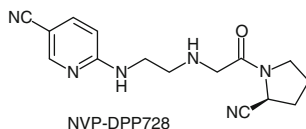


1 sitagliptin phosphate monohydrate

4.2 Endogenous Glucoregulatory Peptide Hormones and Dipeptidyl Peptidase IV (DPP4) Inhibitors

Glycaemic control is crucial in the therapy of type 2 diabetes mellitus. Physiologically, insulin, produced by the β -islet cells in the pancreas in response to an increase in blood glucose concentrations, facilitates the clearance of blood glucose, acting on specific insulin receptors to increase glucose uptake into the liver, muscle and fat cells and stimulating lipid metabolism. An important stimulus to this insulin production is provided by gastrointestinal hormones, such as gastrin, secretin and incretins. The incretins, *glucagon-like peptide-1* (GLP-1) and *gastric inhibitory peptide* (GIP), produced by the intestinal mucosa, stimulate insulin production by pancreatic β -cells after eating, even before blood glucose begins to rise [3]. GLP-1, as the active GLP-1 (7–36) amide, activates specific G-protein-coupled receptors. However, like GIP, GLP-1 is rapidly degraded in vivo to an inactive metabolite by a serine protease, dipeptidyl peptidase-4 (DPP4), also known as adenosine deaminase complexing protein 2 or CD26 [4]. DPP4 is a complex protein molecule that occurs either as a transmembrane or cell-anchored glycoprotein or as a soluble form in circulation. Both forms cleave X-proline dipeptides from the N-terminus of polypeptides. Substrates include many proline or alanine containing peptides, including growth factors, chemokines, neuropeptides and vasoactive peptides. Expressed on the surface of most cell types, as CD26, DPP4 mediates immune regulation, signal transduction and apoptosis.

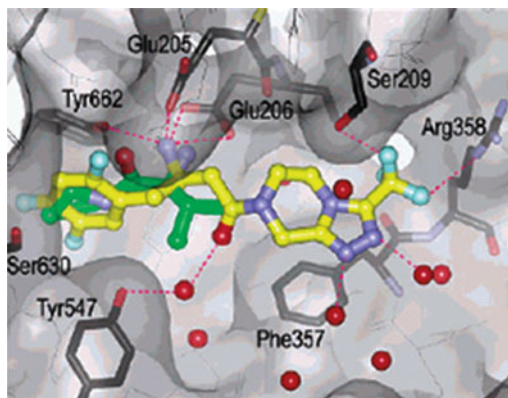
In view of the essential role of DPP4 in the control of GLP-1 activity and glucose homeostasis, it seemed an obvious step to search for small molecule inhibitors of DPP4, which would increase the half-life of active GLP-1 and prolong the glucoregulatory effect of this incretin. Several small molecule inhibitors of DPP4 were designed and have proved effective in preventing degradation of GLP-1 in vivo, lowering blood glucose in the first preclinical studies [5]. Subsequently, *proof-of-concept* (PoC) for the efficacy of DPP4 inhibitors as antidiabetic agents in humans was provided with NVP DPP728, a first-generation small molecule inhibitor [6].



The intensive research that followed resulted in several small molecule DPP4 inhibitors, which all improved glucose tolerance in diabetic patients. Inhibition of DPP4, thus, emerged as a new potential therapeutic approach to the treatment of type 2 diabetes [7].

Although many effective DPP4 inhibitors contain an α -amino acid moiety [8], the β -amino acid-based inhibitors proved to be the most interesting [9]. Sitagliptin phosphate monohydrate (**1**) is an outstanding representative of this latter group of DPP4 inhibitors.

Fig. 4.1 Sitagliptin (yellow) and valine-pyrrolidine (green), bound to DPP4. The interactions of sitagliptin with DPP4 (dotted lines) are discussed in the text (reproduced from [10], with the permission of the American Chemical Society)

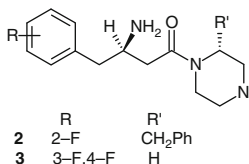


X-ray crystal structure determination shows that sitagliptin binds to the active site of DPP4, so that the amide moiety assumes the opposite orientation to that reported for *R*-amino acid-containing substrates and inhibitors (Fig. 4.1) [10]. The superimposition of compound **1** (yellow) and the substrate analogue, valine-pyrrolidine (green), demonstrates this opposing orientation of the amino carboxylic moiety in the two compounds. The 2,4,5-trifluorophenyl moiety fully occupies the S1 hydrophobic pocket, the (*R*)- β -amino group interacting with the side chains of a tyrosine (Tyr662) and two glutamate residues (Glu205 and Glu206) with a total of four hydrogen bonds. This interaction is analogous to the binding of the N-terminus of the substrate to DPP4 and is consistent with data showing that the (*S*)-enantiomer of **1** is much less potent; (*S*)-**1**, IC₅₀ 440 nM; (*R*)-**1**, IC₅₀ 18 nM. One water molecule bridges the carboxylic oxygen and the hydroxyl of Tyr547. Several other water-mediated interactions are also present between the nitrogen atoms of the triazolopyperazine unit and protein atoms. The pocket that accommodates the trifluoromethyl moiety in **1** is quite tight, and a significant loss in potency is observed when the trifluoromethyl is replaced by larger substituents [10, 11].

All these structural data on the interactions at the active site of DPP4 revealed (*R*)-**1** to be the champion in the design of potent inhibitors of this target protein. The most important aspects of the synthetic chemistry behind this biological achievement are presented in the next section.

4.3 Synthesis with C-acyl Meldrum's Acid as the *N*-Acylating Agent

Sitagliptin was discovered through optimization of β -amino acid-derived inhibitors of DPP4, particularly in relation to metabolic stability and the pharmacokinetic properties of its predecessors **2** and **3** [10].



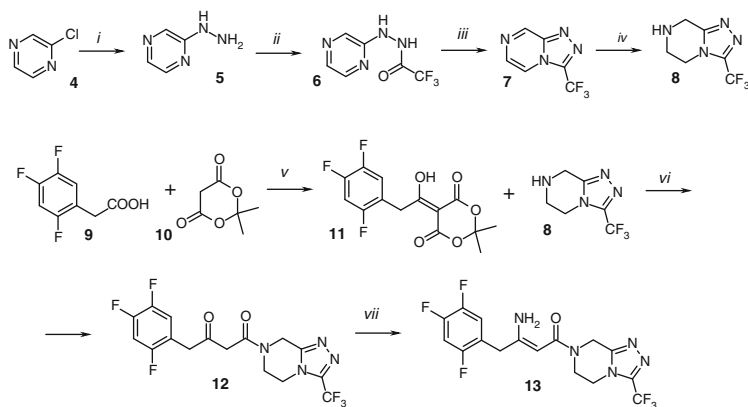
An aspect of this strategy consisted of the replacement of a piperazine moiety with a metabolically robust heterocycle, in particular, by constructing fused heterocycles. From the synthetic point of view, however, the most challenging task was the introduction of a stereogenic centre bearing the amino group in the *R*-absolute configuration. Here, we consider the critical aspects of the enantioselective hydrogenation of β -enamine precursors.

Exploration of the synthetic routes to sitagliptin reveals how catalytic asymmetric hydrogenation of unprotected β -enamides to enantiopure β -amino acid amides was discovered. First, we consider the whole synthetic route to the key precursor **13** (Scheme 4.1).

A plethora of inventive synthetic solutions are available for the specific steps presented in Scheme 4.1. We focus on those that appear to be the most interesting.

The approach to 3-trifluoromethyl-tetrahydro-1,2,4-triazolo-/4,3-*a*-pyrazine (3-trifluoromethyl-1,2,4-triazolo-piperazine), the heterocyclic portion of the sitagliptin molecule, requires construction of the annulated ring on 2-chloropyrazine **4** to yield the intermediate **7**. The latter is selectively hydrogenated in step *iv* to **8**, maintaining the five-membered heteroaromatic ring.

To complete this route to **13**, some unprecedented synthetic solutions were achieved. Starting from 2,4,5-trifluorophenylacetic acid (**9**) and Meldrum's acid (**10**),



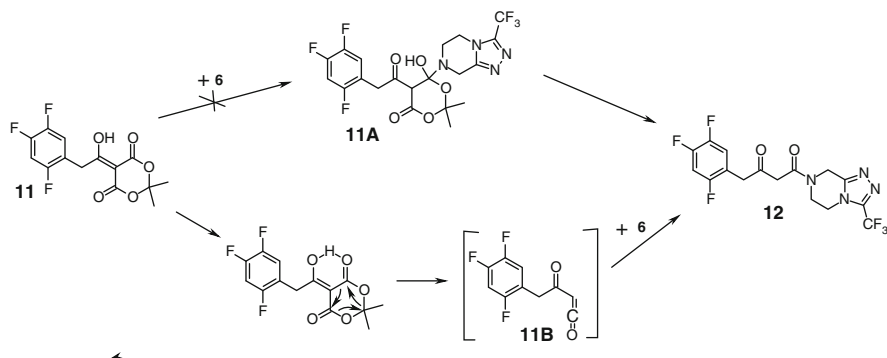
Reagents and conditions: *i*. Neat $\text{NH}_2\text{NH}_2 \cdot x\text{H}_2\text{O}$, 120 °C, 45 min; *ii*. $(\text{CF}_3\text{CO})_2\text{O}$, 0 °C, to r.t.; *iii*. PPA 140 °C, 18 h; *iv*. H_2 , 10% Pd/C, EtOH; *v*. PivCl, DMAP/IPEA + TFA, 50 °C; *vi*. **11**:**8**:IPEA (1:1:2 mol), 70 °C; *vii*. NH_3OAc , MeOH, reflux

Scheme 4.1 Synthetic route to the key precursor **13**

the tricarbonylic intermediate **11** was obtained in step *v* in 95% yield and with 97% conversion. This result required fine-tuning of the reaction conditions; 1.0 equivalent of pivaloyl chloride and 2.1 equivalents of IPEA were used to form the acyl chloride of **9**. This ratio proved sufficient to neutralize HCl and **11** (pK_a 3.1) was generated in this reaction. The tricarbonylic compound **11** is a hidden, or masked, 3-keto-carboxylic acid. On addition of 1 equivalent of triazole **8** as the hydrochloride, decarboxylation of **11** and acylation of **8** proceeded in the same pot; 98% conversion to **12** was achieved within 6 h at 70°C.

The chemical events in these last steps were carefully studied using physicochemical methods, online IR monitoring and kinetic measurements (Scheme 4.2). The detailed kinetic analysis offered mechanistic evidence for the intermediacy of α -oxoketene **11B** on the path to β -ketoamide **12**. This study has also ruled out other possible reaction pathways proposed in the literature, among them addition–elimination via aminoral **11A** [12]. Although intermediate **11B** was not directly observed, even when a special IR probe (Sicomp) was used, its presence is consistent with kinetic results that revealed the decarboxylation step to α -oxyketene **11B** as being rate-limiting. There was no accumulation of **11B** and its steady-state concentration was very low, since amination of ketene is a very fast reaction [13]. This accumulated knowledge suggested the possibility of merging steps *v* and *vi* into a one-pot, three-component procedure for the preparation of the β -keto amide **12** [14].

In step *vii*, the *Z*-isomer of the *N*-unsubstituted β -enamino amide **13** was obtained with complete stereoselectivity, presumably due to the strong hydrogen bonding in the product. This outcome had two important implications for the overall process. First, the unsubstituted β -enamine was clearly the targeted substrate for enantioselective hydrogenation, since all previous processes were based on the fact that the *N*-acyl derivatives required two additional steps, protection and de-protection. Second, the stereochemical homogeneity of the *Z*-isomer would be expected to confer a higher enantiomeric bias during hydrogenation than would a *Z/E* mixture of **13**.

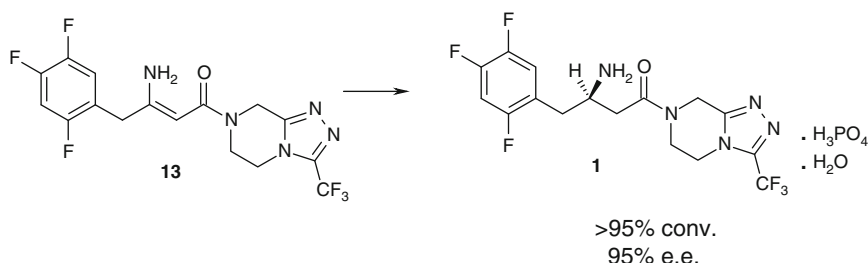


Scheme 4.2 Possible pathways in the formation of β -ketoamide **12** via Meldrum's acid adduct **11**

4.4 Highly Enantioselective Hydrogenation of Unprotected β -Enamino Amides and the Use of Josiphos-Ligands

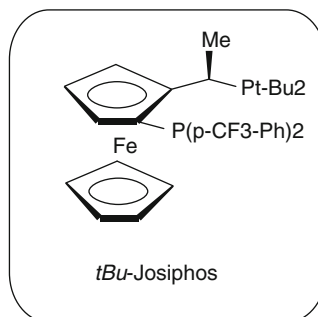
In view of the extensive application in the life sciences of β -amino acids, as components of biologically active peptides and small molecule pharmaceuticals [15], a great deal of research in organic synthesis has been focused on simple, practical and scalable methods for their preparation in an optically pure form [16, 17]. But, because of the obligatory use of *N*-acyl- β -enamines, on the one hand, and their fast equilibration into an *E/Z* mixture, on the other, their asymmetric hydrogenation failed, for a long period, to be utilizable in the large-scale preparation of enantiopure β -amino acids and their derivatives [18–20]. For this reason, in spite of its inherent efficiency and atom economy [20], catalytic asymmetric hydrogenation remained under-explored for the preparation of β -amino acids. A breakthrough was achieved when a method was discovered for the hydrogenation of the free β -enamine **13** [21, 22]. Contrary to the accepted opinion that the *N*-acyl group is a pre-requisite for effective hydrogenation, the authors successfully hydrogenated β -enamine **13** using a catalytic complex that co-ordinates enamine in the *Z* stereof orm.

The search for an effective catalytic metal–ligand complex started with the random screening of commercially available ligands [21, 22]. In a joint effort between the Catalysis Laboratory at Merck and Solvias AG, a company with world-renowned expertise in the field of asymmetric hydrogenation, the asymmetric hydrogenation of **13** was pushed to the limits of its performance. Dozens of ligands and additives were screened, along with the usual parameters such as solvent, temperature and pressure; the optimized reaction is depicted in Scheme 4.3 [22–24].



Optimized reaction conditions:

Catalyst: 0.15 mol% /Rh(COD)₂Cl/2
 0.32 mol% tBu-Josiphos
 Promoter: 0.30 mol% NH₄Cl
 Solvent: MeOH
 Temp., time: 50 °C, 18 h
 Pressure: 150 psig



Scheme 4.3 Optimized conditions for enantioselective hydrogenation of **13** to sitagliptin, *R*-**1**

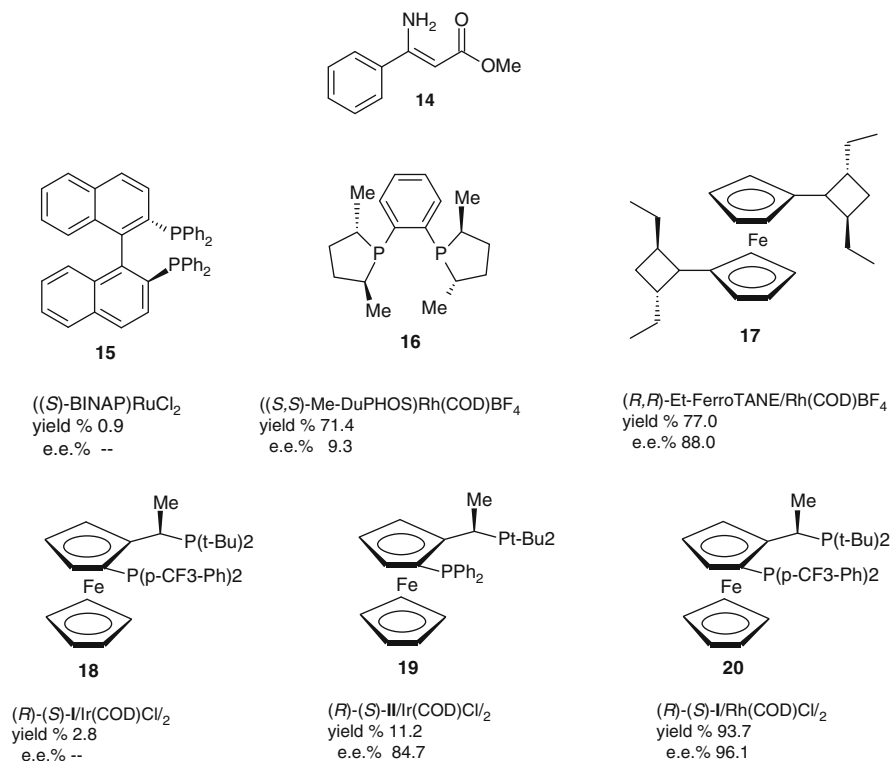
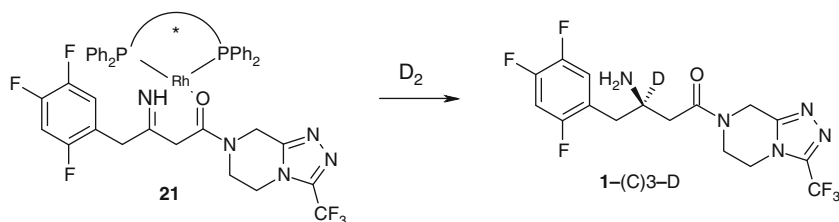


Fig. 4.2 Ligands tested in Ru, Rh and Ir complexes for enantioselective hydrogenation of enamino-ester **15**, and e.e.s obtained

The huge differences in yield and enantioselectivity achieved with some well-known and frequently used bidentate phosphines in screening experiments with the prochiral enamine substrate, methylester **14**, are remarkable (Fig. 4.2) [21].

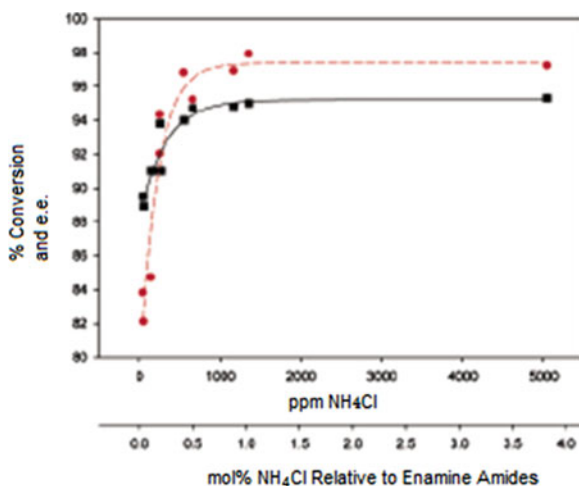
By far, the best results were obtained with Ir- and Rh-ferrocenophosphines **19** and **20**, which contain Josiphos-type, often cited as Solvias Josiphos ligands [23, 24]. Oddly, the Rh complex of the ligand **20** was highly reactive and selective in performing hydrogenation of ester **14**, while its Ir complex **18** proved to be non-selective. Mechanistic studies did not reveal the detailed structure of the catalytic complex, but the accumulated results reveal the intriguing possibility that the imino tautomer is the reactive species in the Rh complex **21** [21, 25].

When amide **13** was reduced in MeOH with D₂ using the catalyst [(COD)RhCl₂], incorporation of deuterium was observed only in the β -position (Scheme 4.4). This finding suggested **21** as the reactive complex, prior to the Rh-D insertion step, a mechanistically analogous situation to that with β -ketoamide hydrogenation [26].



Scheme 4.4 Site-selective incorporation of D-atom reveals the intermediacy of a reactive imino complex

Fig. 4.3 Hydrogenation of enamine amide batches of **13**, containing various amounts of ammonium chloride (● % conversion; ■ % e.e.) (reproduced from [27], with the permission of the American Chemical Society)



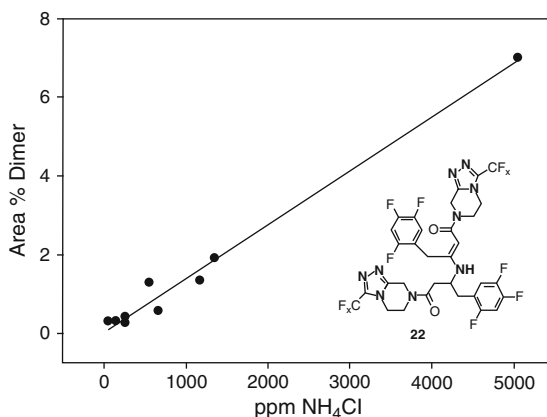
4.5 Ammonium Chloride, an Effective Promoter of Catalytic Enantioselective Hydrogenation

The final improvement in the hydrogenation step was achieved before the large-scale process was set up, enabling production of ~20,000 tons of sitagliptin by 2007 [22]. In Scheme 4.3, 0.3% of ammonium chloride is indicated as the promoter of asymmetric hydrogenation. A positive effect of the inorganic salt was observed when the significant variability in the e.e. and yield was traced to the content of this salt in the various batches of the β -enamine amide **13** [27].

In a separate experiment, a very strong correlation between the concentration of ammonium chloride (up to around 500 ppm), on the one hand, and e.e. and conversion, on the other, was observed (Fig. 4.3) [27].

Data shown by circles in the figure correspond to percent conversion, as measured by liquid chromatography (LC). Data points marked by squares correspond to percent enantiomeric excess, as measured by LC of the areas under the peaks for the *R*-enantiomer of sitagliptin free base. Since solutions of ammonium chloride are

Fig. 4.4 Levels of dimer-like product **22** observed with increasing concentrations of ammonium chloride in the hydrogenation solution (reproduced from [27], with the permission of the American Chemical Society)



weakly acidic, the authors concluded that the correlation between apparent pH and reaction performance may be due to the positive perturbation of enamine–imine tautomerization, so that the equilibrium is shifted in a subtle way to the imine form. The disappearance of the positive effect above 500–1,000 ppm was explained by the promotion of Michael-type addition, a side-reaction leading to the dimer-like by-product **22**. Figure 4.4 shows that if the amount of ammonium chloride present in the reaction is too high, the formation of a dimer-like **22** between enamine amide **13** and sitagliptin **1** reaches a level at which yield of sitagliptin is curtailed [27].

4.6 Conclusion

This study illustrates the fact that many variables, some of them unexpected, may influence a sensitive chemical transformation. When the reaction involved represents the key step in a production process, as shown for the enantioselective hydrogenation of **13** to sitagliptin **1**, optimization of the technological process requires the combined use of synthetic, analytical and physicochemical studies, often based on the serendipity and the imagination of the synthetic chemist.

References

1. Herman GA, Bergman A, Yi B, Kipnes M (2006) *Curr Med Res Opin* 10:1939–1947
2. Raz I, Hanefeld M, Xu L, Caria C, Williams-Herman D, Khatami H (2006) *Diabetologia* 49:2564–2571
3. Drucker DJ (2006) The biology of incretin hormones. *Cell Metab* 3:153–165
4. Kieffer TJ, McIntosh CHS, Pederson TA (1995) *Endocrinology* 136:3585–3596
5. Marguet D, Baggio L, Kobayashi T, Bernard A-M, Pierres M, Nielsen PF, Ribel U, Watanabe T, Drucker DJ, Wagtman N (2000) *Proc Natl Acad Sci USA* 97:6874–6879

6. Ahren B, Simonsson E, Larsson H, Landin-Olson M, Torgeirsson H, Jansson P-A, Sandquist M, Bavenholm P, Efendić S, Eriksson JW, Dickinson S, Holmes D (2002) *Diab Care* 25:869–875
7. Drucker DJ (2003) *Exp Opin Investig Drugs* 12:87–100
8. Magnin DR, Robl JA, Sulsky RB, Augeri DJ, Huang Y, Simpkins LM, Taunk PC, Betebener DA, Robertson JG, Abboa-Offei BE, Wang A, Cap M, Xin L, Tao L, Sitkoff DF, Malley MF, Gougoutas JZ, Khanna JZ, Huang Q, Han S, Parker RA, Hamann LG (2004) *J Med Chem* 47:2587–2593
9. Xu J, Ok HO, Gonzales EJ, Colwell LF Jr, Habulizah B, He H, Leiting B, Lyona KA, Marsilio F, Patel RA, Wu JK, Thornberry NA, Weber AE, Parmee ER (2004) *Bioorg Med Chem Lett* 14:4759–4762
10. Kim D, Wang L, Beconi M, Eiermann GJ, Fisher MH, He H, Hickey GJ, Kowalchick JE, Leiting B, Lyons K, Marsilio F, McCann ME, Patel RA, Petrov A, Scapin G, Patel SB, Roy RS, Wu JK, Wyvratt MJ, Zhang BB, Thornberry NA, Weber AE (2005) *J Med Chem* 48:141–151
11. Rasmussen HB, Branner S, Wiberg FC, Wagtmann N (2003) *Nat Struct Biol* 10:19–25
12. Svetlik J, Goljer I, Turecek F (1990) *J Chem Soc Perkin Trans* 1:1315–1318
13. Chang Y, Guo H-X, Kresge AJ, Tee OS (1996) *J Am Chem Soc* 118:3386–3391
14. Xu F, Armstrong JD III, Zhou GX, Simmons B, Hughes D, Ge Z, Grabowski EJJ (2004) *J Am Chem Soc* 126:13002–13009
15. Drey CN (1985) In: Barrett GC (eds) *Chemistry and biochemistry of the amino acids*, Chap. 3. Chapman and Hill, New York
16. Juaristi E (ed) (1996) *Enantioselective synthesis of β -amino acids*. Wiley-VCH, New York
17. Ma J-A (2003) *Angew Chem Int Ed* 42:4290–4299
18. You J, Drexler H, Zhang S, Fischer C, Heller D (2003) *Angew Chem Int Ed* 42:913–916
19. Drexler H, You J, Zhang S, Fischer C, Baumann W, Spannenberg A, Heller D (2003) *Org Proc Res Dev* 7:355–361
20. Cornelis B, Hermann WA (eds) (1996) *Applied homogeneous catalysis with organometallic compounds*, Vols 1 and 2. Wiley-VCH, NJ
21. Hsiao Y, Riviera NR, Rosner T, Kirska SW, Njolito E, Wang F, Sun Y, Armstrong JD III, Grabowski EJJ, Tillyer RD, Spindler F, Malan C (2004) *J Am Chem Soc* 126:9918–9919
22. Shultz CS, Kirska SW (2007) *Acc Chem Res* 40:1320–1326
23. Blaser H-U, Brieden W, Pugin B, Spindler F, Studer M, Togni A (2002) *Top Catal* 19:3–16
24. The reader may be interested in the origin of the name Josiphos. The inventors explain in ref. 20 that the name refers to the technician, Josi Pueblo, who prepared the first and highly selective ligand of this class!
25. Mohr JT, Krout MR, Stoltz BM (2008) *Nature* 455:323–332
26. Noyori R, Kitamura M, Ohkuma T (2004) *Proc Natl Acad Sci USA* 101:5356–5362
27. Clausen AW, Dziadul B, Capuccio L, Kaba M, Starbuck C, Hsiao Y, Dowling TM (2006) *Org Proc Res Dev* 10:723–726

Chapter 5

Biaryl Units in Valsartan and Vancomycin

Abstract

Biological target: Valsartan is a non-peptide, biaryl antagonist at the angiotensin II type 1 (AT1), G-protein-coupled receptor. It, therefore, blocks the stimulation of vasoconstriction, aldosterone release and salt retention by the kidney, leading to a fall in blood pressure.

Vancomycin is a glycopeptide antibiotic originally isolated from *Streptomyces orientalis*. It blocks the formation of the bacterial cell wall protein murein by forming a complex with D-alanyl-D-alanine.

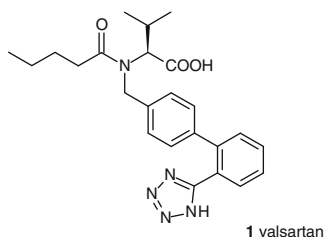
Therapeutic profile: Valsartan is a leading drug for the treatment of hypertension.

Vancomycin is a broad spectrum antibiotic, administered intravenously for the treatment of Gram-positive bacterial infections resistant to other antibacterials.

Synthetic highlights: The Cu-promoted catalytic decarboxylative, biaryl synthesis of valsartan is an example of biomimetic, aerobic decarboxylation and enables C–C bond formation in aqueous solution. The chiral variant of biaryl synthesis is exemplified by the stereoselective approach to the axially chiral biaryl system present in vancomycin.

5.1 Introduction

Valsartan (**1**, (*S*)-3-methyl-2-[*N*-(4-[2-(2*H*-1,2,3,4-tetrazol-5-yl) phenyl]phenyl)methyl]pentanamido]butanoic acid, generic name *Diovan*[®], Novartis) is a representative of a therapeutic class of non-peptidic angiotensin II-(AT1) receptor antagonists, the *sartans*, developed for the treatment of hypertension. With US \$4.2 billion global sales, valsartan holds the largest hypertension market share [1].



5.2 Angiotensin AT1 Receptor, a G-Protein-Coupled Receptor

Hypertension is the most prevalent disease in developed countries, with approximately one billion cases worldwide [2]. Various classes of antihypertensive agents have been introduced into therapy over the last 30–40 years. Yet hypertension remains an under-treated disease and a major health problem worldwide. Valsartan has become an outstanding representative of the angiotensin II type 1 (AT1) receptor antagonists, which are highly effective at reducing blood pressure and at the same time exhibit both renoprotective properties and placebo-like tolerability [3]. They, thus, provided a considerable advance over the earlier angiotensin converting enzyme inhibitors, which inhibited angiotensin II formation, but resulted in coughing due to the concomitant formation of the peptide mediator, bradykinin. The biological target of the newer antihypertensive drugs is the angiotensin AT1 receptor (see Fig 2.1, Chap. 2) that belongs to the largest human gene superfamily, the *G-protein-coupled receptors* (GPCRs) [4]. The GPCRs include around 30% of all drug targets so far investigated, and approximately 30% of all prescription drugs act on GPCRs [5].

The *renin-angiotensin-aldosterone system* (RAAS) is a proteolytic cascade of enzymes that plays an important role in the regulation of blood pressure, and is also involved in the pathogenesis of hypertension. The RAAS is initiated by the release of renin from the kidney, as discussed in Chap. 2 on aliskiren. Renin is responsible for the conversion of angiotensinogen to the inactive decapeptide, angiotensin I, which in turn is cleaved by *angiotensin-converting enzyme* (ACE) to produce the octapeptide, angiotensin II (AngII), the main effector hormone of the RAAS [6, 7]. AngII plays a key role in the pathophysiology of hypertension, and exerts most of its biological functions by activating selective membrane-bound receptors.

Two distinct types of AngII receptors have been identified; type 1 or AT1, and type 2 or AT2. AT1 is a 359-amino acid protein, while AT2 consists of 363 amino acids [8]. The AT1 receptor mediates virtually all known physiological actions of AngII in cardiovascular, neuronal, hepatic and some other cells, while the AT2 receptor appears to be a negative regulator. The interaction of AngII with the AT1 receptor induces a conformational change which activates several effector systems. This receptor is therefore the most direct biological target in the design of inhibitors of the RAAS system. The discovery of losartan and eprosartan, the first potent AngII antagonists, stimulated the design of a large number of their congeners, known as *sartans* [9, 10].

Knowledge of the 3D structure of the AT1 receptor would be of great help in studying receptor–antagonist interaction, as well as in the rationale design of new sartans as highly specific ligands. However, because GPCRs are membrane-bound proteins, their high-resolution structural characterization has still not been achieved. Recently, though, studies were performed to investigate the characteristics of the binding site of the human AT1 receptor, based on the construction of a homology model, to which various types of sartans were docked [11–13].

The structural features that determine the pharmacophoric segment of sartans have also been examined by combination of *quantitative structure-activity relationship* (QSAR) and conformational analysis. The results show that the site of action for sartans as AT1 antagonists include amino acids Lys199, Val108 and His256 located in the mesophase of membrane lipid bilayers [14].

The conformational properties of valsartan have been analyzed both in solution and at the binding site of the AT1 receptor. These studies revealed two low energy conformations of valsartan in solution, *cis/trans* around the amide bond in the ratio of approximately 40:60, while the majority of the docked molecules at the AT1 receptor are bound in the *trans* conformation [15]. A schematic presentation of some of the important interactions of valsartan with the AT1 receptor is given in Fig. 5.1 [16].

Figure 5.1 reveals the interactions between valsartan and Ser105, Ser109 and Lys199 in the AT1 receptor. In this conformation, Ser109 and Lys199 bind to the phenyl-tetrazole group of valsartan. Lys199 binds to the tetrazole group by an ionic H-bond and to the phenyl group by cation- π interaction. Ser109 binds to the phenyl group by OH- π interaction, and Ser105 is assumed to bind to the carboxylic group of valsartan at a distance of 2.9 Å. It is worth noting that the cation- π interaction of Lys199 and the OH- π interaction of Ser109, represent important contributions to the recognition of this small molecule at the protein binding site [17, 18]. All these data reveal the convergent interactions of valsartan at the active site, which contribute to the free energy of binding of -12.24 kcal/mol, and an inhibition constant of 1.06×10^{-9} [16]. On binding, valsartan stabilizes the AT1 receptor in a closed-up, inactive conformation (B), and the authors proposed for valsartan an inverse agonistic effect, emphasizing a more important role for this effect than was initially thought [16, 19].

A more recent molecular modelling study by the same authors, of the binding of valsartan and some other sartans, suggested the presence of binding sites in *transmembrane domains* (TM) 3, 5 and 7 of the AT1 receptor (Fig 5.2a) [20].

Within these three domains, the amino acids responsible for binding interactions are Ser109 of TM3, Lys199 of TM5 and Asn295 of TM7 in the AT1 receptor. Figure 5.2b illustrates these interactions in a 3D model, and in many details corresponds to the findings presented in Fig. 5.1. This is particularly the case with the conformation of the biphenyl unit in the bound valsartan; both models

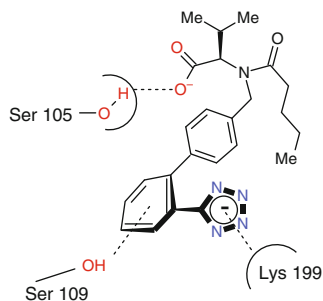


Fig. 5.1 Schematic presentation of interactions of valsartan in the preferred conformation within receptor AT1

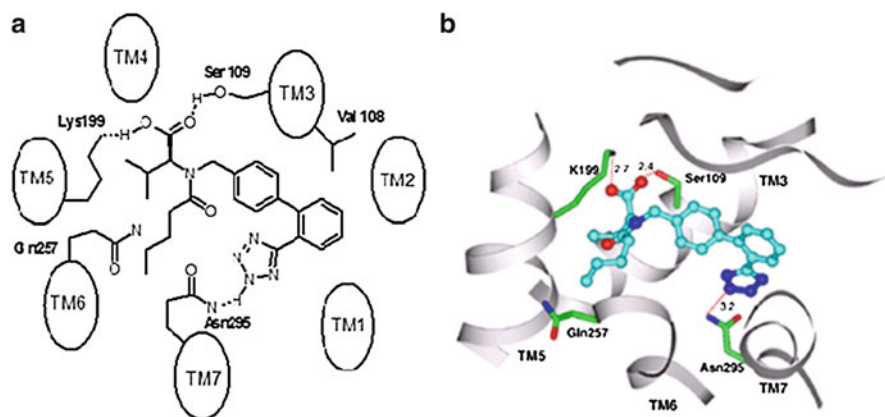


Fig. 5.2 (a) Scheme of binding of valsartan to the AT1 receptor. H-bonding is indicated by *dotted lines* and trans-membrane receptor domains by *ellipses*. (b) Lateral view of valsartan-AT1 (reproduced from [20] with the permission of Elsevier)

reveal the nearly orthogonal position of the two phenyl rings. However, while the tetrazole unit in the first model is exposed towards Lys199, in the second one, it forms a hydrogen bond with Asn295. The authors finally concluded that Lys199 is more important for the interaction with the carboxylate group and that the tetrazole moiety would commonly interact with Asn295 in TM7 [20].

These, sometimes ambiguous, considerations reveal the difficulties in constructing a substrate–enzyme complex at the active site without knowledge of the X-ray structure of the enzyme. In the case of GPCRs, as membrane-bound proteins, crystallographic data are not available, and therefore, modelling of the complex is based on the active-site structure obtained by homology modelling. In such cases, design of biologically more potent compounds might be less straightforward. Nevertheless, correlation for drug-like compounds of high biological activity with specificity and a concerted interaction at the binding site, as well as determination of requirements for the recognition of binding interactions is nowadays crucial for successful drug design. *Sartans* are one of the best examples of achievements in rational drug design.

In part, due to their prolonged therapeutic administration, antihypertensive drugs need to be essentially devoid of side effects. In this respect, it is of considerable interest that AT1 receptor blockade by valsartan reduces diabetogenic factors, including plasma free fatty acid levels by facilitating their uptake by adipocytes, as well as reducing inflammation and oxygen radical production. Therefore, valsartan not only attenuates hypertension but also reduces triggers to metabolic disturbances, which are risk factors for hypertension [21]. Combined therapeutic use of β -blockers, ACE inhibitors and valsartan mutually affects signalling through the β -adrenergic receptor and AT1 receptor in chronic heart failure [22]. However, there is no evidence that this translates into adverse effects on disease outcome.

Most of the beneficial effects provided by valsartan appear to be related to a complete blockade of the angiotensin AT1 receptor. The mechanisms for these beneficial effects of valsartan as an angiotensin II receptor blocker have been studied in model systems and in humans [23]. It was found that valsartan maintains glomerular filtration rate and glomerular pressure and it has been proposed that this might explain the favourable renal outcome with AT1 receptor blocker therapy [24].

5.3 Cu-Promoted Catalytic Decarboxylative Biaryl Synthesis, a Biomimetic Type Aerobic Decarboxylation

The stereogenic centre in valsartan has the *S*-configuration and is introduced with L-valine as the building block. However, the formation of the aryl–aryl bond represents the key step in the synthesis of many *sartans*. The biphenyl unit in valsartan **1** and other *sartans* is a common structural element, and proved to be essential for binding affinity to the receptor and for oral bioavailability. When the barrier for rotation around the central bond is high enough, axially chiral enantiomers can be separated. Some examples of biologically active compounds, intended to illustrate the significance of the biaryl structural motif, are presented in Fig. 5.3.

In addition to the two *sartans*, losartan and telmisartan, a biaryl unit is present in the agrochemical, boscalid; the antibiotic, biphenomycin; and many natural axially chiral polyhydroxy-biphenyls and binaphthyls. Two examples are given in Fig. 5.3. Due to the impeded rotation around the central bond, the last two compounds are configurationally stable.

In recent years, classical methods for biaryl syntheses have been replaced almost completely by mild and selective organometallic complex-catalyzed coupling reactions.

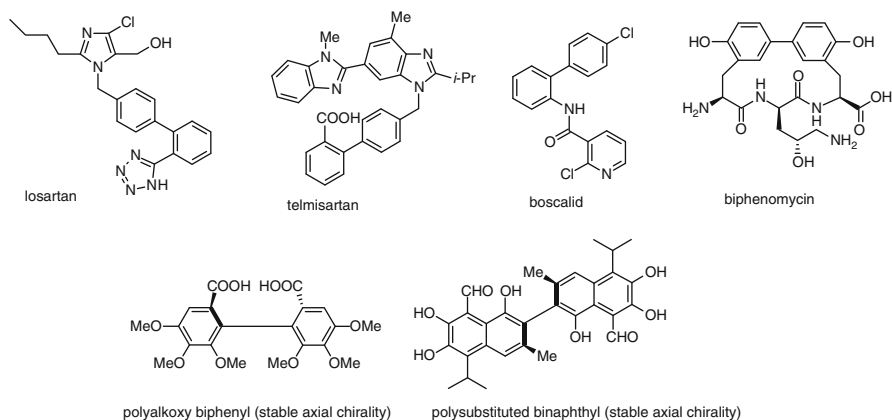


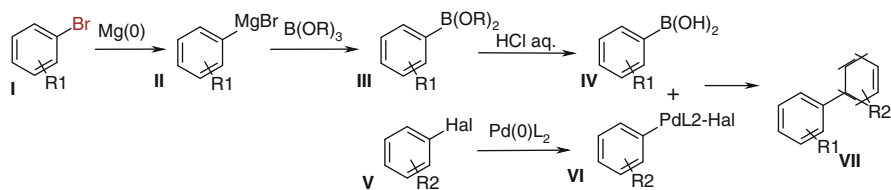
Fig. 5.3 Representative biologically active compounds with a biaryl unit

Among the well-known traditional synthetic approaches to biphenyl derivatives are, first of all, Ullmann-type coupling [25], then the Scholl reaction [26], the Gomberg–Bachmann reaction [27, 28] and their modifications. All of these suffer from the harsh reaction conditions and low yields of unsymmetrically substituted biaryls, making impractical any approach to biaryls with chemically or configurationally sensitive units. Accumulated physicochemical data and mechanistic considerations have revealed that these methods are ineffective at lowering the energy barrier *to synthesis of aryl-carbanion equivalents as nucleophiles*. An effective solution to this problem was found in the mild and catalytic cross-coupling reactions promoted by organometallic species, such as organo-copper, -zinc, -tin and -magnesium complexes [29, 30]. Nowadays, these reactions constitute a generally applicable strategy for the synthesis of biaryls. They all have in common facilitated insertion of metal into the aryl–halide bond as a step towards synthesis of the active complex. This activation of the nucleophile is a key step, while an electrophilic partner is selected to match the electronic requirements of the nucleophile.

A particularly effective and selective method for coupling to biaryls, with the general formula **VII**, is referred to as the Suzuki–Miyaura reaction (Scheme 5.1) [31].

This method consists of coupling of arylboronic acids **IV** with aryl halides **V**, activated as Pd-complexes **VI**. It has been improved continuously over the last decade, and has reached a high level of performance, both on the laboratory and industrial scale [32, 33]. However, even the Suzuki–Miyaura reaction suffers from a drawback common to all cross-coupling reactions; it requires stoichiometric amounts of expensive organometallic compound, in this specific case, arylboronic acid **III**. This reagent must be prepared from sensitive Grignard-type precursor **II** under anaerobic and anhydrous conditions. To achieve such couplings on an industrial scale, formation of the organometallic partner became the most serious issue, as observed in the production of a boscalide intermediate (~1,000 t/a), one of the largest industrial applications of the Suzuki–Miyaura reaction [34, 35] (cf. Sect. 5.4).

Recently, the synthetic breakthrough in this field came only from the work of Goossen and his group [36, 37]. These authors started with an imaginative concept, based on the observation that living organisms, which cannot provide an inert and dry environment, have evolved to generate carbanion equivalents by *enzymatic decarboxylation in aqueous medium* of ubiquitously available arylcarboxylic acids. Bearing this in mind, Goossen et al. designed an efficient catalytic system with a dual capability: to facilitate strongly endothermic extrusion of carbon dioxide



Scheme 5.1 General scheme of the Suzuki–Miyaura reaction

from aryl carboxylates, forming stable aryl–metal compounds, and to mediate cross-coupling of these species with Pd(II) complexes as aryl electrophiles.

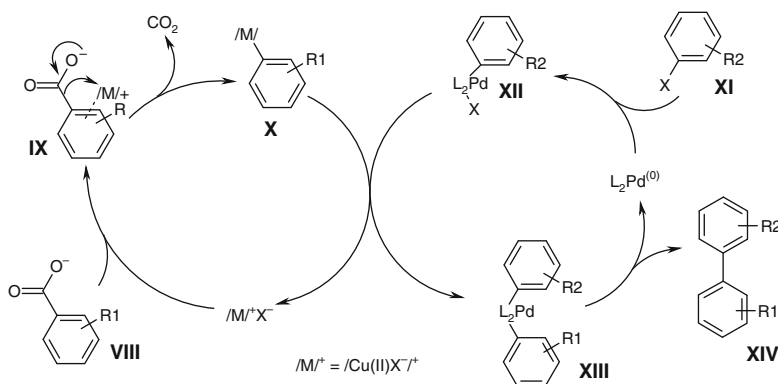
The proposed reaction mechanism of this catalytic process is outlined in Scheme 5.2 [38].

Copper was selected as the metal of choice for the decarboxylation step, **IX** to **X**, as it is widely used in protodecarboxylation procedures [39]. However, taking into account the known, limited catalyst productivity and selectivity of copper in Ullmann-type coupling [25], the authors decided to use a second metal for the cross-coupling step. Here, palladium turned out to be the best choice, as it is known for efficient mediation of a large number of two-electron cross-coupling reactions [40].

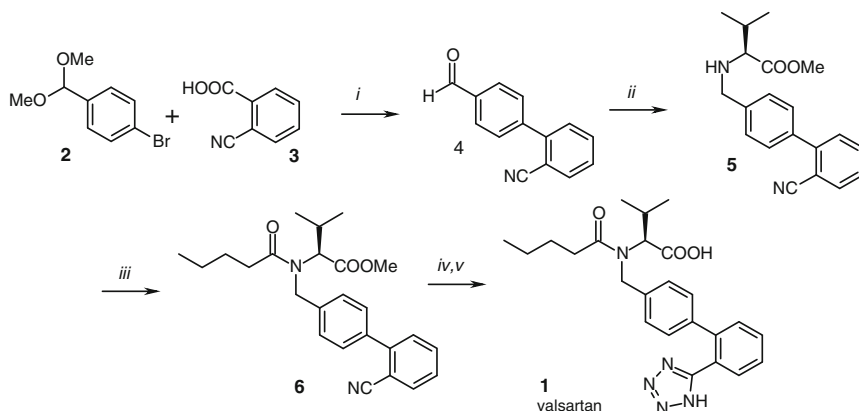
In the left cycle of Scheme 5.2, anion exchange takes place and the Cu(II) ion in the intermediate **IX** is believed to co-ordinate to the aromatic π -system. Then, the Cu ion inserts into the C–C(O) bond with extrusion of CO₂, and shifts to the aryl π -system to form the stable aryl–copper intermediate **X**. In the parallel cycle, aryl halide **XI** adds oxidatively to the palladium catalyst to form the Pd(II)aryl complex **XII**. In the next step, an exciting interplay between two catalytic cycles takes place, resulting in transmetalation to the intermediate **XIII**, that is, transfer of the aryl group from copper to palladium with liberation of the Cu(II) halide. Reductive elimination, in the final step, affords the targeted biaryl **XIV**, regenerating the initial Pd(0) species and restoring the catalytic cycle for palladium. The reaction of copper halide with fresh alkali metal carboxylate, through anion exchange, closes the catalytic cycle for copper.

Synthesis of valsartan represents one of the synthetic highlights on the basis of this methodology, and is outlined in Scheme 5.3 [41].

This apparently simple synthetic route has some hidden pitfalls. Already in the first step, decarboxylative metallation of 2-cyano benzoic acid (**3**), an extremely resistant substrate due to competing co-ordination of cyano group to copper, has the required catalytic system consisting of Cu(II)O and 1,10-phenantroline as bidentate N,N-ligand for Cu(II) ions. This catalytic system proved particularly effective in the specific solvent mixture NMP/quinoline (2:1). Yields of **4** up to 80% were



Scheme 5.2 Coupled catalytic cycles in Goossen et al's synthesis of biaryls



Reagents and conditions: *i*. 15% CuO, ca. 10 mol% of phenanthroline, 2% PdBr₂, NMP/quinoline as solv.; *ii*. NaCNBH₄, L-valine-OMe; *iii*. *n*-BuCOCl/pyridine; *iv*. NaN₃, TBAB, *n*-Bu₃SnCl, *v*. 55% NaOH[−]

Scheme 5.3 Synthesis of valsartan, based on decarboxylative biaryl synthesis

obtained at elevated temperatures without observable formation of side-products. Note the sensitive dimethylacetal unit in **2**. Whereas reductive amination of **4–5** proceeded under standard conditions with a 90% yield, another obstacle appeared in the last step – formation of the tetrazole ring in **1** from the intermediate **6**. 1,3-Dipolar addition of azide anion to aryl nitrile **6** proved troublesome until the authors surmounted the limited reactivity of tri-*n*-butyl-tin chloride and sodium azide by adding tetra-*n*-butylammonium bromide. The mechanistic rationale behind this promotional effect of quaternary ammonium bromide was not explained by the authors. It may reside in the promoted formation of *n*-Bu₃Sn-N₃ via more reactive *n*-Bu₃Sn-Br, formed in equilibrium with initial tin chloride.

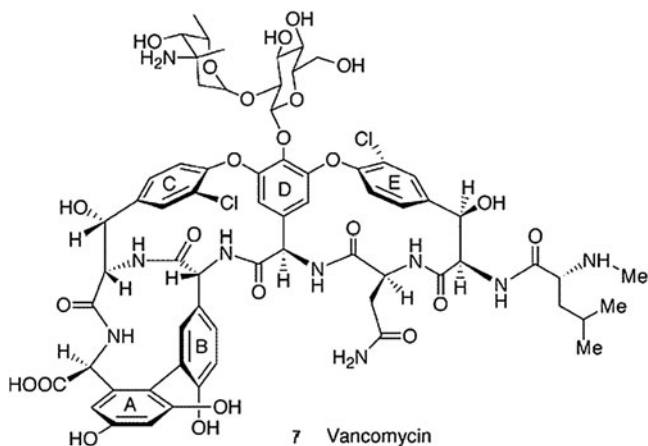
In conclusion, an innovative route to valsartan that comprises *decarboxylative biaryl coupling* afforded this antihypertensive drug in approximately 40% overall yield, which compares favourably with all other reported routes. This approach was the result of meticulous synthetic experimental work. Professor Goosen stated that at the beginning of the project, one of his collaborators had “performed close to 2000 test runs for the model reaction... before he observed the desired product in more than trace quantities” [42]. The route to the “dream reaction” was extensively explored by Goosen’s group. Fine-tuning of many parameters in the Cu(II)-catalyzed decarboxylative biaryl synthesis was performed [38, 41] and the final results were impressive

- Biaryl synthesis can be achieved with activated and non-activated aryl-carboxylic acids, using second-generation catalysts, based on the Cu(II) 1,10-phenanthroline complex.
- Direct coupling of various aryl, heteroaryl and vinyl carboxylic acids with aryl iodides, bromides and even chlorides is possible.

- The scope and potential economic impact of this decarboxylative biaryl coupling is demonstrated by the synthesis of over 40 biaryls, some of them with substantial industrial relevance.

5.4 Stereoselective Approach to the Axially Chiral Biaryl System; the Case of Vancomycin

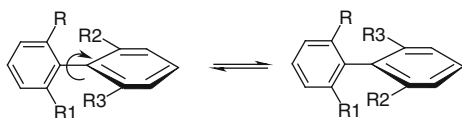
As mentioned in the introduction, optically pure biaryl derivatives are present in a number of natural products of various origins and have a wide range of biological properties [43]. By far, the most important representative of biologically active compounds with axially chiral biaryl unit is vancomycin (7), a clinically used glycopeptide antibiotic from *Streptomyces orientalis* [44].



Vancomycin is a broad spectrum antibacterial, which acts to inhibit the construction of the bacterial cell wall by forming a complex with D-alanyl-D-alanine, required for the synthesis of an essential membrane protein, murein. The antibiotic is administered by infusion and is most commonly used to treat infections with organisms that are resistant to other commonly used antibacterials. Today, this is frequently the case with Gram-positive bacteria such as *Staphylococcus aureus*.

Axial chirality of biaryls, also known as the *atropisomerism phenomenon*, arises from hindered rotation around the central single bond (Scheme 5.4).

Scheme 5.4 Schematic presentation of atropisomerism; equilibrium between enantiomeric biaryls



Configurational stability is usually ensured by the presence of at least two bulky substituents in the *ortho* positions [45].

As creative as coupling to biaryls based on catalytic decarboxylation in aqueous solution may appear, no report has yet appeared on its application to obtain *axially chiral biaryls in the enantiopure form*. This chapter therefore would be incomplete without a brief discussion of selected synthetic methods leading to enantiomerically pure biaryls.

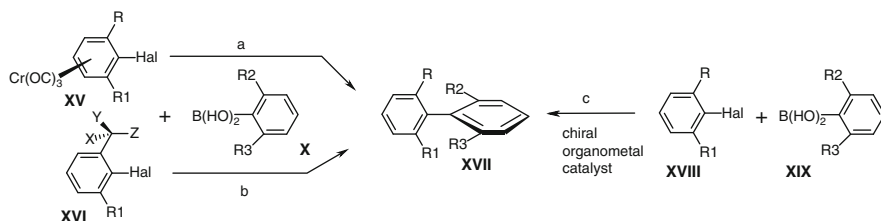
Total syntheses of vancomycin aglycone have been reported by outstanding synthetic teams [46–48], all of whom encountered stereoselective construction of the axially chiral A-B biaryl ring system as an essential problem. One of the most efficient solutions to this problem was reported by Uemura et al. [49–51], and comprises the use of a planar chiral arene chromium complex in the Suzuki–Miyaura cross-coupling reaction.

Before embarking on a more detailed discussion of this approach, let us first consider other chiral variants of the Suzuki–Miyaura reaction in the synthetic approach to enantiopure biaryls **XVII** (Scheme 5.5).

In spite of some of the drawbacks mentioned in Sect. 5.3 of this chapter, the Suzuki–Miyaura reaction is certainly the most widely used method for stereoselective construction of the central bond in biaryls. This method can be classified into diastereoselective (*a* and *b*) or enantioselective (*c*) variants (Scheme 5.5). The former two characterize chiral information present in one of the reacting partners, **XV** or **XVI**. In case *a*, this involves planar-to-axial induction of chirality from **XV** to **XVII**, while in case *b*, central-to-axial chirality is induced from **XVI** to **XVII**. The enantioselective method *c* involves two achiral partners **XVIII** and **XIX**, while the chiral ligand in the palladium complex contributes chiral information to the reacting system.

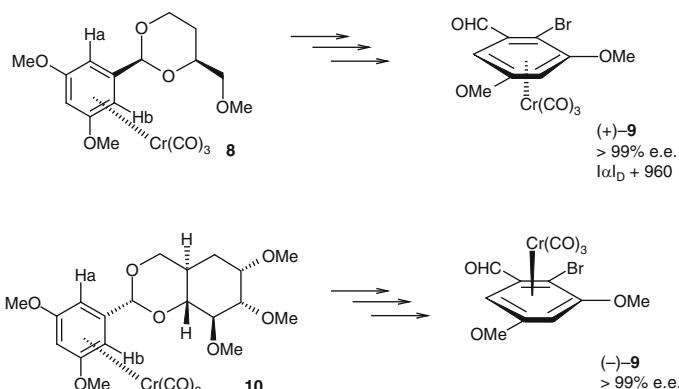
In elucidating a synthetic pathway to enantiopure biaryl **14**, the key intermediate on the pathway to vancomycin, Uemura et al developed a powerful diastereoselective approach, corresponding to method *a* in Scheme 5.5. The most important aspects of this approach are presented in Schemes 5.6 and 5.7 [49–51].

Scheme 5.6 outlines the stereoselective approach to the enantiopure, planar chiral key intermediates, 2-bromo-3,5-dimethoxy-benzaldehyde $\text{Cr}(\text{CO})_3$ complexes (+)-**9** and (–)-**9**, as planar chiral coupling partners [50]. The elegance of

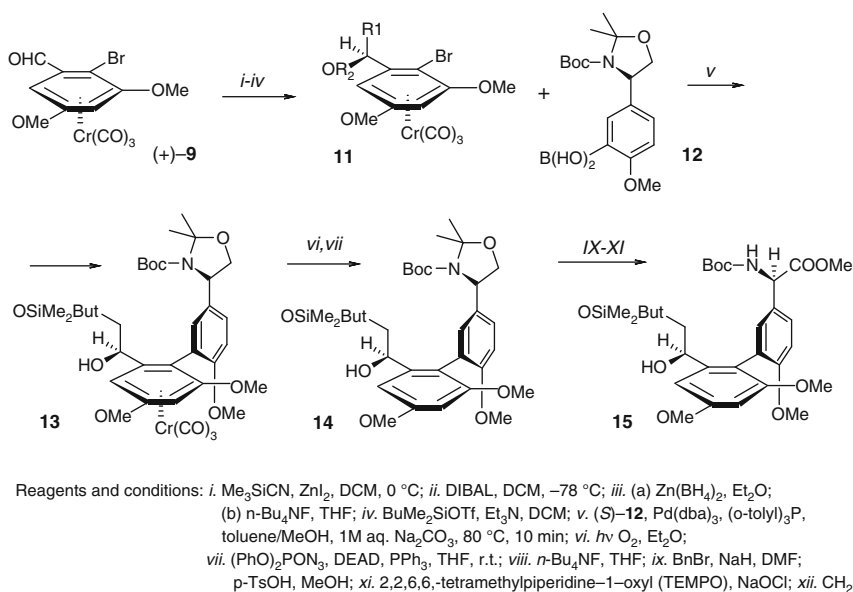


Stereoselective modes of Suzuki–Miyura coupling: *a* and *b* diastereoselective, *c* enantioselective

Scheme 5.5 Alternative variants of Suzuki–Miyaura reaction



Scheme 5.6 Initial steps in Uemura's route to the biaryl system of vancomycin



Scheme 5.7 Final steps in Uemura's route to the biaryl unit in vancomycin

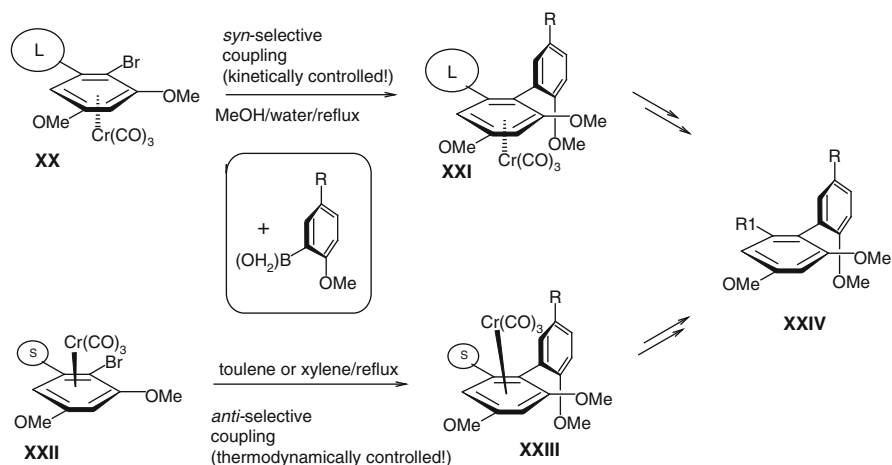
this approach resides in the transfer of centro-chirality in the intermediary acetals **8** and **10** to planar chirality in (+)-**9** and (-)-**9**, respectively. Acetals **8** and **10** are derived from (*S*)-1,2,4-butanetriol and α -D-glucopyranoside, respectively. Transfer to planar chirality of bromo-aldehyde **9** is completed by diastereoselective *ortho*-lithiation and subsequent bromination. In the lithiation step, two diastereotopic protons H_a and H_b in **8** and **10**, respectively, are removed and the resulting Li complexes of aryl carbanions are brominated.

The enantiomerically pure chromium complex **13**, with the correct absolute (*S*)-configuration around the central bond, has been used in the construction of **15**, one of the key chiral building blocks in vancomycin (Scheme 5.7).

This multi-step scheme illustrates the synthetic efforts that have been invested in the construction of homochiral biaryl **15** without loss of enantiomeric purity. It covers many significant modern synthetic reactions: diastereoselective cyanation, of the carbonyl group in (+)-**9** in step *i*, promoted by *anti*-orientation of the carbonyl oxygen to the *ortho*-substituent as the result of a stereoelectronic effect [52]; oxidative removal of the $\text{Cr}(\text{CO})_3$ group in **13** (step *vi*) and stereoselective azidation with inversion of the configuration (step *vii*). For more details, the interested reader should consult the cited literature.

In summary, the chiral economic and, at the same time, aesthetic aspect of Uemura's process, consisting of the dual control of stereoselectivity, is outlined in Scheme 5.8.

The planar chiral tricarbonyl(2,6-disubstituted bromobenzene)chromium complex **XX** can be coupled with the *ortho*-substituted phenylboronic acid derivative, either under kinetic or under thermodynamic control. The former can be achieved in refluxing aqueous methanol, and leads to a *syn*-relationship between the bulky tricarbonylchromium group and the *ortho*-methoxy group in **XXI**. Completing the same reaction in a higher boiling solvent, for example, toluene or xylene, or heating of the *syn*-product in a higher boiling solvent, causes isomerization to the thermodynamically stable *anti*-isomer **XXIII**. Most importantly, axial chirality in both the *syn*- and *anti*-product has the same configuration. This has great practical consequence on elimination of the tricarbonylchromium group, both coupling products can be converted to an identical vancomycin precursor with the general formula **XXIV**.



Scheme 5.8 Overall scheme of Uemura's approach to synthesis of the key biaryl intermediate of vancomycin

5.5 Conclusion

Axially chiral diaryls are a ubiquitous structural motif and frequently targeted intermediates in the multi-step synthetic approach to natural products and their congeners. The therapeutic importance of these compounds has been rediscovered recently and some new heuristic concepts have emerged [53, 54].

References

1. Novartis Annual Report 2006 (2007) Novartis Int. AG, Basel (CH)
2. US Department of Health and Human Services, National Heart, Lung and Blood Institute (2003) NIH Publication No. 03-5233, December
3. Smith DHG (2008) Comparison of angiotensin II type 1 receptor antagonists in the treatment of essential hypertension. *Drugs* 68:1207–1225
4. Hopkins AL, Groom CL (2001) *Nat. Rev Drug Discov* 1:727–730
5. Klabunde T, Hessler G (2002) *Chem BioChem* 3:928–944
6. Unger T (2002) *Am J Cardiol* 89(suppl 3A):310
7. Norris K, Vaughn C (2003) *Exp Rev Cardiovasc Ther* 1:51–63
8. Taccinardi T, Calderone V, Rappelli S, Martinelli A (2006) *J Med Chem* 49:4305–4316
9. Wexler RR, Greenlee WJ, Irvin JD, Goldberg MR, Prendergast K, Smith RD, Timmermans PB (1996) *J Med Chem* 39:626–656
10. Balsamo A, Calderone V, Rapposelli S (2008) *Cardiovasc & Hematol Agents in Med Chem* 6:1–10
11. Koenig AJ (2006) Signal reception: G-protein coupled receptors. In: Davies RW, Morris BJ (eds) *Molecular biology of the neuron*, 2nd edn. Oxford University Press, Oxford, pp 215–248
12. Zoumpoulakis P, Mavromoustakos T (2005) *Drug Des Rev-Online* 2:537–545
13. Cappelli A, Mohr GP, Giuliani G, Galeazzi S, Anzini M, Mennuni L, Ferrari F, Makovec F, Kleinrath EM, Langer T, Valoti M, Giorgi G, Vomero S (2006) *J Med Chem* 49:6451–6464
14. Zoumpoulakis P, Mavromoustakos T (2005) *Drug Des Rev-Online* 2:537–545
15. Potamitis C, Zervou M, Katsiaras V, Zoumpoulakis P, Durdagi S, Papadopoulos MG, Hayes JM, Golic S, Kyrikou I, Argyropoulos D, Vatougia G, Mavromoustakos T (2009) *J Chem Inf Modeling* 49:726–739
16. Miura S, Kiya Y, Kanazawa T, Imaizumi S, Fujino M, Matsuo Y, Karnik SD, Saku K (2007) *Mol Endocrinol* 22:139–146
17. Sulpizi M, Carloni P (2000) *J Phys Chem* 104:10087–10091
18. Zacharias N, Dougherty DA (2002) *Trends Pharmacol Sci* 23:281–287
19. Miura S, Fujino M, Hanazawa H, Kiya Y, Imaizumi S, Matsuo Y, Tomita S, Uehara Y, Karnik SS, Yanagasiwa H, Koike H, Komuro I, Saku K (2006) *J Biol Chem* 281:19288–19295
20. Bhuiyan MA, Ishiguro M, Hossain M, Nakamura T, Ozaki M, Miura S, Nagatomo T (2009) *Life Sci* 85:136–140
21. Leiter LA, Lewanczuk RZ (2005) *Am J Hypertens* 18:121–128
22. Anzai T, Yoshikawa T (2005) *Cardiac Practice* 18:29–36
23. Yasunari K, Maeda K, Nakamura M, Watanabe T, Yoshikawa J, Hirohashi K (2005) *Curr Med Chem Cardiovasc Hematol Agents* 3:61–67
24. Epstein M, Hollenberg NK (2004) *Am J Hypertens* 17:638–639
25. Hassan J, Sevignon M, Gozzi C, Schulz E, Lemaire M (2002) *Chem Rev* 102:1359–1469
26. Kovacic P, Jones MB (1987) *Chem Rev* 87:357–379
27. Gomberg M, Bachmann WE (1941) *Org Synth* 1:113
28. Driggers EM, Hale SP, Lee J, Terrett NK (2008) *Nature Rev* 7:608–624

29. Kumada M (1980) *Pure Appl Chem* 52:669–679
30. Diederich F, Stang P (eds) (1998) *Metal-catalyzed cross-coupling reactions*. Wiley-VCH, Weinheim
31. Miyaura N, Suzuki A (1995) *Chem Rev* 95:2457–2483
32. Mareen AR (2004) *Chem Eng News* 82:49–58
33. Billingsley KL, Anderson KW, Buchwald SL (2006) *Angew Chem Int Ed* 45:3484–3488
34. Kotha S, Lahiri K, Kashinath D (2002) *Tetrahedron* 48:9633–9695
35. Barder TE, Walker SD, Martinelli JR (2005) *J Am Chem Soc* 127:4685–4696
36. Goossen LJ, Deng G, Levy LM (2006) *Science* 313:662–664
37. LJ Goossen, G Deng (2005), PCT DE 2006-001014
38. Goosen LJ, Rodriguez N, Melzer B, Linder C, Deng G, Levy LM (2007) *J Am Chem Soc* 129:4824–4833
39. Smith BM, March J (1992) *Advanced organic chemistry*, 4th edn. Wiley, New York, pp 563–564
40. Liao C-Y, Chan K-T, Tu C-Y, Chang Y-W, Hu C-H (2009) *Chemistry* 15:405–417
41. Goosen LJ, Melzer B (2007) *J Org Chem* 72:7473–7476
42. Synform (2007), 6; A64–A66
43. Bringmann G, Gunther G, Ochse M, Schupp O, Tasler S (2001) In: Herz W, Falk H, Kirby GW, Moore RE, Tamm C (eds) *Progress in the chemistry of organic natural products*, Vol 82. Springer, New York, pp. 1–249
44. Pope SD, Roecker AM (2007) *Expert opin pharmacother* 8:1245–1261
45. Bringmann G, Mortimer AJP, Keller PA, Gresser MJ, Garner J, Breuning M (2005) *Angew Chem Int Ed* 44:5384–5427
46. Evans DA, Dinsmore CJ, Watson PS, Wood MR, Richardson TI, Trotter BW, Katz JL (1998) *Angew Chem Int Ed* 37:2704–2708
47. Nicolaou KC, Mitchell HJ, Nareshkumar JF, Winssinger N, Hughes R, Bando T (1999) *Angew Chem Int Ed* 38:240–244
48. LH Thoresen, K Burgess (2003) *Organic Synth Highlights V*; 297–306
49. Watanabe T, Shakadou M, Uemura M (1999) *Inorg Chem Acta* 296:80–85
50. Kamikawa K, Uemura M (2000) *Synlett*; 938–949
51. Kamikawa K, Tachibana A, Sugimoto S, Uemura M (2001) *Org Lett* 3:2033–2036
52. Solladie-Cavallo A (1989) In: Liebeskind LS (ed) *Advances in metal-organic chemistry*, vol 1. JAI, Greenwich, CT, pp 99–133
53. Ganesan A (2008) *Curr Opin Chem Biol* 12:306–312
54. Bolton R, Williams GH (1986) *Chem Soc Rev* 15:261–289

Chapter 6

3-Amino-1,4-Benzodiazepines

Abstract

Biological target: 3-Substituted 1,4-benzodiazepine-2-one (1,4-BZD) molecules are privileged structures, in that minor changes can produce a wide variety of biological actions. 1,4-BZD drugs have been developed that target a variety of biological ligands. Here, four exemplary 3-amino substituted structures are discussed, three of which inhibit γ -secretase, an enzyme that cleaves amyloid precursor protein (APP) to form amyloid- β -peptide (A β) deposits in the brain of Alzheimer's patients. The fourth, 1,4-BZD, L-768,673, is a potassium channel inhibitor that delays the initiation of the cardiac action potential.

Therapeutic profile: γ -Secretase inhibitors are recently identified candidate molecules for use in the therapy of Alzheimer's disease. Potassium channel blockers are under investigation for several indications; L-768,673 is a potential anti-arrhythmic agent.

Synthetic highlights: Racemization and enantiomerization are two consequences of configurational instability. Enantiomerically enriched 3-amino-1,4-BZDs have been generated via crystallization-induced asymmetric transformation. Enantiomerically pure target products have been obtained by asymmetric Ireland–Claisen rearrangement, highly enantioselective rearrangement of prochiral allylic esters to 1,2-disubstituted carboxylic acids and hydroboration of the terminal C=C bond, an efficient anti-Markovnikov hydration process.

6.1 Introduction

3-Substituted 1,4-benzodiazepine-2-ones (1,4-BZDs) have been extensively investigated as structural scaffolds for drug development. They represent the prototypical “privileged structure”, according to which *minor changes in structure produce a host of different pharmacological profiles* [1, 2]. Figure 6.1 shows some representative 1,4-BZD structures, their respective biological targets and their therapeutic profiles.

In this chapter, we discuss the design and synthesis of four representative lead compounds **1–4**, which are excellent examples of the pharmacological diversity

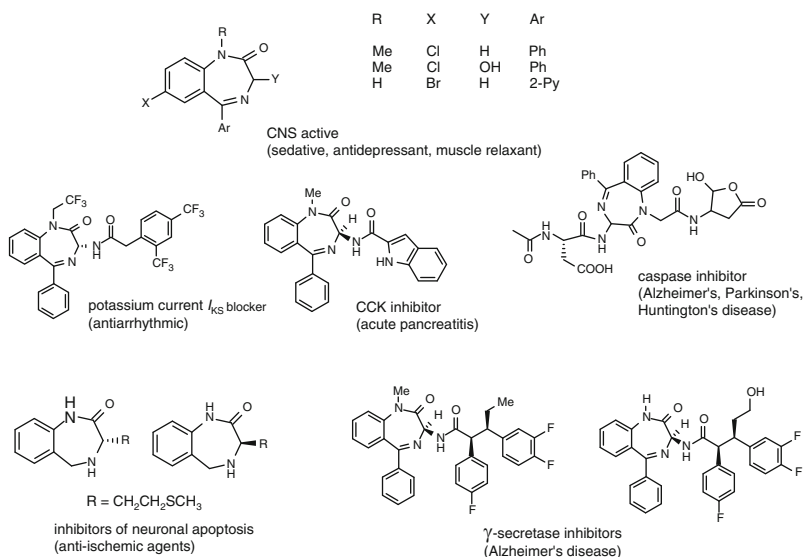
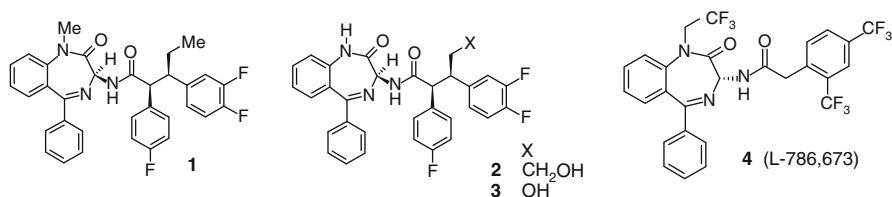


Fig. 6.1 Selected 1,4-BZD structures, their biological targets and therapeutic profiles

among 3-amino-1,4-BZDs. The first three compounds **1–3** exhibit γ -secretase inhibiting activity, while compound **4**, an anti-arrhythmic drug candidate, is an inhibitor of the slowly activating delayed rectifier potassium channel.



6.2 3-Amino-1,4-Benzodiazepine Derivatives as γ -Secretase Inhibitors

Alzheimer's disease (AD) is a progressive neurodegenerative disorder, which over a period of time leads to dementia, of which it is the most common cause, accounting for 60–70% of cases. The disease is associated with an as yet unexplained build-up of extracellular proteins in the brain, including so-called tangles (deposits of the protein, tau) and plaques, formed by deposits of the amyloid- β peptide ($\text{A}\beta$) [3, 4]. This peptide, in its soluble form or when aggregated into

oligomers, fibrils and plaques, is responsible for neuronal toxicity and cell death [5]. A β is produced by the stepwise cleavage of natural proteins by the membrane enzyme β -secretase.

γ -Secretase is a complex of four different structural proteins and a non-essential regulatory protein, CD147. It is an integral membrane protease that cleaves a variety of transmembrane proteins, including amyloid precursor protein (APP) and the biologically broadly distributed membrane signalling protein, Notch. Substrate recognition by the enzyme occurs by binding of the N-terminus of the substrate to one of the four sub-units, nicastrin. The substrate is transferred to a water-containing active site, containing the catalytic aspartate residue, and which carries out hydrolytic cleavage within the hydrophobic environment of the cell membrane. The active site is flexible, since the enzyme is able to cleave APP at multiple locations to generate several A β peptide isoforms, 39–42 amino acids in length. γ -Secretase is, therefore, an attractive target for development of novel synthetic inhibitory drugs with potential for the treatment of AD and several small molecule drug candidates are under investigation [6, 7]. Undesirable side effects are an issue, probably because the enzyme hydrolyses a variety of functional proteins. Very recently, a γ -secretase activating protein has been identified, which only stimulates A β formation, suggesting a possible new approach to selective inhibition of A β production [8].

6.3 Configurational Stability: Racemization and Enantiomerization

Configurational or optical stability is crucial for any chiral compound intended as a drug substance. In view of the different behaviour of enantiomers in a chiral environment, which is regularly present in all compartments of the living organism, the requirement for optical stability is obvious. It is important to note that the chiral environment in biological fluids, either intra- or extracellularly, is generated by the presence of soluble chiral molecules. Insoluble, chiral biopolymers and cell constituents facilitate chiral recognition at the solid–liquid interface.

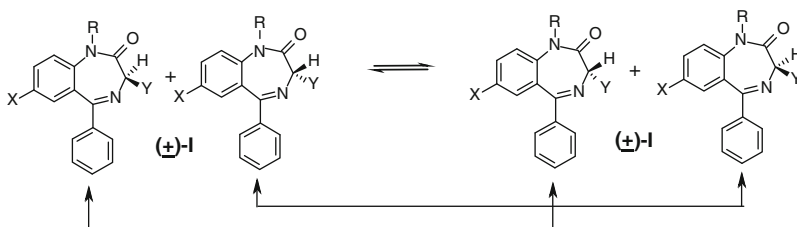
Racemization of an optically active compound is a well-known thermodynamically favourable process that forms a racemic mixture. Racemization is a consequence of the limited configurational stability of the stereogenic centre in chiral compounds. This process can be followed using various chiral methods that allow the determination of the time-dependent ratio of two enantiomers. The most frequently used methods are polarimetry and liquid chromatography (LC) gas chromatography (GC) on chiral stationary phases (CSPs). The importance of the CSP-based chromatography in supplying the required data is clearly emphasized in the policy statement of the US Food and Drug Administration (FDA). This world-leading agency demands unambiguous data on the configurational stability or “stereochemical integrity” of pure enantiomers of chiral drugs and examination of the “potential for the interconversion of the individual isomers” [9].

Enantiomerization is another, less known consequence of low configurational stability, and represents interconversion of two enantiomers in a racemic mixture. Generally, enantiomers of 3-substituted 1,4-benzodiazepines **I**, present in a racemic mixture, may easily interconvert (Scheme 6.1).

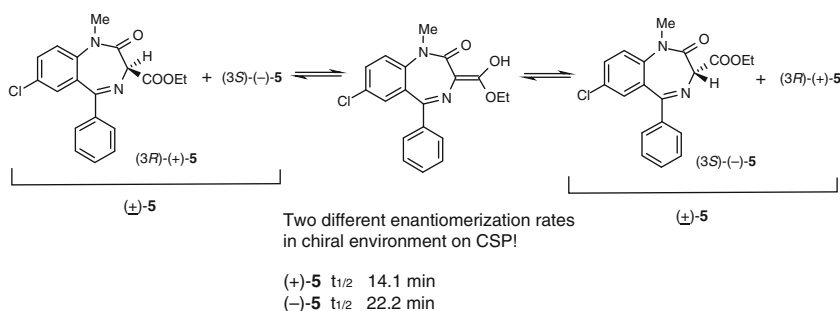
Thermodynamic control of the 1:1 ratio of enantiomers in the racemic mixture does not preclude, however, interconversion of the enantiomers at a defined rate, which can be monitored by chiral means [10, 11]. The most efficient method for determination of kinetic parameters of enantiomerization is chromatography on CSPs. When a racemic mixture of configurationally unstable enantiomers is eluted on CSP and separation into two well-defined peaks is achieved, a change in the chromatographic conditions (e.g. the chemical property of the CSP, flow rate, pH of the eluant or temperature) can provoke substantial changes in the elution profile. This means that originally well-separated peaks become less well separated, then form a plateau, and finally collapse into one peak. Using either simple equations or sophisticated programmes, kinetic and thermodynamic parameters for enantiomerization can be determined to various degrees of accuracy [12, 13].

This process is exemplified by enantiomerization of the 3-carbethoxy-1,4-benzodiazepine derivative **5** (Scheme 6.2) [14].

Enantiomerization is promoted by the basic groups on the CSP and at a defined flow rate, with first-order kinetics and a $t_{1/2}$ of approximately 14 and 22 min for the two enantiomers [14]. At first glance, it may seem surprising that two enantiomers interconvert with different rates. However, this is easily explainable by the chiral



Scheme 6.1 Schematic presentation of enantiomerization process for (±)-**I**



Scheme 6.2 Enantiomerization process of (±)-**5** and half-lives for two enantiomers

environment, in which two enantiomers generally behave as different chemical entities. Such an environment is present during chromatographic separation on the surface of a chiral stationary phase at which bound enantiomers undergo inversion of configuration.

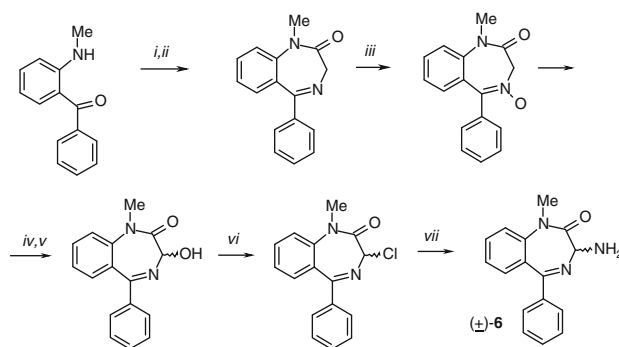
Low configurational stability is used in various inventive modes to recycle “wrong” enantiomers of intermediates for chiral drugs. Recycling of (3*R*)-**6** into (3*S*)-**6** is an important aspect of the process for production of the target compound (3*S*)-**1**, another example of which we shall consider in Chap. 7 (Sertraline).

Compound (3*S*)-**6** is a key building block for the 3-acylamino derivative **1**, a highly potent γ -secretase inhibitor for potential use in Alzheimer’s disease. The structures of all the target compounds **1**–**3** are characterized by three stereogenic centres and an amide bond that connects the 1,2-diaryl carboxylic acid subunits to the (3*S*)-NH₂ group. On the other hand, target structure **4** lacks the two stereogenic centers in the carboxylic subunit.

6.4 Crystallization Induced Asymmetric Transformation

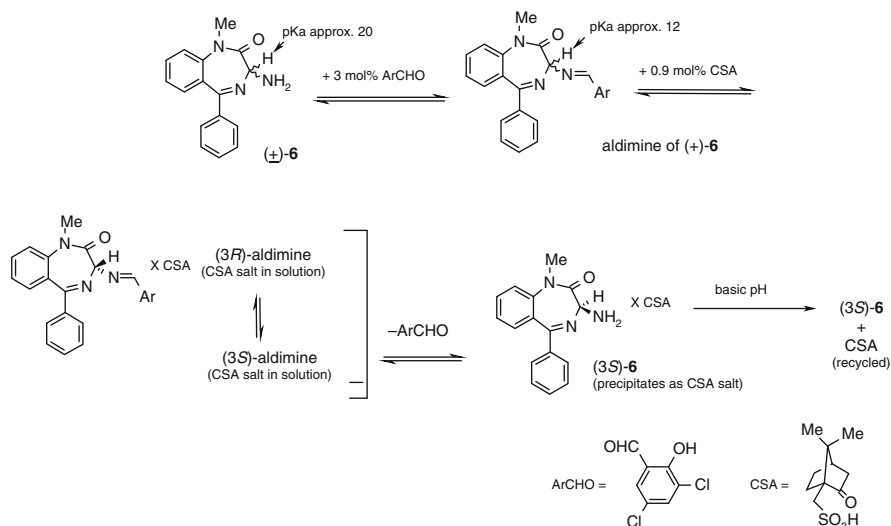
Among chiral 1,4-BZDs, 1-methyl-3-amino-1,4-benzodiazepin-2-one (**6**; Scheme 6.1), represents a particularly interesting structure, syntheses of single derivatives and libraries aimed at specific biological targets having been studied by various teams [15–17]. Synthetic and biological research in the field of 1,4-benzodiazepines were triggered in the early 1960s by the group of Sternbach at Hoffmann-La Roche Research Division, Nutley USA [18]. A synthetic approach to the racemic compound **6** was first reported by S. C. Bell et al. from the Roche team, and was achieved according to Scheme 6.3 [19].

Compound **6** and most of the 3-substituted 1,4-benzodiazepin-2-ones share an important stereochemical characteristic, namely, low configurational stability of the



Reagents and conditions: *i.* ClOCCl₂Br/py; *ii.* NH₃/EtOH; *iii.* AcOH/H₂O₂; *iv.* Ac₂O/D; *v.* KOH in EtOH/H₂O *vi.* SOCl₂/D; *vii.* NH₃/EtOH

Scheme 6.3 Classic synthesis of a racemic 3-amino-1,4-benzodiazepine derivative **6**



Scheme 6.4 Crystallization induced asymmetric transformation of (±)-1-methyl-3-amino-5-phenyl-1,4-benzodiazepine (**6**) into the (3*S*)-enantiomer

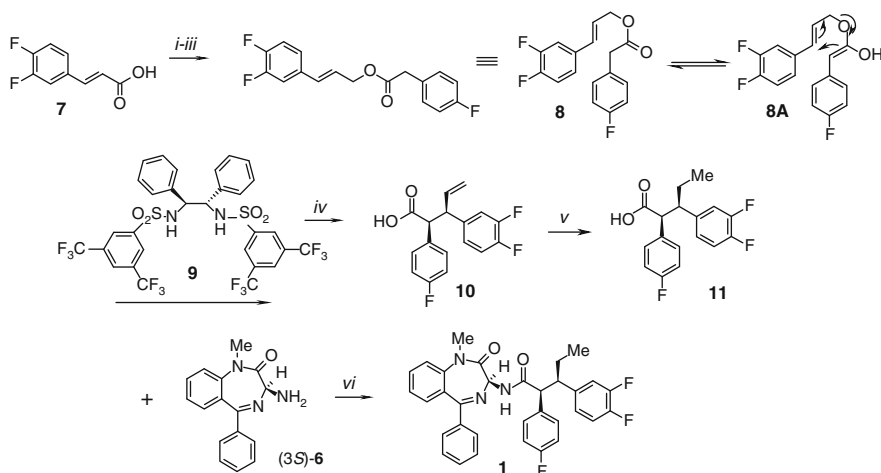
stereogenic centre at C(3). This property permits an important process to be employed for the synthesis of optically pure (3*S*)-**6**, the key intermediate in the synthesis of a number of biologically active 1,4-benzodiazepine derivatives. This process is known as *crystallization induced asymmetric transformation*, and allows for 100% yield of a single enantiomer on separation of the racemic mixture! It is outlined in Scheme 6.4 for transformation of racemic **6** into the (3*S*)-**6** enantiomer [20].

The elegant process, developed by Merck chemists [20], involved a catalytic amount of aromatic aldehyde. This facilitates racemization of the “wrong” enantiomer (3*R*)-**6**, in solution at ambient temperature, via an aldimine intermediate, which possesses a significantly more acidic C(3)-H ($pK_a \sim 12$) than the parent amine ($pK_a \sim 20$). Due to the significantly lower solubility of its (+)-camphor-10-sulphonic acid (CSA) salt, the desired enantiomer, (3*S*)-**6**, continuously crystallizes from the system in equilibrium. This efficient one-pot resolution-racemization process has been used on a multi-kilo scale, affording (3*S*)-**6** for production of various biologically active compounds.

6.5 Asymmetric Ireland–Claisen Rearrangement

Synthetic highlights on the pathway to the optimized leads **1–3** provide instructive examples of the intensive engagement of batch-wise synthetic chemistry at a relative early stage of lead optimization for future NDEs, as presented in Fig. 1.2.

With the availability of an efficient method for the synthesis of enantiomerically pure (3*S*)-**4**, a multidisciplinary team at Merck Sharp and Dohme Research and



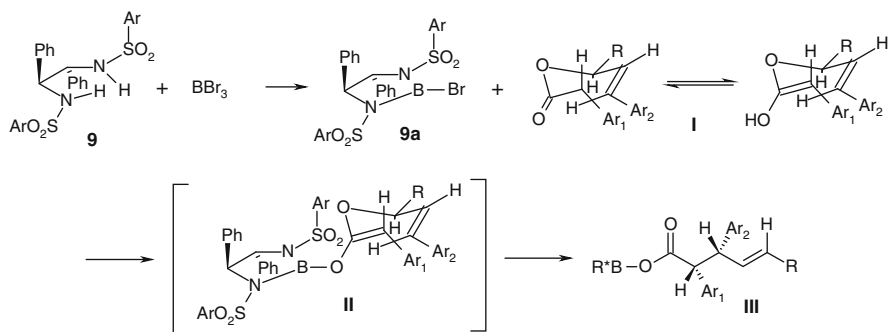
Scheme 6.5 Synthetic route to a γ -secretase inhibitor **1**

Merck Research Laboratories designed and prepared a class of highly potent 1,4-benzodiazepines with γ -secretase inhibitory activity that incorporated a substituted hydrocinnamide unit at C(3) in (3*S*)-**1** (Scheme 6.5) [21, 22].

In developing a route to the target molecule **1**, an original approach was taken to obtain an enantiopure building block, based on the asymmetric Ireland–Claisen rearrangement [23]. In the presence of the catalyst **9**, prochiral allylic ester **8** was converted, in a pericyclic process, into 2,3-aryl-4-pentenoic acid **10** with the defined (2*R*,3*S*)-absolute configuration. The actual reactive species was the enolic form **8A**, which rearranges in a pericyclic $4\pi + 2\sigma$ reaction, promoted by the organocatalyst introduced by Corey et al. [23] for highly enantioselective rearrangement of allylic esters. This rearrangement has been reviewed [24], as a milestone in the development of *chiral variants of pericyclic reactions*.

The mechanism of the rearrangement of the allylesters **1**, promoted by the catalyst **9**, is shown in Scheme 6.6. *E/Z*-Diastereoselectivity of this process is determined by the topology of the intermediate boron enolate **II** in its preferred geometry. The enantioselective formation of (2*S*,3*S*)-**III** is governed by the absolute (*S,S*)-configuration of the *bis*-aryl-sulphonamide unit in the boron reagent **9A**.

According to Corey's early study, the *E/Z* ratio in this reaction is usually over 90:10, and for transformation of **8**→**10** it reaches 99:1 [23]. Since in this rearrangement, the terminal C=CH₂ bond is formed, no diastereoselectivity around the unsaturated C=C bond can be expected. To optimize the yield and e.e. of **10**, the authors modified the original protocol so that addition of the ester **8** to the bromoborane catalyst in step *iv* was carried out at −78 °C, and after 1 h stirring at this temperature, the reaction was continued at ambient temperature for 16 h [22]. Following this protocol, approx. 80% yield of the (2*R*,3*S*)-*E*-isomer of **10** with



Scheme 6.6 Mechanism of asymmetric Claisen rearrangement of allyl esters catalyzed by chiral bis-tosylamide **9**

>99% e.e. was achieved! In the final steps, reduction of the $\text{C}=\text{C}$ bond in **10** was performed, and acylation of (3*S*)-**5** with **11** afforded the target compound **1**, the first representative of a novel class of β -secretase inhibitors. This compound exhibited inhibitory activity at nanomolar concentrations (see Table 6.1).

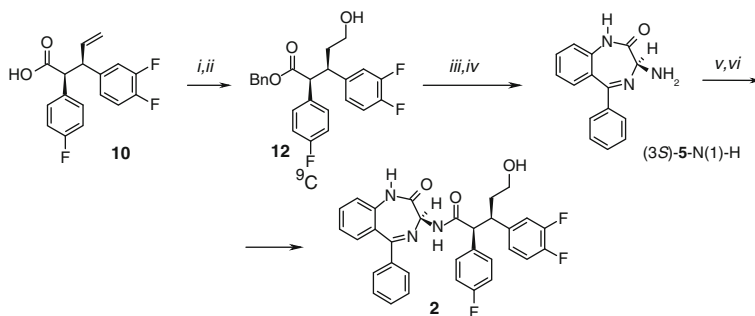
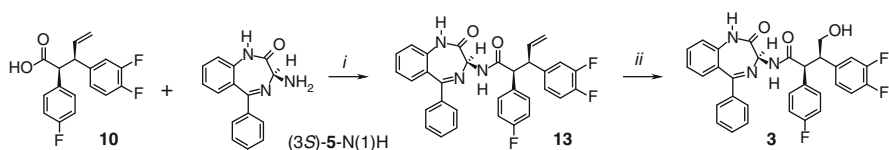
6.6 Hydroboration of the Terminal $\text{C}=\text{C}$ Bond: Anti-Markovnikov Hydration

To obtain more potent lead compounds, two modifications of this structure were anticipated. The synthetic approach to **2** and **3** requires site-selective transformation of structurally complex 3-acylamino-1,4-benzodiazepine precursors, as outlined in Schemes 6.7 and 6.8.

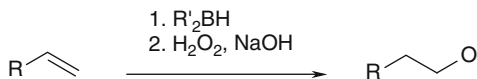
The first step in Scheme 6.7 represents *anti*-Markovnikov-type hydration of the terminal $\text{C}=\text{C}$ bond in **10** to obtain **12**. This transformation requires addition of elements of water so that the electronegative OH group appears on the more electronegative terminal C-atom and the proton on the more positive internal C-atom; in other words, an obvious mismatch of charges is present [25].

The old synthetic problem of *anti*-Markovnikov hydration of the terminal $\text{C}=\text{C}$ bond, to obtain the *prim*-alcohol **3** from **13**, was elegantly solved by hydroboration (Scheme 6.8) [26]. Because of its general importance, the mechanism of this process is outlined in Scheme 6.9, and the energetic profile in Fig. 6.2.

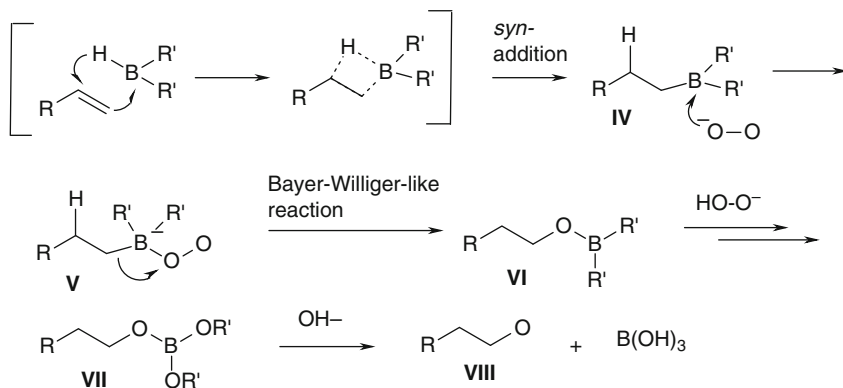
Hydroboration of alkenes was first developed by Brown [26, 27], a Nobel laureate for his contribution to the organic chemistry of boron. The process is based on a multi-step reaction. This consisted of *syn*-addition of borane to the $\text{C}=\text{C}$ bond to form **IV**, followed by peroxide attack and Bayer-Williger-type rearrangement of the intermediate boron-peroxide **V–VI**, and finally hydrolytic splitting of the boronate ester **VII** to the *prim*-alcohol **VIII**, as outlined in Scheme 6.9.

**Scheme 6.7** Final steps in the synthesis of γ -secretase inhibitor **2****Scheme 6.8** Final steps in the synthesis of γ -secretase inhibitor **3**

Overall process



Mechanism

**Scheme 6.9** Mechanisms of hydroboration; anti-Markovnikov addition of elements of water to the terminal C=C bond

The driving force for this process is found in the preferred formation of the *prim*-alkyl borane **IV**, due to the preferred addition of the electropositive boron atom to the terminal, more electronegative C-atom of the C=C bond. An opposite charge distribution occurs during addition of H–OH to the double bond, favouring interaction of the heteroatom with the internal C-atom. Relative energies of all species along the reaction coordinate of hydroboration are presented in Fig. 6.2 [28].

The calculated reaction coordinate reveals higher stability and lower energy of the transition state alkyl borane on the *prim*-C-atom than on the *sec*-C-atom, although the energy content of the product *prim*-alcohol is higher than that of the *sec*-alcohol. The whole process is a typical example of a kinetically controlled reaction.

Achiral and chiral dialkyl boranes, most frequently used in hydroboration reactions are given in Fig. 6.3.

Chiral boranes are easily available from the chiral pool of Nature, specifically from terpenes and sesquiterpenes, as indicated by the retrosynthetic arrow in the Fig. 6.3. They enable enantioselective hydroboration of alkenes in which a stereogenic centre is generated on addition of an hydride ion. This important synthetic aspect of oxidative hydroboration, however, is beyond the scope of this chapter.

On completion of hydroboration in step *ii*, in Scheme 6.7, all remaining steps on the path to **2** (*iv*–*vi*) consist of the manipulation of the benzylic protecting group and coupling to benzodiazepine (3*S*)-**4**-N(1)H to yield the desired target lead compound.

The route to the third target molecule **3**, Scheme 6.8, involves the critical step of ozonolysis of the C=C bond in the intermediate **13**, coupled to reduction of the intermediary aldehyde by the borohydride [29]. This two-step, one-pot reaction is

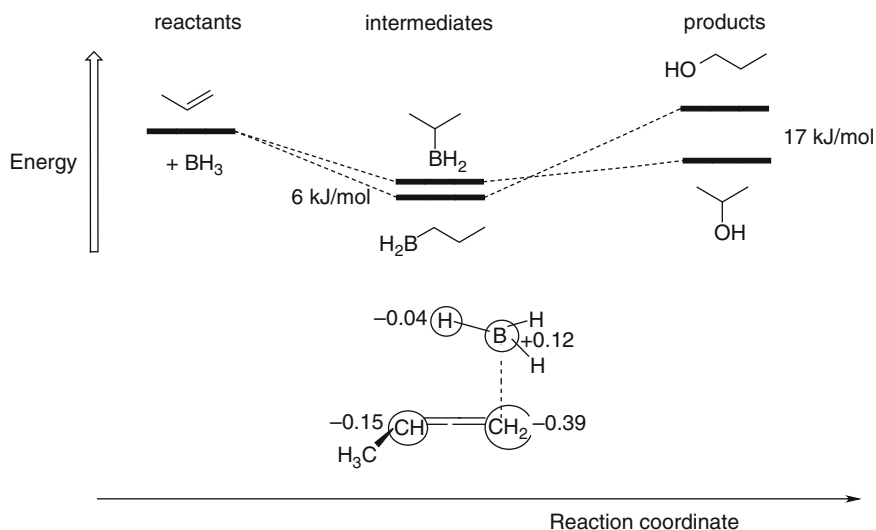


Fig. 6.2 G3MP3 energies and the reactant charges for addition of BH₃ to propene and conversion to propanol-1 (modified according to [28])

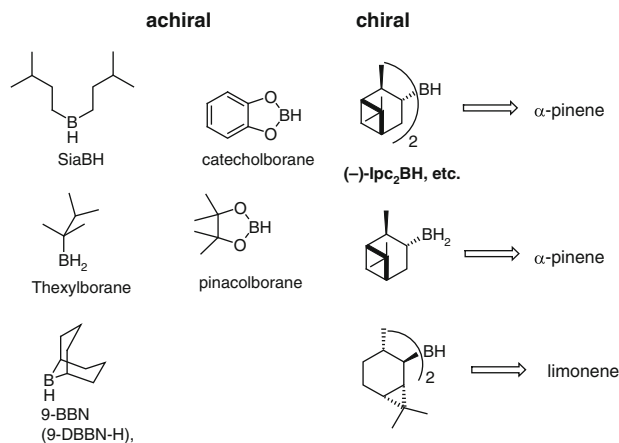


Fig. 6.3 Most frequently used achiral and chiral boranes in hydroboration of alkenes

Table 6.1 γ -Secretase inhibitory activities of selected 2',3'-diarylcaboxylic amides of 3-amino-5-phenyl-1,4-benzodiazepin-2-ones

Compound	IC ₅₀ \pm SD (nM)
1	212 \pm 160
2	35 \pm 23
3	0.06 \pm 0.03

performed with complete site-selectivity, i.e. without cleavage or reduction of any other unsaturated functionality, and has allowed the preparation of the target compound **3** with one C-atom shorter side-chain than in **1** and **2**.

The rationale behind the modification of the structure of the first lead compound **1**, by introducing the terminal hydroxyl group in **2** and **3**, is discussed in detail in the original papers [21, 22]. The biological results for the three selected lead molecules are reported in Table 6.1. It is clear that systematic optimization of hydroxylated derivatives yielded highly potent compounds. Approximately 10^4 -fold enhanced biological activity of **3** in comparison to **1** was the result of well-targeted modification of the chiral carboxylic acid unit on the C(3) of the 3-amino-1,4-benzodiazepine counterpart.

6.7 Crystallization-Induced Asymmetric Transformation in the Synthesis of L-768,673

A second example of crystallization-induced asymmetric transformation of a 3-amino-1,4-benzodiazepine derivative is illustrated by the key step in the highly convergent synthesis of **4** (L-768,673), an anti-arrhythmic drug candidate [30, 31].

Compound **4** is an inhibitor of the slowly activating delayed rectifier K(+) current which repolarizes the cardiac ventricular cell membrane. As a result, the refractory period of the spontaneously contracting heart muscle is prolonged and the cardiac action potential is delayed. This helps to reduce the potentially fatal cardiac ventricular fibrillation which can result from ischaemic heart damage, leading to myocardial infarction.

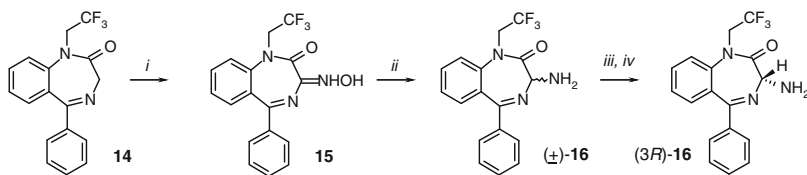
Structurally, compound **4** is a 1-trifluoroethyl-(3*R*)-amino-1,4-benzodiazepine derivative, N-acylated by the strongly lipophilic 1,4-bis-trifluoromethyl-phenylacetyl group. It is interesting to observe that the (3*S*) enantiomer of 1-trifluoroethyl-3-amino-1,4-BZD is present in **4**, whereas the (3*R*) enantiomers of its N-alkyl congeners are preferred in the γ -secretase inhibitors **1–3**!

The synthetic route to the intermediary (3*R*)-amino derivative **16**, including crystallization induced asymmetric transformation as the key step, is presented in Scheme 6.10.

Two details in the above scheme are worth mentioning. Initial attempts at nitrosation of 1,4-BZD ring at C(3) with isoamyl nitrite, the most frequently used agent, failed, due to concomitant attack by isoamyl alkoxide on the oxime. Indeed, when the sterically more crowded *t*-butyl nitrite (t-BuONO) was substituted for isoamyl nitrite oxime, **15** was obtained reproducibly in 85% isolated yield. Second, the effective resolution of racemic **16** was completed with (*R*)-(–)-mandelic acid. For complete conversion of the racemate to the mandelate of (3*R*)-**16**, however, 1–2 mol equivalents of water in *iso*-propylacetate were required, in addition to the salicaldehyde derivative, whose function is explained in Scheme 6.2. On isolation and structural determination, it became clear that the mandelate of (3*R*)-**16** crystallizes as the hydrate.

Comparison of the conditions for crystallization-induced asymmetric transformation of **4** and **13**, which differ in the CH₃ and CH₂CF₃ group at N(1), reveals how considerable serendipity and experience must be invested in solving specific, non-trivial problems on the path to chiral drugs in an optically pure form.

In the final step, acylation of (3*R*)-**16** by 2,4-trifluoromethyl-phenylacetic acid was completed under standard conditions, in 92% yield and, more importantly, without any significant racemization; the e.e of the final product, (3*R*)-**4**, was 99% [31].



Reagents and conditions: *i.* t-BuONO, t-BuOK, THF/toluene, –40 °C, 5h, 95%; *ii.* 5% Ru/C, H₂, 40 psi, 70 °C, 90%; *iii.* 3,5-dichlorosalicylaldehyde 2 mol%, water 1.5–2.0 mol equiv., (*R*)-mandelic acid, *iv.* *i*-PrOAc, r.t. 24 h, 92% yield, 99.4% e.e.

Scheme 6.10 Synthesis of (3*R*)-**16**, the chiral key intermediate for the anti-arrhythmic agent **4**

6.8 Conclusion

Design of new lead molecules offers to the synthetic organic chemist immense opportunities for creative synthesis. Design of the target lead structures, however, requires critical discussion with molecular biologists, pharmacologists and other members of a multidisciplinary team. The many elegant synthetic solutions that resulted in the lead compounds **1–3**, with a hydrocinnamide side chain at the C(3)-NH₂ of the 1,4-benzodiazepine scaffold, illustrate the often high requirements demanded of the structure of selected leads. In spite of such creative synthetic contributions at the hit-to-lead stage in the development of a chiral NDE, subsequent steps, in particular those involving ADME studies and toxicity data, often hamper further development. The team approach is called for and further structural modifications may be required with a costly repetition of the iterative discovery cycle. Consequently, the medicinal chemist is called upon, not only to find unusual solutions to demanding, potentially chiral structures, but to contribute to biologically potent and specific compounds which are easily absorbed and distributed in the body without inducing undesirable toxicity. The challenge is great!

References

1. Huang Z, Huang PL, Panahian N, Dalkara T, Fishman MC, Moskowitz MA (1994) *Science* 265:1883–1885
2. Patchett AA, Nargund RP (2000) *Ann Rep Med Chem* 35:289–298
3. Jhee S, Shiovitz T, Crawford AW, Cutler NR (2001) *Expert Opin Invest Drugs* 10:593–605
4. Sambumartu K, Grieg NH, Lahiri DK (2002) *Advances in the cellular and molecular biology of the β -amyloid protein in Alzheimer's disease. NeuroMol Med* 1:1–31
5. Selkoe DJ (2001) *Physiol Rev* 81:741–766
6. Tsai Y-Y, Wolfe MS, Xia W (2002) *Curr Med Chem* 9:1087–106
7. Zettl H, Weggen S, Schneider P, Schneider G (2010) *Trends Pharmacol Sci* 31:402–410
8. He G, Luo W, Li P, Remmers C, Netzer WJ, Hendrick J, Bettayeb K, Flajolet M, Gorelick F, Wennogle LP, Greengard P (2010) *Nature* 467:95–98
9. FDA Document (1992) *Chirality* 4:338–340
10. Schoetz G, Trapp O, Schurig V (2000) *Anal Chem* 72:2758–2764
11. Oswald P, Desmet K, Sandra P, Krupčik J, Majek P, Armstrong DA (2002) *J Chromatogr B* 779:283–295
12. Schurig V (1998) *Chirality* 10:140–1460
13. Trapp O, Schoetz G, Schurig V (2001) *Chirality* 13:403–414
14. Abatangelo A, Zanetti F, Navarini L, Kontrec D, Vinkovic V, Sunjic V (2002) *Chirality* 13:12–17
15. Micale N, Vairagoundar R, Yakovlev AG, Kozikowski AP (2004) *J Med Chem* 47:6455–6458
16. Evans BE, Rittle KE, Bock MG, Dipardo RM, Freidinger RM, Whitter WL, Lundell GL, Veber DF, Anderson PS, Chang RSL, Lotti VJ, Cerino DJ, Chen TB, Kling PJ, Kunkel KA, Springer JP, Hirshfeld J (1988) *J Med Chem* 31:2235–2246
17. Bock MG, Dipardo RM, Evans BE, Rittle KE, Whitter WL, Veber DF, Anderson PS, Freidinger RM (1989) *J Med Chem* 32:13–16

18. Sternbach L (1979) *J Med Chem* 22:1–7
19. Bell SC, McCaully RJ, Childress SJ (1968) *J Org Chem* 33:216–220
20. Reider PJ, Davis P, Hughes P, Grabowski EJJ (1987) *J Org Chem* 52:955–957
21. Churcher I, Ashton K, Butcher JW, Clarke EE, Harrison T, Owens AP, Teall MR, Williams S, Wrigley JDJA (2003) *Bioorg Med Chem Lett* 13:179–183
22. Churcher I, Williams S, Kennard S, Harrison T, Castro JL, Shearman MS, Lewis HD, Clarke EE, Wrigley JDJ, Behr D, Tang YS, Liu W (2003) *J Med Chem* 46:2275–2278
23. Corey EJ, Lee D-H (1991) *J Am Chem Soc* 113:4026–4028
24. Enders D, Knopp M, Schiffrers R (1996) *Tetrahedron Asymm* 7:1847–1882
25. Beller M, Seayad J, Tillack A, Jiao H (2004) *Angew Chem Int Ed* 43:3368–3398
26. Bubnov Y (2004) In: Kaufmann DE, Matteson DS (eds) *Science of synthesis*, Vol. 6. Thieme, Stuttgart, 945–1072
27. Clay JM (2007) Brown hydroboration reaction. *Name Reactions for Functional Group Transformation*, 183–188
28. Ilich P-P, Reckertsen LS, Becker E (2006) *J Chem Educ* 83:1681–1685
29. Uysal B, Buyuktas BS (2007) *ARKIVOC* 14:134–140
30. Selnick HG, Liverton NJ, Baldwin JJ, Butcher JW, Claremon DA, Elliott JM, Freidinger RM, King SA, Libby BE, McIntyre CJ, Pribush DA, Remy DC, Smith GR, Tebben AJ, Jurkiewicz NK, Lynch JL, Salata JJ, Sanuinetti MC, Siegl PKS, Slaughter DE, Vyas K (1997) *J Med Chem* 40:3865–3868
31. Shi YJ, Wells KM, Pye PJ, Choi WB, Churchill HRO, Linch JE, Maliakal A, Sager JW, Rossen K, Volante RP, Reider PJ (1999) *Tetrahedron* 55:909–918

Chapter 7

Sertraline

Abstract

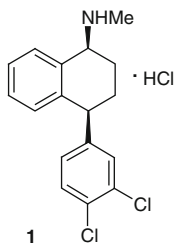
Biological target: Sertraline is an aryl-substituted tetrahydronaphthalene derivative which selectively inhibits the plasma membrane serotonin transporter (SERT) and thereby blocks serotonin re-uptake from the neuronal synapse.

Therapeutic profile: As a selective serotonin reuptake inhibitor (SSRI), sertraline is a widely used drug for the treatment of depression and anxiety-related disorders.

Synthetic highlights: A variety of pathways have been taken in the synthetic approach to sertraline. These include stereoselective reduction of ketones and imines under kinetic and thermodynamic control, using diastereoselective or enantioselective catalysts and reagents, desymmetrization of oxabenzonorbornadiene followed by the Suzuki coupling of arylboronic acids and vinyl halides and Pd-Catalyzed (Tsuji-Trost) coupling of arylboronic acids and allylic esters. For the production of sertraline, the simulated moving bed (SMB), a cost-effective technology, has been introduced.

7.1 Introduction

Sertraline hydrochloride [**1**, (1*S*,4*S*)-1-methylamino-4-(3',4'-dichlorophenyl)-tetrahydronaphthalene, *Zoloft*[®]] is an inhibitor of serotonin re-uptake, and an important pharmaceutical agent for the treatment of depression as well as dependency- and other anxiety-related disorders [1, 2].



7.2 Synaptosomal Serotonin Uptake and Its Selective Inhibitors (SSRI)

Serotonin (*5-hydroxytryptamine*, 5-HT) occurs in the intestinal wall, where it regulates motility and secretion; in blood platelets, where it modulates platelet aggregation and vascular blood flow; and in the CNS, where it acts as a neurotransmitter in areas of the midbrain. At least seven different receptors for serotonin have been characterized, which mediate a wide variety of different physiological effects. Depression and anxiety are thought to be the result of actions on 5-HT_{1A} receptors in the brain limbic system. Following release from neurons by a depolarizing action potential at central synapses, the activity of 5-HT is terminated by neuronal reuptake. This is performed by a synaptic membrane amine transporter protein, specific for 5-HT, which also co-transporters sodium and chloride ions to repolarize the neuronal membrane.

Sertraline belongs to the group of *selective serotonin reuptake inhibitors* (SSRIs), the most commonly prescribed group of anti-depressants which have revolutionized the treatment of depression and anxiety disorders. They exert their effects by inhibiting the *plasma membrane serotonin transporter* (SERT). This group of drugs includes fluvoxamine (*Luvor*[®]), fluoxetine (*Prozac*[®]), paroxetine (*Payil*[®]) and citalopram (*Celexa*[®]), Fig. 7.1. All of them differ structurally and pharmacologically from the earlier *monoamine oxidase inhibitors* (MAOs) and *tricyclic antidepressants* (TACs, illustrated below by amitriptyline).

SSRIs and sertraline in particular, represented a significant advance over the frequent adverse effects of the earlier drug classes [3]. Further progress in this field has been achieved with dual- and triple-uptake inhibitors, which inhibit the uptake of serotonin, dopamine and adrenaline, three neurotransmitters that are most closely linked to depression [4].

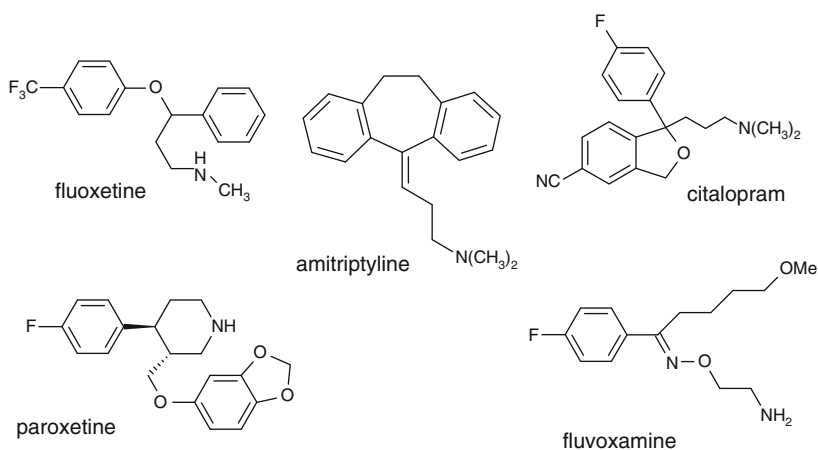


Fig. 7.1 Some representatives of selective serotonin reuptake inhibitors (SSRIs)

7.3 Action of Sertraline and Its Protein Target

The difference in biological properties between *cis*- and *trans*-diastereomers of **1**, and in particular between (1*S*,4*S*)- and (1*R*,4*R*)-enantiomers of *cis*-**1** is well documented, and enabled the selection of (1*S*,4*S*)-**1** for further progression as a drug [5, 6]. Early comparison of the structure of the potent and chiral serotonin uptake inhibitor (1*S*,4*S*)-sertraline with that of the chiral conformer of (*R*)-fluoxetine indicated a close three-dimensional correspondence. This suggested that the conformer of (*R*)-fluoxetine, rather than the mirror image conformer, is the form which binds to the receptor in the absolute conformation, similar to those adopted by (1*S*,4*S*)-sertraline [7]. Recently, the structure was reported of the binding site in the LeuT-sertraline complex (Fig. 7.2) [8]. LeuT is the bacterial homologue of the human membrane serotonin transporter (SERT), which allowed the crystal structures of four SSRIs, including sertraline, to be studied.

Due to the high degree of homology between human SERT and bacterial LeuT [9], X-ray data obtained for the sertraline complex with the bacterial protein allowed conclusions to be drawn on the binding interactions that are important for its inhibitor activity. Structural data for the three LeuT-SSRI structures revealed common conformational characteristics of the bound drugs, in particular, that specificity of SERT for SSRIs is dependent on the interaction of the drug halogens with the protein *halogen binding pocket* (HBP). The amino acid sequence in this pocket, indicated in Fig. 7.2, is highly conserved between LeuT and SERT, further supporting the value of the bacterial protein model. Notably, in the bound sertraline molecule, the dichlorophenyl ring is approximately perpendicular to the tetrahydronaphthalene ring, which is tilted slightly from the membrane plane. The amine nitrogen forms a salt bridge with the carboxyl group of Asp404, and simultaneously interacts with the back-bone oxygen of Asp401 via a bound water molecule, as evidenced in Fig. 7.2. The dichlorophenyl ring in the bound sertraline molecule is rotated around the C4–C13' bond by 180° compared to the unbound molecule [10].

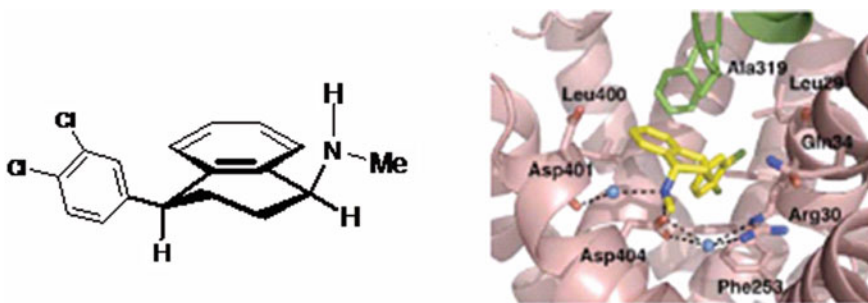


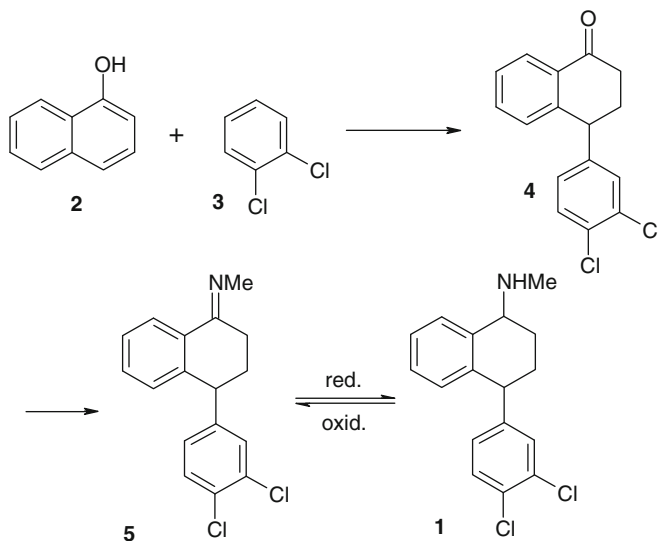
Fig. 7.2 Stereoformula of sertraline and X-ray structure of LeuT-sertraline complex (reproduced from [8], with the permission of the Nature Publishing group, a division of Macmillan Publishers Ltd.)

The sertraline molecule is rather rigid, indicating that the drug molecule maintains its low-energy conformation upon binding to its protein target. Since the absolute conformation of an unbound organic molecule is defined by the sign of the dihedral angles, and these are directed by the absolute configuration of the stereogenic centre(s), it is obvious why usually one enantiomer adopts the reactive conformation at the binding site. (1*S*,4*S*)-Sertraline is a good example of such stereorecognition by the biological receptor, and all efforts made to synthesise the pure enantiomer, as described in the following sections, are clearly understandable.

7.4 General Synthetic Route

The structure of sertraline is characterized by two stereogenic centres with absolute (1*S*,4*S*) configuration and relative *cis*-configuration. The compound can be obtained from an enantiomerically pure natural chiral compound, as presented in Sect. 7.7. However, a more effective approach was initiated from achiral materials by transforming them diastereoselectively, followed by chiral separations of the enantiomers [11].

Before discussing the stereochemical issues of the individual steps, the overall synthetic route is presented in Scheme 7.1, in which the absolute configurations at the stereogenic centres are not shown. It is important to note that **4** and **5** are racemic while target compound **1** comprises two diastereomeric racemates which can equilibrate in an epimerization process, based on amine-imine redox equilibrium at C(1),



Scheme 7.1 General synthetic route to sertraline

or on the base-catalyzed epimerization at C(4). Synthetically useful aspects of both processes will be discussed.

It is estimated that about 20% of all drugs contain at least one stereogenic centre linked to an amino group, as in sertraline. There is thus an enormous demand for new methods for the enantioselective synthesis of chiral amines in an optically pure form, and for racemisation processes that can recycle the “wrong” enantiomer. Some of these methods were successfully applied along the pathway to sertraline, and in this chapter examples of these highly inventive approaches are given.

7.5 Stereoselective Reduction of Ketones and Imines Under Kinetic and Thermodynamic Control

The first three examples of catalytic processes developed for (1*S*,4*S*)-sertaline are characterized by the use of *metals as the catalysts* in various synthetic transformations (Sect. 7.5.1–7.5.3). In the fourth example, chiral oxazaborolidine is used as the reducing agent (Sect. 7.5.4).

The most direct route to *rac*-tetralone **4**, namely, arylation of α -naphthol (**2**) with 1,2-dichlorobenzene (**3**) mediated by aluminium chloride, is depicted in Scheme 7.1. The mechanism of this highly interesting C–C bond-forming reaction involves the formation of a strong carbocation-like species on co-ordination of AlCl_3 to the carbonylic tautomer of **2**, and its arylation by dichlorobenzene. This racemic ketone is the starting material for all the routes that are described below.

7.5.1 Diastereoselectivity of Hydrogenation of *rac*-tetralone-Methylimine: The Old ($\text{MeNH}_2/\text{TiCl}_4/\text{Toluene}$) Method Is Improved by Using $\text{MeNH}_2/\text{EtOH-Pd}/\text{CaCO}_3$, 60–65°C in a Telescoped Process

Traditionally, condensation of **4** with methylamine was promoted by TiCl_4 in toluene with an excess of methylamine, producing the hazardous by-products, titanium dioxide and methylamine hydrochloride [12]. An extremely simple, innovative approach was recently described that provides conversion of **5**–**1** and avoids this disadvantage [13]. It relies on the low-solubility of imine **5** in alcohols, driving the reaction equilibrium towards the final product. The reaction is performed in a pressure vessel at 60–65°C providing >95% conversion to **1**.

This inventive step is followed by diastereoselective hydrogenation of **5** to otherwise thermodynamically less stable *cis*-**1** (in the racemic form), using Pd/CaCO_3 (1% w/w). This improves diastereoselectivity by up to 95% d.e., well above the 80% previously achieved. Moreover, this catalyst was found to perform best in alcohols, providing the conditions for development of a “telescoped process”. This process is characterized by

the use of the *same solvent and one reaction vessel* for completion of the three steps; transformation of **4**–**5** and **5** to *rac*-**1** and resolution of *rac*-**1** by crystallization with mandelic acid.

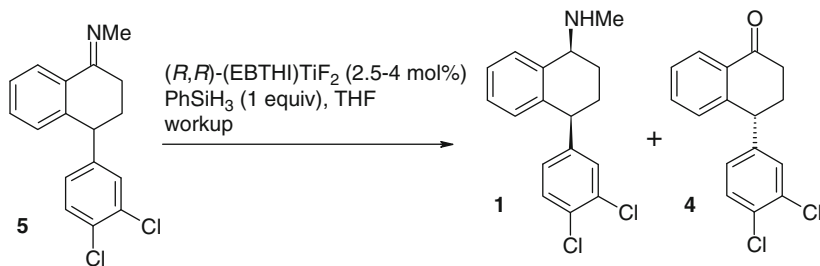
7.5.2 Kinetic Resolution of Racemic Methylamine: Hydrosilylation by (*R,R*)-(EBTHI)TiF₂/PhSiH₃ Catalytic System

Another highlight on the synthetic route to sertraline is the kinetic resolution of *rac*-imine **5** by hydrosilylation with the (*R,R*)-(EBTHI)TiF₂/PhSiH₃ catalytic system, according to Scheme 7.2 [14].

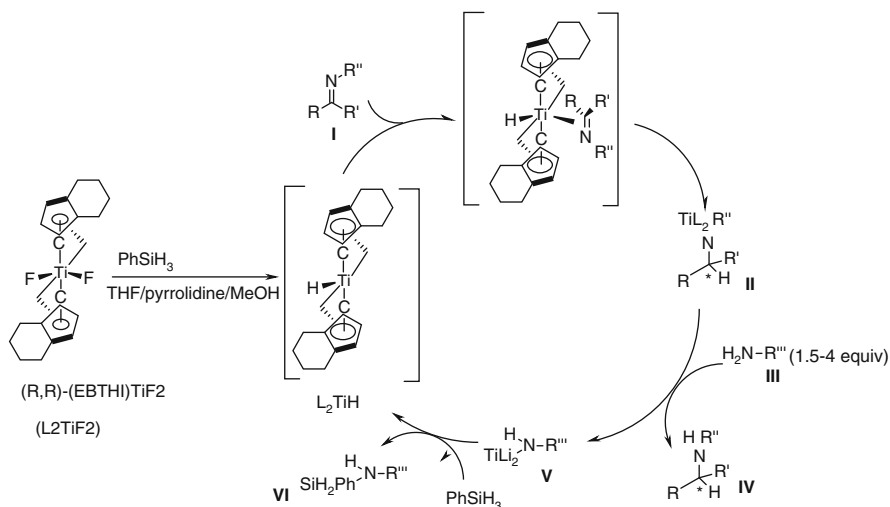
Both (*R,R*) and (*S,S*) enantiomers of ethylenebis(η^5 -tetrahydroindenyl)titanium difluoride (EBTHI)TiF₂, were developed by Buchwald et al. and used in many efficient enantioselective hydrogenations of ketones [15] and imines [16]. The utility of this process was demonstrated in the enantio- and diastereo-selective preparation of sertraline according to Scheme 7.2. The enantioselectivity and yield in this reaction ranged between 90 and 96% e.e. and 40–50%, respectively. The yield is based on the racemic **5**, and amounts to 76–96% when based on the (*4S*)-enantiomer. Workup in this reaction requires chromatographic separation of (*1S,4S*)-**1**, from the (*4R*)-ketone **4**. Later, in Sect. 7.5.4, we shall discuss an independent research project that resulted in the efficient recycling of the “wrong” enantiomer of this ketone.

The key mechanistic aspects of the reaction are outlined in Scheme 7.3.

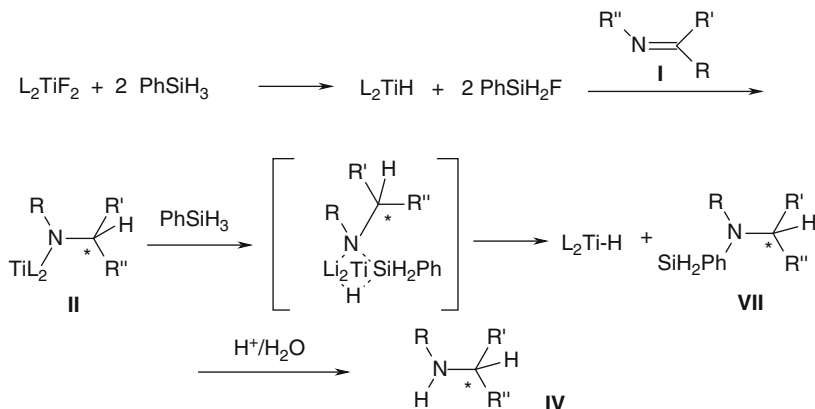
Activation of the (*R,R*)-(EBTHI)TiF₂ complex by PhSiH₃ leads, in the first step, to the Li₂TiH complex. Initial insertion of the imine in the Ti–H bond is followed by proton-transfer and departure of the chiral intermediate **II**, followed by formation of the Ti–N bond in **V** and the chiral product **IV**. The cycle is completed by the intervention of phenylsilane and regeneration of the L₂TiH catalytic species. High enantioselectivity of the hydride transfer is controlled by the steric demand of the chiral ligand in the titanocene complex, in which diastereotopicity of the two sites of the C=N bond assures stereoselection.



Scheme 7.2 Enantioselective hydrogenation of *rac*. imine **5** to (*1S,4S*)-**1**



Scheme 7.3 Mechanism of enantioselective hydrogenation of imines by $(R,R)\text{-(EBTHI)TiF}_2/\text{PhSiH}_3$ catalytic system



Scheme 7.4 Mechanism of hydride transfer via Li_2TiH -imine complex

Another mechanistic proposal argues that the formation of the intermediary **II** is thermodynamically driven by formation of the Ti–H bond due to cleavage of the Ti–F bond (ca. 140 kcal/mol) and formation of an Si–F bond of unusually high bond energy (150–165 kcal/mol) [17]. The final σ -bond metathesis and formation of **VII** is outlined in Scheme 7.4, in which a water molecule is invoked to split the Si–N bond in the last step to the chiral amine **IV**.

It is important to note that the reaction outlined in Scheme 7.2 does not involve a simple *kinetic resolution*, in which one enantiomer reacts faster than the other without the creation of a new chiral centre. Instead, a chiral centre at C(1) in **5**

allows the formation of two diastereomeric racemates. Remarkably, the chiral reducing agent selects the (4*S*) enantiomer of **5** and reduces the imino unit in a *cis*-fashion, affording (1*S*,4*S*)-**1**, only a *single stereoisomer of four different possibilities*! The authors achieved high stereoselectivity in favour of the (1*S*,4*S*)-*cis*-diastereomer; d.e.s were found between 98 and 99% [14].

7.5.3 Catalytic Epimerization of the Trans- to the Cis-Isomer of Sertraline

Generally, racemization of chiral *sec*-amines can be represented as shown in Scheme 7.5.

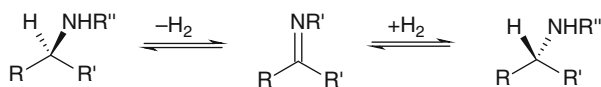
In these equilibria, both enantiomers interconvert via the prochiral intermediate, and are present in equal quantities, irrespective of the enantiomer that is in excess at the beginning of the process. When racemization of the “wrong” enantiomer is coupled with further conversion of the “right” one from the resulting mixture, this tandem transformation is named *dynamic kinetic resolution* (see also concluding statement of the Sect. 10.4.2).

While many heterogeneous catalysts and some homogenous catalytic complexes are known to racemize optically active *sec*-alcohols via corresponding ketones [18, 19], there is little precedence for the racemization of amines [20, 21]. Moreover, most of them do not meet industrial criteria for *turn over number* (TON), price of the catalyst, loading capacity of the catalyst or reaction conditions, in particular when high temperatures are required.

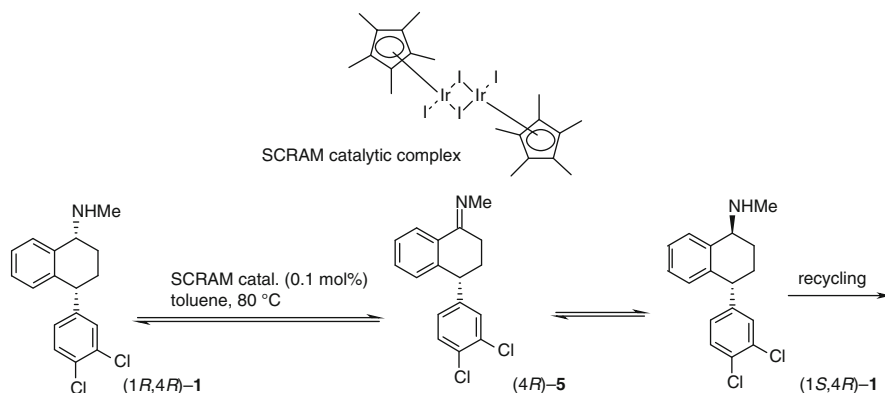
Recently, it has been reported that a SCRAM catalyst can dehydrogenate a “wrong” (1*R*,4*R*)-enantiomer of sertraline to the imine, which depending upon the reaction conditions, is then reduced back to the amine [22]. The whole process for epimerisation of the “wrong” enantiomer of sertraline is presented in Scheme 7.6.

Sertraline is an interesting case whereby epimerization of the *sec*-amine is under thermodynamic control, affording a more stable *trans*-diastereomer with up to 90% d.e. and the correct (1*S*) configuration at the stereogenic centre bearing the amino group. Since the second stereogenic centre at C(4) can be equilibrated with a strong base, a technological process has been devised in which the three “waste” isomers from sertraline production can be racemized and turned into the (1*S*,4*S*)-enantiomer, present in the drug substance.

It is important to note the delicate nature of SCRAM-type catalysts. When an analogous complex with the chloride anion as the ligand was used, ~120-fold



Scheme 7.5 General scheme of redox-type racemization of imines



Scheme 7.6 SCRAM-catalyzed epimerization of (1*R*,4*R*)-**1** to (1*S*,4*R*)-**1** and recycling

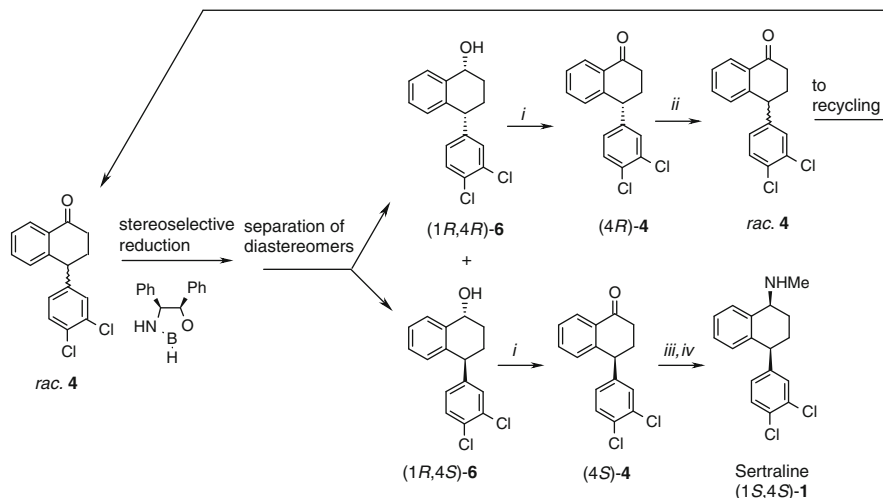
decrease in the rate of racemization was observed. Such a large effect of the anionic ligand on the catalytic activity can be explained by the *effective positive charge on the metal*, that is, its ability to act as a Lewis acid and to accept/donate hydride ion. The high rate of this reversible, first-order redox process for sertraline, with a $t_{1/2}$ of 22 min, makes this process highly attractive for the large-scale epimerization of (1*R*,4*R*)-**1** [22].

7.5.4 Stereoselective Reduction of Tetralone by Chiral Diphenyloxazaborolidine

There are numerous methods for asymmetric reduction of aryl-alkyl ketones [23, 24]. Stereoselective reduction of racemic ketones, substrates that already possess one stereogenic centre, is diastereoselective if one configuration prevails at the newly created stereogenic centre. Diastereoselectivity of reduction is controlled by the stereogenic centre already present, but it can be controlled twice when a chiral reducing agent is used. A favourable or matching situation appears when the chiral reducing agent, or catalyst, enhances enantioselectivity; otherwise “mismatch” of the two controllers lowers diastereoselectivity. To avoid the second and favour the first relation, usually a “trial and error” approach is required, applying both enantiomers of the reagent or catalyst. Nowadays, in silico design of the transition state structures facilitates selection of the reagent, or catalytic system with the “correct” absolute configuration.

This situation was faced when the sertraline precursor *rac.* ketone **4** was reduced (Scheme 7.7). Two diastereomers were separated by crystallization and the “right” diastereomer (1*R*,4*S*)-**6** converted to sertraline via the (4*S*)-ketone **4**, then the imine, and finally *cis*-diastereoselective hydrogenation was carried out.

Generally, benzylic-type alcohols, such as **6**, can be re-oxidized to ketones by various methods [25, 26]. Racemic ketone **4** is reduced by the chiral



Reagents and conditions. *i.* pyridinium chlorochromate (PCC); *ii.* NaOH/MeOH/ Δ ; *iii.* MeNH₂, EtOH; *iv.* H₂, *cis*-selective.

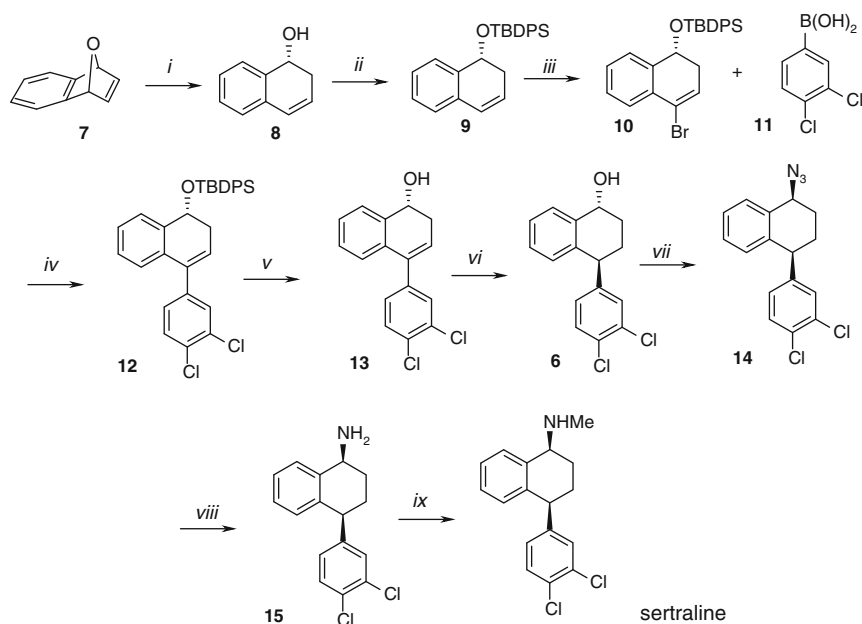
Scheme 7.7 Stereoselective reduction of *rac.* ketone **4** and recycling of the “wrong” diastereomer

diphenyloxazaborolidine with 95% d.e to the preferred (1*R*,4*S*)-diastereomer **6**. Such a high diastereoselectivity was achieved within the framework of a research project which combined a synthetic study and *ab initio* calculations to determine the relationship between the oxazaborolidine structure and diastereoselective bias [27]. Sixteen oxazaborolidines were synthesized and tested for the stereoselective reduction of tetralones! This study revealed that the primary requirement of a catalyst to generate high diastereoselectivity was to completely block one face of oxazaborolidine, and led to the invention of the catalyst in Scheme 7.7. Along with the “*telescopic process*” described in Sect. 7.5.1 this process was competitive for industrial scale production until the SMB-based process, described in the Sect. 7.8, was developed.

7.6 Desymmetrization of Oxabenzonornbornadiene, Suzuki Coupling of Arylboronic Acids and Vinyl Halides

This section describes an original, multistep synthesis pathway to sertraline, as outlined in Scheme 7.8 [28, 29].

This approach is based on the chiral dihydronaphthalene motif, represented by compound (*R*)-**8**. Generally, this motif is found in a number of biologically active molecules and therefore it is a chemically “privileged structure” in the sense of being a starting point for the identification of a lead compound for evaluation [30].



Reagents and conditions: *i.* $\text{Ni}(\text{COD})_2/(\text{S})\text{-BINAP}$, DIBAL-H, THF, r.t.; *ii.* TBDPSCl, imidazol, DCM/DMAP; *iii.* Br_2 , TEA/DCM, then DBU/toluene; *iv.* $\text{Pd}(\text{PPh}_3)_4$, KF, toluene, H_2O , 100°C , 3h; *v.* TBAF/AcOH, THF; *vi.* H_2 /10 mol% $[\text{Ir}(\text{COD})\text{pyCy}_3]\text{PF}_6$, DCM; *vii.* dppa/DBU, THF; *viii.* H_2 /Pd/C, EtOH; *ix.* $\text{ClCOOEt}/\text{MeCN}$, K_2CO_3 , then $\text{LiAlH}(\text{OMe})_3$, THF.

Scheme 7.8 Enantioselective synthesis of sertraline based on desymmetrization of oxabenzonorbornadiene **7** and Suzuki coupling to (*R*)-**12**

In Chap. 6, we have already considered 1,4-benzodiazepines as a group of “privileged structures”, but defined in a somewhat different way [31].

The bicyclic structure **7** is desymmetrized by reductive C–O bond splitting in the presence of the Ni complex of (*S*)-BINAP and diisobutylaluminum hydride (DIBAL-H). This couple ensures enantioselective hydrometalation-elimination from one of the *enantiotopic carbon atoms* in the bridge to the C–O bond, affording dihydronaphthalenol (*R*)-**8** in 88% yield and 98% e.e. In the following steps, protection of **8** as the silyl ether **9** was completed before addition of bromine to the double bond in the presence of triethylamine. This intermediate was treated with DBU (1,8-diazabicyclo[5.4.0]undec-7-ene, strong, crowded base) without isolation, and on regioselective elimination of hydrogen bromide, vinylbromide **10** was isolated in 83% yield.

An intensive search was made for a successful coupling strategy to introduce the aryl group in **12** [29]. Various Stille coupling conditions, with an SnMe_3 group instead of the boronate group in **11**, resulted in low yields of **12**. Finally, Suzuki coupling of **10** with arylboronic acid **11** led, under the optimized conditions indicated for step *iv* in Scheme 7.8, to **12** in 53% yield. Numerous methods have

been published for Suzuki coupling using a wide variety of bases and catalyst precursors [32], and some aspects of the Suzuki-Miyaura reaction are discussed in Sect. 5.4.

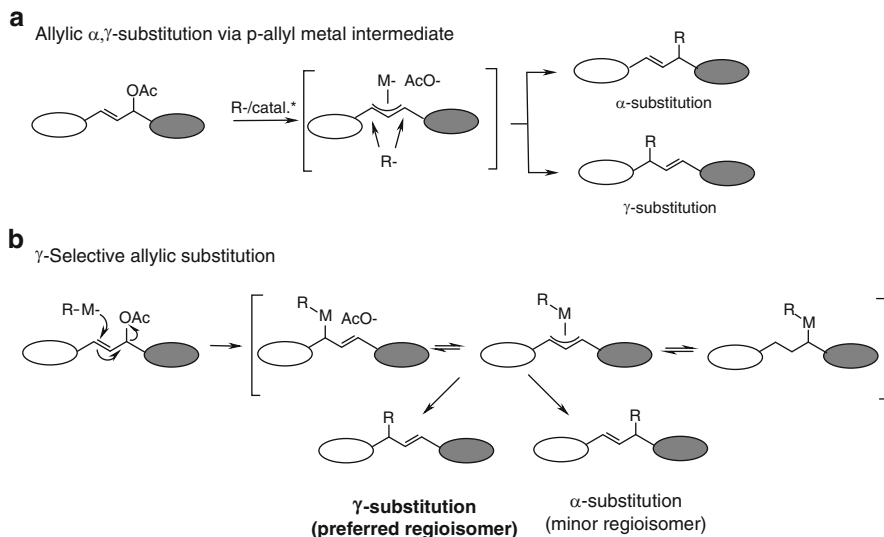
In the next steps, **12** was deprotected, and the C=C bond in **13** diastereoselectively hydrogenated to the *trans*-(1*R*,4*S*)-diastereomer **14**. Suitable selection of a catalytic system and increasing the pressure of hydrogen to 1,000 psi led in step *vi*, to **6** in 88% yield and 28:1 *trans*-selectivity. This compound was used as an intermediate in Scheme 7.7, in which it was oxidized to ketone (*S*)-**4**. Along the synthetic pathway in Scheme 7.8, however, the authors decided to control stereochemistry by substituting the benzylic alcohol with nitrogen functionality (step *vii*). For this purpose, modified Mitsunobu conditions were applied, using *diphenylphosphorylazide* (dppa) in the presence of DBU [33]. Under these conditions, the benzylic hydroxyl is activated and displaced by azide with complete inversion of the configuration, affording **14** in 88% yield and 99% e.e. The authors noted that classic Mitsunobu conditions (PPh₃, DEAD, HN₃) lead to significant epimerization at the reacting stereocentre.

In the last steps, all that remained was to reduce the azide and methylate the resulting amine. Reduction of azide was cleanly effected by hydrogen over Pd/C. The problem of selectivity in reduction of carbamate to Me group was circumvented, however, by using LiAlH(OMe₃) in refluxing THF.

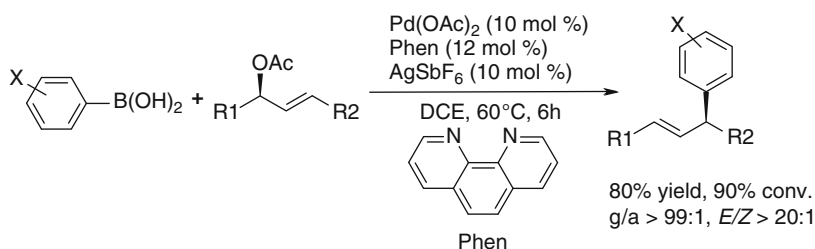
When this synthesis was completed, the authors attempted to reduce the number of isolated intermediates, most of them are sensitive to the workup and purification procedures. This resulted in a 9-step process and 38% overall yield of sertraline. This approach, though declared by the authors as “expedient total synthesis” [28], is hardly competitive on a large-scale, with the robust approaches described in the former sections. Still, the many elegant synthetic solutions to issues encountered in individual steps makes this approach fascinating and inspiring for synthetic and medicinal chemists.

7.7 Pd-Catalyzed (Tsuji-Trost) Coupling of Arylboronic Acids and Allylic Esters

Transition metal-catalyzed allylic substitution reactions with carbon nucleophiles are among the most important carbon-carbon bond formation methods in modern organic synthesis, because of their broad substrate scope under mild reaction conditions. In addition, they are applicable to enantioselective reactions, as well as exhibiting versatility towards the alkene functionality adjacent to the chiral centre for stereoselective derivatization. Tsuji-Trost allylic substitution, involving a (π -allyl) metal intermediate, has provided a particular advance in this regard [34, 35]. Most recently, Sawamura et al. [36, 37] have improved the regioselectivity of this reaction with unsymmetrically substituted allylic esters, and thus opened a new approach to sertraline.



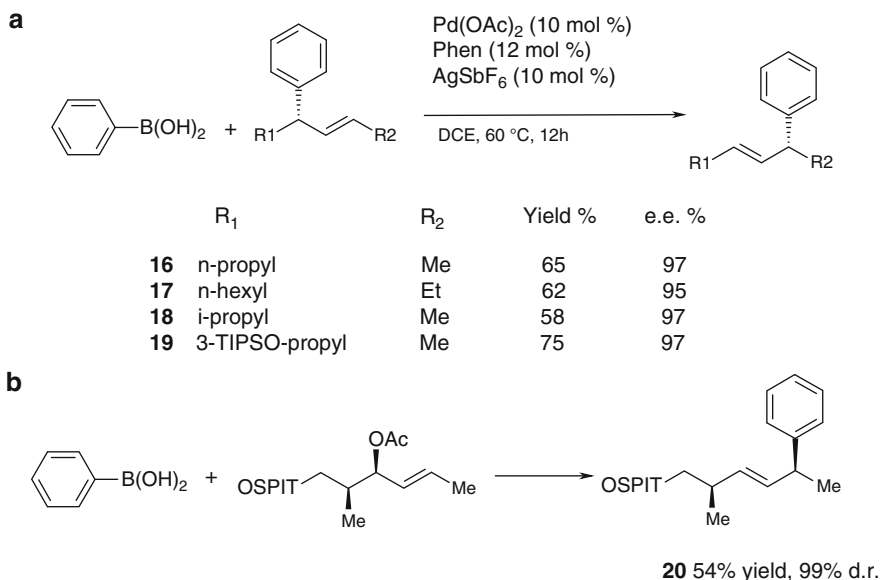
Scheme 7.9 Two types of metal-mediated allylic substitutions

Scheme 7.10 General scheme of γ -selective coupling

Generally, allylic substitution of unsymmetrically substituted allylic substrates occurs competitively at the α - and γ -positions due to formation of a (π -allyl) metal intermediate (Scheme 7.9a). One way to address the issue of the regiochemical control in allylic substitution is to employ strongly nucleophilic, mostly ate-type, organometallic reagents (R-M-), such as monoalkyl heterocuprate reagents ([R-Cu-X]-). 2,3 Allylic substitution reactions of this type show characteristic γ -regioselectivity (Scheme 7.9b) [37].

According to these considerations, the authors have developed Pd-catalyzed γ -selective and stereoselective allyl-aryl coupling between allylic ester and arylboronic acids according to the general Scheme 7.10.

In order to achieve high yield, conversion, regio- and stereoselectivity, along with high stereospecificity, reaction conditions indicated in Scheme 7.10 were the result of meticulous optimization. Thus, screening of solvents showed that dichloroethane (DCE) was optimal and eliminated many ethereal and aromatic solvents. The use



Scheme 7.11 Examples of 1,3-*syn* chirality transfer

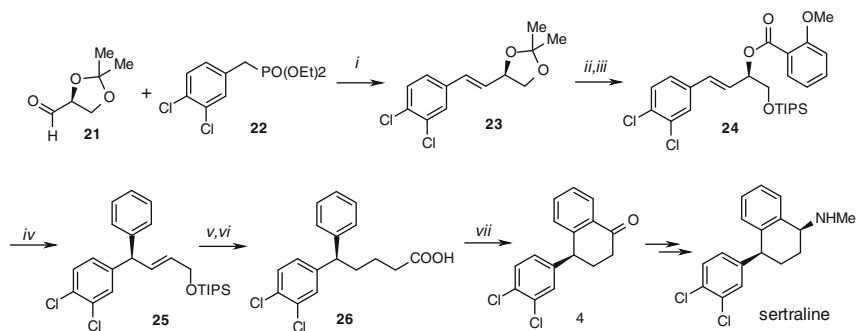
of Pd(OAc)_2 as a source of Pd(II) was essential for promotion for regioselectivity; other acyloxy ligands and other metals proved less effective. Ligand screening showed that *1,10-phenanthroline* (Phen) and 2,2'-bipyridine were equally effective and that the use of the ligand with bisimine structure ($-\text{N}=\text{C(R)}-(\text{CR})=\text{N}-$) was essential for the efficiency of the catalytic system. Finally, model experiments have shown that this reaction can be completed with excellent α - to γ -chirality transfer and *syn*-stereoselectivity (Scheme 7.11) [35].

While the first four examples, Scheme 7.11a, demonstrate the high enantioselectivity of the process, the last example, Scheme 7.11b, provides an example of diastereoselective transfer. These latter results prompted the concise formal total synthesis of sertraline according to Scheme 7.12 [37].

Starting from L-ascorbic acid, a chiral building block from nature, 2,3-isopropylidene-L-glyceraldehyde **21** was obtained and subjected to an *E*-selective Horner–Wadsworth–Emmons-type reaction [38] with phosphonate **22** to give *E*-alkene **23**. Two-step manipulation of the diol unit in **23** afforded **24** which underwent γ -allylic coupling to (*R*)-**25** with 97% e.e. and 77% yield. In the last three steps, cyclic ketone (4S)-**4** was obtained, with approximately 65% yield. This can be converted to sertraline by one of the routes described above.

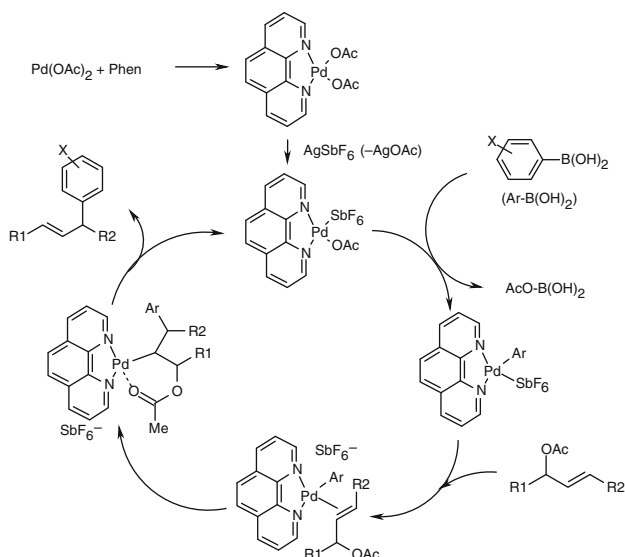
The key step in this approach, allyl-aryl coupling between allylic ester **24** and phenylboronic acid to **25**, provides a catalytic cycle in which the catalytic components indicated in Scheme 7.10 participate as outlined in Scheme 7.13.

Each step in the above cycle was experimentally confirmed by spectroscopic means and stoichiometric reactions of Pd-complexes that were considered relevant for the catalysis.



Reagents and conditions: *i.* LDA, THF/DMPU, r.t., 60%; *ii.* 1N HCl/THF, r.t., then TIPSCl, imidazole, r.t.; *iii.* 2-OMe-C₆H₄COCl, pyridine, DMAP, DCM, r.t., 80% for 3 steps; *iv.* Pd(OAc)₂, 1,10-Phen, AgSbF₆, t₁, then PhB(OH)₂, DCE, 40 °C, 2h, 77%; *v.* H₂, Pd/C, THF r.t. then TBAF, THF, r.t.; *vi.* Jones oxid., 79% for 3 steps; *vii.* ClSO₃H, 80%.

Scheme 7.12 Synthesis of sertraline, (1*S*,4*S*)-**1**; in the key step Tsuji-Trost reaction affords (*R*)-**25**



Scheme 7.13 Catalytic cycle of allyl-aryl coupling between allylic esters and arylboronic acids

7.8 Simulated Moving Bed in the Commercial Production of Sertraline

The search for a cost-effective synthetic method for the production of (4*S*)-tetralone **4**, the intermediate on the pathway to sertraline, was shifted to technology that is still new to the pharmaceutical industry – continuous chromatographic separation

of enantiomers based on a simulated moving bed (SMB) process [39, 40]. As an indication of the rapidly growing interest in SMB technology, over 1,700 papers and patents on the development and application of SMB technology are cited in electronic databases. Approximately 1,100 citations have appeared since the year 2000. Here we refer the reader to several recent monographs [41–43] and review articles [44, 45].

The operating mode of SMB is illustrated in Fig. 7.3, which presents the 12-column system. The eluent and feed streams enter the chromatographic system continuously. A counter-current solid stream is “simulated” by shifting the inlet ports periodically in the direction of the internal recycle flow. This leads to the desired separation of the feed components, two enantiomers in the case of separation of racemate, which can be withdrawn through the extract and raffinate ports which are redirected in the same manner as the inlets [46].

Conventional fixed bed chromatographic columns can be used in SMB, and the inlet and outlet ports to the unit are redirected periodically in the direction of the fluid flow to simulate, in a discontinuous manner, the continuous counter current movement of the chiral stationary phase (CSP), as presented in Fig. 7.3. Continuous

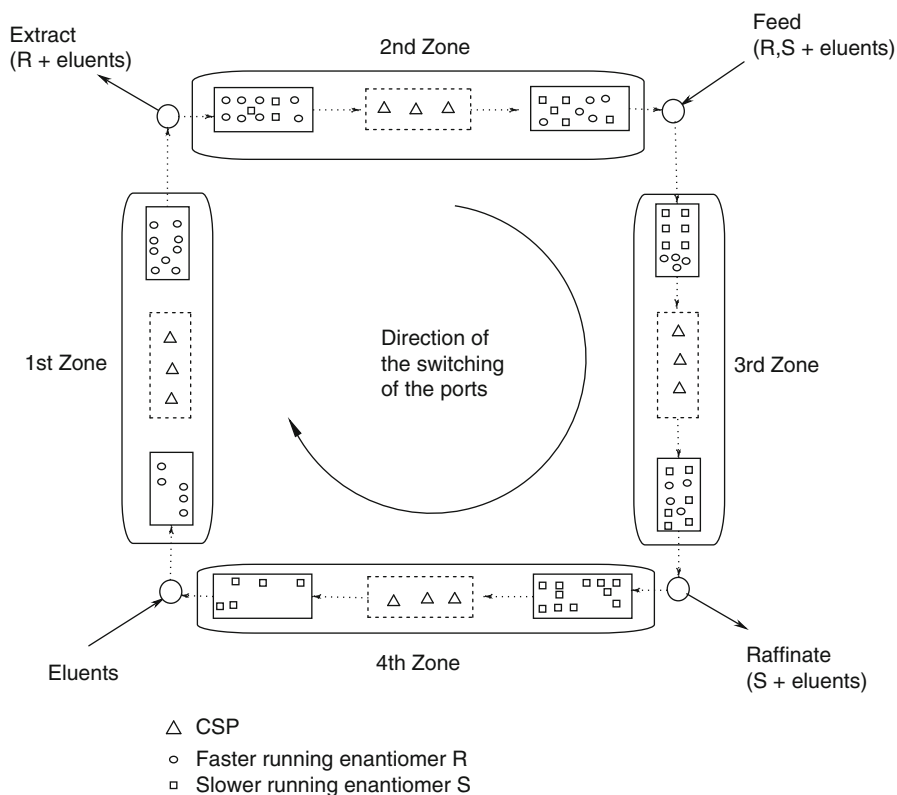


Fig. 7.3 Principle of the simulated moving bed process with twelve columns (modified from [46])

movement is simulated better when the four SMB sections consist of a large number of fixed bed columns and the port switch occurs at high frequency.

Nowadays, SMB is the technology of choice for industrial separation of larger quantities of racemates, motivated by the following benefits:

- Easy scale up of the separation process
- Short times required for implementation of the production process under good manufacturing practice (GMP) requirements
- Reduced production costs
- Broad productivity range, typically between 0.2 and 3 kg/kg CSP/day.

The following are key practical steps in the development of SMB technology:

- Screening of CSPs by standard HPLC methods
- Determination of the most effective couple CSP/eluent system
- Determination of loading capacity and adsorption isotherms for the most effective system
- Identification of the system providing the highest productivity and lowest solvent consumption.

In-process control of SMB separation has recently been improved by various automated on-line enantiomeric analysis systems. An example, comprising an analytical HPLC set-up with two UV detectors sharing the same light source, employed to monitor the internal composition profile, is presented in Fig. 7.4 [47].

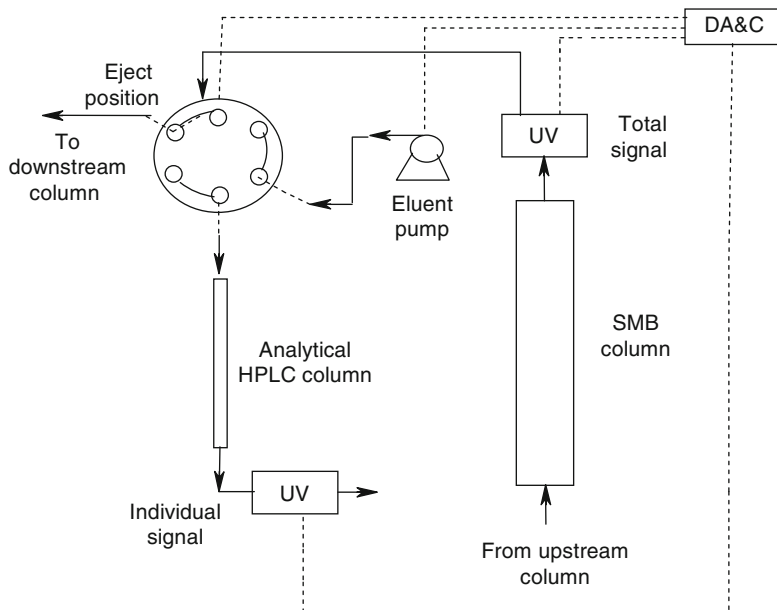


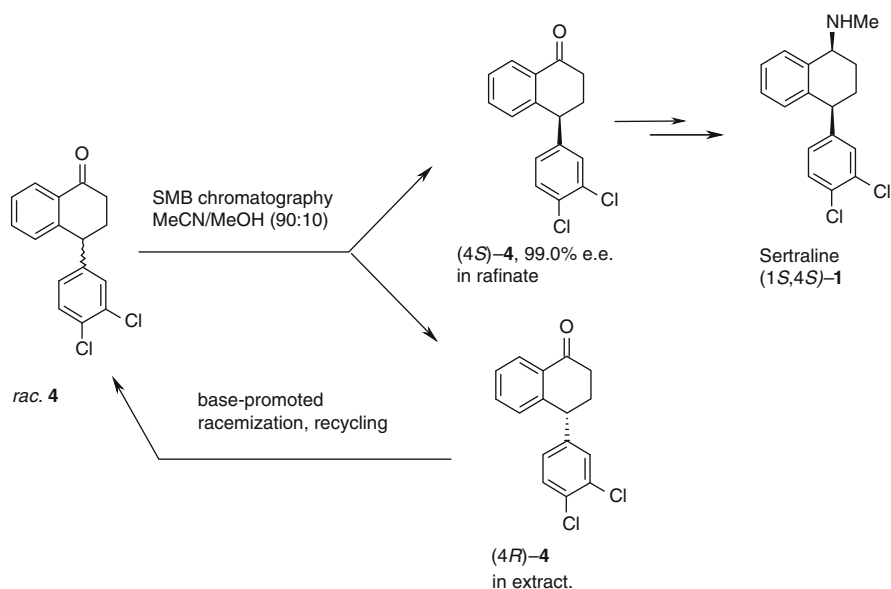
Fig. 7.4 Schematic diagram of the on-line chiral monitoring system. The main equipment comprises a six-port two-position valve, an analytical HPLC column, one HPLC pump, and two UV detectors. The set-up is fully automated (modified from [47])

This and similar monitoring systems are used in combination with combined technological steps, such as:

- SMB + separation by crystallization
- Bioreactors + SMB separation of the product
- SMB + racemization of the “wrong” enantiomer

This last tandem process was developed for the production of sertraline, and is one of the most thoroughly investigated applications of SMB technology on a large-scale [48, 49]. It provides the technology for a cost-effective production of (4*S*)-tetralone (**4**), the key intermediate in the synthetic route to sertraline. Investment in SMB technology led to a commercial production process for sertraline that increased throughput by eliminating the processing of the “wrong” (4*R*)-tetralone throughout the entire process [50, 51]. This illustrates the general rule for synthesis of chiral compounds in an enantiomerically pure form; if you have to undertake separation of enantiomers during the synthetic process, then do it as early as possible. Research at Pfizer Inc. culminated in the process depicted in Scheme 7.14 [51].

For the success of the whole process, fast, base-catalyzed racemization of the “wrong” enantiomer (4*R*)-**4** in the extract, and feeding the racemate back into the SMB unit proved to be crucial. The most important operating parameters for the pilot scale performance are given in Table 7.1 [51]. An impressive, nearly 100% recovery of the target enantiomer (4*S*)-**4** was achieved.



Scheme 7.14 SMB production scheme for enantiomerically pure 1*S*,4*S*-1

Table 7.1 Pilot-scale operating parameters and performance for SMB separation of *rac*-tetralone **4**

Column	Amylose (3-chloro-4-methyl-phenylcarbamate)
Mobile phase	MeCN/MeOH (90:10)
Number of columns	6
Column length	9.9 cm
Column diameter	4.8 cm
Feed concentration	30 g/L
Flow rate	37 ml/min
Pressure	25 bar
(4 <i>S</i>) tetralone e.e.	99.7%
(4 <i>S</i>) tetralone recovery	98.4% yield
Productivity	370 kg enantiomer/year/kg CSP

7.9 Conclusion

This overview of “chiral methodologies” used in the synthetic route to sertraline reveals the high competitiveness of lesser known methods in the production of chiral drugs in an optically pure form. The economic benefits achieved and the fast implementation of the large-scale process places SMB technology in an increasingly stronger position among other methods.

References

- McRae AL, Brady KT (2001) *Exp Opin Pharmacother* 5:883–892
- Chen Z, Skolnick P (2007) *Exp Opin Pharmacother* 9:1365–1377
- Ban TA (2001) *J Neural Trans* 108:707–716
- Skolnik P, Basile AS (2006) *Drug Discov Today Ther Strateg* 3:489–494
- Welch WM, Kraska AR, Sarges R, Koe BK (1984) *J Med Chem* 27:1508–1515
- Roman DL, Walline CC, Rodriguez GJ, Barker EL (2003) *Eur J Pharmacol* 479:53–63
- Ives JL, Heym J (1989) *Ann Rept Med Chem* 24:21
- Zhou Z, Zhen J, Karpowich NK, Law CJ, Reith MEA, Wang D-N (2009) *Nature Struct Mol Biol* 16:652–658
- Yamashita A, Singh SK, Kawate T, Jin Y, Gouaux E (2005) *Nature* 437:215–223
- Caruso F, Besmer A, Rossi M (1999) *Acta Crystallogr C* 55:1712–1714
- Quallich GJ (2005) *Chirality* 17:120–126
- Welch WM, Krasak AR, Sarges R, Koe BK (1984) *J Med Chem* 27:1508–1515
- Taber GP, Pfisterer DM, Colberg C (2004) *Or Proc Res Develop* 8:385–388
- Yun J, Buchwald SL (2000) *J Org Chem* 65:767–774
- Yun J, Buchwald SL (1999) *J Am Chem Soc* 121:5640–5644
- Verdauger X, Lange UEW, Buchwald SL (1998) *Angew Chem Int Ed* 37:1103–1107
- Verdauger X, Lange UEW, Reding MT, Buchwald SL (1996) *J Am Chem Soc* 118: 6784–6785
- Fujita K, Furukawa S, Yamaguchi R (2002) *J Organomet Chem* 649:289–292
- Cshernyik G, Bogar K, Backwall J (2004) *Tetrahedron Lett* 36:6799–6802
- Ell AH, Samec JSM, Brasse C, Backvall JE (2002) *Chem Commun.* 1144–1145

21. Samec JSM, Ell AH, Backvall JE (2005) *Chem-Eur J* 11:2327–2334
22. Blacker AJ, Stirling MJ, Page MI (2007) *Org Process Res Develop* 11:642–648
23. Berkessel A, Goroger H (2005) Asymmetric reduction of ketones by organocatalysis, Chap. 11. In: *Asymmetric organocatalysis*. Wiley-VCH, Weinheim, pp. 314–322
24. Pozzi G (2008) *Handbook of asymmetric heterogeneous catalysis*. Wiley-VCH Verlag GmbH&Co. KGaA, Weinheim, Germany, pp 181–208
25. Kuang Y, Islam NM, Nabae Y, Hayakawa T, Kakimoto M (2010) *Angew Chem Int Ed* 49:436–440
26. Figiel PJ, Leskela M, Repo T (2007) *Adv Synth Catal* 349:1173–1179
27. Quallich GJ, Blake JF, Woodall TM (1994) *J Am Chem Soc* 116:8516–8525
28. Lautens M, Rovis T (1997) *J Org Chem* 62:5246–5247
29. Lautens M, Rovis T (1999) *Tetrahedron* 55:8967–8976
30. Thompson LA, Ellman JA (1996) *Chem Rev* 96:555–572
31. Patchett AA, Nargund RP (2000) *Ann Rep Med Chem* 35:289–298
32. Miyaura N, Suzuki A (1995) *Chem Rev* 95:2457–2483
33. Thompson AS, Humphrey GR, Demarco AM, Mathre DJ, Grabowski EJJ (1993) *J Org Chem* 58:6886–5890
34. Trost BM, Van Vranken DL (1996) *Chem Rev* 96:395–422
35. Trost BM, Crawley ML (2003) *Chem Rev* 103:2921–2943
36. Ohmiya H, Makida Y, Tanaka T, Sawamura M (2008) *J Am Chem Soc* 130:17276–17277
37. Ohmiya H, Makida Y, Li D, Tanabe M, Sawamura M (2010) *J Am Chem Soc* 132:879–889
38. D Enders, M Bartsch, D Backhaus (1995) *Synlett*; 869–870
39. Juza M, Mazzotti M, Morbidelli M (2000) *Simulated moving-bed chromatography and its application to chirotechnology*. *Tibtech* 18:108–118
40. Abel S, Juza M (2007) Less common applications of enantioselective HPLC using the SMB technology in the pharmaceutical industry. In: Subramanian G (ed) *Chiral separation techniques*, 3rd edn. Wiley-VCH, Weinheim, pp 203–273
41. Cox GB (2005) *Preparative enantioselective chromatography*. Blackwell, Oxford/Ames, IA
42. Guiochon G, Fellinger A, Shirazi SG, Katti AM (2006) *Fundamentals of preparative and nonlinear chromatography*. Academic, Boston, MA
43. Schmidt-Traub H (2005) *Preparative chromatography of fine chemicals and pharmaceutical agents*. Wiley-VCH, Weinheim
44. Blaser H-U, Pugin B, Spindler F (2005) *J Mol Catal A* 231:1–20
45. Farina V, Reeves JT, Senanayake CH, Song JJ (2006) *Chem Rev* 106:2734–2793
46. Toumi A, Engell S, Diehl M, Bock HG, Schloder J (2007) *Chem Eng Process* 46:1067–1084
47. Araujo JMM, Rodrigues RCR, Eusebio MFJ, Mota JPB (2008) *J Chromatogr A* 1189:292–301
48. Lode A, Houmard M, Miglioroni C, Mazotti M, Morbidelli M (2001) *Chem Eng Sci* 56:269–291
49. Barker PE, Ganetsos G, Ajongwen J, Akintoye A (1992) *Chem Eng J* 50:B23–B28
50. Barker PE, Ganetsos G, Ajongwen J (1993) *J Chem Technol Biotechnol* 57:21–26
51. O Dapremont, F Geiser, T Zhang, SG Subramanian, RM Guinn, GJ Quallich (2002) U.S. Pat. 6,444, 854

Chapter 8

1,2-Dihydroquinolines

Abstract

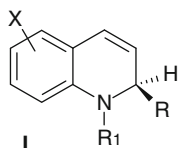
Biological target: 1,2-Dihydroquinolines (1,2-DQs) are potential candidate molecules for use as selective, non-steroidal antagonists at the glucocorticoid receptor (GCR).

Therapeutic profile: GCR antagonists have potential for use in adrenocortical hyperplasia, as in Cushing's disease. Development of GCR agonists from 1,2-DQs would expand indications to those for the broad anti-inflammatory effects of glucocorticoids.

Synthetic highlights: The synthesis of 1,2-DQs exemplifies asymmetric organo-catalysis in which enantioselective synthetic reactions are catalyzed by small organic molecules. To generate 1,2-DQs, achiral thiourea and axially chiral bi-phenols are used as catalysts for the enantioselective Petasis reaction. This is an illustration of a multicomponent reaction (MCR), for which the general concept and examples are also described.

8.1 Introduction

This chapter is not devoted to the development of a specific NDE or marketed drug, but to a synthetic process, exemplified by its application to the synthesis of a potential NDE class. It is inspired by the achievement of *asymmetric organocatalysis*, a catalytic variant of a multi-component reaction (MCR). The resulting methodology was utilized in the synthetic pathway to enantiopure 1,2-dihydroquinolines with the general formulae **I**.



R₁ = alkyl, alkenyl, or the like

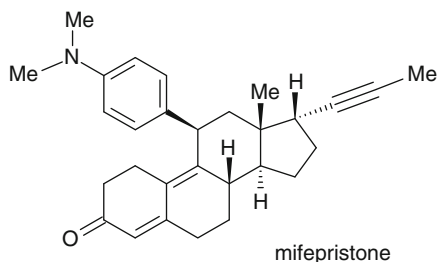
R = *ibid.*

X = aryl, heteroaryl, halogen, O-, or N-functionality

8.2 Glucocorticoid Receptor

1,2-Dihydroquinolines **I** are promising *glucocorticoid receptor* (GCR) antagonists, and therefore potential drugs for the treatment of various pathological states. The GCR is a member of the cytoplasmic steroid receptors, which are the target molecules for the actions of endocrine gluco- and mineralo-corticoid, oestrogenic and protestagenic hormones. The lipid soluble glucocorticosteroids diffuse across the cell membrane in order to bind to the GCR. This interaction initiates a variety of signal transcription reactions and translocation of the steroid–receptor complex to the cell nucleus. On binding to nuclear glucocorticoid response elements, the steroid either causes transactivation, the active expression of biologically active proteins, or transrepression, the inhibition of protein expression. The protein profile thus generated modulates essential physiological processes such as energy and bone metabolism, cell growth and differentiation, maintenance of blood pressure and immune responses [1]. Chronic excessive activation of glucocorticoid receptors induces obesity, insulin resistance, glucose intolerance, dyslipidemia, hypertension and cardiovascular disease [2, 3].

The main strategy towards pharmacological modulation of the GCR, over many years, has been the development of steroidal receptor agonists, with varying potencies, for use as anti-inflammatory drugs [4]. Recently, this search has been focused on the dissociation of anti-inflammatory actions from metabolic side effects. In contrast, despite intensive research, the only glucocorticoid receptor antagonist that is available for clinical use is the steroid, mifepristone (RU486).



Although developed as a potential GCR antagonist, mifepristone also has potent affinity for the progesterone receptor, which resulted in its marketing as an abortifacient. Although this activity limits the drug's utility as a GCR antagonist, it has received orphan drug approval for the treatment of Cushing's disease (adrenal cortex hyperplasia) and is under investigation for use in depression. There is, thus, still an unmet need for *selective non-steroidal GCR antagonists* [5]. It is, therefore, not surprising that among other structural classes being investigated, the discovery that enantiopure 1,2-dihydroquinolones act as GCR antagonists prompted a search for original approaches to the synthesis of this class of chiral heterocyclic compounds.

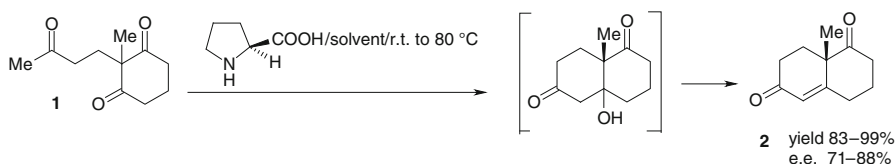
Using the reaction leading to enantiopure 1,2-dihydroquinolines **I** as an example, this chapter addresses both the principles of asymmetric organocatalysis in the Petasis-type reaction (Sect. 8.3), as well as representative *multi-component reactions* in organic synthesis (Sect. 8.4).

8.3 Asymmetric Organocatalysis: Introducing a Thiourea Catalyst for the Petasis Reaction

Asymmetric organocatalysis can be defined as enantioselective synthetic reactions that are catalyzed by small organic molecules. The term was introduced for what was long referred to as “metal-free catalysis” [6]. As opposed to transition metal complexes with organic ligands, of which many examples are given in Chaps. 5, 9, 13, 14 and 16, the catalytic activity of organocatalysts resides in the low-molecular weight organic molecule, and no transition metal is required. To some extent, organocatalysis is related to organometallic catalysis, in the same way as reactions catalyzed by enzymes which have no metal ion at the active site can be related to reactions catalyzed by metalloenzymes. It is surprising how effectively small organocatalyst molecules that mimic the active-site topology of an enzyme in the transfer of chiral information, can catalyse some reactions in a highly enantioselective manner.

In this context, it is well worth citing the classic example of the L-proline-catalyzed intramolecular asymmetric aldol reaction, involving cyclodehydration of achiral triketone **1** to yield the unsaturated Wieland–Miescher diketone **2** (Scheme 8.1) [7, 8]. In early papers, it was reported that in the presence of 20 mol% of L-proline, the diketone **2**, an important intermediate in steroid synthesis, is obtained in high yield and in approximately 70–90% enantiomeric excess (e.e.).

Due to the technological importance of this reaction, its study over a quarter of century has resulted in some fascinating improvements. For instance, the quantity of the catalyst was lowered from 200 to 3 mol%, while enantioselectivity was enhanced from 71% in MeCN at 80°C, to 88% in DMF [9, 10].



Scheme 8.1 L-Proline-catalyzed enantioselective cyclization of triketone **1** into the Wieland–Miescher ketone **2**

8.3.1 General Consideration of the Petasis Reaction

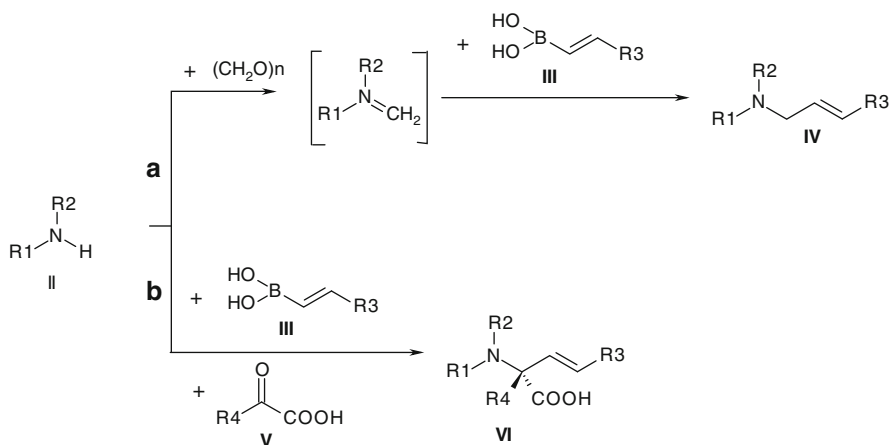
Many other fascinating examples of organocatalysis have been presented in a recent monograph and reviews [6, 11, 12]. In its original form, the Petasis reaction was developed as a three-component, non-catalytic condensation of amine, aldehyde and vinyl boronic acid (Scheme 8.2) [13, 14].

The Petasis reaction represents a boronic acid variant of the Mannich reaction, and therefore is also referred to as a borono-Mannich reaction. It was first explored with formaldehyde as the carbonyl component and alkenyl, or α,β -unsaturated organoboronic acid (**III**) as a nucleophile (route *a* in Scheme 8.2) [13]. It was later developed in a practical synthesis of α -amino acids (**VI**) from α -keto acids (**V**) and alkenyl boronic acids (**III**) [14] (route *b* in Scheme 8.2).

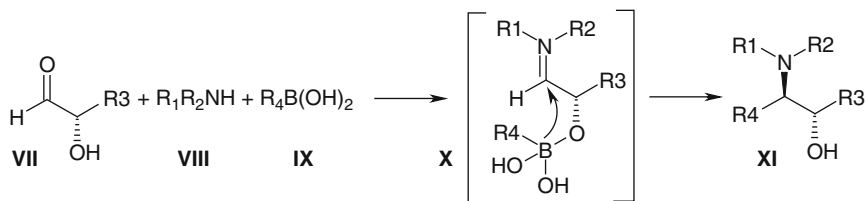
A favourable feature of the Petasis reaction, in relation to NDE synthesis, is its triple convergence to form products with multiple sites for introduction of chemical diversity. Moreover, ready availability of alkenyl boronic acids in stereochemically (*E* or *Z*) pure forms and their easy handling, prompted development of this new method for broad application in organic synthesis. Particularly important is the extension of the Petasis reaction to α -keto-carboxylic acids (**V**) in a practical synthesis of β,γ -unsaturated α -amino acids (Scheme 8.2, route *b*).

Before consideration of the catalytic, asymmetric Petasis reaction, examples of the non-catalytic, stereocontrolled, Petasis reaction are discussed. Studies on asymmetric induction in this reaction led to remarkable progress, particularly in developing the diastereoselective process with chiral α -hydroxy aldehydes (Scheme 8.3 [15]).

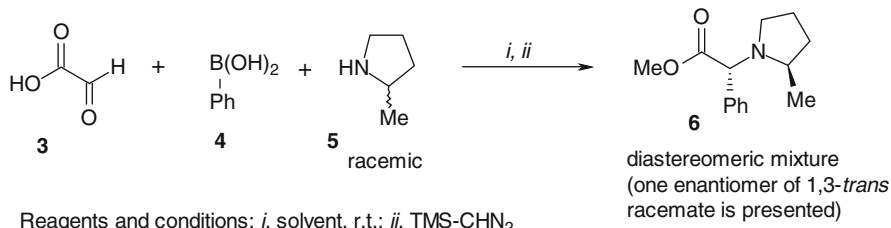
When optically pure aldehyde was used, stereocontrolled “back-side” boronation of the intermediary complex **X** assured formation of α,β -aminoalcohol **XI** in the *trans* relative configuration and defined the absolute configuration at the second stereogenic centre.



Scheme 8.2 Two variants of a three-component Petasis reaction; synthesis of; (a) β,γ -unsaturated amines, (b) β,γ -unsaturated α -amino acids



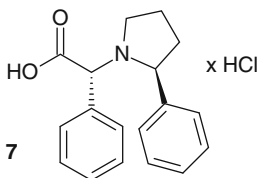
Scheme 8.3 The Petasis reaction in diastereoselective synthesis of α,β -aminoalcohols **XI**



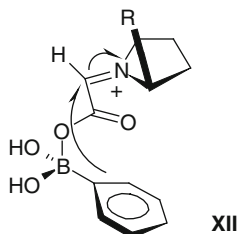
Scheme 8.4 Diastereoselective synthesis of pyrrolidine-derived arylglycine methylester **6**

This type of diastereoselective Petasis reaction was elaborated by Nanda et al in pyrrolidine-derived arylglycine synthesis (Scheme 8.4) [16].

When this reaction was completed in *hexafluoroisopropanol* (HFIP), the diastereomeric ratio was enhanced to approximately 95:5 (90.0% d.e.), and the reaction time shortened from a few days to 20 h. To establish the relative 1,3-*trans* stereochemistry between the two stereogenic centres, a single crystal X-ray structure was obtained for hydrochloride **7** (as the racemate), and from the NMR data this same stereochemistry was proposed for a series of congeners.



The observed diastereoselectivity is consistent with the addition of the aryl group to the intermediate immonium ion, in which approach of the aryl group occurs from the side opposite to the pyrrolidine 2-substituent, as presented in formula **XII**.



In a related paper, high diastereoselectivity with *secondary* amines was confirmed, while the use of chiral *primary* amines generally gives products with low to moderate diastereoselectivity [17]. Factors affecting the efficiency and stereoselectivity of this reaction, in particular of the structure of the boronate ester and amine, were also determined.

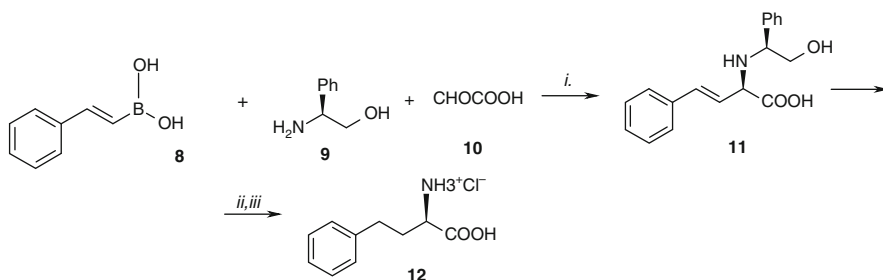
In contrast, an early paper by Petasis et al. reported that the use of a chiral amine in the optically pure form resulted in effective asymmetric induction (Scheme 8.5). Preparation of (*R*)-homophenylalanine (**12**) with >99% e.e. was achieved when (*S*)-2-phenylglycinol (**9**) was used as a chiral auxiliary [15].

It is important to note that the Petasis reaction in Scheme 8.5 is a more convenient method for preparation of α -amino acids than, for instance, Strecker or Ugi syntheses! The latter two rely on the use of undesirable cyanide ion or isocyanide reagents, and require more stringent experimental conditions. More details on both reactions are given in the next section.

Low stability of the functionalized allyl boronates may limit their synthetic application. Alternative progress towards a workable Petasis borono-Mannich reaction offers a new solution to this problem: in situ generation and use of allylboronates [18]. This one-pot route to stereo-defined α -amino acids is outlined in Scheme 8.6.

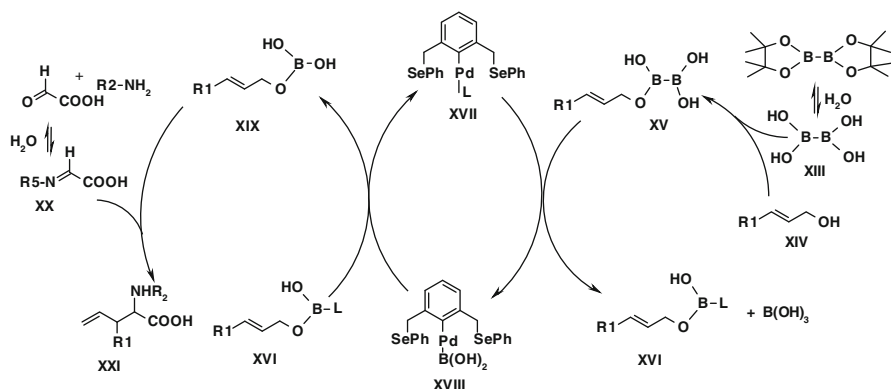
The central catalytic cycle is characterized by the use of the pincer complex **XVII**. The authors supposed that the boronate group is transferred from diboronate **XIII** to catalyst **XVII**, affording the η^1 -boronato complex **XVIII**. The boronato group substitutes the activated hydroxyl group in **XV** to give allyl boronic acid **XVI** and boric acid. Importantly, this step ensures that the waste product of the reaction is non-toxic boric acid.

Another interesting observation was made in the last step; addition of keto-acid and amine, separately, gives higher yields than addition of imine **XX** formed in the separate process. This suggests pre-co-ordination of amine to the boron atom of **XIX**, which is probably important for the in situ formation of imine **XX**. A series of β -substituted α -amino acids **XXI** obtained by this method revealed the large substrate scope of this reaction and the high *trans*-diastereoselectivity of the process. In addition, high regioselectivity was obtained, as the consequence of migration of the R_1 group from γ - to the β -position in the α -amino acids **XXI**.



Reagents and conditions: *i.* DCM, 25 °C, 12h; *ii.* H₂, Pd/C; *iii.* HCl in Et₂O.

Scheme 8.5 Petasis reaction in the synthesis of D-homophenylalanine **12**



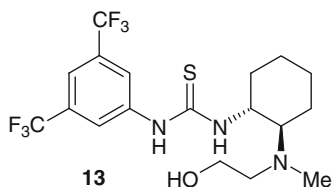
Scheme 8.6 Suggested mechanism for the one-pot four-component Petasis borono-Mannich reaction (modified from [18])

Since the Petasis boronic-Michael reaction generally requires prolonged stirring at room temperature for 24 h or more, some studies have been devoted to acceleration of this process. Ionic liquids have been shown to be convenient solvents, shortening the reaction times down to 3–4 h at room temperature [19]. The recovered ionic liquid was re-used up to five times without loss of activity. In some cases, microwave activation has been shown to achieve acceptable conversion within short reaction times [20].

Water was also reported as a suitable medium for the Petasis borono-Mannich reaction [21, 22]. Using salicaldehyde as the carbonyl component, the broad scope of this method was demonstrated, and parallel DFT calculations corroborated the experimentally observed solvent effect on the reaction rate.

8.3.2 Catalytic, Enantioselective Petasis Reaction

The enantioselective, organocatalytic variant of the Petasis reaction, developed by Takemoto and coworkers from the University of Kyoto, represents a breakthrough in the synthesis of *enantiopure 1,2-dihydroquinolines*. As mentioned before, this structural unit is present in many natural products and biologically active compounds, and therefore an effective and short synthetic route via the Petasis-type reaction to enantiopure compounds in this class is a major leap forwards. Screening of the new thiourea catalysts in the Takamoto group resulted in a highly effective catalyst **13**, specifically designed for the Petasis reaction.

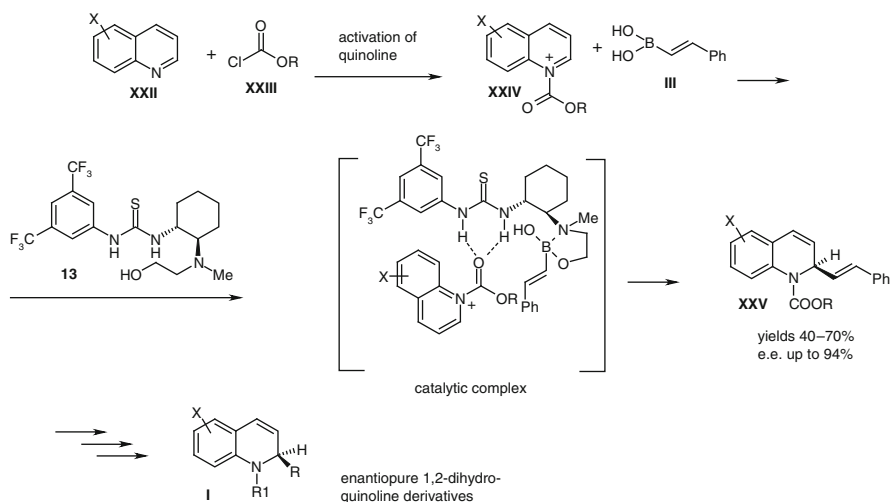


Thiourea derivatives are a specific group of organocatalysts. Most of them were developed by the groups of Jacobsen [23, 24] and Takemoto [25, 26], and designed for enantioselective or chiral variants of classic synthetic reactions, such as the Mannich reaction, Michael addition, the aza-Henry reaction, Strecker cyanide addition and some others.

All organocatalytically active thiourea derivatives comprise a set of H-bond donor/acceptor units within a chiral scaffold, activating the reaction partners by hydrogen bonding in the reactive complex. The thiourea catalyst **13** has a chelating, chiral, aminoalcohol functional group, in addition to the thiourea unit. This combination of functional groups can activate organoboronic acids, by co-ordination to the boron centre, and direct the stereochemical outcome of the Petasis reaction by concomitant co-ordination of the quinolone carboxylic acid ester, as outlined in Scheme 8.7 [26].

In this reaction, the chiral thiourea moiety acts as a Bronsted acid and activates both the N-acylated quinolinium salt **XXIV** and unsaturated boronic acid **III**, enhancing the electrophilic character of the quinolinium unit in the “ate” catalytic complex with bifurcal hydrogen bond. Such activation of the two reaction partners permits enantioselective formation of the C–C bond at the stereogenic centre C(2) as a result of interaction between the nucleophilic terminal carbon of the C=C bond in boronic acid and the electrophilic C(2)-atom α - to the ammonium cation in the quinolinium unit.

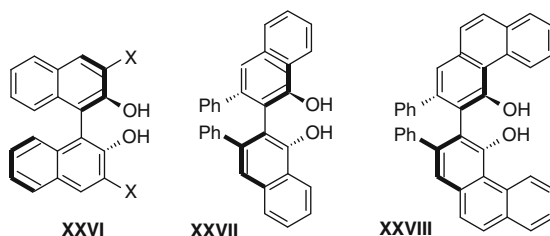
The broad application of the organocatalytic Petasis reaction is revealed by the total syntheses of quinoline alkaloids and their congeners with biological activity. The enantiomeric purity obtained in this reaction of 1,2-dihydroquinolines with the



Scheme 8.7 The chiral thiourea **13** catalyzed Petasis reaction as a source of enantiopure 1,2-dihydroquinoline derivatives **I**

general formulae **I**, amounts to approximately 95% e.e. [27, 28], affording valuable chiral building blocks for the synthesis of NDEs. This is particularly applicable to inhibitors of hormone sensitive lipase, used in the treatment of lipid and glucose disorders [29], or agents for the treatment of diseases associated with inhibition of the glucocorticoid receptor [30].

Broad biological potential of enantiopure 1,2-dihydroquinolines prompted the recently reported organocatalytic, asymmetric Petasis reaction, catalyzed by chiral biphenols [31]. Since it was observed that chiral biphenol derivatives **XXVI–XXVIII** serve as proficient catalysts for asymmetric reactions involving boronates [32, 33], the authors postulated that they could be used as ligands in multi-component condensation reactions, and the Petasis reaction in particular.



Exploratory research revealed the particular efficacy of vaulted biaryl phenol **XXVIII** as organocatalysts. Under optimized conditions, the *secondary* amines, ethyl glyoxalate and diethyl boronate ester afforded α -amino acid esters **14–17** in high yield and with over 90% e.e. (Table 8.1) [33].

The course of this reaction has been studied by spectroscopic methods, NMR and ESI-MS, and single ligand exchange was observed [33]. Monitoring of the reaction by ^{11}B NMR demonstrated conversion of a trivalent vinyl boronate to a tetravalent boronate species, and the involvement of aminals in this process.

In view of the multi-component nature of the Petasis reaction, a general consideration of the MCR concept is briefly presented in the next section, in order to complete the picture of the mechanism and synthetic scope of these reactions.

Table 8.1 Asymmetric Petasis reaction catalyzed by biaryl phenol **XXVIII**

Entry	R_1NHR_2	Product	Yield %	e.e. %
1	BnNHMe	14	81	90
2	BnNHt-Bu	15	73	86
3	BnNH(CH ₂) ₂ Ph	16	82	94
4	BnNH(CH ₂) ₂ CN	17	80	97

8.4 Multi-component Reactions: General Concept and Examples

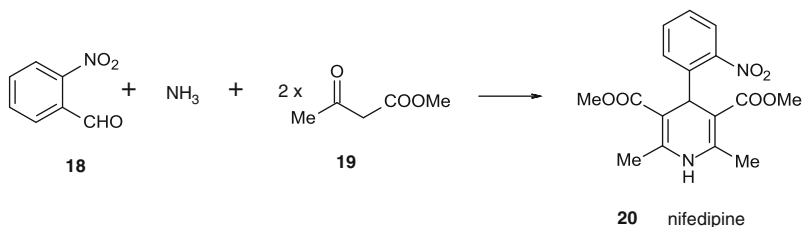
The organocatalytic Petasis reaction is a three-component reaction, since in the critical step of the reaction process one molecule of thiourea catalyst, an *N*-acylquinolinium or *N*-acyliminium ion, and boronic acid form the productive complex. It represents a specific case of an MCR in the sense that one component has a catalytic effect in promoting covalent bond formation between the other two partners. It is important to emphasize, however, that in MCRs *not all reacting molecules undergo simultaneous interaction*, which represents an entropically highly unfavourable event. Rather, an MCR is a well-defined sequence of bimolecular interactions, in which the intermediate formed during the first and the second stages, interacts with the third, and in some cases with the fourth component in the MCR.

8.4.1 General Concept of Multi-component Reactions

Multi-component reactions are highly variable, enabling the synthesis of a large number of products from only a few starting substances. Since MCRs are one-pot reactions and single-step conversions, they are, therefore, economical with resources and come close to what is defined as an “ideal synthesis” [34]. Despite this, the broad value of MCRs was not recognized until 1961, when I. Ugi described the most important variants of the *four-component reactions* [35]. This is a shame, because some *three-component reactions* had already been widely in use for 150 years before Ugi’s discovery! They became “name reactions”, honouring their inventors, such as Strecker synthesis of α -amino acids, that was first published in 1850 [36]; Hantsch synthesis of 1,4-dihydropyridines [37], the Mannich reaction [38], and the somewhat less known Biginelli [39] and Passerini reactions [40]. Chronologically, one of the earliest examples is the Hantsch four-component synthesis of 1,4-dihydropyridines [37]. This reaction soon entered the laboratory manuals and most recently became the basis for production of 1,4-dihydropyridines for the therapy of cardiovascular diseases; the example of nifedipine (**20**) synthesis is given in Scheme 8.8 [41].

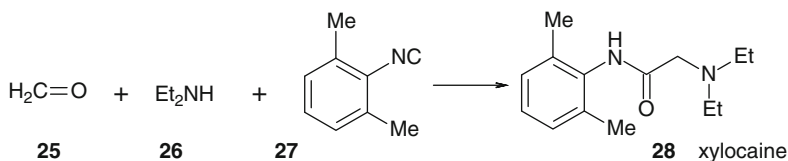
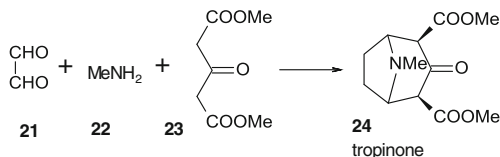
Robinson’s synthesis of alkaloid tropinone (**24**), an achiral, *meso*-structure, represents an elegant application of the Mannich reaction to dialdehyde **21**, methylamine **22**, and C–H acid keto-diester **23** (Scheme 8.9) [42].

Nowadays, MCRs are widely recognized as powerful tools for the synthesis of compound libraries, but also as an economic approach to selected single molecules. Examples include effective approaches to heterocycles, such as indoles [43] and benzofuranes [44]. According to SciFinder, only during the period 2005–2010, approximately 2,700 MCRs were reported.



Scheme 8.8 The four-component Hantzsch reaction in the synthesis of nifedipine **20**

Scheme 8.9 The three-component Mannich reaction in the synthesis of tropinone **24**



Scheme 8.10 Three-component Ugi reaction in the synthesis of xylocaine **28**

8.4.2 Efficient, Isocyanide-Based Ugi Multi-component Reactions

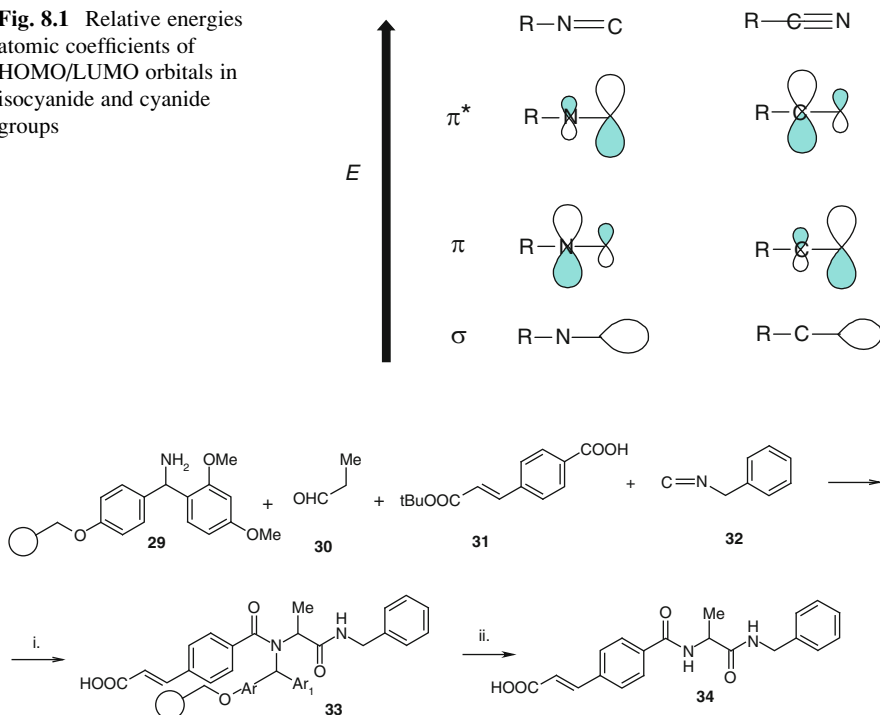
A final example is the one-step, three-component variant of the Ugi reaction (Scheme 8.10), according to which an important local anaesthetic agent, xylocaine (**28**), was synthesized from formaldehyde, diethylamine and 2,6-dimethyl-phenylisocyanide [45].

Why are Ugi's MCRs so efficient? The answer lies in the low activation energies of all the elementary steps, which are either equilibrium processes or irreversible steps. This concept of energetically preferred reactions is discussed in Chap. 15, in relation to click-reactions of azides and alkynes. Low-energy elementary reactions either occur in concert and are pericyclic or involve two reacting groups with highly matching electron distribution.

The high nucleophilic character of the isocyanide group can be explained by the ambivalent electronic nature of the two-valent carbon atom of this group, which determines its extraordinary reactivity (Fig. 8.1) [46].

The high reactivity of isocyanides and cyanides is due to the atomic coefficients of their respective HOMO/LUMO orbitals. Compared to alkyl nitriles, the atomic

Fig. 8.1 Relative energies atomic coefficients of HOMO/LUMO orbitals in isocyanide and cyanide groups



Reagents and conditions: i. MeOH/CHCl₃, r.t.; ii. 10% TFA/DCM.

Scheme 8.11 The four component Ugi reaction; one component is maintained on a solid support

coefficient of the π^* -orbital (LUMO) is higher in the C-atom of isocyanide, conferring high nucleophilic properties to this atom. Electrophiles first react with the σ -orbital (HOMO) and thereafter again with the C-atom of isocyanide. Thus, depending on the reacting partner, the C-atom of isocyanides behaves either as an electrophilic or a nucleophilic centre. This property results in the controlled formation of α -adducts with both reacting species, in contrast to cyanides which react at the C-atom with electrophiles and at the nitrogen with nucleophiles.

Bearing in mind the exceptional electronic character of the R-N=C group, and the divalent nature of the carbon atom in this group, let us now consider one of the most fascinating reactions in organic synthesis: Ugi's 4-component reaction (4CR) [35, 46]. This is illustrated in Scheme 8.11 by the specific case in which the Rink resin acts as the carrier of the amino-component and allows the synthesis of a library of structural congeners [47].

After completion of the 4CR-step, washing with 10% TFA leads to concomitant hydrolysis of the *tert*-Bu ester group and cleavage of the product **34** from the polymer. A common element of the library, prepared according to Scheme 8.11, was *tert*-butyl-4-carboxycinnamate **31**, and by variation of the aldehyde and isocyanide component other members were obtained. A multi-component approach to

34, representative of the library of potent inhibitors of haematopoietic (blood-forming) protein-tyrosine phosphatase, was reported by chemists at Ontogen [47, 48]. Compound **34** exhibited high activity at micromolar concentrations (IC_{50} 3.9 μM) [47]. Since this enzyme is over-expressed in acutely leukemic cells, these compounds exhibited a promising biological profile for the treatment of leukemia.

8.5 Conclusion

Most multi-component reactions are particularly convenient for the production of compound libraries, also called compound collections during the pioneering phase of this MCR methodology. To build up such libraries, a particularly convenient approach is to anchor one component on a solid-phase, while combining the other three components in solution, as exemplified in Scheme 8.11. Many variants of 4CRs have found broad application in innovative pharmaceutical companies for building up compound libraries with rather complex scaffolds. This method also allows for structural variations that are inaccessible to multi-step synthesis. The story of MCRs, from named reactions to highly specific new reactions, such as Petasis and Ugi reactions, reflects the development of synthetic organic chemistry towards entropically unfavourable processes, and the synthesis of new structures beyond the reach of classical methods.

References

1. Odermatt A, Gummy AC (2008) *Chimia* 62:335–339
2. Steffensen KR (2006) *Advances in molecular and cellular endocrinology*. Elsevier BV, 63–89
3. Walker BR (2007) *Eur J Endocrin* 157:545–559
4. Tanaka H, Yoshikawa N, Shimizu N, Morimoto C (2007) *Inflamm Regen* 27:486–493
5. Mohler ML, He Y, Wu Z, Hong S-S, Miller DD (2007) *Expert Opin Ther Pat* 17:59–81
6. Berkessel A, Groger H (2005) *Asymmetric organocatalysis*. Wiley-VCH, Weinheim
7. Eder U, Sauer G, Wiechert R (1971) *Angew Chem Int Ed* 10:496–497
8. Hajos ZG, Parish DR (1974) *J Org Chem* 39:1612–1615
9. Eder U, Wiechert R, Sauer G, (for Schering AG), DE 2014757
10. Hajos ZG, Parish DR, (Hofmann la Roche and Co., AG), DE2102623
11. Notz W, Tanaka F, Barbas CF III (2004) *Acc Chem Res* 37:580–602
12. Donniell MJO (2004) *Acc Chem Res* 37:506–517
13. Petasis NA, Akritopoulou I (1993) *Tetrahedron Lett*: 583–586
14. Petasis NA, Zavialov IA (1997) *J Am Chem Soc* 119:445–446
15. Petasis NA, Zavialov IA (1998) *J Am Chem Soc* 120:11798–11799
16. Nanda KK, Trotter RW (2005) *Tetrahedron Lett* 46:2025–2028
17. Southwood TJ, Curry MC, Hutton CH (2006) *Tetrahedron* 62:236–242
18. Selander N, Kipke A, Sebelius S, Szabo KJ (2007) *J Am Chem Soc* 129:13723–13731
19. Yadav JS, Subba Reddy BV, Naga Lakshmi P (2007) *J Mol Catal A* 274:101–104
20. McLean NJ, Tye H, Whittaker M (2004) *Tetrahedron Lett* 45:993–996

21. NR Candeias, LF Veiros, CAM Alfonso, PMP Gois (2009) *Eur J Org Chem*: 1859–1863
22. Candeias NR, Cal PMSD, Andre V, Duarte MT, Veiros LF, Gois PMP (2010) *Tetrahedron* 66:2736–2745
23. Yoon TP, Jacobsen EN (2003) *Science* 299:1691–1693
24. Yoon TP, Jacobsen EN (2005) *Angew Chem Int Ed* 44:466–468
25. Hoashi Y, Okino T, Takemoto Y (2005) *Angew Chem Int Ed* 44:4032–4035
26. Inokuma T, Hoashi Y, Takemoto Y (2006) *J Am Chem Soc* 128:9413–9419
27. Yamaoka Y, Miyabe H, Takemoto Y (2007) *J Am Chem Soc* 129:6686–6687
28. AA. *Synthesis (Synform)* 2007/04, A46–A48
29. Ebdrup S, Hansen HK, Vedso P, Cornelis De Jong J, Jacobsen P (for Novo Nordisk), PCT WO 2003/05 1842 A3
30. Matsuda M, Mori T, Kawashima K, Nagatsuka M, Kobayashi S, Yamamoto M, Kato M, Takai M, Oda T (for Santen Pharmaceutical Co.) PCT WO 2007/03 2556 A1
31. Wu TR, Chong MJ (2005) *J Am Chem Soc* 127:3244–3245
32. Lou S, Moquist PN, Schaus SE (2007) *J Am Chem Soc* 129:15398–15404
33. Lou S, Schaus SE (2008) *J Am Chem Soc* 130:6922–6923
34. Wender PA, Handy ST, Wright DL (1997) Towards the ideal synthesis. *Chem Ind*: 765–772
35. Ugi I, Steinbruckner C (1961) *Chem Ber* 94:734–742
36. Stecker A (1850) *Liebigs Ann Chem* 75:27–45
37. Hantsch A (1882) *Liebigs Ann Chem* 215:1–82
38. Tramontoni M, Angiolini L (1994) *Manich bases-chemistry and use*. UCR, Boca Raton, FL
39. Biginelli P (1891) *Ber Dtsch Chem Ges* 24:1317–1319
40. Passerini M (1922) *Gazz Chim Ital* 52:432–443
41. Bossert F, Meyer H, Wehinger R (1981) *Angew Chem Int Ed* 20:762–769
42. Robinson R (1917) *J Chem Soc* 111:876–899
43. Heravi MM, Baghernejad B, Oskooie HA, Hekmatshoar R (2008) *Tetrahedron Lett* 49:6101–6103
44. Chen RE, Wang YL, Chen ZW, Su WK (2008) *Can J Chem* 86:875–880
45. Ugi I, Steinbruckner C (1959) (for A. B. Astra) DE-B, 1, 103, 337
46. Domling A, Ugi I (2000) *Angew Chem Int Ed* 39:3168–3210
47. Cao X, Moran EJ, Siev D, Lio A, Ohashi C, Mjalli AMM (1995) *Bioorg Med Chem Lett* 5:2953–2958
48. Moran EJ, Shashar S, Cargill JF, Shabaz MM, Lio A, Mjalli AMM, Armstrong RW (1995) *J Am Chem Soc* 117:10787–10790

Chapter 9

(–)-Menthol

Abstract

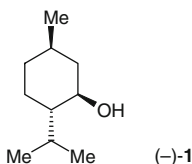
Biological target: Menthol is a natural terpenoid with agonist activity at the thermoreceptive, non-selective cation channel, transient receptor potential melastatin type 8 (TRPM8). Present on nerve fibres and skin cells, these channels are activated by a fall in temperature and mediate analgesia. Menthol is also an agonist at GABA_A receptors, for which (+)-menthol reveals stereoselectivity.

Therapeutic profile: (–)-Menthol is a household medicament, widely used as a local anaesthetic and analgesic, to reduce itching, as a gastric sedative agent and as a decongestant.

Synthetic highlight: Diastereoselective production of *rac*-menthol from its aromatic precursor is achieved by site-selective isopropylation and diastereoselective hydrogenation to the *all-trans* racemate. Enantioselective allylic amine–enamine–imine rearrangement of an acyclic diene–allylic amine, catalyzed by an Rh(I)–(–)-BINAP complex, affords (–)-menthol; the process has been scaled-up to production of 1,000 tons/year.

9.1 Introduction

(–)-Menthol (**1**, (1*R*,3*R*,4*S*)-1-methyl-3-hydroxy-4-isopropyl-cyclohexane; IUPAC name (1*R*,2*S*,5*R*)-2-isopropyl-5-methylcyclohexanol), is a natural compound, a fragrant terpenoid present in peppermint and other mint oils.



(–)-Menthol has been used for centuries as a local anaesthetic, a topical analgesic, an antipruritic agent, a gastric sedative agent, and is also widely used as an *over-the-counter* (OTC) decongestant cold medication [1]. It is a weak inhibitor of inflammation and the associated increased sensitivity to pain (hyperalgesia), and is

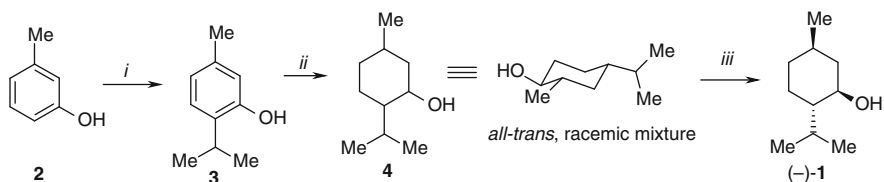
used as a promoter of drug penetration through the skin [2]. At least some of the pharmacodynamic actions are related to the agonistic activity of (–)-menthol at the cold-activated cation channel, *transient receptor potential melastatin type 8* (TRPM8), which is highly sensitive to temperature and extracellular calcium. TRPM8 channels on nerve fibres and skin cells not only respond to a decrease in ambient temperature, but their activation also mediates analgesia. There are reports of the antibacterial activity of (–)-menthol [3] and induction of peripheral vasodilatation (which in the scalp, can be hair-growth promoting) [4].

A recent study on (+)-menthol, which is an enantiomer also present in varying amounts in the natural product, revealed its activity at the γ -aminobutyric acid (GABA_A) receptor for which the natural compound is only a weak agonist [5]. GABA_A receptors are predominant ionotropic receptors for fast inhibitory neurotransmission in the central nervous system (CNS). These receptors are recognized as important targets for modulation by sedative, anxiolytic and general anaesthetic agents [6]. It is, therefore, of considerable interest that (+)-menthol acts as a general anaesthetic with a potency that corresponds to its ability to enhance the GABA current, comparable to that of well-known CNS active compounds. This suggests a more selective agonist action of the (+)-enantiomer at GABA_A receptors.

9.2 Natural Sources and First Technological Production of (–)-Menthol

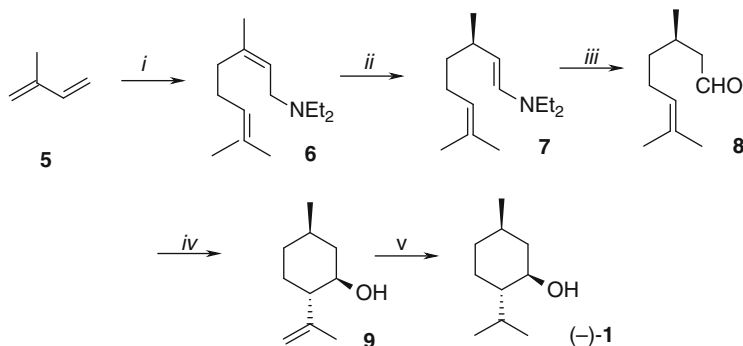
World-wide production of (–)-menthol has reached 4,500 tons/year, prompted by its use as an important ingredient in personal care products, perfumes and in the pharmaceutical industry. Being a natural product, until 1984, all (–)-menthol on the world market originated from the natural source, *Mentha arvensis*, and the restricted supply has maintained its high price. It is worth noting that natural sources (e.g., rose oil) provide a mixture of enantiomers containing up to 80% e.e. (–)-menthol [4]. Syntheses of racemic menthol have been reported, and the separation of the (–)-enantiomer has been claimed by crystallization of diastereomeric derivatives [7], even at elevated pressure [8]. An overview of the various methodologies applied in the production of enantiomerically pure (–)-menthol has been published [9]. Most of these have remained little more than academic achievements until the revolutionary breakthrough made by Japanese chemists, both from academia and industry.

The first successful industrial production of (–)-menthol was based on 3-methyl-phenol **2**, which was transformed in two steps into 2-isopropyl-5-methyl cyclohexanol **4**, i.e., into the menthol skeleton (Scheme 9.1) [10]. This structure has three stereogenic centres and therefore $2^3 = 8$ stereoisomers. The inherent beauty of this process resides in the complete regioselectivity of isopropylation, controlled stereoelectronically by the two substituents on the aromatic ring, and the high diastereoselectivity of hydrogenation to the *all-trans* product, one of three possible racemic diastereomers.



Reagents and conditions: *i.* propylene-SiO₂/Al₂O₃; *ii.* H₂-Cu chromate catal.; *iii.* optical resolution

Scheme 9.1 An early production process for racemic menthol and resolution to (–)-menthol



Reagents and conditions: *i.* NHEt₂–LiNEt₂; *ii.* Rh(I)–BINAP; *iii.* H₂SO₄; *iv.* ZnBr₂; *v.* H₂–catal.

Scheme 9.2 Takasago Co. process for production of (–)-menthol

9.3 Enantioselective Allylic Amine–Enamine–Imine Rearrangement, Catalysed by Rh(I)-(–)-BINAP Complex

The enantioselective approach to (–)-menthol is outlined in Scheme 9.2 [11]. It is a real challenge to our understanding of synthetic chemistry that such a simple short synthetic route, which starts from the achiral natural hydrocarbon isoprene, well known for its huge consumption by the rubber industry, can afford a chiral, cyclic alcohol with three stereogenic centres in defined absolute configurations and with high enantiopurity!

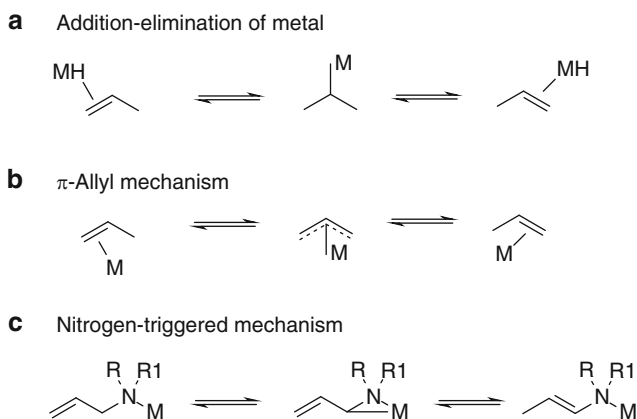
All the knowledge accumulated over the years at Takasago Research Institute, Tokyo, headed by S. Akutagawa, and by the research team of R. Noyori, Nobel Laureate for chemistry in 2001, prompted the development of an industrial process for the production of (–)-menthol by this method. Superficial observation of this scheme, and the list of reagents cited for the steps *i*–*v*, do not reveal the impressive mechanistic knowledge which has been gained on nearly all steps on this route to (–)-menthol. Already in the first step (*i*), reaction conditions in the alkylation of

the diethylamide anion by isoprene **5** allow complete control of the formation of *Z-cis*-allyl amine **6**. This stereochemical outcome (stereoselective in two dimensions!) defines enantioselectivity in the next step (*ii*), Rh(I)-(–)-(BINAP) catalyzed formation of the C(3) stereogenic centre in the enamine **7** with the (*R*)-configuration. Mechanistic details behind the enantioselective bias for allylic migration in step *ii* are discussed below. By hydrolysis of the enamine **7**, the aldehyde **8** is produced in a very high yield, and with enantiomeric purity greater than 98%. The unsaturated aldehyde undergoes intramolecular ene-reaction, mediated by zinc dibromide, step *iv*, which is completely controlled by the first chiral centre. The unsaturated precursor of (–)-menthol, (–)-isopulegol (**9**), also present in nature, is formed in an *all-equatorial* form with high optical purity. By one crystallization step at -50°C , the e.e. can be increased to 100%, and this material is used in the hydrogenation step (*v*) to obtain essentially optically pure (–)-menthol (**1**).

The mechanistic and stereochemical aspects of the individual steps of Scheme 9.2, which contribute to the elegance of this route, will now be discussed in more detail.

Let us start with a consideration of the metal ion-promoted migration of an allylic C=C bond (Scheme 9.3). There are various mechanisms involved in this process, dependent on the electronic properties of the metal ion [12]. In the first case (a), the reactive metal hydride undergoes addition to π -electrons of the double bond, forming a covalent bond with the more electronegative carbon atom. Abstraction of the hydride ion from the second terminal carbon completes the migration process. More “soft” metal ions form co-ordinative bonds through their d-electrons and promote migration of the C=C bond *via* the delocalized π -allylic system (b).

The final mechanistic pathway (c), the so-called nitrogen-triggered mechanism, is responsible for the enantioselective route to (–)-menthol. It comprises, first, co-ordination to the electronegative N-heteroatom followed by abstraction of the acidic α -proton and formation of the three-membered metallacycle. This intermediate



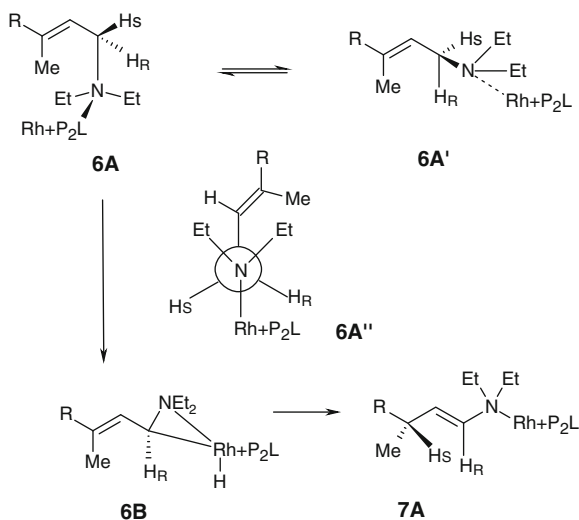
Scheme 9.3 Mechanisms of metal-mediated, double-bond migration

facilitates migration of the double bond to the enamine position, forming a relatively unstable species.

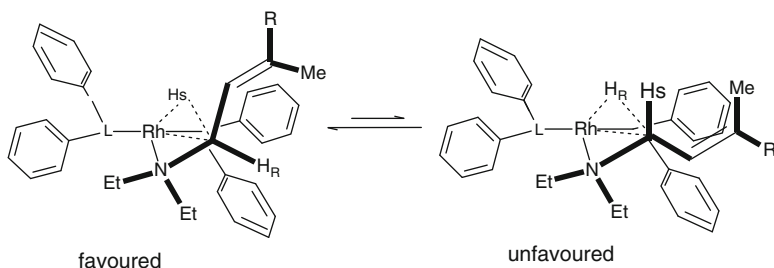
More detailed insight into the stereochemistry of the allylic migration is presented in Scheme 9.4, which accounts for the formation of the stereogenic centre in the prochiral substrate **6** [13]. For the co-ordination of Rh(I) and chirality transfer, the most effective chiral diphosphine proved to be BINAP, discussed below. Two allylic protons H_S , H_R , in the complex **6A** became diastereotopic, i.e. chemically non-equivalent. Free rotation around the C–C single bond permits equilibrium with **6A'**, with an inverted position of the two diastereotopic H-atoms. To control the stereoselectivity of this process, the topology of the complex must be well defined and the energy of the preferred conformer, **6A** or **6A'** in the Scheme 4, should be significantly lower. Assuming that the chiral topology of the R^+P_2L unit in the complex stabilizes conformer **6A''**, the hydride ion H_S will be abstracted by Rh(I), as a consequence of Rh C–H insertion, and an Rh-hydride complex **6B** is formed. This complex favours suprafacial hydride transfer and its appearance as an H_S atom at the front side of the γ -carbon that in **7A** becomes a stereogenic centre with an *S*-absolute configuration.

Visualization of the steric preference for abstraction of H_S in **6A** is given in Scheme 9.5.

Two orientations of the allyl amine, with the *E*- (*trans*) configuration around the C=C bond in the Rh(I)-(S)-(-)BINAP complex, are presented. The detailed topology of (-)-BINAP, however, is of the outmost importance for the understanding of the enantioselectivity or stereochemical bias of allylic migration. Therefore, structural formulae of BINAP enantiomers and the X-ray structure of the Ru(II) dicarboxylate complex of (S)-(-)-BINAP are presented in Figure 9.1 [14]. The structure of the complex is characterized by the axial chirality of the dinaphthyl unit and the “butterfly like” disposition of the aromatic rings in the diphenylphosphine unit.



Scheme 9.4 Conformational equilibrium that controls stereochemistry of the Rh(I)-catalyzed allylic migration



Scheme 9.5 Presentation of two possible transition states in the step **6A–6B**

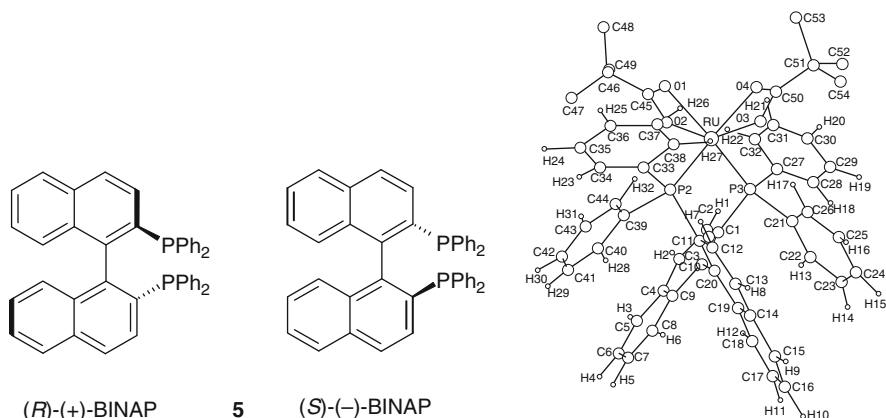


Fig. 9.1 Structural formulae of (*R*)-(+)- and (*S*)-(–)-BINAP and X-ray structure of the Ru(II)-dicarboxylate complex of (*S*)-(–)-BINAP (Reproduced from [14], with the permission of the American Chemical Society)

The whole assembly forms a well-defined chiral cleft that can accommodate the reacting prochiral molecule. Such favoured and unfavoured orientations of the allylic amine substrate, in the transition state of allylic migration within the Rh(I)-(–)-BINAP complex, are schematically presented in Scheme 9.5. As a consequence, in the favoured complex, the H_S proton is abstracted and suprafacially transposed to the γ -carbon atom creating a stereogenic centre with the (*R*)-configuration.

9.4 Production Scale Synthesis of Both Enantiomers

The synthetic method presented in Scheme 9.2 was scaled-up for industrial production of 1,000 tons/year of (–)-menthol. It represents a brilliant application of (–)-BINAP as a chiral ligand in organometallic catalysis [15]. The technical process development required, among other factors, enhancement of catalyst productivity, expressed as

turnover number (TON, in moles of enamine produced by 1 mol of the catalyst), to cope with the high prices of metal (Rh) and ligand. The already high efficiency of the catalytic system was enhanced impressively; from a TON of approximately 100, at the initial laboratory stage, to about 400,000 in the continuous production of (–)-menthol. The efficiency and enantioselectivity of the isomerization process, at this level, compares well with many enzyme-catalyzed reactions. In view of the recently observed biological activity of the non-natural enantiomer, (+)-menthol [5], it is important to note the entirely equal availability of enantiomeric (*R*)-(+)-BINAP, the ligand in the catalytic complex which will afford this enantiomer of menthol with exactly the same efficacy and optical purity!

9.5 Conclusion

In developing a pathway to the large-scale production of (–)-menthol, organic chemical synthesis has demonstrated its versatility and efficiency. The efficacy of the Rh(I)-BINAP system in allowing asymmetric isomerization of the allylamine **6** to enamine **7**, and the complete selectivity of the zinc bromide catalyzed ene-reaction to form the substituted cyclohexane derivative **9**, with all three stereogenic centres in the right configuration, demonstrate that relatively inefficient laboratory procedures may be transformed into economic industrial processes. Late-stage development of a drug and its successful marketing heavily depend on such contributions from synthetic chemistry, reduced to practice by the collaboration of many creative laboratory chemists and engineers in the production plant.

References

1. (2003) Skin Protecting Drugs for Over-the-counter Use, US Federal register 68 (107): 33362–33381
2. Kang CW, Yap PF, Lim C, Chen YZ, Ho PC, Chan YW, Wong GP, Chan SY (2007) J Control Release 120:211–219
3. Kotan R, Kordali S, Cakir A (2007) J Biosci 62:507–513
4. Kaneda K, Matsuda K, (2007) Jpn Kokai Tokkyo Koho. JP 2007169233, A 20070705
5. Watt EE, Betts BA, Kotey FO, Humbert DJ, Griffith TN, Kelly EW, Veneskey KC, Gill N, Rowan KC, Jenkins A, Hall AC (2008) Eur J Pharmacol 59:120–126
6. Krasowski MD, Harrison NL (1999) Cell Mol Life Sci 55:1278–1303
7. House DW (1983) Resolution of d,l-menthol. US 4418225, A 19831129
8. Cahn RP (1992) Optical isomer separation by crystallization under pressure. Jpn Kokai Tokkyo Koho, JP 04260401, A 19920916
9. Hopp R (1996) (–)-Menthol, an example of the various methodologies applied in the production of enantiomers. Rivista Italiana EPPOS 7:111–130
10. Chaplin JA, Gardiner NL, Mitra RK, Parkinson CJ, Portwig, Madrie; Butana AM, Dickson MDE, Brady D, Marais SF, Reddy S (2002) Process for preparing (–)- menthol and similar compounds via enzymic resolution. PCT Int Appl, WO 2002004384 A2

11. Tani K, Yamagata T, Akutagawa S, Kumobayashi S, Taketomi T, Takaya H, Miyashita A, Noyori R, Otsuka S (1984) *J Am Chem Soc* 106:5208–5217
12. Rylander PN (1973) *Organic synthesis with noble metal catalysts*, Chap. 5. Academic, New York
13. Yamakawa M, Noyori R (1992) *Organomet* 11:3167–3169
14. Ohta T, Takaya H, Noyori R (1988) *Inorg Chem* 27:566–569
15. Akutagawa S (1998) A practical synthesis of (–)-menthol with Rh-BINAP catalyst. In: Collins AN, Sheldrake GN, Crosby J (eds) *Chirality in Industry*. Wiley, NJ, pp 313–324

Chapter 10

Fexofenadine Hydrochloride

Abstract

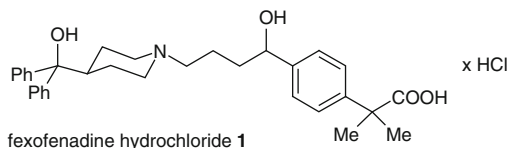
Biological target: Fexofenadine is a racemic carboxylic analogue of terfenadine and a highly hydrophilic zwitterionic amino acid, which is a specific antagonist at H_1 histamine receptors.

Therapeutic profile: The drug is a second-generation antihistamine, lacking sedative activity, for the treatment of allergic diseases, including allergic rhinoconjunctivitis, seasonal allergic rhinitis, urticaria and atopic dermatitis.

Synthetic highlights: Although not feasible from a cost–benefit point of view, racemic switch to the R(+) enantiomer is discussed. Retrosynthetic analysis of the fexofenadine molecule is presented together with some inventive synthetic steps employed. These include $ZnBr_2$ -catalyzed transposition (rearrangement) of α -haloketones to terminal carboxylic acids and microbial oxidation of the non-activated C–H bond. The concept of bioisosterism is exemplified by the silicon switch of fexofenadine to sila-fexofenadine.

10.1 Introduction

Fexofenadine hydrochloride (**1**, (\pm)-2-[4-]-1hydroxy-4-(hydroxydiphenylmethyl)-1-piperidino]butyl]phenyl]-2-methylpropanoic acid, *Allegra*[®]) is an antihistamine agent, acting as an H_1 antagonist.



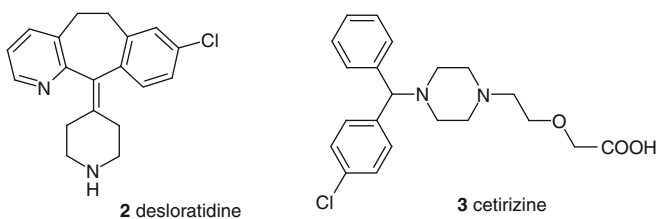
It is clinically effective in the treatment of seasonal allergic rhinitis and chronic idiopathic urticaria and is not associated with adverse cardiac or cognitive/psychomotor effects. These qualities have led to the ranking of fexofenadine in eighth place among the 200 best marketed drugs, and in 2007, it led to approximately \$0.9 billion in sales.

10.2 Histamine Receptors as Biological Targets for Anti-allergy Drugs

Histamine is a major chemical mediator in the pathogenesis of allergic disease. It is released, predominantly by mast cells, in response to cross-linking by allergens of specific immunoglobulin E antibodies bound to the cell membrane, as well as by some chemical stimuli. Activation by histamine of H₁ receptors, present on various types of smooth muscle, endothelial cells and in the heart, causes many of the typical symptoms of allergic diseases. These include sneezing, swelling (due to plasma leakage), erythema (due to dilation of blood vessels) and itching, all of which can be effectively blocked by specific antagonists of the action of histamine at H₁ receptors. H₁-receptor antagonists are widely used as the primary therapeutics for allergic diseases, such as skin urticarias, allergic conjunctivitis and hay fever [1–3].

Histamine H₁ receptors are a sub-class of the super-family of G-protein-coupled receptors, along with the other three histamine receptor subtypes: H₂, H₃ and H₄. The H₂ receptor plays a major role in controlling gastric acid secretion, whereas the H₃ receptor regulates the activity of histamine and other neurotransmitters in the CNS. Due to the high homology of all histamine receptors, selectivity is the prime issue in development of new drugs acting at only one receptor sub-type. First-generation H₁ receptor antagonists, such as chlorpheniramine, promethazine and clemastine, cross the blood–brain barrier and exert CNS side effects including drowsiness and sedation.

As a class, second-generation antihistamines, also known as non-sedative antihistamines, are highly selective for the H₁ receptor. The most important representatives: fexofenadine, desloratidine and cetirizine (1–3) are characterized by limited effects on the CNS and low cytochrome P450 inhibition.



Second-generation H₁-receptor antagonists potently and selectively bind to the H₁ receptor, stabilizing it towards the inactive state, with relatively long dissociation times. These properties contribute to the effectiveness of the second-generation antagonists in alleviating histamine-mediated allergic symptoms as well as to their long duration of action. This newer class of antihistamines does not cross the blood–brain barrier, and therefore, many side effects, in particular sedation are avoided [4, 5].

Racemic fexofenadine hydrochloride (1), sold under the registered names of *Allegra*[®] and *Telfast*[®], was discovered as the major active metabolite of

Table 10.1 Main pharmacokinetic properties of racemic fexofenadine

Absorption (T_{\max} /h)	1–3
Duration of action (h)	24
Volume of distribution (L/kg)	5.4–5.8
Metabolites (% of dose)	5
Terminal elimination half-life (h)	11–15
Urinary excretion (%)	11
Faecal excretion (%)	80

Table 10.2 Pharmacokinetic parameters of fexofenadine enantiomers (in human subjects, p.o.)

Parameter	(+)-enantiomer	(–)-enantiomer
C_{\max} (ng/ml)	169 ± 48	73 ± 23
T_{\max} (h)	2.4 ± 0.6	2.6 ± 0.3
$t_{1/2}$	4.0 ± 2.1	4.2 ± 2.7
AUC (ng/h/ml)	$1,075 \pm 236$	495 ± 140

terfenadine (**4**). The main pharmacokinetic and metabolic properties of fexofenadine are presented in Table 10.1.

Fexofenadine is rapidly absorbed and has a long duration of action, making it suitable for once daily administration, and it provides a more improved quality of life than any other antiallergic drug [6–8].

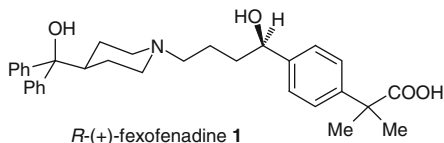
Pharmacokinetic parameters observed for fexofenadine enantiomers are comparable except for the *area under the curve* (AUC) for plasma concentrations (Table 10.2) [9].

In a detailed clinical study, it was demonstrated that both enantiomers of fexofenadine possess equal potency but differ in selected pharmacokinetic parameters [10]. A 63:37 steady-state ratio of *R*-(+)-**1** and *S*-(–)-**1** was observed in plasma and this remained constant across time and dosing. In a later study, it was found that the AUC and the maximum plasma concentration (C_{\max}) of *R*-(+)-**1** were significantly greater than those of the *S*-(–)-enantiomer [11]. Furthermore, plasma and renal clearance of oral *S*-(–)-fexofenadine were both significantly greater than for the *R*-(+)-enantiomer.

10.3 Absolute Configuration and “Racemic Switch”

All these studies of non-racemic fexofenadine were prompted by the development of an HPLC method for the chiral separation of fexofenadine enantiomers in human plasma [11, 12]. Based on these and additional studies on the pharmacokinetic [13] and enantioselective disposition of fexofenadine in the presence of verapamil [14],

it was proposed that the use of *R*-(+)-fexofenadine only might provide a more predictable therapeutic effect and less drug–drug interactions [15].



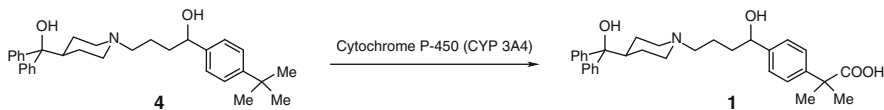
A “racemic switch”, that is, replacement of racemic fexofenadine on the market by the *R*-(+)-enantiomer, is not likely, however, since the cost-benefit considerations are unfavourable due to the relatively minor positive therapeutic effect and the considerably higher production costs of the pure *R*-(+)-enantiomer. Nevertheless, because of the exciting enantioselective syntheses and stereochemical properties of the enantiomers of fexofenadine, these will be considered in the next section.

As mentioned in the previous section, fexofenadine is the metabolite of terfenadine (**4**), a first generation antihistamine for the therapy of allergy (Scheme 10.1).

Oxidative metabolism of xenobiotica and of drugs, in particular, is a well known process by which the organism transforms foreign substances into more hydrophilic metabolites, enabling their faster elimination in the urine. There are many cases in which drug metabolites have been found to be more convenient and effective drugs than the original compounds [16]. One of the best known examples is the discovery of oxazepam, the C3-hydroxylated metabolite of diazepam, as the more active and selective sedative. Some of the details of this discovery are discussed in Chap. 6.

Fexofenadine, as the carboxylic analogue of terfenadine, is an amino acid with a highly hydrophilic zwitterionic structure. Its enantiomers have been separated repeatedly by chromatographic methods [9, 17, 18], and the CD spectra reveal a positive extreme for the *R*-(+)-enantiomer at ~205 nm with a shoulder at ~225 nm. The absolute configuration of the fexofenadine enantiomers was determined by chemical correlation with the alcohol *S*-(–)-**12**, for which the prediction of absolute configuration is based on the configuration of the chiral catalysts used in reduction. Details are presented in Scheme 10.9.

Recently, a validated LC method was reported for the separation of the structural (*meta/para*) isomers of fexofenadine hydrochloride with a chiral mobile phase [19]. This is an interesting example in which an *achiral reversed-phase ODS column* is used for the separation of enantiomers *in chiral combination with the mobile phase*, pH 3 aqueous buffer-MeCN (60:40), containing 5 g/L β -cyclodextrin as a chiral additive.



Scheme 10.1 Metabolic oxidation of terfenadine (**4**) to fexofenadine (**1**)

Despite the cost-benefit limitations to the development of a single-enantiomer drug, many original syntheses of pure enantiomers have been reported. Some of these are discussed in the following section, after a brief overview of non-stereoselective approaches.

10.4 Retrosynthetic Analysis of Fexofenadine

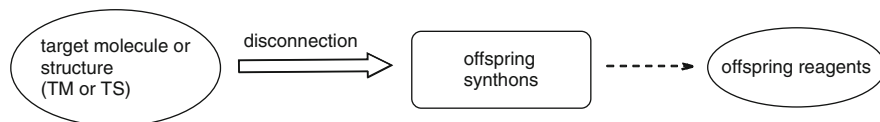
Fexofenadine serves as a good example of a *target molecule* (TM) that can be approached by *retrosynthetic analysis*, also known as the *disconnection approach* or the *synthon approach*. This methodology enables the organic chemist to design a synthetic route to the TM, starting from simple and readily available materials. It is important to note that the disconnection approach is an imaginary process, the reverse of an actual chemical reaction, which breaks a bond in the target molecule to yield the structure of a new compound from which the TM can be made.

Besides the terms, *disconnection* and *target molecule* (TM), a number of other basic terms are used in retrosynthetic analysis: *functional group interconversion* (FGI), *synthon*, *reagent* or *synthetic equivalent*. The exact meaning of these terms is discussed by S. Warren [20–22], and the whole approach has found its place in most modern organic chemistry textbooks [23–26]. Here it is sufficient to mention that *disconnection* is an analytical, cognitive process, involving reversal of the synthetic direction that results in hypothetical structures, called *synthons*, which are charged species, radicals or radical ions. Based on these structures, real species, reagents or synthetic equivalents are then identified, as generally outlined in Scheme 10.2.

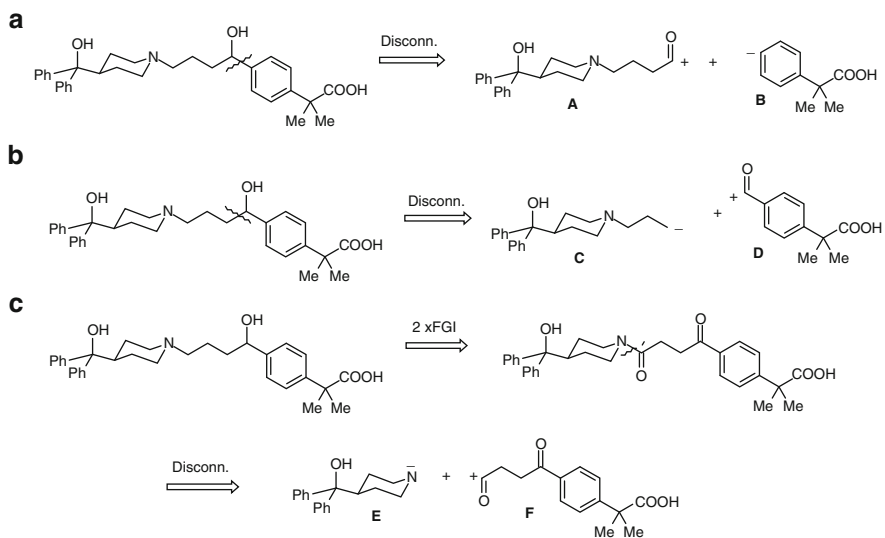
Each intermediate in retrosynthetic analysis is a new target molecule, and combination, in the last step, of the last two intermediates into the TM corresponds to highly *convergent synthesis*, the advantages of which, compared to *consecutive synthesis*, have been repeatedly discussed in textbooks on organic synthesis.

There are three key rules to be followed in retrosynthetic analysis: disconnection should follow the *correct mechanism*, allow *maximal simplification* of the TM and lead to *available starting materials*. The fexofenadine molecule can be maximally simplified by disconnections made at critical bonds (Scheme 10.3). These are disconnections at the CH₂–aryl bond (a) and an alternative disconnection of the CH₂–CH₂Ar bond (b). In addition, disconnection of the N–CH₂ bond, after FGI of the amine to an amide group, represents another possibility (c), which can be completed to create a pathway to the sila-bioisostere of fexofenadine, as described in Sect. 10.4.3.

Two synthons, cationic **A** and anionic **B**, which are the result of disconnection (a), have a couple of synthetic equivalents, for example, (1) and (2) in Table 10.3.



Scheme 10.2 General scheme of the flow of events in retrosynthetic analysis



Scheme 10.3 Three disconnections of fexofenadine at critical bonds, which provide maximal simplification of the target molecule

Table 10.3 Possible synthetic equivalents (reagents) for the synthons envisaged by disconnections a–c

Disconnection a.	
(1)	
(2)	
Disconnection b.	
(3)	
Disconnection c.	
(4)	

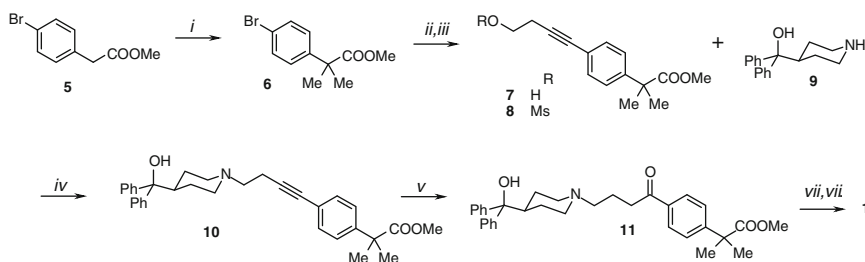
Two synthons **C** and **D** are the result of an alternative disconnection *b* of the CH₂–CH₂Ar bond. Finally, retrosynthetic analysis *c* suggests two functional group interconversions followed by disconnection of the amide N–CO bond, affording synthons **E** and **F**. This analysis has been used in the synthesis of the sila-bioisostere of fexofenadine (**49**), as described in Sect. 10.4.3.

Three syntheses of fexofenadine reported in the literature actually follow these retrosynthetic considerations, starting from reagents presented in (1) to (3) (Table 10.3). The fourth disconnection (4) is applied in the synthesis of the sila-bioisostere of fexofenadine (**49**), discussed in Sect. 10.4.3.

10.4.1 ZnBr₂-Catalyzed Rearrangement of α -Haloketones to Terminal Carboxylic Acids

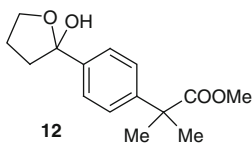
Kawai et al. [27] have reported the synthesis of alkyne **7** after the stepwise formation of phenyl-2,2-dimethylacetic acid by double methylation of *para*-bromo-phenylacetic acid (Scheme 10.4).

This seven-step route is characterized by a high average yield, but requires complete elimination of Hg ions and chromatographic purification of the ketone intermediate **11**, which renders the whole process impractical for large-scale production of fexofenadine. Recently, a modification of this step has been claimed, which uses the free carboxylic acid of the ester **10** for hydration and does not require chromatographic purification of the ketone [28]. Another hydration protocol has been claimed, consisting of the use of platinum(II)chloride in THF/water as an hydrating agent for **10** [29]. However, this method also required chromatographic purification of the ketone **11**. It is interesting to note that the attempts at conversion of alkyne **8** to the ketone via mercury-catalyzed hydration resulted in the loss of the mesyl group and formation of the hemiketal **12**.



Reagents and conditions: *i.* MeI (2.4 equiv.)/NaH (3 equiv.), THF; *ii.* 3-butyne-1-ol, Pd(0)Cu₂Br₂/TEA, reflux; *iii.* MsCl (2 equiv.), pyridine/DCM, r.t., 12h; *iv.* azacyclanol (**9**).HCl (1.1 equiv.), K₂CO₃ (3.3 equiv.), MeCN; *v.* Hg(II)O, H₂SO₄/H₂O/MeOH, 55 °C, chromatography; *vi.* NaBH₄ (1.5 equiv.), MeOH, r.t.; *vii.* 1N NaOH/MeOH (1:1 v/v), 80 °C.

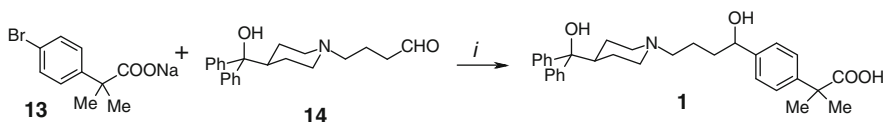
Scheme 10.4 Synthetic route to fexofenadine according to Kawai et al



The bond-forming reaction, according to retrosynthetic step 2, reported by Patel et al. [30] is presented in Scheme 10.5.

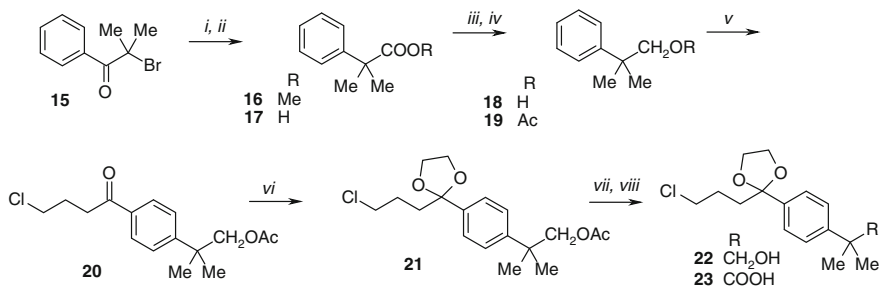
In this step, the sodium salt of 2-(4-bromophenyl)-2,2-dimethylacetic acid **13** was lithiated via a metal–halogen exchange using *t*-BuLi, and subsequently 4-[4-(hydroxydiphenylmethyl)piperidini-1-yl]butyraldehyde **14** was arylated to afford fexofenadine.

This synthesis of fexofenadine uses either the ester (**6**) or salt (**13**) of 4-bromo-2,2-dimethylphenylacetic acid as the C₁₀ building block. However, neither this nor the parent 2,2-dimethylphenylacetic acid is an easily available compound. An original approach to synthesis of the 2,2-dimethylphenylacetic acid unit was taken by Di Giacomo et al. (Scheme 10.6) [31]. In the key step, skeletal rearrangement was made of the α -halo-isopropylmethyl ketone **15** to the methyl ester of the corresponding phenylalkanoic acid **16**.



Reagents and conditions: *i*. *t*-BuLi/THF, Li-Br exchange.

Scheme 10.5 Arylation of aldehyde in the last step of the convergent synthesis of fexofenadine



Reagents and conditions: *i*. ZnBr₂, MeOH, 115 °C, 5 h; *ii*. 0.4 N NaOH, MeOH/H₂O (2:1, v/v), 80 °C, 12 h; *iii*. LiAlH₄, Et₂O; *iv*. Ac₂O, TEA, 4-PPy, r.t. 20 min; *v*. 4-chlorobutyryl chloride, AlCl₃, CS₂, 0 °C, 15 h; *vi*. ethylene glycol, *p*-TsOH, benzene, reflux, 24 h; *vii*. NaOH, MeOH r.t. 30 min; *viii*. Jones oxydation.

Scheme 10.6 Transposition of α -bromoketone **15** to 2,2,-dimethylacetic acid **16** and subsequent steps on the pathway to fexofenadine

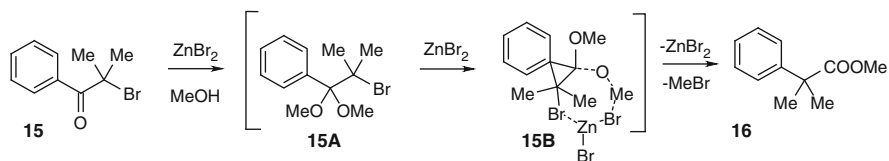
The authors proposed a possible mechanism for this transposition, shown in Scheme 10.7 [32].

The reaction proceeds via ZnBr_2 catalysis with formation of an acetal intermediate **15A**, and polarization of the C–Br bond. Transposition of the hemiacetal intermediate **15B** and 1,2-migration of phenyl group affords the 2,2-dimethylphenylacetic acid ester **16**.

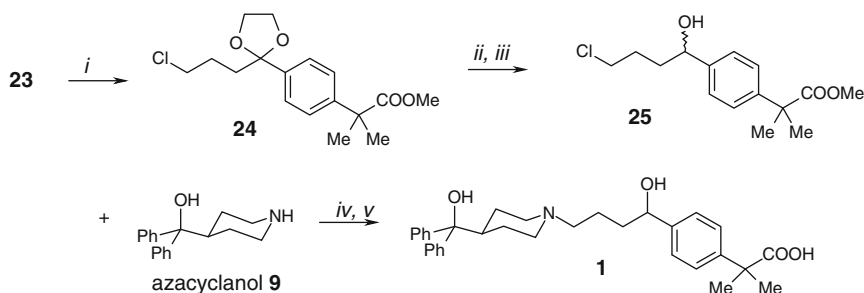
The final steps in Scheme 10.6 are completed under standard conditions. One may question why reduction of the ester to alcohol **18** and its protection as acetate **19** should be performed before Friedel–Crafts acylation, since both the dimethylcarboxy and dimethylhydroxymethyl groups are expected to be *para*-orientated due to the strong steric perturbation of the *ortho*-substitution. Quite unexpectedly, the dimethylcarboxy group proved to have a *meta/para* orientation, so that acylation of **18** resulted in the formation of a mixture of *meta*- and *para*-isomers that were difficult to separate.

With the availability of the intermediary acid **23**, the authors achieved synthesis of racemic fexofenadine **1**, as outlined in Scheme 10.8 [32].

According to retrosynthetic analysis (3), the C–C bond to the benzylic C atom can be formed from the suitably selected couple, the Grignard reagent of an alkyl bromide and aryl aldehyde. This is the key step in the synthesis of fexofenadine, as reported by Fang et al. [33] (Scheme 10.9).

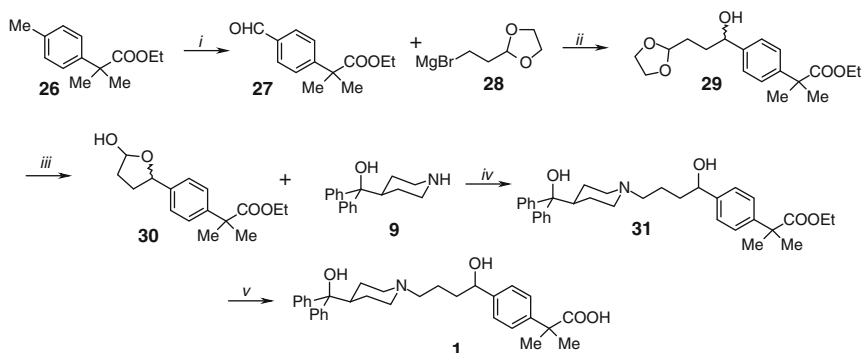


Scheme 10.7 Mechanism of transposition of α -bromoketone to the 2,2-dimethylacetic acid derivative

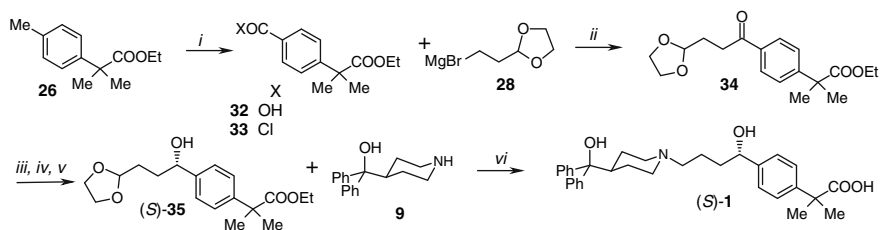


Reagents and conditions: *i.* CH_2N_2 , Et_2O , 0°C ; *ii.* 2% HCl/THF , r.t., 1.5 h; *iii.* NaBH_4 , MeOH/THF , 0°C , 30 min; *iv.* azacyclanol, K_2CO_3 , KI , benzene/DMF (8:2, v/v), reflux 7 h; *v.* 10% NaOH , MeOH , reflux, 2 h.

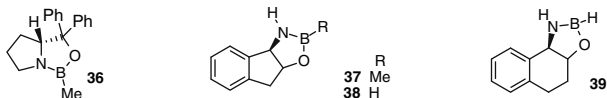
Scheme 10.8 Final steps on the route to fexofenadine



Scheme 10.9 Synthetic route to fexofenadine based on the formation of a C–C bond to the benzylic carbon



Ligands **36–39**, tested in enantioselective reduction of **34**, step *iii*.



Scheme 10.10 Enantioselective route to (*S*)-fexofenadine, and chiral ligands tested in asymmetric hydrogenation

The same authors have developed an enantioselective route to *S*-(–)-fexofenadine **1** (Scheme 10.10) [27].

This route offers some interesting solutions to selectivity problems. Two reactions have been performed with *complete site-selectivity* involving oxidation of the aryl-Me group in **26** to the carboxylic group in **32**, in the presence of two geminal Me groups on the benzylic carbon. This was followed by a Grignard reaction of **28** with a carboxylic acid chloride in the presence of a carboxylic ester group, moderated by an Fe-oxo complex. Enantioselective reduction of the ketone carbonyl

group was achieved with oxazaborolidine-based borane catalysts, **36–39**. More details on the scope and mechanism of enantioselective reduction by boranes are presented in Chap. 11.

In this context, it is interesting that a patent claimed by Aventis Pharmaceuticals, directed towards the development of a novel method for asymmetric reduction of ketones catalyzed by Cp_2TiH , was used in the preparation of intermediates in the synthesis of fexofenadine [34].

10.4.2 Microbial Oxidation of Non-activated C–H Bond

One of the key structural elements of fexofenadine is the aryl-2,2-dimethylacetic acid unit. The 2,2-dimethylacetic acid group cannot be conveniently incorporated as a C_4 building block. In contrast, the *tert*-butyl group can be conveniently introduced into the aromatic ring by alkylation with *iso*-butene [35]. Therefore, an efficient method for the selective oxidation to a COOH group of one of the three Me groups in the *tert*-butyl unit would elegantly solve the problem. Such a level of chemoselectivity is difficult to obtain by chemical means, however, and biocatalytic oxygenation is the method of choice.

Since most chemical syntheses presented in the previous section are multi-step and laborious, the bio-oxidation of the *tert*-butyl group in terfenadine (**4**) has been investigated as an alternative solution [36–40]. This process is presented in Scheme 10.1 with CYP3A4 as the oxidant. With most micro-organisms tested, side products were observed and the desired carboxylic acid, fexofenadine, was obtained in low yields. Detailed study of the regioselective oxidation of terfenadine to fexofenadine with the filamentous fungus *Cunninghamella blakesleeana* was reported by Weuster-Botz et al. [41]. The authors followed the method described in a previous report on the regioselective microbial oxidation of ebastine, a close structural congener of terfenadine, with *C. blakesleeana* [42]. This process was scaled up to lab-scale in a stirred tank reactor (Fig. 10.1), by optimizing the following parameters: solubility of the substrate terfenadine; reaction temperature; oxygen tension; pH and the use of additives such as glycerol, mineral salts, and so on.

It was found that the fungus, *C. blakesleeana*, was not able to perform the complete oxidation of terfenadine to fexofenadine, because the reaction stopped at the level of the *prim*-alcohol. Since the *prim*-alcohol cannot be selectively oxidized with strong agents, such as RuCl_3 or H_5IO_6 , but rather this occurs with the secondary hydroxy group, the result was disappointing for the scale-up process.

Further progress was made by Buisson et al. [40]. These authors screened a series of micro-organisms for their ability to oxidize the *tert*-butylphenyl group in terfenadine. They defined the culture conditions required to increase the formation of the carboxylic acid and to avoid the formation of alcohols and other side products. Table 10.4 shows the products detected in crude extracts after 96 h incubation [40].

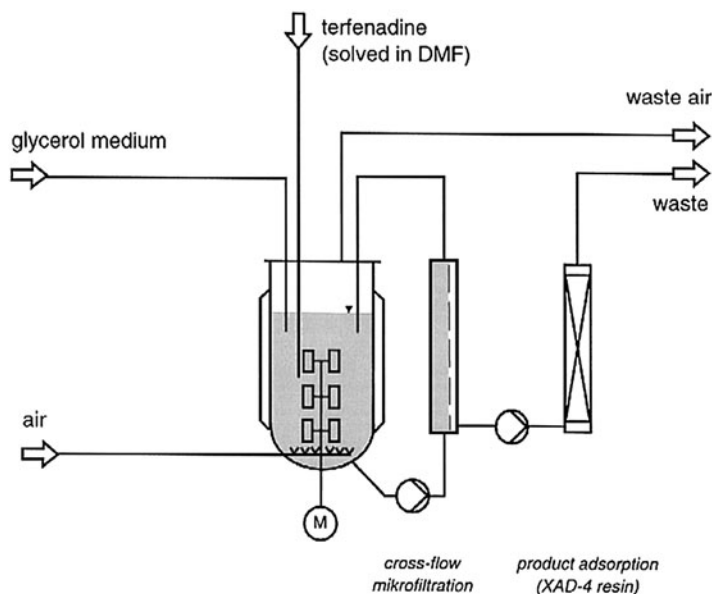


Fig. 10.1 Scheme of the membrane reactor system for continuous biotransformation of terfenadine to fexofenadine with *C. blakesleeana* AT1 (reproduced from [41], with the permission of Elsevier)

Table 10.4 Oxidation of the *tert*-butylphenyl group of terfenadine by selected micro-organisms

Micro-organisms	Culture medium	Terfenadine	
		Fexofenadine	Alcohol
<i>Cunninghamella blakesleeana</i> ATTC 8688a	YM	+	—
	YMS	—	+
<i>Cunninghamella echinulata</i> ATTC 9245	YM	—	—
	YMS	+	—
<i>Streptomyces risomes</i> NRRL 2234	YM	—	—
	YMS	+	—
<i>Streptomyces platensis</i> NRRL 2364	YM	+++	—
	YMS	++	++
<i>Absidia corymbifera</i> LCP 63 1800	YM	++	++
	YMS	+++	—

— no products formed

+ product observed (<20%)

++ alcohol and acid presence (20–50%)

+++ main or unique product observed (>75%)

Two strains of bacteria and three strains of filamentous fungi were selected and cultivated in a culture medium supplemented (YMS) or not (YM) with soybean peptones (Table 10.1). Soybean peptones obtained by proteolytic digestion [43] are well known nutrient media for growing bacteria and fungi. They were found to induce oxidative activity in all strains tested.

The best results were obtained with *Absidia corymbifera* cultured in YMS, with which complete transformation of terfenadine to fexofenadine was achieved. The preparative experiments carried out in 1 L of YMS and 200 mg of terfenadine led to 193 mg (93% yield) of fexofenadine. Some variation of the protocol for microbial oxidation to fexofenadine by *A. corymbifera* was recently reported by the same author, but no significant improvement in productivity was achieved [44].

In conclusion, it is important to note that microbial oxidations were performed with racemic terfenadine and did not exhibit *kinetic resolution* to a single enantiomer. Thus, the biocatalytic approach excluded *dynamic kinetic resolution* as an attractive “racemic switch” approach to the complete conversion of *rac*-terfenadine to the therapeutically desirable (*R*)-(+)-**1** enantiomer of fexofenadine [45, 46].

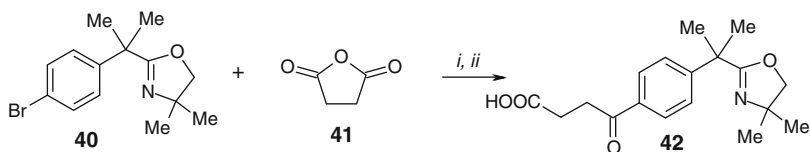
10.4.3 Bioisosterism: Silicon Switch of Fexofenadine to Sila-Fexofenadine

Silicon switch of marketed drugs is a relatively new concept and consists of sila-substitution (C/Si exchange) of existing drugs in the search for drug candidates that have improved biological properties providing a beneficial intellectual property (IP) status. It has been shown that silicone molecules can be accessed in a relative straightforward manner and can have a pharmacological or pharmacokinetic benefit over their carbon counterparts [47–49].

C/Si bioisosterism has been considered repeatedly due to some fundamental differences between carbon and silicon that are useful in drug design [50–52]. These include:

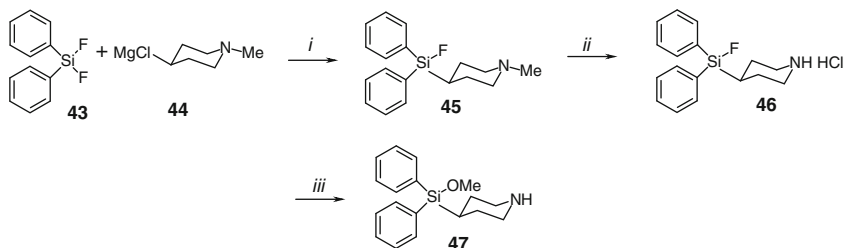
- Differences in the electronegativity of the two elements, silicon being a more electropositive element than carbon.
- Differences in covalent radius ($r_{\text{C}} = 77 \text{ pm}$, $r_{\text{Si}} = 117 \text{ pm}$), which lead to differences in bond distances and in the steric arrangement of the bonds. While the average length of a C–C bond is 1.54 \AA , the C–Si bond has a length of 1.87 \AA . These differences can lead to differing steric requirements and to varying shapes of carbon and silicon analogues, and consequently, to changes in the way in which they interact with biological binding sites.
- Silicon allows for chemical reactions, which are not accessible to standard carbon chemistry, prompting the synthesis of novel drug-like scaffolds.
- Due to the higher electropositivity of silicon, silanols (Si–OH) are more acidic than carbinols (C–OH), and the hydrogen bond strength of silanols is higher than that of carbinols [53, 54].

The properties of bioisosteric compounds prompted Tacke et al. to prepare sila-fexofenadine (**49**) and to study the bioisosterism of this and some related H_1 -receptor antagonists [55, 56]. Replacement with a silicon atom of the *tert*-carbon atom bearing the OH group in fexofenadine was attempted, and the synthesis of sila-fexofenadine was achieved according to Schemes 10.11–10.13.



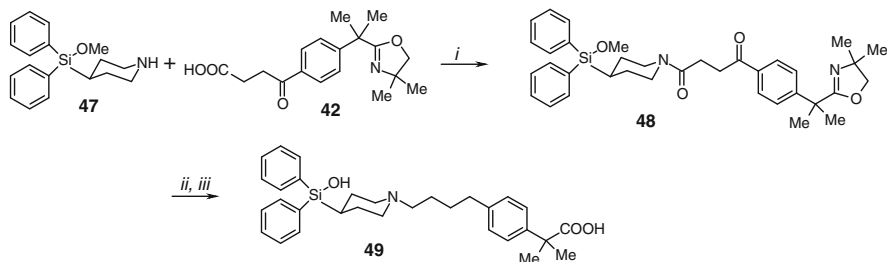
Reagents and conditions: *i.* Mg, THF, -78 °C to r.t.; *ii.* 2M aq. HCl, ether.

Scheme 10.11 Synthesis of all-carbon building block **42** on the path to sila-fexofenadine



Reagents and conditions: *i.* Mg/l₂ 80 °C, 0.5 h, then THF, 65%; *ii.* Cl(CO)OCHClMe, DCM, 0 °C to 20 °C, 1.5 h, 58%; *iii.* MeONa/MeOH, 20 °C, 1 h, 82%.

Scheme 10.12 Synthesis of the Si-containing building block for sila-fexofenadine



Reagents and conditions: *i.* Et₃N/CICOOEt, THF; *ii.* LiAlH₄/THF; *iii.* aq. HCl, then aq. NaOH in MeOH/water, over-all yield 42%.

Scheme 10.13 Final steps in the synthesis of sila-fexofenadine

The phenyl-2,2-dimethylacetic acid building block was prepared according to Scheme 10.11, which comprised an interesting variant of the Grignard reaction of bromophenyl derivative **40** with anhydride **41** by protecting the carboxylic group in **40** as the 1,3-oxazoline [56].

The second building block, with an incorporated silanol unit, was prepared according to Scheme 10.12.

The starting material, diphenyl-difluorosilane, is easily generated from the corresponding dichlorosilane with hexafluorosilicate under anhydrous conditions [57]. The final steps of this convergent synthetic route are presented in Scheme 10.13.

They comprised *N*-acylation, simultaneous reduction of the amide and ketone units, and in the final step, simultaneous hydrolysis of the Si-OMe group and the protective oxazoline group. Since all steps proceeded in high yield, intermediates were not isolated, and the final product was crystallized from methanol in an overall yield of 42%.

Finally, both fexofenadine and its sila-bioisostere exhibited similar in vitro pharmacological profiles. Evaluation of the effects in vivo of the C/Si switch, though, was not reported.

10.5 Conclusion

Although of considerable interest as examples of approaches to enantioselective synthesis, these creative reactions on the route to enantiomerically pure fexofenadine remain chemical curiosities unless a way is found to make them economically viable. Perhaps this may prove to be the case with a future improvement on the fexofenadine molecule.

References

1. Druce HM, Kaliner MA (1988) JAMA 259:260–263
2. Lindquist M, Edwards IR (1997) Lancet 349:1322
3. Meeves SG, Appajosyula S (2003) J Allergy Clin Immunol 112:69–77
4. Adelsberg BR (1997) Arch Intern Med 157:494–500
5. Izumi N, Mizuguchi H, Umehara H, Ogino S, Fukui H (2008) Allergol Int 57:1–7
6. Markham A, Wagstaff AJ (1998) Drugs 55:269–274
7. Simpson K, Jarvis B (2000) Drugs 59:301–321
8. Howard DR, Haribhakti R, Kittner B, Agrawala P (2005) Curr Med Res Opin 21:769–775
9. Surapaneni S, Khalil SKW (1994) Chirality 6:479–483
10. Robbins DK, Castels MA, Pack DJ, Bhargava VO, Weir SJ (1998) Biopharm Drug Dispos 19:455–463
11. Miura M, Uno T, Tateishi T, Suzuki T (2007) Chirality 19:223–227
12. Miura M, Uno T, Tateishi T, Suzuki T (2007) J Pharm Biomed Anal 43:741–745
13. Tateishi T, Miura M, Suzuki T, Uno T (2008) Br J Clin Pharmacol 65:693–700
14. Sakugawa T, Miura M, Hokama N, Suzuki T, Tateishi T, Uno T (2009) Br J Clin Pharmacol 67:535–540
15. Miura M, Uno T (2010) Expert Opin Drug Metabol Toxicol 6:69–74
16. Eichelbaum M, Testa B (2003) Stereochemical aspects of drug action and disposition. Springer, Heidelberg
17. Zamani K, Conner DP, Ween HB, Yang SK, Cantilena CR (1991) Chirality 3:467–470
18. Chan KY, George RC, Chen T, Okerhom RA (1991) J Chromatogr 571:291–297
19. Sakalgaonkar AA, Mirgane SR, Pawar RP (2008) Chromatographia 68:143–146
20. Warren S (1989) Designing organic synthesis, a programmed introduction to the synthon approach, 5th edn. Wiley, New York
21. Warren S (1989) Organic synthesis, the disconnection approach, 4th edn. Wiley, New York
22. Warren S (1989) Workbook for organic synthesis, 4th edn. Wiley, New York

23. Serratos F, Xicart J (1996) *Organic chemistry in action, the design of organic synthesis*. Elsevier, Amsterdam
24. Fuhrhopf J, Penzlin G (1994) *Organic chemistry, concepts, methods, starting materials*. VCH, Weinheim
25. Smith M (1994) *Organic synthesis*. McGraw-Hill, Inc., New York
26. Chiron C, Tomas RJ (1997) *Exercises in synthetic organic chemistry*. Oxford University Press, London
27. Kawai SH, Hambalek RJ, Just G (1994) *J Org Chem* 59:2620–2622
28. Castaldi G, Barreca G, Tarquini A, US Patent Publ. 2005/0277775 A1
29. Castaldi G, Barreca G, Tarquini A, US Patent 6,815,549
30. Patel S, Waykole L, Repić O, Chen K-M (1996) *Synth Commun* 24:4699–4610
31. Giordano C, Castaldi G, Uggeri F, Gurzoni F (1985) *Synthesis*: 436–437
32. Di Giacomo B, Coletta D, Natalini B, Ni M-H, Pellicciari R (1999) *Farmaco* 54:600–610
33. Fang QK, Senanayake CH, Wilkinson HS, Wald SA, Li H (1998) *Tetrahedron Lett* 39: 2701–2704
34. Aventis Pharm (2000) US Patent 6407119
35. Modrogan E, Valkenberg MH, Hoelderich WF (2009) *J Catal* 261:177–187
36. Michels PC, Zirbes EL (1993) US Patent 5,204,246
37. Meiwes J, Worm M (1999) US Patent 5,990,127
38. Azerad R, Biton J, Lacroix I (1999) WO Patent 47693
39. Senanayake CH, Pflum DA (1999) *Chim Oggi* 17:21–26
40. Mazier C, Jaouen M, Sari M-A, Buisson D (2004) *Bioorg Med Chem Lett* 14:5423–5426
41. Schmitz G, Franke D, Stevens S, Takors R, Wuester-Botz D, Wandrey C (2000) *J Mol Catal B Enzymatic* 10:313–324
42. Schwartz H, Liebig-Weber A, Hochstatter H, Bottcher H (1996) *Appl Microbiol Technol* 44: 731–735
43. Payne JW (1976) *Peptides and micro-organisms*. *Adv Microb Physiol* 13:55–113
44. El Quarradi A, Salard-Arnaud I, Buisson D (2008) *Tetrahedron* 64:11738–11744
45. Bäckvall JE (2006) *Asymmetric catalysis via dynamic kinetic resolution*. In: Christmann M, Bräse S (eds) *Asymmetric synthesis – the essentials*. Wiley-VCH, Weinheim
46. Martín-Matute B, Bäckvall JE (2008) *Dynamic kinetic resolutions*. In: Gotor V, Alfonso I, García-Urdiales E (eds) *Asymmetric organic synthesis with enzymes*. Wiley-VCH, Weinheim, pp 89–113
47. Showell GA, Mills JS (2003) *Drug Discov Today* 8:551–556
48. Bains W, Tacke R (2003) *Curr Opin Drug Discov Devel* 6:526–543
49. Mills JS, Showell GA (2004) *Expert Opin Investig Drugs* 13:1149–1157
50. Schmid T, Diass JO, Ilg R, Surburg H, Tacke R (2003) *Organometallics* 22:4343–4346
51. Bains W, Tacke R (2003) *Curr Opin Drug Discov Rev* 6:526–543
52. Pooni PK, Showell GA (2006) *Mini Rev Med Chem* 6:1169–1177
53. Reichstatt MM, Mioč UB, Bogunović LJ, Ribnikar SV (1991) *J Mol Struct* 244:283–290
54. Tossel AT, Sahai N (2000) *Geochim Cosmochim Acta* 64:4097–4099
55. Tacke R, Schmid T (2004) For Amedis Pharmaceuticals Ltd. GB Patent 2394714
56. Tacke R, Schmid T, Penka M, Burschka C, Bains W, Warneck J (2004) *Organometallics* 23: 4915–4923
57. Lickiss PD, Lukas R (1996) *J Organomet Chem* 510:167–172

Chapter 11

Montelukast Sodium

Abstract

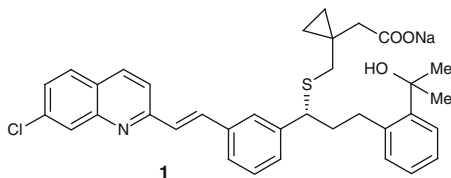
Biological target: Montelukast is a 7-chloroquinoline-substituted derivative of the leukotriene D₄ (LTD₄) molecule and a second generation antagonist at the CysLT-1 receptor for LTD₄, a bronchoconstrictor mediator in allergic inflammation.

Therapeutic profile: The drug is used in the oral treatment of chronic, particularly nocturnal asthma.

Synthetic highlights: With only one stereogenic centre but a complex assembly of functional groups, the synthesis of montelukast has been approached from several angles. These include hydroboration of ketones with boranes from α -pinenes, involving a non-catalytic enantioselective reduction protocol; a non-linear effect (NLE) is observed in this reaction. Organometallic complexes of Ru(II) have also been employed to catalyze enantioselective hydrogen transfer, using formic acid as the source of hydrogen; CeCl₃-THF solvate was found to be a valuable promoter of the Grignard reaction. In a biocatalytic process with ketoreductase KRED (*KetoREDuctase*), a “self driven” process was scaled-up to a 200 kg batch and >99.9% e.e of montelukast.

11.1 Introduction

Montelukast sodium (**1**, 2-[1-[[[(1*R*)-1-[3-[2-(7-chloroquinolin-2-yl)ethenyl]phenyl]-3-[2-(2-hydroxypropan-2-yl)phenyl]propyl]sulphanylmethyl] cyclopropyl]acetic acid, sodium salt, *Singulair*[®], originator Merck Co.), a once-a-day oral antagonist of leukotriene D₄ (LTD₄) was selected for clinical development in 1991, and introduced in 1997 for the treatment of both adult and pediatric chronic asthma. This compound is recognized as one of the most significant advances in asthma therapy in the last 25 years [1] and is commonly used for the treatment of nocturnal asthma.



11.2 Leukotriene D₄ Receptor (LTD₄), CysLT-1 Receptor Antagonists

The design of montelukast was the result of structural development by several companies through various phases of complexity, from the first to the second generation of leukotriene D₄ antagonists [2].

During research into mediators of allergy and asthma in the mid-twentieth century, *slow reacting substance* (SRS, a bronchial smooth muscle slow contracting substance) was identified by biologists as an important endogenous factor in the pathophysiology of human asthma, without any knowledge of its chemical structure [3]. Using *slow reacting substance of anaphylaxis* (SRS-A) of biological origin as the agonist [4], the first in vitro tests were developed, and compound FPL-55712 (Fig. 11.1) identified as an antagonist of the *smooth muscle contracting activity* of SRS-A [5].

Compound FPL-55712, therefore, represents the first putative antagonist of SRS-A. In 1979, Bengt Samuelson at the Karolinska Institute (Stockholm) reported the structure of SRS-A as a variable mixture of three substances, designated leukotriene C₄, leukotriene D₄ and leukotriene E₄ (LTC₄, LTD₄ and LTE₄). Each molecule differs in the nature of the cysteine-containing peptide attached at C6 (Fig. 11.1) [6]. All three leukotrienes were subsequently shown to be derived from arachidonic acid by catalytic oxidation via the 5-lipoxygenase pathway and conjugation of the intermediate LTA₄ with amino acids derived from glutathione. This discovery enabled the more rationale design of LTD antagonists. It is important to note that the complexity of the biological target, the “peptido-leukotriene receptor”, consisting of a mixture of membrane proteins, precluded crystallization of single receptor components or their complexes with potential antagonists, and thus their more effective design. (The cysteinyl leukotrienes are now known to act on two seven transmembrane domain G-protein-coupled receptors, CysLT-1 and CysLT-2, the former being the main receptor sub-type on bronchial smooth muscle). The chemical development pathway which is described below was, therefore, the result

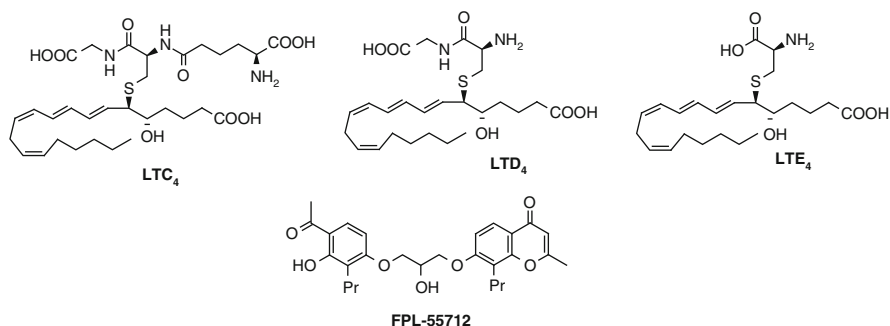


Fig. 11.1 FPL-55712, the first antagonist of SRS-A, and the three main components of SRS-A (LTC₄, LTD₄, LTE₄)

of continuous fine-tuning of the lead structures based on the assumed interactions at the active site(s).

It was shown that LTD₄ exhibits potent contractile activity on smooth muscle [7], including bronchoconstriction, together with changes in vascular permeability in the airways [8]. LTD₄ is an extremely potent spasmogenic mediator of respiratory smooth muscle, being 10,000 times more potent than histamine in eliciting contraction of human lung tissue [9], mainly through actions at the CysLT-1 receptor [10].

These and other studies led to the strengthening of the hypothesis that blockers of LTD₄ might yield novel effective therapy of asthma. The *first generation* of LTD₄ antagonists consisted of leukotriene analogues **2–4**, which retained recognizable structural elements of the natural compounds (Fig. 11.2).

Replacement of the polyene chain in **2** for substituted aryl mimetics in **3** and **4** led to moderately active compounds with improved metabolic stability, but these compounds lacked the required pharmaceutical properties of good oral absorption and a half-life suitable for further evaluation.

The second generation LTD₄ antagonists **5–8** were characterized by a clear departure from the biological lead structure (Fig. 11.3).

The important observation that the styryl-quinoline analogue **5** had similar potency to LTD₄, i.e. IC₅₀ = ca. 0.5 μM, led to the conclusion that an extended conjugated system could interact with the LTD₄ receptor in a manner similar to that proposed for the natural LTD₄. Previously, a hypothetical model of the leukotriene D receptor had been postulated that recognized the flat π-system and the two polar

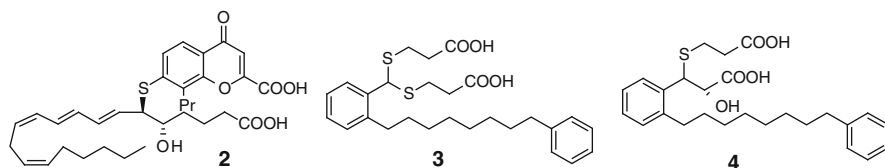


Fig. 11.2 First generation of selective LTD₄ antagonists

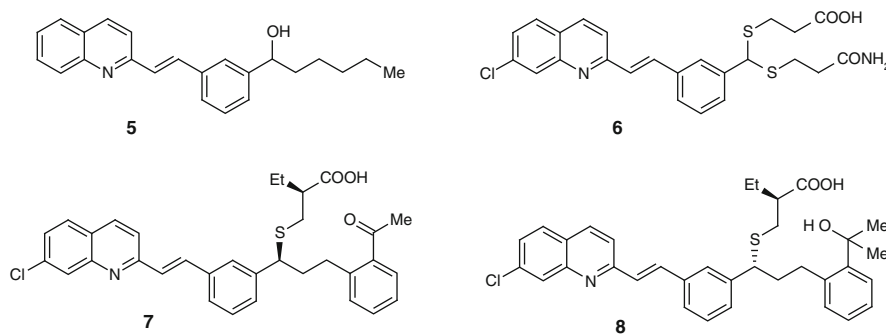


Fig. 11.3 Second generation selective LTD₄ antagonists

acidic chains [11]. Studies were, therefore, initiated to derive structure activity relationships (SAR), in particular to define where one might best add polar and acidic functionalities to these planar, conjugated molecules. As a result, a few hundred compounds were tested and lead molecules **6–8** emerged. They are characterized by a 7-chloroquinoline unit conjugated to the second aromatic ring, in addition to a carboxylic and another polar group.

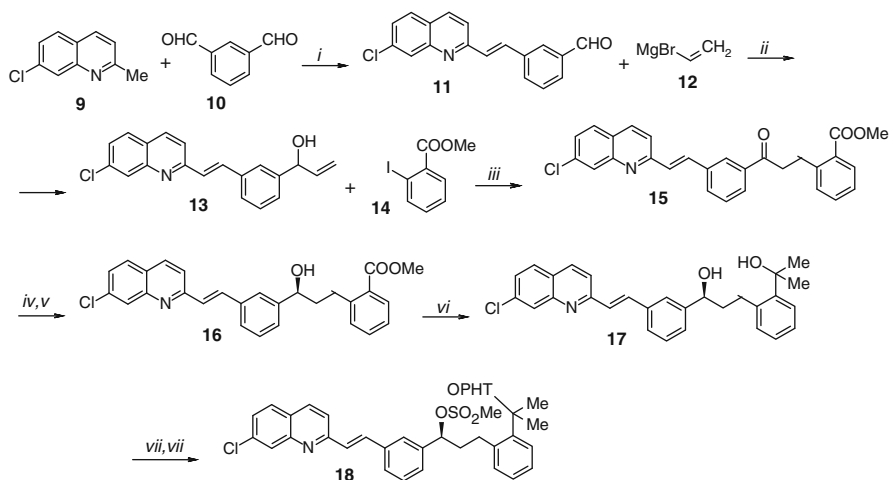
Compound **6** was evaluated in clinical studies under the name verlukast, and it was soon observed that its dithioacetal unit is metabolically unstable, being the site of oxidative metabolism. Replacement of dithioacetal by a thioether moiety was shown to yield compounds with comparable intrinsic potency. Further studies indicated that incorporation of an aromatic ring into the alkyl side chain yielded compounds **7** and **8** with the highest potency at the CysLT1 receptor. Not surprisingly, these two diastereomers, with opposite configurations at the stereogenic centre bearing the S-atom, exhibited remarkably different biological effects; peroxisomal enzyme-induction was observed with compound **7**, bearing the (*R*)-configuration at the benzylic centre, while the (*S*)-diastereomer **8** was inactive and exhibited some degree of toxicity [12].

Final lead optimization included examination of compounds that incorporate thioalkanoic acid moieties, with particular emphasis on the steric bulk in the side-chain. This allowed selection of the optimized compound, montelukast sodium [(*R*)-**1**], incorporating a cyclopropyl unit at the β -position. Montelukast exhibited the best overall potency profile, lack of liver toxicity and superior pharmacokinetics (PK). Interestingly, this final lead optimization, which resulted in a clinical candidate and its successful marketing as a drug, was achieved with one stereogenic centre less than in most of its immediate precursors. In view of the exponential enhancement of synthetic complexity for each additional stereogenic centre in a chiral molecule, it is reasonable that the number of stereogenic centres in a potential NDE should be kept to a minimum.

11.3 Hydroboration of Ketones with Boranes from α -Pinenes and the Non-linear Effect in Asymmetric Reactions

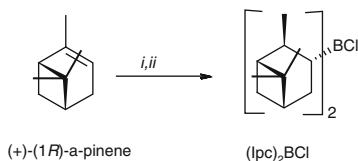
Montelukast has only one stereogenic centre but a complex assembly of functional groups. Various synthetic approaches have been claimed [13–16] and published [17–20]. In this and Sect. 11.4, we discuss selected and – from the synthetic chemistry point of view – most demanding steps, on the pathway to montelukast presented in Schemes 11.1, 11.7 and 11.9.

Condensation of 2-methylquinolone **9** with dialdehyde **10** (1.5 mol equiv), in the presence of acetic anhydride afforded, after elimination of approximately 20% of *bis*-adduct, compound **11** in 65% overall yield as a pure *E*-isomer. Grignard reaction with vinylmagnesium bromide **12**, under standard conditions, gives the expected *sec*-alcohol **13**, which is condensed with methyl-2-iodobenzoate **14**, in the presence of palladium acetate and lithium acetate in DMF, to yield ketone **15**.



Reagents and conditions: *i.* Ac_2O /xylene, reflux; *ii.* toluene, -10°C , then at -5 to 0°C ; *iii.* $\text{Pd}(\text{OAc})_2$, LiOAc , toluene, reflux under N_2 , 12 h; *iv.* $(\text{Ipc})_2\text{BCl}$, hexane, *v.* $(i\text{-Pr})_2\text{EtN}$ in THF, then 3.5 h at -20°C ; *vi.* MeMgCl , CeCl_3 , THF; *vii.* MeSO_2Cl , $(i\text{-Pr})_2\text{EtN}$, toluene/ MeCN ; *viii.* $\text{DHP}/\text{Ph}_3\text{PH}^+\text{Br}^-/\text{toluene}$.

Scheme 11.1 Initial steps en route to montelukast sodium; synthesis of intermediate (*S*)-18



Reagents and conditions: *i.* $\text{B}_3\text{H}_3\text{Me}_2\text{S}$, THF, 0°C ; *ii.* $\text{HCl}/\text{Et}_2\text{O}$, -78°C to 0°C

Scheme 11.2 Transformation of natural α -pinene to chiral borane ligand

Formation of this product, in the Heck coupling reaction, is the consequence of the migration of the $\text{C}=\text{C}$ bond repeatedly observed in this catalytic reaction [21], and transitory formation of the enol form of ketone **15**. Reduction of this ketone to the *S*-enantiomer of benzylic alcohol **16** is the key step on the path to the (*R*)-enantiomer of montelukast **1**. The second Grignard reaction (*vi*), with subsequent activation of the benzylic OH group (*vii*) and protection of *tert*-OH group (*viii*) afforded the first key intermediate **18**.

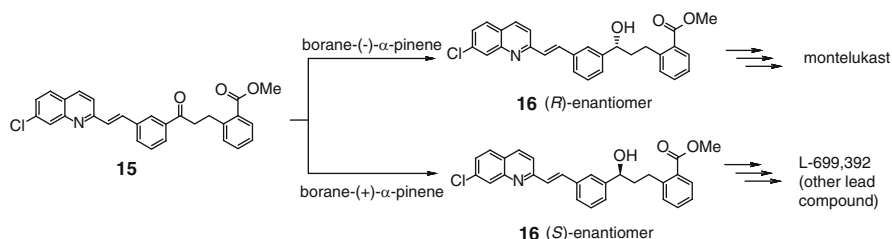
Enantioselective reduction of the ketone was studied in detail by a variety of groups, and most conveniently achieved with (–)-chloro-diisopinocampheyl borane, $(\text{Ipc})_2\text{BCl}$, available from natural (+)-pinene according to Scheme 11.2.

This chiral reducing agent was developed by Chandrasekharan and Brown [22, 23] and can be prepared *in situ* from both enantiomers of α -pinene. Later, the Merck group made an important observation on the (–)-isomer; the reducing agent prepared from 98% optically pure (–)- α -pinene gave benzylic alcohol **S-16**

with 97% e.e. [17–20]. The same reagent, prepared from less expensive 70% optically pure (–)- α -pinene, yields the alcohol **S-16** with similar optical purity of 95% e.e., which can be extended even to 99.5% e.e. by using an excess of the reagent. This effect, known as the *non-linear effect* (NLE) or *asymmetric amplification*, is observed in the reductive step **15**–**16** with both enantiomers of borane- α -pinene reagent and has been explored on an industrial scale (Scheme 11.3).

This observation is underpinned by the general principle for enantioselective reactions, first formulated by Wynberg and Feringa that “when a chiral substance undergoes a reaction, the reaction rate and the product ratio will depend, *inter alia*, upon the enantiomeric excess present in the starting material” [24]. This is not always the case, however, as was first observed by H. B. Kagan and C. Agami, who also suggested that the phenomenon be called the non-linear effect (NLE) [25]. The NLE appears when the enantiomeric purity of the product is not proportional to that of the catalytic chiral auxiliary, and is schematically presented in Fig. 11.4.

Deviations from a linear relationship can be divided into two types: a positive NLE appears when the product e.e. is greater than that calculated from the e.e. of



Scheme 11.3 Opposite enantioselectivities in hydroboration of **15**–**16** by boranes from enantiomeric α -pinenes

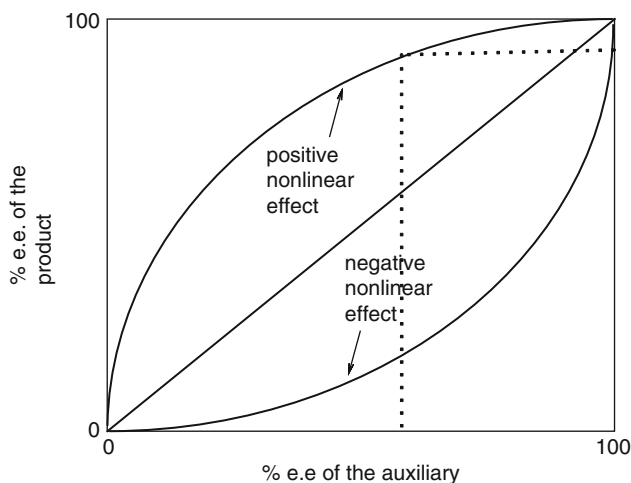
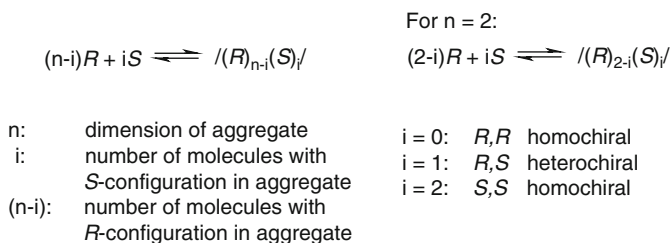


Fig. 11.4 Schematic presentation of the non-linear effect (NLE)

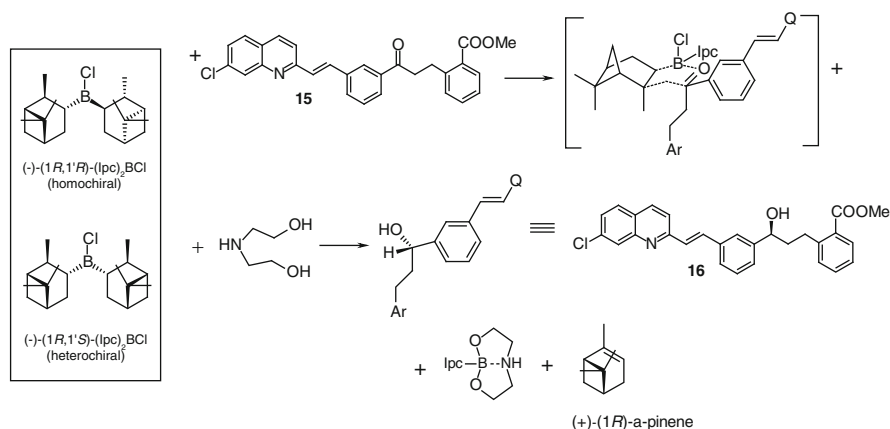
the chiral auxiliary. A negative NLE appears when the enantiomeric excess of the product is less. To explain this phenomenon, Kagan and Agami suggested that dimeric complexes give rise to an NLE. Suppose a metal binds two ligands [25]. An enantiopure system, in this case, contains only homochiral complexes, ML_RL_R or ML_SL_S , but in an enantio-impure system, heterochiral, or *meso*-complexes, ML_RL_S , also can be formed. The enantiopure complex, ML_SL_S , of the minor enantiomer, is least probable. If the *meso*-complex is active, it competes with the homochiral catalyst, and because the *meso*-complex forms racemates, the product e.e. is less than that expected of the chiral auxiliary. But if the *meso*-complex is inactive, the homochiral complex is effectively enriched. Product enantiomeric excess of the chiral auxiliary is consequently higher than expected. This relation can also be presented in terms of the equilibria shown in Scheme 11.4.

The most simple system in which an NLE is possible appears when $n = 2$, so that dimerisation, as the most simple type of aggregation, can take place. Here, possible optically active options are homochiral (*R,R*) and (*S,S*) and inactive heterochiral (*R,S*) aggregates.

This situation actually arises in the hydrogenation of **15** (Scheme 11.5). In this case, the competitive reducing agent can be either the homochiral $(-)-(1R,1'R)-(Ipc)_2BCl$



Scheme 11.4 Possible equilibria between homo- and heterochiral complexes or aggregates



Scheme 11.5 Mechanism of hydroboration by $(-)-(1R,1'R)-(Ipc)_2BCl$, exemplified by ketone **15**

or the heterochiral complex. Only the former can reduce **15** by enantioselective hydrogen transfer in the intermediary complex. The co-ordinated ketone extends the large aryl group into the less hindered *pseudo-equatorial* position whereas the alkyl group is accommodated in the *pseudo-axial* position of the chelate ring. The boron moiety initially formed is removed in this example by precipitation with diethanolamine, which allows recycling of the chiral auxiliary, although some other work-up procedures are possible.

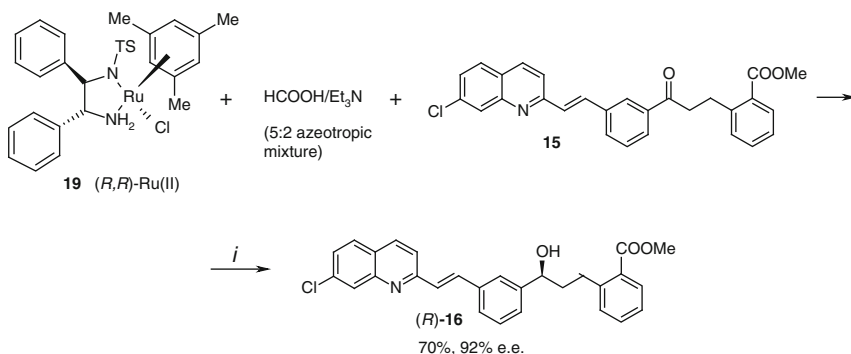
In conclusion, hydrogenation of the intermediary ketone **15** with borane derived from (–)- α -pinene proved to be highly site- and enantioselective, confirming the practical value of this non-catalytic reduction protocol.

11.4 Ru(II) Catalyzed Enantioselective Hydrogen Transfer

Another method of enantioselective hydrogenation of **15** en route to montelukast was studied by Noyori et al. using Ru(II)-catalyzed *asymmetric hydrogen transfer* and formic acid as the source of hydrogen [26]. The catalytic complex **19** and the reductive process are presented in Scheme 11.6.

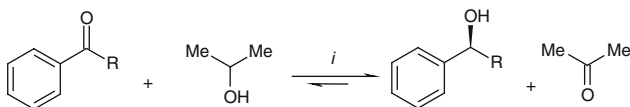
Before considering the mechanism of this important variant of asymmetric hydrogen transfer, let us first look at earlier methods used in the field. Most of them were based on 2-propanol as the favourable organic source of hydrogen, and represent catalytic variants of the Meerwein-Verley-Ponndorf “name reaction” which uses large quantities of Al-isopropoxide at elevated temperatures (Scheme 11.7) [27, 28].

Although catalytic transfer hydrogenation of ketones to alcohols with 2-propanol, according to this scheme, offers an attractive alternative to the reaction with dihydrogen (molecular hydrogen), it encountered inherent chemical problems when



Reagents and conditions: *i*. HCOOH/Et₃N as the solvent, 28 °C, substrate/catalyst ratio 200:1

Scheme 11.6 Catalytic asymmetric hydrogen transfer on the pathway to montelukast



Reagents and conditions: *i*. chiral organometallic catalysts, base

Scheme 11.7 General scheme of catalytic hydrogen transfer from 2-propanol

attempted in its asymmetric or “chiral” version. First, the occurrence of the reversal reaction, resulting from the structural similarity and close electrochemical potentials in the above redox process of the hydrogen donor and product, both being *sec*-alcohols, frequently compromises the enantiomeric purity of the chiral product [29]. Besides, the unfavourable ketone-alcohol equilibrium ratio often prevents a high conversion.

An elegant solution to these problems was found in the use of formic acid as the source of hydrogen. This hydrogen donor can be viewed as an adduct of H_2 and CO_2 , and effects the reaction irreversibly with truly kinetic enantioselection, usually with 100% conversion. Use of formic acid in enantioselective reduction of ketones has remained elusive because of the lack of a suitable transition metal catalyst, until Noyori et al. made a breakthrough in this field [26, 30]. These authors enormously improved asymmetric catalysis by the discovery of Rh(II) complexes, modified with an arene ligand and a chiral *N*-tosylated 1,2-diamine, as effective catalysts in the presence of formic acid-triethylamine azeotropic mixture. Reduction according to Scheme 11.6 can be conducted conveniently in an open vessel using a mixture of $/RuCl_2(\eta^6\text{-mesitylene})_2/\text{complex}$ and *(1R,2R)*-*N*-(*para*-tolylsulfonyl)-1,2-diphenylethylene diamine (TsDPEN) in a formic acid-triethylamine solvent, without isolating the *(R,R)*-Ru(II) catalytic complex **19**.

The reactivity and enantioface-differentiation capability of the complex **19** results from the compromise between the steric and electronic properties of the $\eta^6\text{-mesitylene}$ ligand and the chiral diamine. In complex **19**, mesitylene displays a better enantioselectivity, with somewhat decreased reactivity, than the unsubstituted benzene. Even more interestingly, the presence of the NH_2 terminus in the TsDPEN ligand proved of crucial importance. The $NHMe$ analogue showed a comparable enantioselectivity but with much lower reactivity, whereas the NMe_2 derivative gave very poor reactivity and enantioselectivity! In the reduction of **15** another important aspect is complete site-selectivity, involving reduction of the carbonyl group without affecting the olefinic bond, ester function, quinoline ring or the hydrogenolysis of the halogen atom.

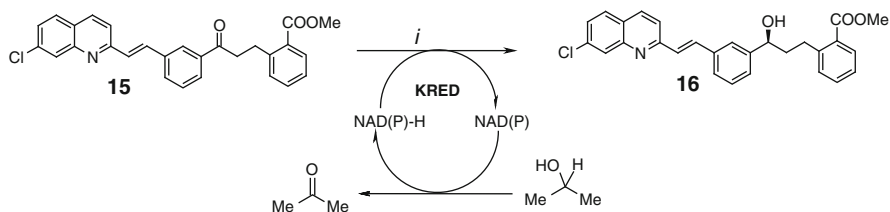
Successful application of the *(R,R)*-Ru(II) catalyst **19** in the synthetic route to montelukast sodium is an elegant example of how fundamental knowledge of a catalytic process enables development of a robust and effective catalyst, which is useful on an industrial scale in the synthetic development of a chiral drug.

11.5 Biocatalytic Reduction with Ketoreductase KRED (KetoREDuctase)

In spite of these two relatively efficient reductions of the carbonyl group in **15**, two research teams have jointly developed a biocatalytic process as an alternative approach, applicable to large scale production of the enantiopure intermediate **16** [31]. Through synergistic efforts in process chemistry, molecular biology, bioinformatics and high throughput screening, a ketoreductase KRED (*KetoREDuctase*) with very high enantioselectivity, >99.9% e.e., was developed. This biocatalytic process was scaled-up to produce a >200 kg batch (Scheme 11.8) [31].

KRED reductase was developed by enzyme evolution technology, and targeted enzyme activity was approximately 1,000-fold higher than that of the initial enzyme [32]. Fine-tuning of the enzyme evolution through 19 mutations gave the final strain with activity at 45°C that yielded 100 g of substrate **15**/L in 24 h at an enzyme concentration of 3 g/L.

The main technological issue in developing this process was the highly hydrophobic nature of the substrate **15** (clog *P* approx 7; for comparison *n*-heptane has clog *P* approx 4), rendering it virtually insoluble in water. Since the two reactions in Scheme 11.8 form an equilibrium, elimination of the acetone side-product *via* distillation is required to drive reduction of **15** to completion. Fortunately, both problems were solved, and the crystalline monohydrate of **16** was obtained using a mixture of the solvents (*iso*-PrOH/toluene/aq. buffer) and slow distillation of the acetone formed in the reaction. The resulting reaction was “self-driven” to 99% conversion by continuous precipitation of the product **16** from the reaction mixture.



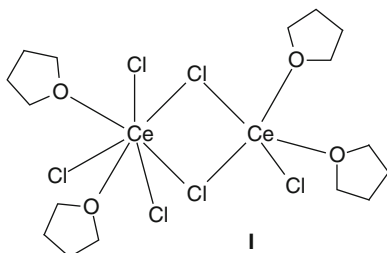
Reagents and conditions: *i*: 100g/L substrate **15** loading, *i*-PrOH/toluene/Et₃N buffer, pH 8 (5:1:3), KRED 3-5 wt.%, r.t., 40-45h.

Scheme 11.8 Codexis' biocatalytic reduction of **15**–**16**

11.6 CeCl₃-THF Solvate as a Promoter of the Grignard Reaction: Phase Transfer Catalysis

The extraordinary effect of Ce(III) chloride on the Grignard reaction in step *vi* of the Scheme 11.1, giving significantly better yields of the *tert*-alcohol **17** than in the reaction performed in its absence, deserves analysis and comment. This step was

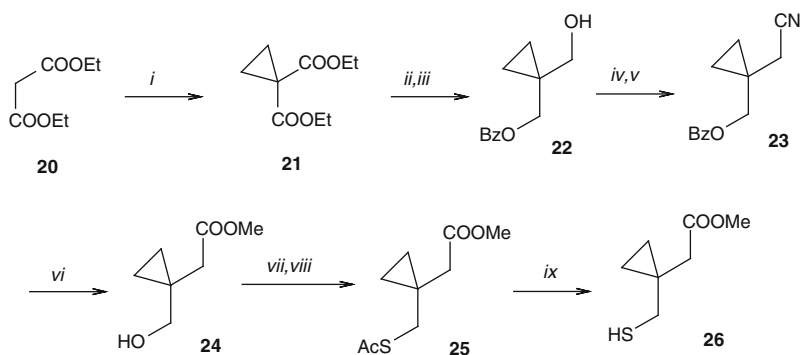
studied in detail, and it was demonstrated that the use of properly activated Ce(III) chloride overcomes undesired reactions, such as enolization, reduction and condensation, competing with the formation of *tert*-alcohols [33].



The activated Ce(III) chloride was identified as the THF solvate **I**, and its crystal structure was determined. It was shown that the total water content in the system during the Ce(III) chloride activation is a critical factor controlling selectivity towards the *tert*-alcohol **17**. Under optimized reaction conditions, formation of the methyl ketone was suppressed by 12–20% to 0.74%, and selectivity of conversion to the diol **17** enhanced by up to 99.2% with 100% conversion of **16**. The beneficial effect of hydrated Ce(III) chloride complex is postulated to be due to suppression of the enolization of the methyl ketone intermediate and formation of less basic and more nucleophilic species with the Grignard reagent. Despite extensive efforts, the structure of this reagent formed from Ce(III) chloride and Grignard reagents remains unknown [33].

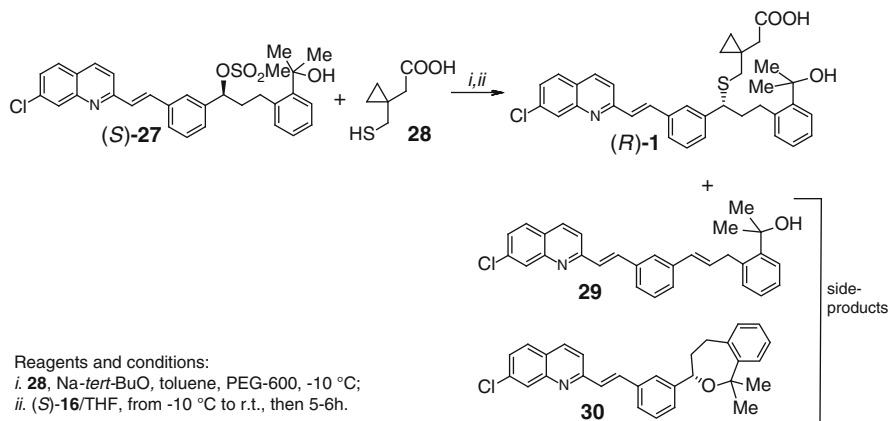
The route to the second key intermediate **26**, an achiral thiol bearing a cyclopropyl unit, requires nine steps from diethylmalonate (Scheme 11.9).

It is worth mentioning here the method by which the hydroxyl group in **24** is replaced by the thiol group in **26**. It is based on the high nucleophilicity of the soft Cs-salts of thioacids and the selective split of the S–C(=O) bond in the



Reagents and conditions: *i*. 1,1,2-dibromoethane, NaH/toluene; *ii*. LiAlH₄/THF, *iii*. BzCOCl/pyridine; *iv*. MsCl, Et₃N; *v*. NaCN/DMSO; *vi*. KOH, EtOH/H₂O; *vii*. MsCl, Et₃N; *viii*. AcSCe, DMF; *ix*. NH₂NH₂.

Scheme 11.9 Synthesis of the cyclopropane-derived building block **26** on the path to montelukast



Scheme 11.10 Alternative process for thiolation step on the pathway to (R)-1

intermediary thioesters by hydrazine under mild conditions [34]. Importantly, substitution of the thiobenzoic or thioacetic acids in DMF by caesium salts allows the reaction to proceed virtually without racemization of the optically pure *sec*-mesylates or tosylates, which can be deacylated with hydrazine or ammonia to afford enantiomerically pure thiols [35].

With thiol **26** available, the process was improved using free acid **28** as a thiolating agent, and non-THP protected (S)-**27** (Scheme 11.10). Formation of the C–S bond in (S)-**27**, with inversion of the configuration, is the last crucial step in the synthesis of montelukast. It was soon observed that the original conditions for steps *i* and *ii* in Scheme 11.10 needed improvement, since the yield of montelukast in the product mixture was regularly low and large quantities of the side-products **29** and **30**, up to 60%, were observed [36].

To avoid this inconvenience, stabilization of the disodium salt of thiol carboxylic acid **28** was achieved through solvating metal by linear and cyclic polyethers. They acted as *phase transfer catalysts* (PTCs), which can solvate metal ions and thus increase the solubility and reactivity of nucleophilic reagent. The increased reactivity of the nucleophilic reagent, the dialkali metal salt of **28**, resulted in higher selectivity of the process and unwanted competitive reactions were suppressed. Polyethylene glycol (PEG-600) proved a particularly effective component of the reacting system. Using the conditions indicated in Scheme 11.10, a scale-up process was developed on a kg-scale, affording (R)-**1** in 85.7% yield at 93% conversion.

11.7 Conclusion

There are many synthetic routes to montelukast [13–20]. As for other successful drugs on the market, many of these routes have been developed by chemists in companies that are not primarily involved in development of new drug entities

(NDEs, see Sect. 1.1). These are usually referred to as *generic companies*, since they focus their R&D and business activities on active pharmaceutical ingredients (APIs) for which patent protection will expire. Contrary to general belief, generic companies are by no means pirate companies just awaiting the expiration of patent protection. To the contrary, their investment in R&D is growing and their research targets are becoming increasingly sophisticated. Such companies generally initiate their R&D projects 8–10 years before termination of the patent protection of an API. Their aim is to make innovative contributions, such as developing original and more effective synthetic routes or inventive pharmaceutical forms that make possible new routes of therapy, in particular those based on new polymorphs with favourable bioavailability and pharmacokinetic (PK) properties. Obviously, in view of their long-term targets, interdisciplinary research and high total costs, such research projects become much more like NDEs and approach the philosophy of *innovative companies*. In other words, the borderline between these two enterprises is disappearing, and in the future they will tend to merge.

References

1. Young RN (2001) *Progr Med Chem* 38:249–277
2. Young RN (1999) *Eur J Med Chem* 34:671–685
3. Grant JA, Lichtenstein LN (1974) *J Immunol* 112:897–904
4. Ishizaka T, Ishizaka K, Tomioka H (1972) *J Immunol* 108:513–520
5. Chand N (1979) *Agents Actions* 9:133–140
6. Murphy RC, Hammarstrom S, Samuelsson B (1979) *Proc Natl Acad Sci USA* 76:4275–4279
7. Lewis RA, Austen KF, Drazen J, Clark DA, Marfat A, Corey EJ (1980) *Proc Natl Acad Sci USA* 77:3710–3714
8. Snyder DW, Fleisch JH (1989) *Annu Rev Pharmacol Toxicol* 29:123–143
9. Drazen J (1981) In: Holgate S, Dahlen S (eds) *SRS-A to Leukotrienes*. Blackwell Science, Oxford, pp 189–201
10. Coleman RA, Eglen RM, Jones RL, Narumiya S, Shimizu T, Smith WL, Dahlen S, Drazen J, Gardiner PJ, Jackson WT, Jones TR, Krell RD, Nicosia S (1995) *Adv Prostaglandin Thromboxane Leukot Res* 23:283–285
11. Yang RN (1988) *Drugs Future* 13:745–759
12. Labelle M, Prasit P, Belley M, Blouin M, Champion E, Charette L, Deluca JG, Dufresen C, Frenette R, Gauthier JY, Grimm E, Grossman SJ, Guay D, Herold EG, Jones TR, Lau CK, Leblanc Y, Leger S, Lord A, McAuliffe M, McFarlane C, Masson P, Metters KM, Oimet N, Patrick DH, Perrier H, Pickett CB, Piechuta H, Roy P, Williams H, Wang Z, Xiang YB, Zamboni RJ, Ford-Hutchinson AW, Young RN (1994) *Bioorg Med Chem Lett* 4:463–468
13. Merck Frosst Canada Inc. Unsaturated hydroxyalkylquinoline acids as leukotriene antagonists, EP 480717
14. Merck&Co., Inc. Process for the preparation of leukotriene antagonists, WO 9518107
15. Merck&Co., Inc. Process for the preparation of 1-(thiomethyl)-cyclopropaneacetic acid, US 5523477
16. Chemigas Ltd. Process for preparing montelukast and precursors thereof, US 2006/0223999 A1
17. McNamara JM, Leazer JL, Bhupathy M, Amato JS, Reamer RA, Reider PJ, Grabowski EJJ, Org J (1989) *J Org Chem* 54:3618–3721
18. Labelle M, Belley M, Gareau Y, Frenette R, Guay D, Gordon R, Grossman SJ, Jones TR, Leblanc Y, McAuliffe M, McFarlane C, Masson P, Metters KM, Oimet N, Patrick DH,

- Piechuta H, Sawyer N, Yiang YB, Pickett CB, Ford-Hutchinson AW, Zamboni RJ, Young RN (1992) *Bioorg Med Chem Lett* 2:1141–1146
19. Labelle M, Belley M, Gareau Y, Frenette R, Guay D, Gordon R, Grossman SJ, Jones TR, Leblanc Y, McAuliffe M, McFarlane C, Masson P, Metters KM, Oimet N, Patrick DH, Piechuta H, Sawyer N, Yiang YB, Pickett CB, Ford-Hutchinson AW, Zamboni RJ, Young RN (1995) *Bioorg Med Chem Lett* 5:283–288
 20. Guay D, Gauthier JY, Dufresne C, Jones TR, McAuliffe M, McFarlane C, Metters KM, Prasit P, Rochette C, Roy P, Sawyer N, Zamboni R (1998) *Bioorg Med Chem Lett* 8:453–458
 21. Negishi E, de Meijere A (2002) *Handbook of organopalladium chemistry for organic synthesis*, Chapter IV.2. The Heck Reaction (Alkene substitution via carbopalladation–dehydropalladation). J Wiley Interscience, New York
 22. Chandrasekharan L, Ramachandran PV, Brown HC (1985) *J Org Chem* 50:5446–5448
 23. Brown HC, Chandrasekharan L, Ramachandran PV (1986) *J Org Chem* 51:3394–3396
 24. Wynberg H, Feringa B (1976) *Tetrahedron* 32:2831–2834
 25. Puchot S, Samuel O, Dunach E, Zhao S, Agami C, Kagan HB (1986) *J Am Chem Soc* 108: 2353–2357
 26. Fujii A, Hashiguchi S, Uematsu N, Ikaraya T, Noyori R (1996) *J Am Chem Soc* 118: 2521–2522
 27. Zassinovich G, Mestroni G, Gladiali S (1992) *Chem Rev* 92:1051–1069
 28. Evans DA, Nelson SG, Gagne MR, Muci AR (1993) *J Am Chem Soc* 115:9800–9801
 29. Yang H, Alvarez M, Lugan N, Mathieu R (1995) *J Chem Soc Chem Commun*: 1721–1722
 30. Hashiguchi S, Fujii A, Takehara J, Ikariya T, Noyori R (1995) *J Am Chem Soc* 117: 7562–7563
 31. Lang J, Lalonde J, Borup B, Mitchell V, Mundorff E, Trinh N, Kochrekar DA (2010) *Org Process Res Dev* 14:193–198
 32. Fox R, Huisman GW (2008) *Trends Biotechnol* 26:132–138
 33. Conlon DA, Kumke D, Moeder C, Hardiman M, Hutson G, Sailer L (2004) *Adv Synth Catal* 346:1307–1315
 34. Kellogg RM, Hof RP (1996) *Perkin Trans* 1:1651–6157
 35. Strijtveen B, Kellogg RM (1986) *J Org Chem* 51:3664–3671
 36. Halama A, Jirman J, Boušková O, Gibala P, Jarrah K (2010) *Org Proc Res Dev* 14:425–431

Chapter 12

Thiolactone Peptides as Antibacterial Peptidomimetics

Abstract

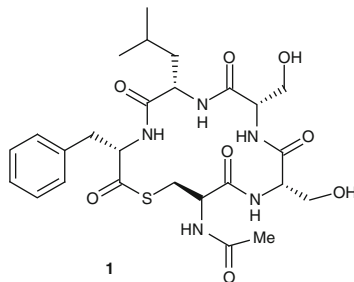
Biological target: Thiolactone peptides are macrocyclic peptides that bind, on the surface of *Staphylococcus aureus* bacteria, to the accessory gene regulator C. This acts as a receptor for auto-inducing and quorum-sensing peptides produced by the bacteria and regulates the bacterial growth.

Therapeutic profile: In mimicking the quorum-sensing peptides, the thiolactone peptides act as antibacterials, naturally regulating the growth of the bacteria.

Synthetic highlights: This chapter describes the background for the development of modern peptide syntheses. This involves chemical ligation of unprotected peptides carried out with chaotropes. Using a transient thioester-linked intermediate, native chemical ligation (NCL) of two unprotected peptides is achieved. With Fmoc protecting groups and the use of Rink resin, chemoselectivity of peptide synthesis is feasible. The development of NCL, as applied to thiolactone peptide synthesis, is considered in detail.

12.1 Introduction

This chapter is devoted to a biologically active macrocyclic compound **1**, which is neither a drug molecule that has been introduced into therapy nor was its stereochemistry created by a synthetic chemist. Compound **1** is both a cyclic polypeptide and a macrocyclic thiolactone at the same time.



The therapeutic importance of peptides and cyclopeptides is well known [1–4]. Their therapeutic profile ranges from anti-diabetic and cytostatic agents in addition

to a wide variety of other activities [5–7]. Recently, it was discovered that thiolactone peptides act as potent anti-microbials, thanks to their specific mechanism of action. This discovery has opened the door to a new concept for the therapy of infective diseases and initiated research into original synthetic routes to this class of compounds.

Huge progress has been made in synthetic methodologies for the construction of cyclopeptides, and of *thiolactone peptides* in particular. The original methods developed by peptide chemists in constructing large peptides, and cyclopeptides containing a thiolactone group, represent an exceptional achievement by the pharmaceutical industry. In comparison with the classical peptide synthetic procedures, these new methods have broadened the capacity for the preparation of large proteins with considerable implications for the development of molecular biology (genome construction). On the other hand, they have created the potential to synthesize polypeptides with additional functionalities, such as a thioester group, that are not easily amenable to classical *liquid-phase protein synthesis* (LPPS) or *solid-phase protein synthesis* (SPPS). These new synthetic concepts are referred to as *chemical ligation* (CL) and *native chemical ligation* (NCL) and will be discussed in more detail in relation to the synthesis of the target thiolactone peptide **1**.

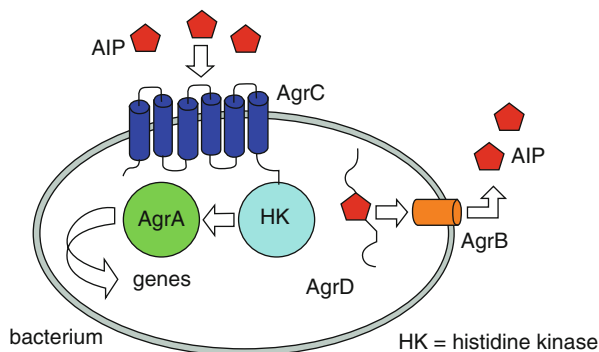
This compound is a cyclic, non-natural peptide with a thiolactone unit and a representative of the group of cyclic peptide inhibitors of staphylococcal virulence. Thiolactone peptides are expected to act as anti-bacterial therapeutics by a highly specific mechanism, as outlined in the following sections.

12.2 Virulence and Quorum-Sensing System of *Staphylococcus aureus*

An ever-increasing number of modified bacterial strains, and in particular, the emergence of antibiotic resistance in microbial species have become serious concerns for the therapy of microbial infections [8, 9]. It is clear that pathogens continue to adapt more quickly than new antibiotics can be developed. Consequently, there is a pressing need to identify new types of antibacterial agents, and it has been suggested that *interference with the expression of microbial virulence* (the inherent disease-causing capacity of a micro-organism) may represent a promising anti-bacterial approach [10, 11]. Targeting bacterial systems associated with virulence rather than their essential cellular processes is becoming a preferred research approach to anti-bacterial therapy.

The discovery of a global regulatory system for virulence in *S. aureus*, mediated by small *auto-inducing peptides* (AIPs) has opened a new avenue to the interruption of microbial defences, and consequently, to overcoming resistance to many antibiotics. Microbial defensive mechanisms, based on mutation, drug efflux pathways, biofilm formation and the secretion of virulence factors, have become the major threat to modern antibiotic therapy.

Fig. 12.1 Proposed mechanism of the two-component *agr* auto-induction system in *S. aureus* (reproduced from [14], by permission of The Royal Society of Chemistry. <http://dx.doi.org/10.1039/B517681F>)



To begin with, let us briefly consider the function of AIPs and their role in *quorum sensing*. AIPs function as extracellular signalling molecules that allow individual organisms to sense the surrounding bacterial population density. Once a critical bacterial count is achieved, designated a “quorum”, the bacteria modulate their gene expression and thereby their rate of reproduction. This results in co-operative behaviour that confers sustainability to the whole developing colony. Remarkably, each of the secreted AIPs can activate an accessory gene regulator (*agr*) within the same colony and inhibit the *agr* response in strains belonging to other colonies [12, 13].

Thus, to a large extent, local cell density, as one of the most important factors in the pathogenesis of *S. aureus*, can be regulated by “quorum sensing” mediated by a group of small macrocyclic peptides. The quorum-sensing system in *S. aureus* is encoded by the *agr* locus and is shown schematically in Fig. 12.1 [14].

Accessory gene regulator B (AgrB) processes the propeptide AgrD to generate an AIP and secretes this into the extracellular milieu. The AIPs bind to the AgrC receptor, the intracellular unit of which is a *histidine kinase* (HK) that phosphorylates the intracellular response regulator AgrA. This second signalling component then promotes gene transcription that induces increased virulence and produces more *agr* proteins, completing the auto-induction circuit.

The surface protein receptor, AgrC, is an especially attractive and viable target for therapeutic control, as its *inhibitors need not permeate the cell membrane*. This greatly simplifies the constraints regarding pharmacokinetic properties of drug candidates, which require only a low molecular weight and sufficient lipophilicity to achieve membrane permeability. More precisely, knowledge of the structure and composition of the *S. aureus* auto-inducing peptides, AIPs I–IV (Fig. 12.2), permitted the design of synthetic analogues with inhibitory properties.

The key step in the synthesis of analogues of AIPs I–IV consists of the insertion of the highly reactive thiolactone unit in between the cysteine SH group and the carboxylic group of amino acids at the C-terminus. Generally, thioesters are regarded as activated carboxylic acids, useful intermediates in the synthesis of more stable derivatives such as esters and amides. Formation of thioesters is, therefore,

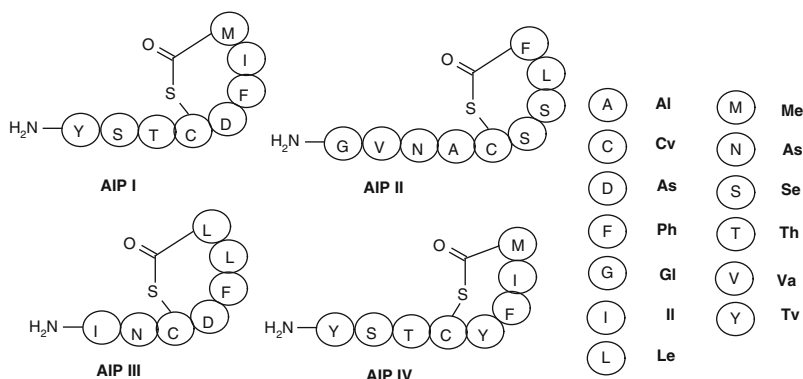


Fig. 12.2 Schematic representation of auto-inducing peptides **AIP I-IV** from *S. aureus* species

an energetically “uphill” process, which requires very specific protocols in order to be successful.

Before entering the specific topic of insertion of the thioester unit into peptidomimetics, it is first relevant to overview briefly two related achievements in synthetic peptide chemistry methodology.

12.3 Development of Chemical Ligation in Peptide Synthesis

At the turn of the last century, most proteins were obtained by recombinant DNA-based expression of proteins in genetically engineered cells [15]. This method revolutionized the study of proteins by enabling the production of large amounts of proteins of defined molecular composition, and allows for the variation of the amino acid sequence of the proteins [16]. As the cell is used as a protein factory, such molecular structures are inherently limited to the 20 genetically encoded amino acids. The technology is further limited by the dimensions of proteins, usually only those with a molecular weight of below 30 kD are easy to express. Large multi-domain proteins that are often toxic to the cell are difficult to generate [17].

Chemical synthesis of proteins, as an attractive alternative to biological methods of protein production, also has its advantages and inherent limitations. It promises unlimited variation of the covalent structure of the polypeptide chain, including incorporation of non-natural amino acids. However, synthesis of even small protein molecules by the standard methods of peptide chemistry has remained a daunting task. Such synthesis has often required large teams and taken years to complete, with no guarantee of success. By the classical methods, routine and reproducible preparation of synthetic polypeptides was limited to products of up to 50 amino acid residues. Historical progress in polypeptide synthesis, from coupling of *N*-carbobenzyloxy (N-Cbz) protected amino acids (AAs) in solution (LPPS) via SPPS to the recently introduced chemical ligation (CL), is presented in Fig. 12.3 [18].

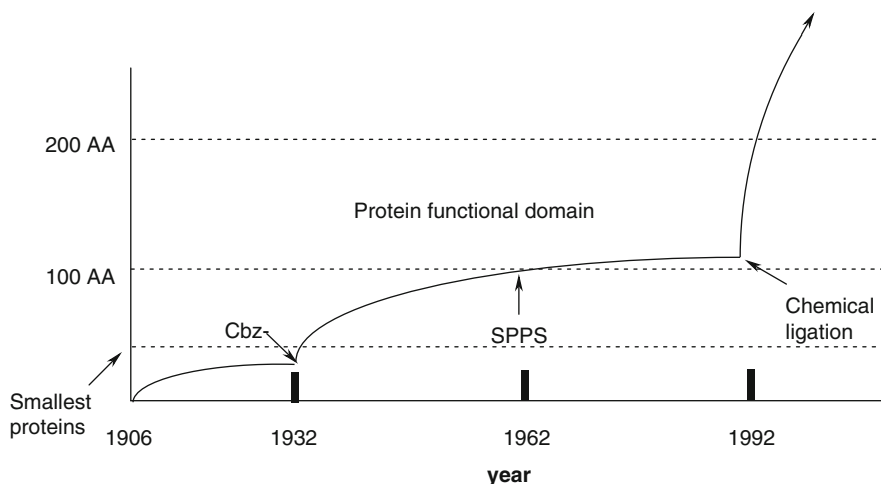


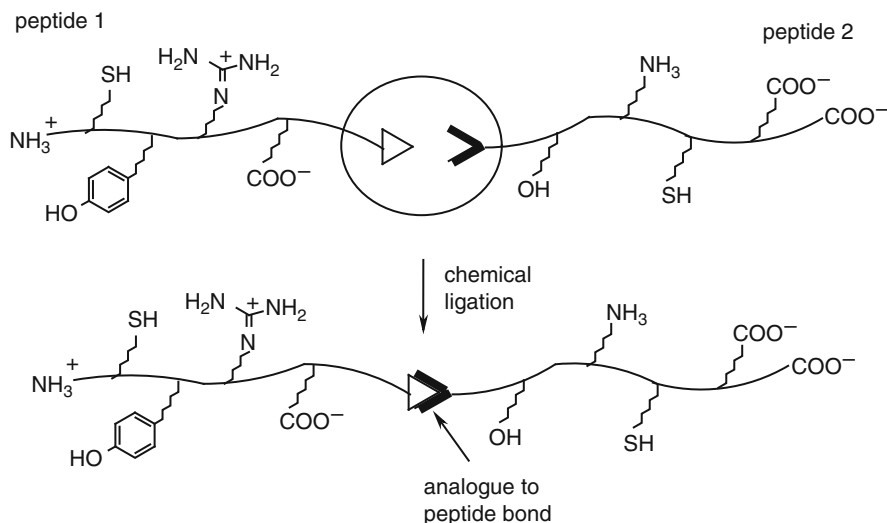
Fig. 12.3 Historical progress in the size of synthetically accessible polypeptides (modified from [18])

None of these methods, however, allowed for the synthesis of functional proteins or of enzymes in particular. Their inherent limitations include the technically demanding preparation of protected AAs and smaller protein segments and the lack of an effective method for the purification of protected segments. Most importantly, the lack of ionisable groups in fully protected peptides precludes direct analysis by *electrospray mass spectrometry* (ESM), a powerful tool in the analysis of large molecules. The poor solubility of fully protected peptides in organic solvents made them difficult to manipulate, and the low attainable concentrations of reacting segments often led to slow and incomplete reactions [19].

Usually, unprotected peptide segments are readily soluble, can be more easily handled and can be directly characterized by ESM. The most efficient method for the synthesis of unprotected peptides is SPPS, introduced by Merrifield in 1963 [20], and by 1980, it had been developed into a powerful tool for the synthesis, in good yield and high purity, of peptides with up to 50 AAs [18].

With these available achievements, the situation was ripe for the most important discovery in protein synthesis, *chemical ligation* (CL) of unprotected peptide segments [21–24]. The method is based on the principle of *chemoselective reactions*, which are facilitated by mutually reactive functional groups in the presence of other, notably, less reactive functionalities. This novel chemical ligation approach to peptide chemistry relies on the principles outlined in Scheme 12.1 [23].

Two reactive functional groups are usually incorporated into each peptide by chemical synthesis. Their mutual recognition triggers a *chemoselective reaction* and allows the use of completely unprotected peptide segments, which led to a marked increase in the size of available synthetic peptides in recent years, as presented in Fig. 12.3. The fact that such chemoselective reactions may be carried out in aqueous buffers is of considerable methodological importance. In addition,



Scheme 12.1 Principles of chemical ligation (modified from [23])

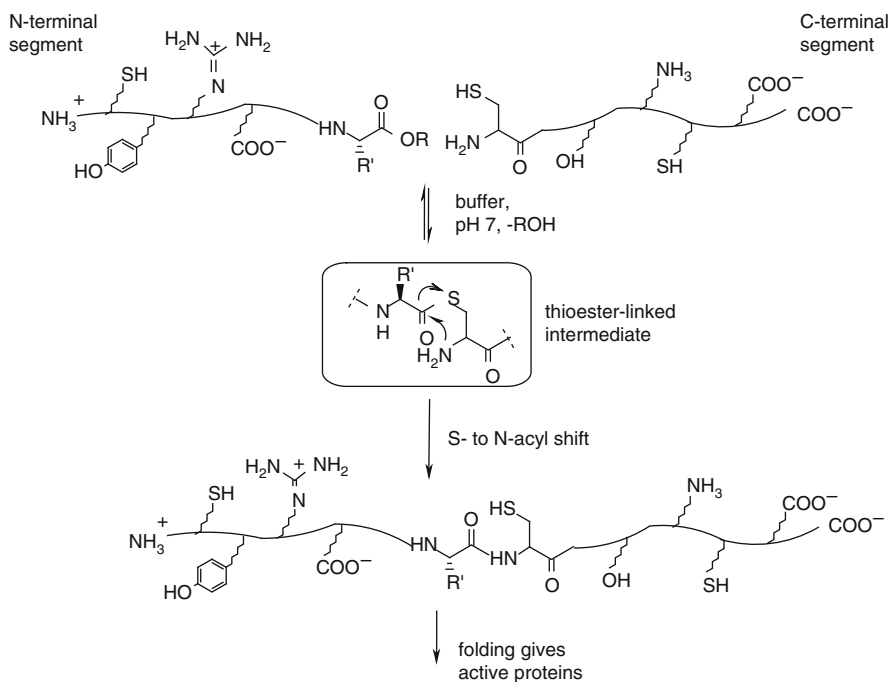
the reactions are carried out with *chaotropes*, polar salts that increase the concentration of the reacting segments by a specific salting-in effect and consequently enhance the rate of reaction. The broadly used *chaotrope*, 6 M guanidine hydrochloride, increases the solubility of the reacting peptides, thereby, allowing the use of higher peptide concentrations to accelerate the CL reaction.

As simple as this methodology can be, it is not without a principal drawback. This is presented by the formation of an unnatural bond at the site of ligation between the two peptide segments. Such bonds include thioester- [25], oxime- [26], thioether- [27], disulfide- [28] and thiazole-forming [29] CL. These unnatural structures, however, are often well tolerated within the folded protein and examples exist of fully active protein molecules synthesized by CL [23].

12.4 Development of Native Chemical Ligation; Chemoselectivity in Peptide Synthesis

On the basis of these methodologies that afforded proteins in high yield and good purity from unprotected building blocks, only one step remained to achieve the synthesis of large peptides *with a natural amide bond at the ligation site*. In 2004, Dawson et al. discovered an ingenious extension of the CL principle, and named it NCL [30]. This process is outlined in Scheme 12.2 [23].

Simply mixing two peptide segments together that contain correctly designed and mutually reactive functional groups led to the formation of a single polypeptide product containing a *native peptide bond at the ligation site*. The essential feature of

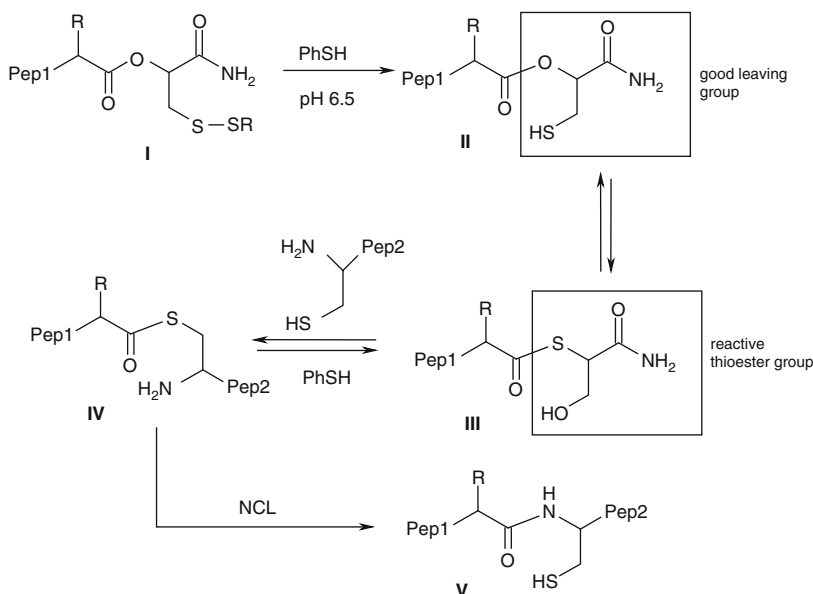


Scheme 12.2 Schematic presentation of native chemical ligation (NCL) (modified from [23])

the NCL method is the transient formation of the thioester bond followed by an *S*-to-*N*-acyl shift. The thioester bond is expressly designed to undergo spontaneous rearrangement via intramolecular nucleophilic attack of the amino group to form the amide-linked product.

The critical feature of the NCL method is that *ligation occurs at an N-terminal Cys residue*, no matter how many additional internal Cys residues are present in either segment. Such fascinating chemoselectivity allows the use of unprotected functional groups present in either of the two reacting proteins. For detailed studies of the mechanism of the NCL reaction, the interested reader should consult the studies by Dawson et al. [31, 32]. Here it suffices to say that transesterification of esters into thioesters represents an energetically “uphill” process in view of the higher reactivity (lower stability) of the latter. It can be achieved if the subtle interplay between entropic and enthalpic factors favours the process, or if the product is present in a low steady-state concentration, and is consumed in the subsequent irreversible step, as for the NCL process shown in Scheme 12.2.

More recent improvements of the NCL methodology have been reported by Botti et al. [33] and Danishefsky et al. [34, 35]. Botti has developed a strategy that allows the formation of thioester peptides compatible with an Fmoc protecting group, thus solving an old problem in peptide chemistry [29, 30]. The elegance of this method is demonstrated in Scheme 12.3 [33].

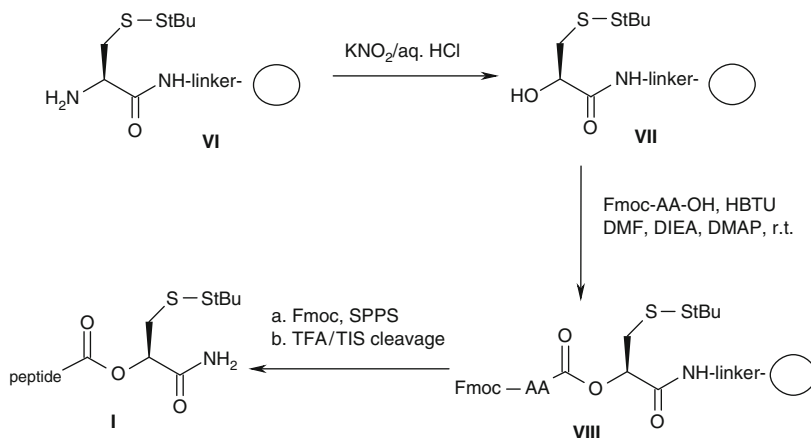


Scheme 12.3 Native chemical ligation through an in situ *O*- to *S*-acyl shift (modified from [33])

This simple scheme apparently hides a highly inventive solution to the *chemo-selective reactivity* problem. The electron-withdrawing carboxamido group is introduced into **I**, adjacent to the O-atom in the ester bond, activating the C–O bond in the C(O)–O–C_α unit. The carboxamido group makes the hydroxyl a better leaving group in **II** and allows the unfavourable, “energetically uphill” *O*- to *S*-acyl migration to form **III**. The reactive thioester intermediate **IV** is formed on addition of the second peptide unit, then withdrawn from the equilibrium with the formation of the new peptide bond in **V** (Scheme 12.3).

This key step has enabled the synthesis of peptides in the solid phase, preferably on the Rink-amide resin, according to Scheme 12.4 [33].

Under solid-phase conditions, *fluorenylmethyloxycarbonyl* (Fmoc)-Cys-(*tert*-butylthio)-OH is coupled, in a first step, to the amino Rink-PEGA resin using standard HBTU coupling. This yields, after Fmoc group removal, the starting resin **VI**. A detailed explanation of the structure and use of the Rink-amide resin is given in the next section. The N-terminal free amino group is transformed into hydroxyl group in **VII** via the diazo salt, reacting with KNO₂ under aqueous conditions. These steps generate the carboxamide 3-*tert*-butylsulfanyl-2-hydroxypropionamide template, which is esterified to **VIII** by *O*-benzotriazole-*N,N,N'*, *N'*-tetramethyl-uronium-hexafluorophosphate/*diisopropyl-ethylamine* (HBTU/DIEA) coupling reagents. Further steps in Scheme 12.4 afford peptide **I**, with a protected cysteine unit at the ligation site, ready for deprotection and ligation according to Scheme 12.3.



Scheme 12.4 Preparation of peptide-C α oxy-(2-tert-butylthiophenyl-1-carboxamide) ethyl ester **I** on the Rink-amide resin (modified from [33])

12.5 Development of NCL in Thiolactone Peptide Synthesis

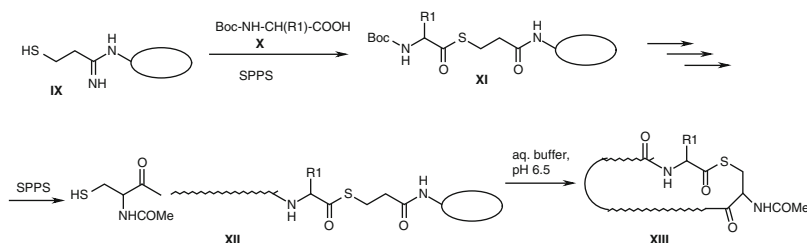
As mentioned in the introduction to this chapter, the recent discovery of thiolactone peptides as potential antimicrobial agents, based on their ability to act as antagonists of natural *auto-inducing peptides* (AIP), prompted the new synthetic achievements, which permitted the synthesis of these cyclic peptide inhibitors. Here, we discuss the most recent achievement in the synthesis of AIP mimics, based on an original linker for the Fmoc-based solid-phase methodology.

Previous AIP syntheses involved a combined solid-phase solution route. According to this new method, a linear unprotected peptide, α -thioester **XI**, prepared by *tert*-butoxycarbonyl (*tert*-Boc)-SPPS undergoes cyclization to **XII** through *trans*-thioesterification, and elimination of the resin in aqueous buffer to yield the thiolactone peptide **XIII** (Scheme 12.5) [36].

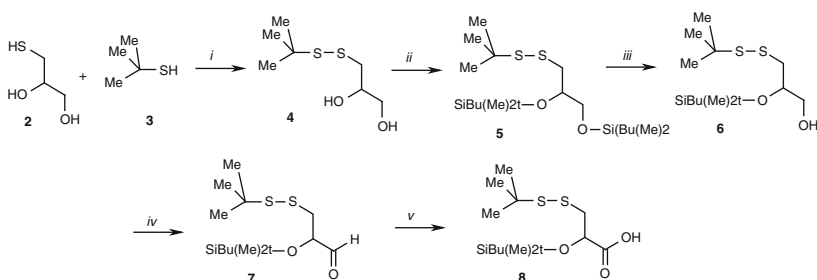
In all of the peptide bond-forming steps, N-Boc-AA is activated by the HBTU/DIEA system, and the Boc group removed with anhydrous HF. The latter creates a bottleneck in the process, and the replacement of Boc by an Fmoc protecting group became the key objective.

This problem was first addressed by Muir et al. [36], adopting the Botti methodology [33]. In this approach, Fmoc-cysteine-(*t*-BuS)-COOH was first coupled with poly[acriloyl-bis(aminopropyl)polyethyleneglycol] (PEGA) resin, followed by α -aminodiazotization, as shown in Scheme 12.4. Subsequent hydrolysis under aqueous conditions affords the α -hydroxycysteine resin. The crucial drawbacks of this method are the low isolation yields due to the limited options for resins that have good swelling properties in water.

Design of the new linker, its synthesis and successful application to novel AIP synthesis was recently achieved by the same group [36]. To overcome the limitations



Scheme 12.5 Schematic presentation of the synthesis of thiolactone peptide **XIII** with N-Boc protected amino acids (modified from [36])



Reagents and conditions: *i.* mol. ratio **2**:**3**:TEA = 1:10: 2.5, solvent, MeOH bubbling O₂ overnight, r.t., >10; *ii.* Mol. ratio **4**: *tert*-Bu(Me)₂SiCl: imidazole: DMAP (1²:3:6:0.06), solvent, anhydr. DMF, bubbling N₂ overnight, r.t.; *iii.* cold 1:1 mixture TFA/water added dropwise to **5** in THF, stirring at 0 °C for 4.5h; *iv.* DCM, mol. ratio Dess-Martin periodinane: **6** (1.2:1) stirring under N₂ at r.t. for 2h; *v.* NaOCl, 2-methyl-2-butene, Na-phosphate buffer.

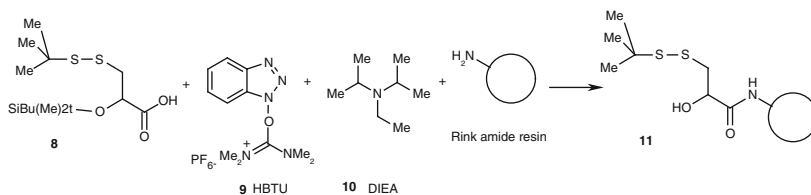
Scheme 12.6 Preparation of the linker **8** (modified from [36])

mentioned earlier, the authors designed a solution-phase synthesis of an original linker, 2-(*tert*-butyl-dimethyl-silyloxy)-3-*tert*-butyldisulphanyl-propionic acid (**8**). This molecule is an α -hydroxycysteine congener that acts as a masked thioester and can be coupled with any resin using standard procedures. Preparation of **8** is outlined in Scheme 12.6 [36].

This linker was bound to a Rink-amine resin, and the *O*-*tert*-butyldimethylsilyl (OTBS) protecting group removed by *tetrabutylammonium fluoride* (TBAF) in THF, affording **11** (Scheme 12.7). A detailed description of the reaction and work-up conditions in this scheme will serve to demonstrate the sensitivity of this initial step in SPPS technology.

Selective deprotection of the Fmoc protecting group, either on the Rink resin or on the first AA bound to the Rink resin, is presented in Scheme 12.8.

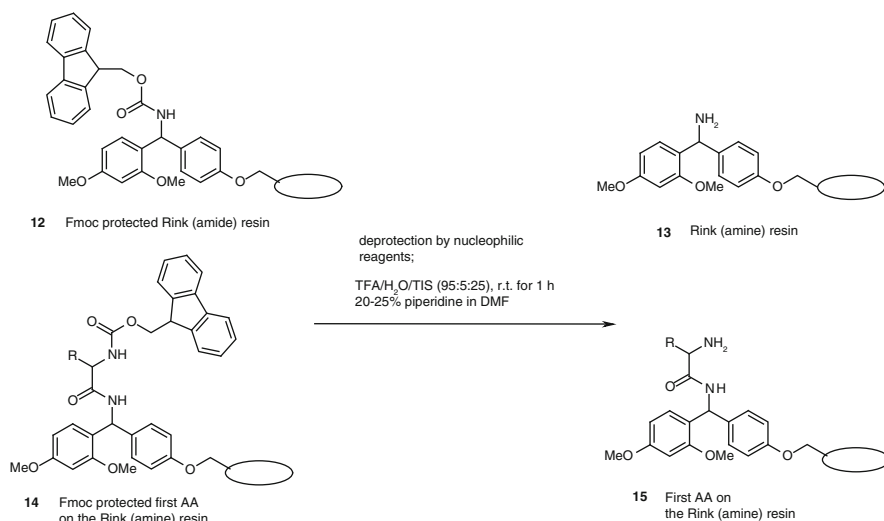
This solid phase comprises a polystyrene-bound benzylamine unit, in which removal of the prepared peptide unit is triggered by the formation of a benzylic carbocation, stabilized by the three alkoxy *electron donating groups* (EDG). With the linker bound to the Rink resin (**11**), the authors completed the *O*-acylation with N-Fmoc-Phe to obtain **17** (Scheme 12.9).



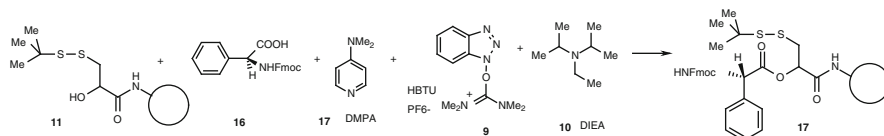
Reagents and conditions: DMF, mol. ratio 8: HBTU: DIEA: Rink resin (1:1:1.0:2.6:1.0), first 8, HBTU, DIEA in DMF for 3 min at r.t. then Rink resin, stirred by bubbling N_2 at r.t. for 4 h

Work-up: remaining amino groups acylated by Ac_2O /DIEA/DMF (1:1:8); two treatments for 10 min, deprotection of TBS by TBAF (1M in THF), r.t., overnight

Scheme 12.7 Formation of amide **11** using O,S-protected, 3-dithio-2-hydroxypropionic acid and Rink resin



Scheme 12.8 Schematic presentation of Fmoc deprotection on the Rink resin and of the first AA bound to N-Fmoc



Standard reagents and conditions: solvent DMF
mol. ratio 8: HBTU: DIEA: Rink resin (1:1:1.0:2.6:1.0),
first 8, HBTU, DIEA in DMF for 3 min at r.t.
then Rink resin, stirred by bubbling N_2 at r.t. for 4 h.

Work-up: remaining amino groups acylated by Ac_2O /DIEA/DMF (1:1:8); two treatments for 10 min, deprotection of TBS by TBAF (1M in THF), r.t., overnight.

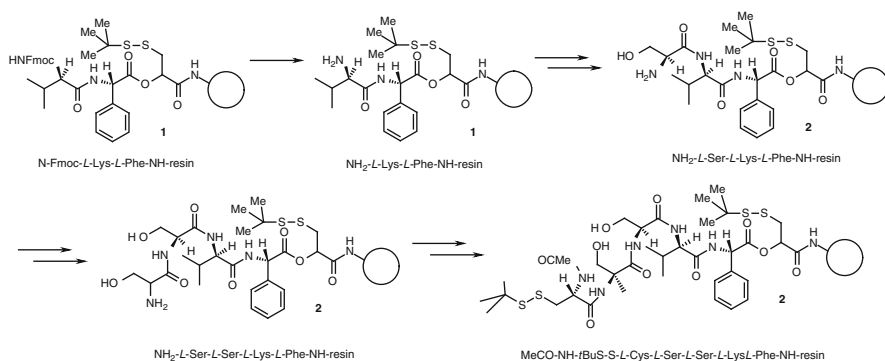
Scheme 12.9 Preparation of O-acylated linker with N-Fmoc-Phe **17**

Scheme 12.9 once again shows the details of the reaction conditions and work-up. The work-up requires protection of all the remaining amino groups by acetylation, and removal of the TBS group by a non-hydrolytic agent in THF.

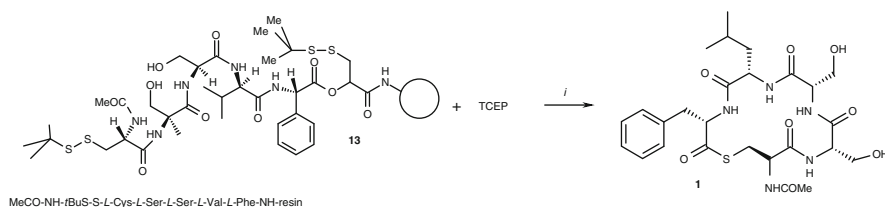
SPPS of the thiolactone peptide precursor **22** was completed by sequential addition of N-Fmoc protected AAs (Phe, Lys, Ser, Ser and Cys). This sequence is presented in Scheme 12.10.

In the last step, removal of the pentapeptide was completed with simultaneous formation of the thiolactone unit, as outlined in Scheme 12.11.

The key reagent in the final step is the addition of the mild reducing agent, *tris*-(2-carboxy)ethyl phosphine (TCEP), which permits the formation of the thiol group, deprotonated at pH 6.6–6.8 and its intramolecular attack on the activated ester group. In this step, the cyclopeptide **1** is removed from the solution and purified by semi-preparative HPLC.



Scheme 12.10 SPPS of **22**, the acyclic precursor of the thiolactone peptide **1**



Reagents and conditions: *i.* solvent; 20% MeCN/80% 6 M guanidinium chloride in 0.1 M phosphate buffer pH 6.5 then added TCEP and pH adjusted to 6.6–6.8 with 4M NaOH. Rocked at r.t. for 2–24 h,

Work-up: purification by semipreparative HPLC (Vydac C18 column), eluent linear gradients.

Scheme 12.11 Final step in the SPPS of the thiolactone peptide **1**

12.6 Conclusion

The crucial steps in the synthesis of peptides by SPPS, CL and NCL, avoiding the massive introduction and elimination of protecting groups, illustrate the elegance and novelty of this approach. The methods have prompted the development of new solutions to solid-phase synthesis, as in the instructive approach to the auto-inducing antibacterial peptidomimetic **1**. This compound, with its congeners, is expected to act as a blueprint for new antibacterials to treat infections with highly resistant micro-organisms, thus, solving one of the most important current problems in the therapy of infectious diseases.

References

1. Yan L (1983) A small peptide. *Science* 220:64–65
2. Mor A (2001) Peptides; biological activity of small peptides. In: *Encyclopedia of life sciences*. Wiley, Published Online: 19 April 2001, DOI: [10.1038/npg.els.0001329](https://doi.org/10.1038/npg.els.0001329)
3. Sewald N, Jakubke HD (2009) Peptides: chemistry and biology. Wiley-VCH, Weinheim
4. Kastin A (2006) Handbook of biologically active peptides. Academic, MA
5. Gomez-Paloma L, Bruno I, Cini E, Khochbin S, Rodriguez M, Taddei M, Terracciano S, Sadoul K (2007) Design and synthesis of cyclopeptide analogs of the potent histone deacetylase inhibitor, FR235222. *Chem Med Chem* 2:1511–1519
6. Sainas I, Fokas D, Vareli K, Tzakos AG, Kounnis V, Briasoulis E (2010) Cynobacterial cyclopeptides as lead compounds to novel target cancer drugs. *Mar Drugs* 8:629–657
7. Yu R, Wang J, Li J, Wang Y, Zhang H, Chen J, Huang L, Liu X (2010) A novel cyclopeptide from the cyclization of PACAP (1-5) with potent activity towards PAC1 attenuates STZ-induced diabetes. *Peptides* 31:1062–1067
8. Fluit AC, Wielders CLC, Verhoef J, Schmitz F-J (2001) *J Clin Microbiol* 39:3727–3732
9. Anderson DI (2003) *Curr Opin Microbiol* 6:452–456
10. Roychoudhury S, Zelinski NA, Ninfa AJ, Allen NE, Jungheim LN, Nicas TI, Chakraborty AM (1993) *Proc Natl Acad Sci USA* 90:965–969
11. Ji G, Beavis R, Novick RP (1995) *Proc Natl Acad Sci USA* 92:12055–12059
12. Ji G, Beavis R, Novick RP (1997) *Science* 276:2027–2030
13. Lina G, Jarraud S, Ji G, Greenland T, Pedraza A, Etienne J, Novick RP, Vandensch F (1998) *Mol Microbiol* 28:655–662
14. Gorske BC, Blackwell HE (2006) *Org Biomol Chem* 4:1441–1445
15. Matthews BW (1993) *Ann Rev Biochem* 62:139–160
16. Smith M (1994) *Angew Chem Int Ed* 33:1214–1221
17. Cleland JL, Craik CS (1996) Protein engineering: principles and practice. Wiley Interscience, New York, pp 518–542
18. Kent SBH (1988) *Ann Rev Biochem* 57:957–984
19. Gatos D, Athanassopoulos P, Tzavara C, Barlos K (1999) In: Bajusz S, Hudecz F (eds) *Peptides*. Akademia Kiado, Budapest, pp 146–148
20. Merrifield RB (1986) *Science* 232:341–347
21. Stephen BH, Kent D, Alewood P, Alewood M, Baca A (1992) In: Epton R (ed) *Innovation and perspectives in solid phase synthesis*. Andover, UK, pp 1–22
22. Muir TW, Kent SBH (1993) *Curr Opin Biotechnol* 4:420–427
23. Dawson PE, Kent SBH (2000) *Ann Rev Biochem* 69:923–960

24. Macmillan D (2006) *Angew Chem Int Ed* 45:7668–7672
25. Schnolzer M, Kent SBH (1992) *Science* 256:221–225
26. Rose K (1994) *J Am Chem Soc* 116:30–33
27. Englebretsen DR, Garnham BG, Bergman DA, Alewood PF (1995) *Tetrahedron Lett* 36:8871–8874
28. Baca M, Muir TW, Schnolzer M, Kent SBH (1995) *J Am Chem Soc* 117:1881–1887
29. Liu CF, Rao C, Tam JP (1996) *J Am Chem Soc* 118:307–312
30. Dawson PE, Muir TW, Clark-Lewis I, Kent SBH (1994) *Science* 266:769–779
31. Dawson PE, Churchill MJ, Ghadiri MR, Kent SBH (1997) *J Am Chem Soc* 119:4325–4329
32. Hackeng TM, Griffin JH, Dawson PE (1999) *Proc Natl Acad Sci USA* 96:10068–10073
33. Botti P, Vilani M, Manganiello S, Gaertner H (2004) *Org Lett* 6:4861–4864
34. Warren JD, Miller JS, Keding SJ, Danishefsky SJ (2004) *J Am Chem Soc* 126:6576–6578
35. Wu B, Chen J, Warren JD, Chen G, Hua Z, Danishefsky SJ (2006) *Angew Chem Int Ed* 45:4116–4125
36. George EA, Novick RP, Muir TW (2008) *J Am Chem Soc* 130:4914–4924

Chapter 13

Efavirenz

Abstract

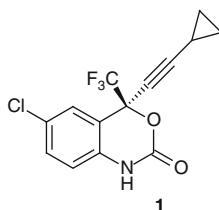
Biological target: Efavirenz is a non-nucleoside analogue, direct inhibitor of reverse transcriptase (RT) and thus blocks the transcription of human immunodeficiency virus-1 (HIV-1) viral RNA into the genome of infected cells. The binding at the active site of RT involves unique steric interactions.

Therapeutic profile: The drug is a first choice therapy for patients with HIV-1 infection.

Synthetic highlights: The initial step in the synthetic pathway to efavirenz involves the asymmetric addition of an alkyne anion to the ketone C=O bond. The generation of chiral Li^+ aggregates elegantly determines the stereoselectivity of the reaction. Scale-up of alkynylation is promoted by the use of Et_2Zn as a weak Lewis acid.

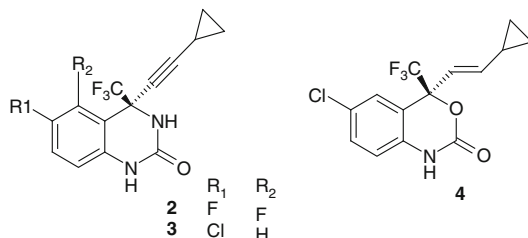
13.1 Introduction

Efavirenz ((S)-**1**, (–)-6-chloro-4-cyclopropylethynyl-4-trifluoromethyl-1,4-dihydro-2H-3,1-benzoxazin-2-one, *Sustiva*[®], *Stocrin*[®]) is widely prescribed for the treatment of the *acquired immunodeficiency syndrome* (AIDS) and symptomatic HIV-1 infections [1, 2].



AIDS is caused by two types of viruses, *human immunodeficiency viruses* HIV-1 and -2, the former being the most prevalent. In 2008, an estimated 33.4 million people worldwide were living with an HIV infection, and around 2 million of these die each year [3]. The AIDS epidemic remains a challenge to worldwide healthcare. In the USA alone, since 1980, \$170 billion has been spent on AIDS research, and

more than \$20 billion is still being invested annually. Patients infected with HIV require long-term therapy with effective and inexpensive drugs administered at convenient once-daily doses, without pronounced side effects, and with lowered capacity to induce resistance in the rapidly mutating HIV-1 virus [4, 5]. Although the effective suppression of HIV infection is achievable with a combination of drugs, the individual drugs are still prone to the development of resistance [6]. Therefore, new generations of more potent structural congeners of existing drugs are under continual investigation. A prime example of such an active compound is efavirenz (**1**), a successor to its active congeners **2–4**.



Efavirenz is well absorbed orally and has a relatively long plasma half-life of up to 55 h, permitting once daily administration. Although, like other drugs of this class, it can exert undesirable CNS side effects, it has become the drug of choice in initial standard triple therapy of HIV-1 infections, referred to as *highly active anti-retroviral therapy* (HAART).

13.2 HIV-1 Reverse Transcriptase Inhibitors

HIV is an RNA retrovirus that binds to surface molecules (CD4 and chemokine receptors) on white blood cells that are crucial for host defence. The virus then enters the cell and uses its own biochemical machinery to transcribe the viral RNA into DNA, which is then integrated into the DNA of the host cell chromosomes. The host cell then starts generating viral proteins, which are modified by viral proteases and used to construct new viruses that leave the cell to infect other cells.

While novel compounds are under development that inhibit the integration of viral DNA into nuclear chromatin, as well as others that block new virus construction, the three main targets of current anti-HIV drug therapy are the surface molecules that bind the virus at the cell surface, the viral enzyme, *reverse transcriptase* (RT), which converts viral RNA into DNA and the viral proteases that modify viral proteins for incorporation into new viruses. Reverse transcriptase inhibitors (RTIs) were the first to be developed and remain the mainstay of HAART combinations. There are three classes of RTI: the original nucleoside analogues, which act as false message carriers in the nucleotide transcription process; non-nucleoside analogues, which inhibit the enzyme directly, and the nucleotide analogue, tenofovir, which is a pro-drug, activated by tissue esterases. Efavirenz is a *non-nucleoside reverse transcriptase inhibitor* (NNRTI), inhibiting HIV-1 RT by inducing

a conformational change in the enzyme to lock the polymerase active site into an inactive conformation [7].

13.2.1 *Steric Interactions at the Active Site*

Due to the importance of its three-dimensional structure, including the absolute (*S*)-configuration of efavirenz and the mechanism of its inhibition of HIV-1 RT, some structural aspects of the interaction of efavirenz with the active site of RT will be considered here in detail. The RT is responsible for the reverse transcription of viral RNA into complementary DNA as soon as the virus enters the host cell. It is therefore a preferred, deterministic biological target and detailed structural and functional studies on the protein have been reported [8]. It possesses a specific, largely hydrophobic pocket and not surprisingly, NNRTIs are targeted at this pocket. Characteristically, the shape of efavirenz and many NNRTI congeners of the first and second generations show surprising similarity, sharing a common butterfly-like conformation consisting of two wings, representing two specific π -electron-containing moieties that do not share a common plane [9, 10].

This three-dimensional frame of efavirenz is governed by its single stereogenic centre, the absolute *S*-configuration inducing a helical-like arrangement (with a very short pitch) of the four substituents at the stereogenic centre. It is crucially important for the biological effects of the drug that the direction of helicity, which is hidden in the three-dimensional structure of (*S*)-**1**, matches the helicity at the TR active site. Detailed studies of this interaction have demonstrated the orientation of efavirenz in the bound HIV-1/RT complex [11, 12]. It was found that the cyclopropylethynyl group is positioned within the top sub-pocket at the active site, surrounded by the aromatic units of four amino acids (Tyr181, Tyr188, Trp229 and Phe227). This binding interaction is complemented by the interactions of the benzoxazin-2-one ring, sandwiched between the side chains of a single leucine (Leu100) and one valine (Val116) residue. A graphical representation of the attractive (red) and repulsive (blue) interactions between efavirenz and the individual amino acid residues of HIV-1 is given in Fig. 13.1 [13].

The net attractive interaction between efavirenz and the surrounding amino acid residues amounts to ~22 kcal/mol, the most important contribution, ~11.3 kcal/mol, being provided by two hydrogen bonds between the backbone Lys101 and the carbamate group of the benzoxazin-2-one ring, as schematically presented in Fig. 13.2.

These hydrogen bond interactions have not been observed in other HIV-1-RT/antiviral agent complexes and are considered to be a distinguishing property of efavirenz. Most importantly, these interactions provide the basis for the capacity of efavirenz to dimerize two critical subunits of HIV-1 RT and inhibit DNA polymerization. These two subunits are p66 and p51, which form a heterodimer with

Fig. 13.1 Graphical representation of the attractive (*red*) and repulsive (*blue*) interactions of efavirenz and individual residues of HIV-1 RT (reproduced from [13], with permission of Elsevier)

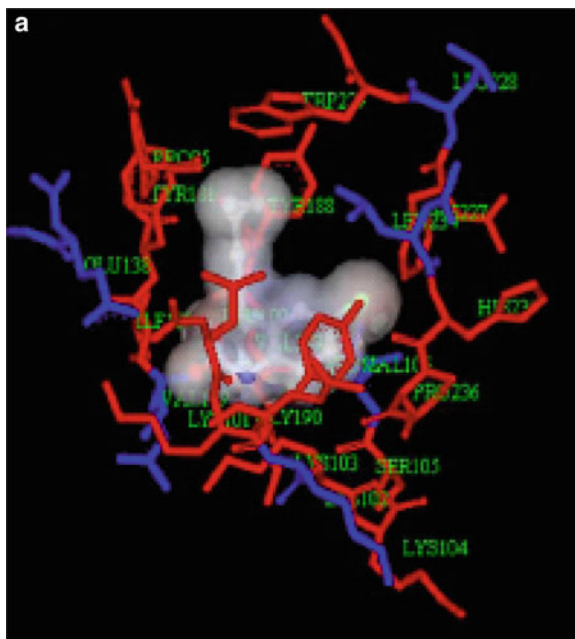
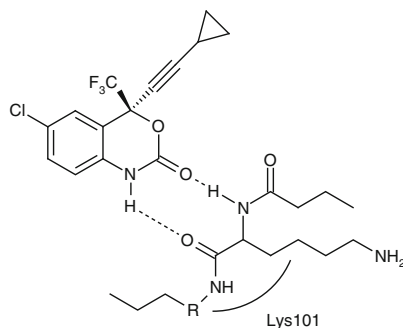


Fig. 13.2 Hydrogen bonding between efavirenz and Lys101 at the RT active site



a pocket of ~ 10 Å at the active site. The p66/p51 heterodimer has a chiral structure [13]. The four sub-domains form a segment of the right-handed helix, which perfectly explains the requirement for the well-defined chirality of efavirenz and its congeners as HIV-1 inhibitors. Efavirenz binding induces structural changes in the dimeric face of the p66/p51 heterodimer, which account for its increased subunit affinity and prevents its catalyzation of DNA polymerization.

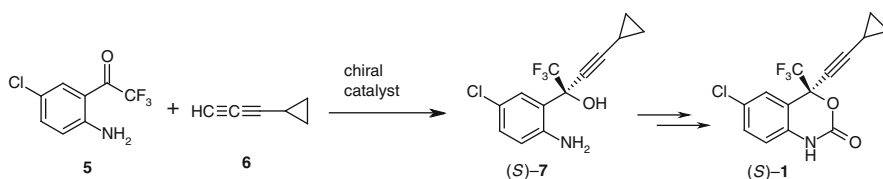
Efavirenz **1** and its congeners **2–4** are prepared in a higher than 98% enantiomeric excess on a scale of up to 5,000 kg. All of them either reached a late stage of clinical testing or have been introduced into the regular therapy of AIDS [14, 15]. The remarkable synthetic achievements that resulted in the availability of this valuable drug on the world market are outlined in the following sections.

13.3 Asymmetric Addition of Alkyne Anion to C=O Bond with Formation of Chiral Li⁺ Aggregates

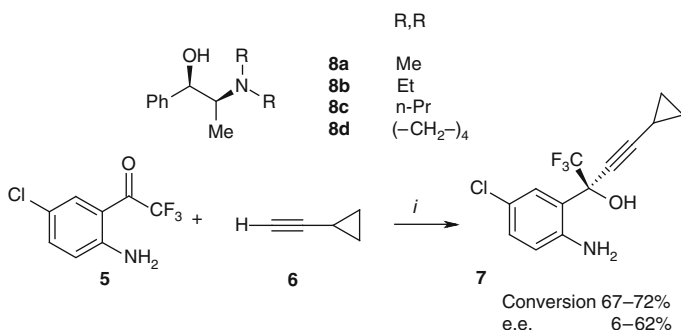
The initial step on the synthetic pathway to (*S*)-**1** requires complete enantioselective addition of cyclopropylacetylide carbanion of **6** to the ketone **5** to obtain the carbinol (*S*)-**7**, followed by carbonylation of the 1,3-amino alcohol unit, as outlined in Scheme 13.1.

13.3.1 Mechanism of the Chirality Transfer

The route via racemic carbinol **7** requires its derivatization into a mixture of diastereomers, their separation by crystallization and final removal of the derivatizing agent [16]. Moreover, the “wrong” enantiomer of *tert*-alcohol **7** cannot be racemized via oxidation–reduction, a process that was successfully applied in the synthetic approach to sertraline, as presented in Chap. 7. At Merck Research Laboratories, the enantioselective alkynylation of trifluoromethyl ketone **5** by cyclopropylacetylene **6** was therefore studied as the key step in the asymmetric synthesis of enantiopure efavirenz (*S*)-**1** (Scheme 13.2) [16]. The observation that the Li-acetylide of



Scheme 13.1 Initial enantioselective step on the path to efavirenz, (*S*)-**1**



Reagents and conditions: *i.* *n*-BuLi, chiral modifier **8a–8c**, –25 °C.

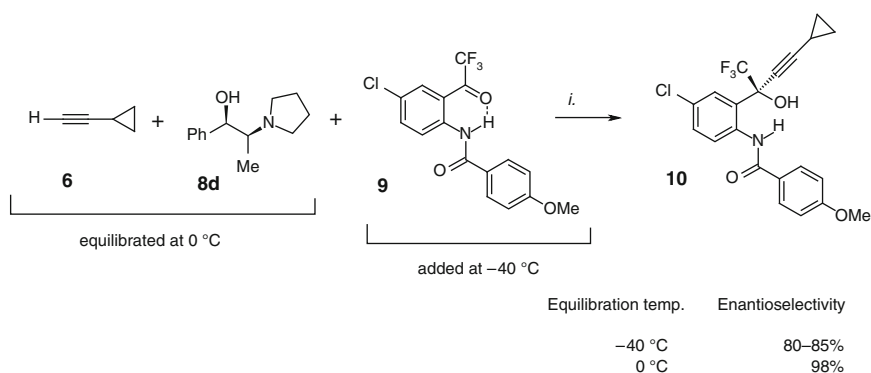
Scheme 13.2 Chiral modifiers **8a–d** used in the enantioselective alkynylation of ketone **5**

6 and Li-aminoalkoxides of chiral auxiliaries **8a–c** form multi-component reactive complexes proved to be critical for the success of this project. In the absence of a reliable working hypothesis, the authors initiated the study of this reaction by treating the unprotected amino-ketone **5** with a mixture of Li-cyclopropylacetylide and Li-alkoxides of chiral amino-alcohols **8a–d** (Scheme 13.2).

All four chiral auxiliaries are available derivatives of ephedrine. Structurally, they are vicinal amino-alcohols, which are able to act as 1,4-N,O-bidentate ligands for many metal cations. The stability of such complexes generally enhances with the hardness of the central metal ion [17].

With the first three chiral auxiliaries, **8a–c**, low to medium e.e.s of **7** were obtained, far from values needed to make the process operate on a large scale. Somewhat higher enantioselectivities were obtained when the reaction was performed at -40°C with an *N*-*para*-methoxybenzoyl (PMB)-protected substrate **9** (Scheme 13.3). Even more important for the research concept than just enhancement of e.e.s were the observations made in these experiments. First, 2 mol of the acetylide and 2 mol of the chiral auxiliary were needed for complete ketone alkynylation. Second, pyrolidino-ephedrine **8d** proved to be the best auxiliary amino-alcohol. With this auxiliary, an e.e. of over 98% was achieved, with complete conversion of the ketone, but only when the acetylide-alkoxide solution was first warmed to 0°C then cooled down to -40°C before addition of the ketone **9** (Scheme 13.3).

This result indicated that the lithium aggregates equilibrated at 0°C to form an effective complex in the transfer of chirality. The experiments also revealed a *non-linear effect* (NLE), suggesting that more than 1 mol of chiral auxiliary was involved in the chirality transfer (more detailed discussion about the origin of non-linearity in chirality transfer is given in Chap. 11).



Reagents and conditions: *i.* *n*-BuLi, -40 to 0°C , THF.

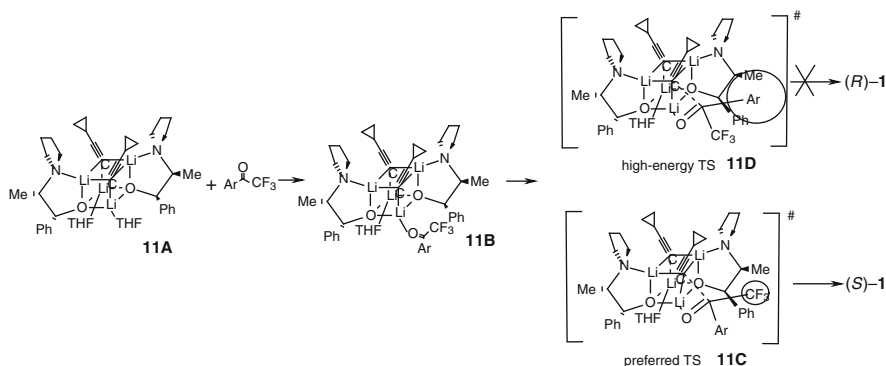
Scheme 13.3 Optimized scheme for production of the key intermediate **10** in the pathway to efavirenz

13.3.2 Equilibration of Lithium Aggregates and the Effect of Their Relative Stability on Enantioselectivity

The strong tendency of lithium cation to undergo multiple co-ordination with hard heteroatoms, in particular oxygen, is well known [17, 18]. In the specific case of the acetylide-pyrrolidino ephedrine alkoxide system, meticulous spectroscopic studies using ^6Li , ^{13}C and ^{15}N NMR techniques, and X-ray characterization of some complexes revealed a variety of interesting structural data [19]. Formation of the cubic tetramer **11A** during high temperature equilibration (Scheme 13.4) was demonstrated by all three NMR techniques. The multiplicity of the signals of the Li-, N- and C-labelled atoms at various temperatures has also revealed that the acetylide-alkoxide complexes *do not equilibrate below* 0°C . These findings suggested the mechanism for the pathway to (*S*)-**1**, starting from the tetramer **11A** to form the preferred transition-state tetramer **11C** (Scheme 13.4) [19, 20].

Two paths are possible for the formation of the C–C bond between the acetylide and carbonyl carbon of the ketone via the two tetrameric transition-state complexes **11C** or **11D**. In the higher energy path, the larger aryl group must share the same space, in a sterically highly crowded environment, as the phenyl and methyl groups of the ephedrine analogue **8d**. In the lower energy path, the aryl group occupies a relatively empty space, whereas the smaller CF_3 group is found in a crowded region. This simple model predicts the enantioselective bias of alkylation toward the (*S*)-enantiomer of **1**, as confirmed experimentally [19].

In concluding this section, it is important to mention that the roles of *aggregation phenomena* have been carefully defined by Noyori, who emphasizes the “softness”, that is, the relatively low kinetic barriers to transitions between various intermediates on the energy surface [21]. The stereoselectivity of diastereometric aggregates in directing the reaction is nicely demonstrated in Scheme 13.4.



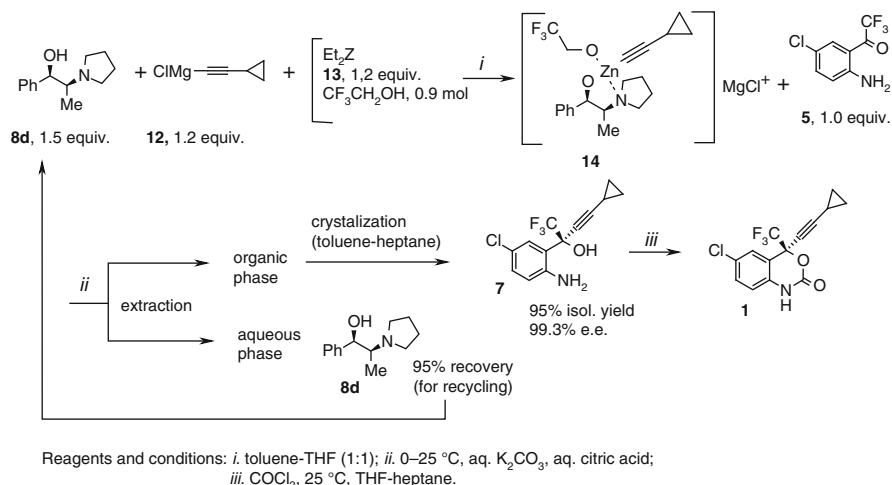
Scheme 13.4 Diastereomeric transition-state tetramers **11C** and **11D** define enantioselective alkylation of aryl-trifluoromethyl ketone

The results of this elegant research provided the basis for the large-scale production of efavirenz (*S*)-**1**. The compound was produced on a 30-kg scale with 98% purity and 98.4% e.e., which on crystallization, produced material with 100% e.e. Later development of this process, as described in the next section, permitted the production of early sales quantities of efavirenz [22].

13.4 Scale-up of Alkynylation Promoted by the Use of Et_2Zn

However, the creativity of the synthetic chemists did not stop with the process shown in Scheme 13.3. A problem emerged due to the use of the N-PMB group in the protection step. To solve this problem, it was reasoned that the Et_2Zn should act as a promoter even in the absence of the N-PMB group. This reagent is a mild base, unable to deprotonate the aniline amino group in the starting ketone **5**, despite the expected enhancement of its N–H acidity. Since Et_2Zn behaves also as a weak Lewis acid, it was used in combination with the Grignard alkyne reagent **12** to generate the Zn-alkynyl species (Scheme 13.5). It was fortuitous that the same ephedrine analogue **8d** used with Li-acetylide was also the best chiral auxiliary in the Zn complex **14**. Moreover, following the observation that trifluoroethanol can serve as the second alkoxy unit, only 1 mol of chiral auxiliary **8d** was needed; in practice, 1.5 mol equivalent was used [22, 23].

The route outlined in Scheme 13.5 has been developed to a large-scale process, providing (*S*)-**7**, which was transformed into efavirenz without loss of enantiomeric purity, with 95% yield and 99% e.e.



Scheme 13.5 Large-scale production method for efavirenz **1** via the key intermediate (*S*)-**7**

13.5 Conclusion

The approach used for efavirenz is cited as one of the most effective synthetic methods ever devised for a chiral drug [16]. At the same time, it is an impressive example of how “basic research” in chemistry can drive technical solutions that are applicable to process chemistry, contributing to effective chirality transfer and satisfying the stringent economy of the production process.

References

1. Young SD, Britcher SF, Tran LO, Payne LS, Lumma WC, Lyle TA, Huff JR, Anderson PS, Olsen DB, Carroll SS, Pettibone DJ, O'Brien JA, Ball RG, Balani SK, Lin JH, Chen I-W, Schleif WA, Sardana VV, Long WJ, Barnes VW, Emini EA (1995) *Antimicrob Agents Chemother* 39:2602–2605
2. Corbett JW, Ko SS, Rodgers JD, Gearhart LA, Magnus NA, Bacheler LT, Diamond S, Jeffrey S, Klabe RM, Cordova BC, Garber S, Logue K, Trainor GL, Anderson PS, Erickson-Viitanen SK (1999) *Antimicrob Agents Chemother* 43:2893–2897
3. WHO/UNAIDS Data and statistics. Global Summary 2009. http://www.who.int/hiv/data/2009_global_summary.gif Accessed 14 October 2010
4. Grob PM, Wu JC, Cohen KA, Ingraham RH, Shih CK, Hargrave KD, McTague TL, Merluzzi VJ (1992) Nonnucleoside inhibitors of HIV-1 reverse transcriptase. *AIDS Res Hum Retroviruses* 8:145–152
5. Havlir DV, Richman DD (1996) Viral dynamics of HIV implications for drug development and therapeutic strategies. *Ann Intern Med* 124:984–994
6. Cane AP (2009) New developments in HIV drug resistance. *J Antimicrob Chemother* 64 (suppl 1):i37–i40
7. Zhou Z, Lin X, Madura JD (2006) *Infect Disord Drug Targets* 6:391–413
8. Ding JP, Das K, Hsiou Y, Sarafianos SG, Clark AD Jr, Jacobo-Molina A, Tantillo C, Hughes SH, Arnold E (1998) *J Mol Biol* 284:1095–1111
9. Sarafianos SG, Marchand B, Kalyan D, Himmel DM, Parniak MA, Hughes SH, Arnold E (2009) *J Molec Biol* 385:693–713
10. De Clercq E (2004) *Chem Biodivers* 1:44–64
11. Mao C, Sudbeck EA, Venkatachalam TV, Ucken F (2000) *Biochem Pharmacol* 60:1251–1265
12. Tachedjian G, Orlova M, Sarafianos SG, Arnold E, Goff SP (2001) *Proc Natl Acad Sci USA* 98:7188–7193
13. Nunriam P, Kuno M, Saen-oon S, Hannongbua S (2005) *Chem Phys Lett* 405:198–202
14. Venezia CF, Howard KJ, Ignatov ME, Holladay LA, Barkley MD (2006) *Biochemistry* 45:2779–2789
15. Wang J, Smerdon SJ, Jager J, Kohlstaedt LA, Rice PA, Friedman JM, Steitz TA (1994) *Proc Natl Acad Sci USA* 91:7242–7146
16. Grabowski EJJ (2005) *Chirality* 17:249–259
17. Thompson A, Corley EG, Huntington MF, Grabowski EJJ (1995) *J Org Chem* 60:1590–1594
18. V Fusi (1999) Cryptand ligands for selective lithium coordination. In: *Coordination chemistry at the turn of the century*, Slovak Techn. Univ. Press, 283–288
19. Thompson A, Corley EG, Huntigton MF, Grabowski EJJ, Remenar JF, Column DB (1998) *J Am Chem Soc* 120:2028–2038
20. Fu X, Reamer RA, Tillyer R, Cummins JM, Grabowski EJJ, Reider PJ, Collumn DB, Huffman JC (2000) *J Am Chem Soc* 122:11212–11218

21. Noyori R, Kitamura M (1991) *Angew Chem Int Ed Engl* 30:49–69
22. Pierce ME, Parsons RL Jr, Radesca LA, Lo YS, Silverman S, Moore JR, Islam Q, Choudhury A, Fortunak JMD, Nguyen D, Luo C, Morgan SJ, Davis WP, Confalone PN, Chen C, Tillyer RD, Frey L, Tan L, Xu F, Zhao D, Thompson AS, Corley EG, Grabowski EJJ, Reamer R, Reider PJ (1998) *Org Chem* 63:8536–8543
23. Tan L, Chen C, Tillyer RD, Grabowski EJJ, Reider PJ (1999) *Angew Chem Int Ed* 38:711–713

Chapter 14

Paclitaxel

Abstract

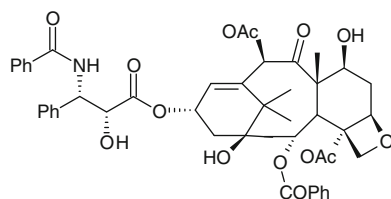
Biological target: Paclitaxel is a natural polysubstituted macrocyclic compound isolated from the bark of the Pacific yew tree (*Taxus brevifolia*). It binds to β -tubulin, causing polymerisation of the tubulin, thereby disrupting normal microtubule dynamics required for cell division.

Therapeutic profile: Paclitaxel (*Taxol*[®]) is an anticancer agent with a broad spectrum of activity against tumours that are often refractive to other drugs.

Synthetic highlights: The partial synthesis of paclitaxel was necessary to enhance the availability of the drug substance and avoid unsustainable use of yew trees. Many different synthetic routes have been reported and three inventive pathways for the enantioselective or site-selective approaches to various segments of the paclitaxel molecule are described. These are all promoted by organometal catalytic complexes. Reactions presented include use of the intramolecular Heck reaction in the synthetic pathway to baccatine III; the Sharpless reaction and the introduction of a trifunctional catalyst for biomimetic synthesis of chiral diols; synthesis of the paclitaxel side-chain; and use of a Zr-complex catalyst in the reductive N-deacylation of taxanes to primary amine, the key precursor of paclitaxel.

14.1 Introduction

Paclitaxel (**1**, (2 α ,4 α ,5 β ,7 β ,10 β ,13 α)-4,10-bis(acetyloxy)-13-[[[(2*R*,3*S*)-3-(benzoylamino)-2-hydroxy-3-phenylpropanoyl]oxy]-1,7-dihydroxy-9-oxo-5,20-epoxytax-11-en-2-yl benzoate, *Taxol*[®]) is a natural compound that disrupts the cell division and growth of many malignant tumors.



1 paclitaxel

Because of the limited natural availability of the compound, as discussed in Sect. 14.3, and despite the complexity of the molecule, huge synthetic efforts have been made to achieve the total synthesis of paclitaxel. These endeavours have resulted in many elegant partial or total synthetic approaches [1–3], and these have been reviewed repeatedly [4, 5]. Numerically, by 2010, there were 156 citations in SciFinder related to the synthesis of taxol and 7,875 citations related to the general terms, taxol *and* synthesis. In addition to total chemical synthesis, the strategy of *site-selective* transformation of the complex mixture in the natural taxanes, together with *enantio*- and *diastereo-selective* transformation of paclitaxel molecular fragments, complete the palette of selective transformations that have been studied.

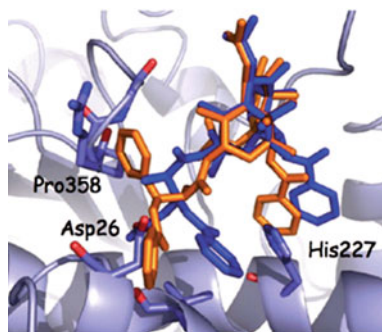
It is not possible in just a brief chapter to cover all the different synthetic approaches that have been taken. However, with a careful selection of a few of the many methods for the total synthesis of paclitaxel and its asymmetric side-chain, we hope to give the reader an impression of the complexity and huge demand on human resources and time that such endeavours require. We have selected for consideration three highly inventive synthetic reactions that were carried out to construct various segments of the paclitaxel molecule. All of them are promoted by *organometal catalytic complexes*, follow an original mechanistic route, and are either site-selective or enantioselective.

14.2 Disturbed Dynamics of Cellular Microtubules by Binding to β -Tubulin

Paclitaxel was first approved by the FDA for ovarian cancer, then for breast cancer, while other new clinical uses are also anticipated [6, 7]. It has activity against a broad range of tumour types, including breast, ovarian, lung, head and neck cancers. The drug is also active in other malignancies that are refractory to conventional chemotherapy, including previously-treated lymphoma and small cell lung cancers and oesophageal, gastric endometrial, bladder and germ cell tumours. Paclitaxel is also active against AIDS-associated Kaposi's sarcoma.

Tumours are formed by continuously dividing and proliferating cells, which have lost their ability to regulate their division and growth. Cell division, the basic process in cell and tissue growth, involves the separation of the paired sets of chromosomes in the cell nucleus, each of which is divided into a daughter cell in a process called mitosis. The separation of the chromosomes requires complex changes in the cell skeleton, composed of microtubules, which are responsible for cell shape, motility and attachment. The basic units of the microtubules are heterodimers of the globular proteins, α - and β -tubulin. Paclitaxel binds to β -tubulin, causing polymerisation of the tubulin, which can no longer disassemble, thereby disrupting the normal microtubule dynamics required for cell division. The paclitaxel molecule shows a T-shaped or 3D butterfly structure, optimized within the β -tubulin. This structure of the bioactive form has been challenged by the group of

Fig. 14.1 T-Taxol (PTX, *blue*) in β -tubulin in which the PTX-NY (*orange*) conformer is superimposed on matching atoms in the baccatin core (reproduced from [9], with the permission of the American Chemical Society)



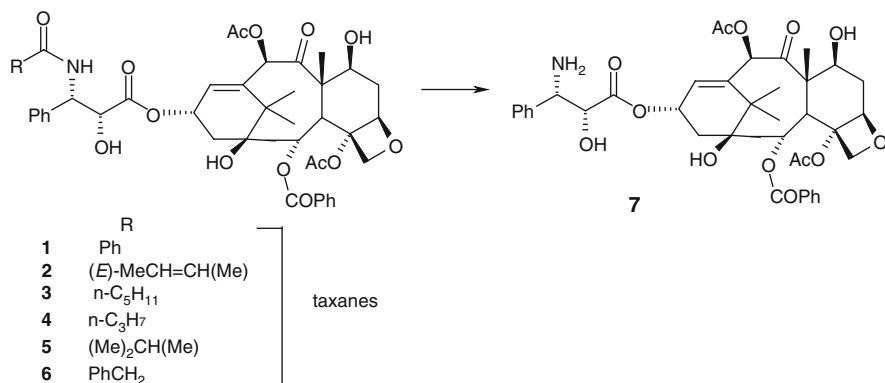
I. Ojima who suggested the “PTX-NY” conformer, in which the C-13 side chain is proposed to adopt a different conformation and an alternative hydrogen-bonding pattern in the tubulin binding site [8]. The two conformers were compared to show that only T-Taxol fits the PTX-derived electron crystallographic density [9].

As seen in Fig. 14.1, the PTX conformer is greatly preferred over PTX-NY, since the placement of the latter leads to severe steric interactions at Asp26 and Pro358 residues. This work has been extended, using molecular mechanics and quantum chemical methods, to reveal that the PTX-NY conformation is relatively less stable, on average, by 10–11 kcal/mol. PTX conformers fitted into the electron crystallographic binding site of tubulin demonstrate that PTX-NY cannot be accommodated unless the pocket is reorganized in violation of the experimental constraints.

All these results underlined the remarkable, nearly perfect fit of the natural product into a naturally unrelated biological target, and directed most of the synthetic efforts towards partial or total synthesis of paclitaxel rather than of its structural congeners. In the following three sections, the specific achievements of the three reactions catalyzed by organometallic complexes are presented, showing the key transformations that provide the key building blocks for paclitaxel.

14.3 Three Selected Synthetic Transformations on the Pathway to Paclitaxel

Paclitaxel was originally isolated in 1962 from extracts of the bark of the Pacific yew tree (*Taxus brevifolia*) [10]. In spite of attempts by many research groups worldwide to develop a workable synthesis of paclitaxel, yew trees remained the main source for a long period. In 1977, the National Cancer Institute in the USA ordered 3.5 tons of yew bark, requiring the felling of 1,500 yew trees [11]. Already in 1984, however, it would have been necessary to fell 360,000 trees to treat ovarian cancer patients in the USA for 1 year. This unsustainable situation prompted a new search for highly inventive solutions. The cultivation of fungi that grow on the bark of the tree and produce paclitaxel was one of them [12]. Nursery-grown ornamental yew trees were also used as a source of primary taxanes **2–6**, a mixture of congeners



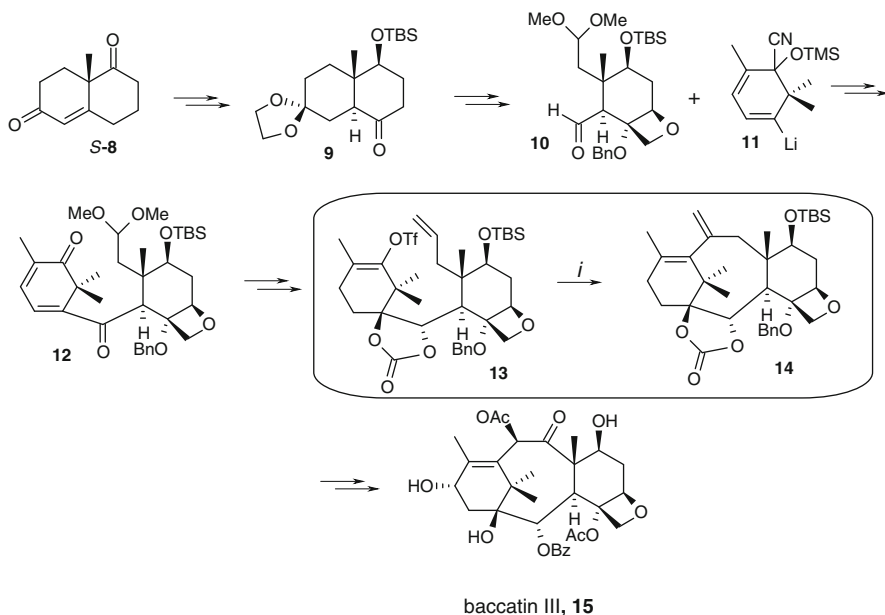
Scheme 14.1 N-Deacylation of taxanes **1–6** to primary amine **7**

of paclitaxel **1**, which were extracted from the pruned tree tops [13]. The fast-growing yew trees regenerate their tops in approximately 2 years, and branch cuttings can be used to grow 1–2 million new yew trees per year. This sustainable availability of taxanes provided the opportunity for their chemical transformation into paclitaxel. As with many natural products, the chemical modification of taxanes to paclitaxel carries a specific requirement, namely, the chemical modification of a defined site in the molecule, while retaining unaltered all other similar functionalities. N-Deacylation of taxanes is outlined in Scheme 14.1, and the solution to this formidable task of site-selectivity is discussed in Sect. 14.3.3.

14.3.1 Intramolecular Heck Reaction on the Synthetic Route to Baccatin III

Although with the current availability of taxane intermediates, the total synthesis of paclitaxel now has limited practicality, the achievement of this feat is worth considering here, in relation to an innovative specific transformation accomplished as part of the total synthesis reported by Danishefsky et al. [14]. They employed an intramolecular Heck reaction, forming a C–C bond between two vinylic carbon atoms, and creatively applied this reaction to an organometal-catalyzed cyclization, forming the highly functionalized 8-membered ring of baccatin III (**15**). This synthesis is outlined in Scheme 14.2, in which only a few selected intermediary structures are presented. The whole process consists of a total of 30 defined synthetic steps, and ends up with baccatin III (**15**), as an immediate precursor of paclitaxel **1** [14]!

An advantage of this total synthesis is the use of optically pure ketone **S-8**, commercially available and produced on an industrial scale by a biocatalytic process with L-proline as a cheap organocatalyst (see Chap. 8). Scheme 14.2 indicates only the reagents and conditions required for step *i*, the Heck-type ring closure of **13–14**.

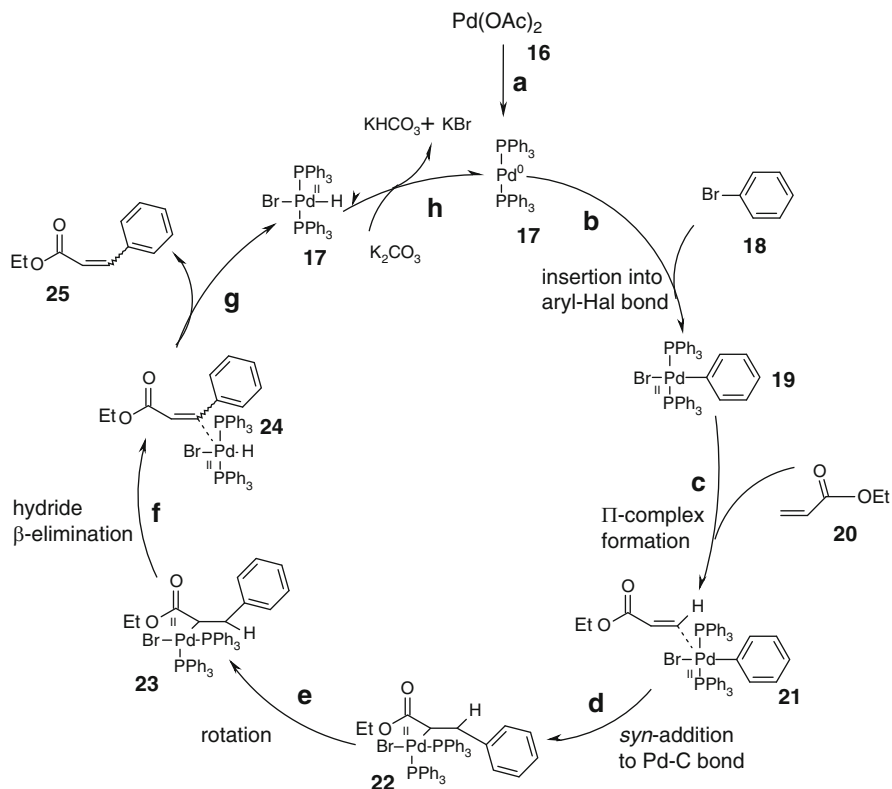


Reagents and conditions: *i.* Pd(PPh)₄, K₂CO₃/MeCN, 4A MS, 90 °C, 49%.

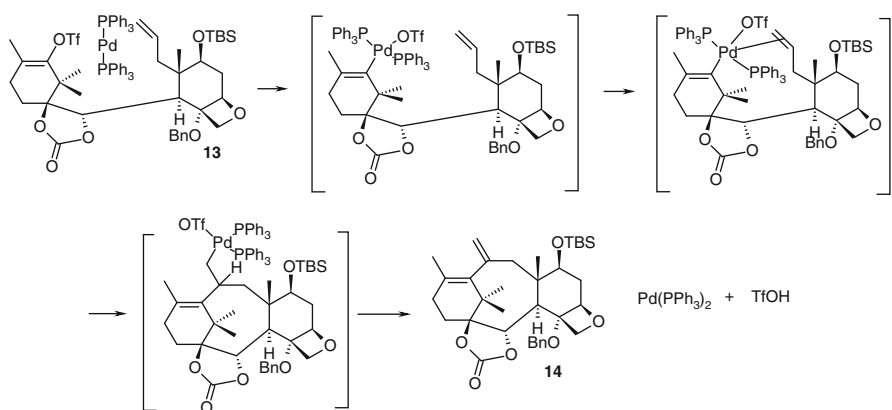
Scheme 14.2 Outline of Danishefky's synthesis of baccatin III **15**

In its original form, the Heck reaction is an organometal-catalyzed process that promotes coupling of aryl-halides and alkenes to form arylalkenes [15]. Standard protocols for the Heck reaction use Pd(II) salts, such as Pd(PPh₃)₄, PdCl₂ and Pd(OAc)₂, mono- or di-phosphine ligands, like PPh₃ or BINAP, and organic or inorganic bases as the scavengers of haloacids [15, 16]. The catalytic cycle for preparation of cinnamic ester **25** is outlined in Scheme 14.3.

This mechanistic scheme envisages the insertion of Pd into an aryl-halogen bond, which is most effective for Ar–I, less so for Ar–Br and least efficient with Ar–Cl, as the strength of the bond increases [16]. Stability of the Ar–Pd bond in the complex **19** is crucial for the continuation of the cycle, something that cannot be expected for a vinylic C–Pd bond. Without entering into other details of this catalytic cycle, it is conceivable that vinyl halides are less suitable partners than aryl halides due to their inherent instability and the deactivating effect of the relatively π -electron rich C=C bond, while simple terminal alkenes are less reactive than enones. Therefore, in the critical step *i* in Scheme 14.2, Danishevsky used the extremely reactive nucleofugal trifluoroacetoxy group on the vinylic carbon, expecting that the terminal C=C bond would react with its internal, more electro-positive carbon, forming the entropically unfavourable central 8-membered ring of the baccatin III skeleton. Mechanistically, this intramolecular process corresponds to the general scheme, and is outlined in Scheme 14.4 [14].



Scheme 14.3 Catalytic cycle of the Heck reaction



Scheme 14.4 Proposed mechanistic path for construction of the 8-membered ring in the baccatin III precursor **14** by the intramolecular Heck reaction

Insertion of Pd(0) into the allylic C=C-OTf bond was followed by the formation of the π -complex with the second C=C bond, transient formation of a Pd-C bond and final hydride elimination to close the catalytic cycle.

Generally, the Heck reaction requires elevated temperatures. With the specific, highly functionalized substrate **13**, the reaction was successfully achieved at 90°C in MeCN. To the author's great satisfaction, it proceeded with an acceptable yield, forming exclusively the 8-membered ring in **14**. The subsequent final steps in the synthesis of baccatin III (**15**) have been reported repeatedly [17, 18].

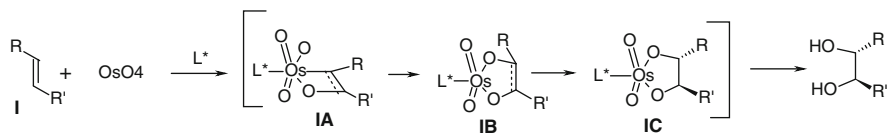
14.3.2 Trifunctional Catalyst for Biomimetic Synthesis of Chiral Diols: Synthesis of the Paclitaxel Side-Chain

Combination of a catalytic process on the one hand and a one-pot multi-step synthesis on the other is one of the most attractive strategies in synthetic organic chemistry. Inventive solutions in this direction represent considerable scientific advances and at the same time they offer economic synthetic approaches to commercially important compounds or their key building blocks. This was the achievement of a group of chemists from the Indian Institute of Chemical Technology in Hyderabad. In the search for multifunctional catalysts, both homogeneous and heterogeneous, the authors concentrated on the *trifunctional catalytic system*, $\text{Na}_2\text{PdCl}_4\text{-K}_2\text{OsO}_4\text{-Na}_2\text{WO}_4$ (PdOsW), and its heterogeneous analogues [19], and applied this catalyst in an efficient synthesis of the paclitaxel side-chain [20, 21].

This catalytic system allows three independent transformations to occur in sequence; the Heck reaction, N-oxidation and *asymmetric dihydroxylation* (AD). The mechanism of the Heck reaction is discussed in the previous section. Here we take a closer look at the last two steps. They are coupled processes, based on the *Sharpless asymmetric dihydroxylation* reaction [22, 23]. Several recent reviews on Sharpless asymmetric dihydroxylation cover the general synthetic aspects [24–27], together with methods for immobilization of the osmium catalysts [28].

As a starting point for a discussion of trifunctional catalysis, Scheme 14.5 provides a general overview of the Sharpless AD reaction.

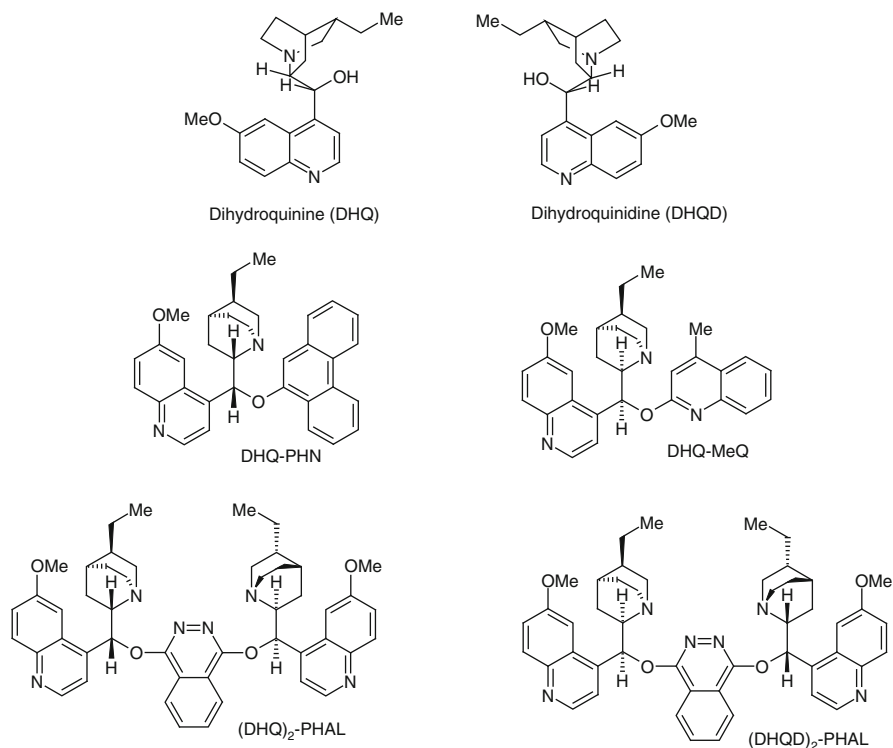
Roles of the osmaoxetane complexes **IA** and **IB** as intermediates has been proposed, and the fundamental mechanism for face-selectivity involves the reaction between the olefin and OsO_4 within the chiral binding pocket created by the chiral ligand L^* [29, 30].



Scheme 14.5 General scheme of the Sharpless AD reaction, Os-mediated dihydroxylation of olefins

Sharpless et al. observed that addition of *l*-2-(2-menthyl)pyridine to osmium tetroxide resulted in a chiral complex which reacted with olefins **I**, and generated diols **II** with low enantiomeric excess (3–18% e.e.). The poor enantioselectivity displayed in the reaction was explained by the instability of the pyridine–osmium tetroxide complexes. Tertiary amines like quinuclidine, however, do form considerably stronger complexes with OsO₄ [31], and continuing work in the Sharpless group led to the discovery that derivatives of naturally occurring cinchona alkaloids are substantially better ligands for osmium. Screening of various chiral ligands led to the identification of specific derivatives of dihydroquinine (DHQ) and dihydroquinidine (DHQD) as the most effective ligands (Scheme 14.6) [32]. *Phenanthrenyl* and *4'-methly-2'-quinolyl* derivatives of *dihydroquinine* (PHN and MeQ in the Scheme 14.6) were first generation ligands that accelerated dihydroxylation to 25-fold that of the uncatalyzed reaction, and afforded chiral vicinal diols with an average e.e. of 85–95%.

The dimeric ligands, (DHQ)₂-PHAL and (DHQD)₂-PHAL (PHAL = *phthalazine*), represent the third, most effective generation of chiral ligands derived from cinchona alkaloids. They allow formation of a large U-shaped binding pocket, in



Scheme 14.6 Structure of ligands derived from dihydroquinine (DHQ-PHN and DHQ-MeQ), and the phthalazine class of dimeric ligands (DHQ)₂-PHAL and (DHQD)₂-PHAL

which the important interactions between the alkene and its ligand involve aryl–aryl interactions between the substrate aromatic residue and the two parallel methoxyquinolone units of the ligand [33].

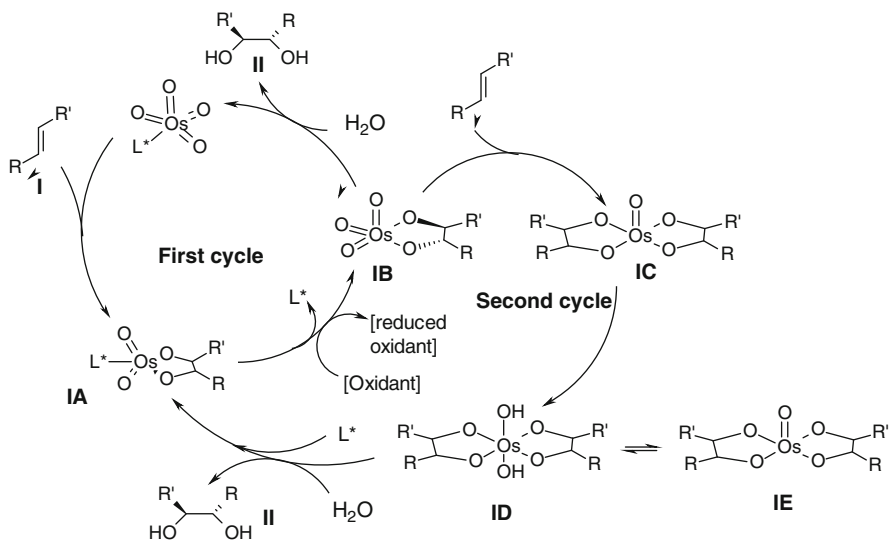
Various catalytic cycles of dihydroxylation have been proposed by Sharpless [34] and Corey [35]. According to Sharpless, two cycles operate in the catalytic reaction (Scheme 14.7). The first one is highly enantioselective, whereas the second cycle, which includes formation of Os complex with two moles of alkene **IC-ID**, is poorly enantioselective [36].

This scheme is valid for one-phase dihydroxylations with *N*-methylmorpholine *N*-oxide (NMO) as the oxidant. When re-oxidation is induced, using $K_3[Fe(CN)_6]$ as the terminal oxidant, the problems raised by the second cycle are efficiently eliminated [37, 38]. When this particular co-oxidant is employed and the dihydroxylation is performed in a heterogeneous solvent system (typically *tert*-butanol–water), the olefin osmylation and the osmium re-oxidation steps are uncoupled since they occur in different phases (Scheme 14.8) [39].

The reaction occurs at either ambient or ice-bath temperature, with a solid, non-volatile Os(IV) salt $K_2OsO_2(OH)_4$, and $K_3Fe(CN)_6$ as oxidant (Scheme 14.9).

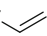
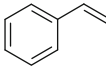
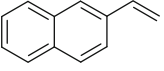
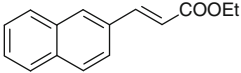
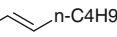
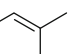
The two alkaloid auxiliaries, DHQ and DHQD, have a pseudo-enantiomeric relationship, defined by opposite configurations at the two central carbon atoms, affording enantiomeric products with similar enantioselectivity (Scheme 14.10).

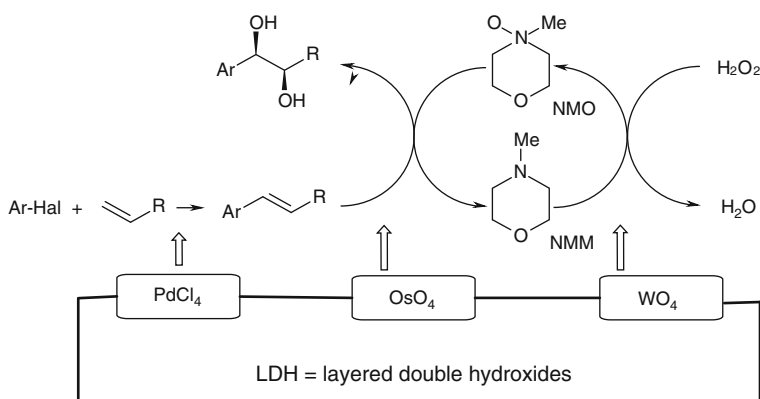
Schemes 14.9 and 14.10 show potassium hexacyanoferrate and NMO as the two re-oxidising agents that are often used, but several other re-oxidation systems, including oxygen, have also been described [40–42]. The examples in Table 14.1 demonstrate the high enantioselectivity of the dihydroxylation of various olefins with representatives of chiral ligands derived from DHQ and DHQD.



Scheme 14.7 Sharpless proposal for the mechanism of asymmetric hydroxylation

Table 14.1 Selected examples of asymmetric dihydroxylation of olefins

Olefin	Ligand	% e.e.	Configurations
n-C8H17 	PHN	74	<i>R</i>
	MEQ	87	<i>R</i>
	(DHQD) ₂ -PHAL	97	<i>R</i>
	(DHQ) ₂ -PHAL	97	<i>S</i>
	MEQ	87	<i>R</i>
	PHN	98	2 <i>S</i> , 3 <i>R</i>
n-C4H9  n-C4H9	PHN	95	2 <i>R</i> , 3 <i>R</i>
n-C4H9 	PHN	84	<i>R</i>
	(DHQD) ₂ -PHAL	98	<i>R</i>
	(DHQ) ₂ -PHAL	95	<i>S</i>

**Scheme 14.11** Catalytic cycle in the transformation of prochiral olefins to chiral diols catalyzed by a trifunctional catalyst

As indicated in the introductory paragraph of this section, the most efficient dihydroxylation was achieved with heterogeneous catalysts. Scheme 14.11 presents the catalytic cycle in the AD reaction catalyzed by the heterogeneous trifunctional catalyst [42].

To get this system working and highly enantioselective, the authors first prepared and characterized heterogeneous catalysts on *layered double hydroxides* (LDH). LDH is a class of layered material, consisting of alternating cationic and anionic layers [43]. The cationic layers contain a wide variety of M(II) cations (Mg, Zn, Ni, Cu) and M(III) cations (Al, Ga, In, Cr, Fe), and are separated by anionic layers containing anions (Cl^- , NO_3^- , CO_3^{2-}) [44]. To obtain the heterogeneous catalyst, LDH-PdOsW, three bivalent anions, PdCl_2^{2-} , OsO_4^{2-} and WO_4^{2-} , were simultaneously co-exchanged onto a single LDH matrix. Importantly, X-ray powder diffraction patterns of the initial LDH and the exchanged catalysts, LDH-PdOsW, revealed that the three anions in the catalyst were located at the edges. As confirmed by FTIR spectra of the exchanged trifunctional catalyst, such coordination results in the retention of the co-ordination geometries of divalent anions anchored to the LDH matrix in their monomeric form [45].

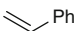
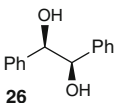

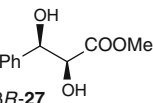
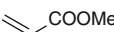
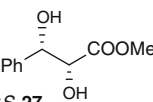
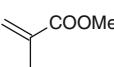
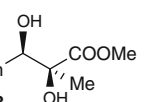
Re-oxidation of NMM to NMO (Schemes 14.10 and 14.11), was completed using peroxide as the second oxidant for recycling the NMM in the process. Technologically, this requires an additional operation unit. Similarly, an additional unit operation is needed for the production of specific prochiral olefin, the substrate for the AD reaction. Hence, development of a multifunctional catalyst for the one-pot synthesis of prochiral substrates, and finally the chiral diol was highly desirable.

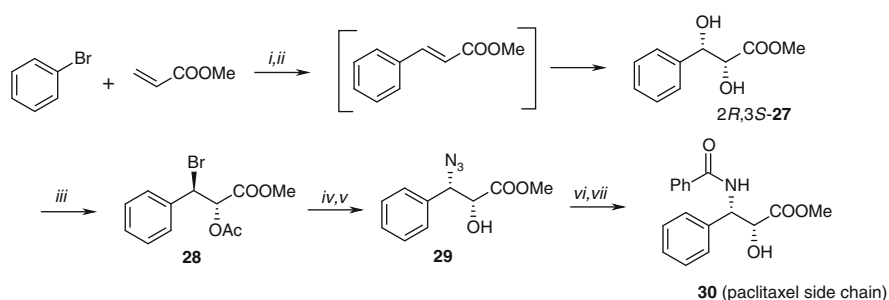
Having created the catalytic system with LDH-PdOsW, the authors optimized the conditions for the cycles in Scheme 14.7, and some of their results are presented in Table 14.2. The methodology based on trifunctional catalysts requires bulk chemicals, such as styrene and acrylates, as starting materials to prepare prochiral substrates, stilbenes and cinnamates, in an “in situ Heck step”. Upon dihydroxylation, they give chiral diols **26–28** in a single-pot reaction, with a remarkably constant 99% e.e, which remained unchanged even after five catalytic cycles. The opposite configuration of the diol product **27**, obtained with the DHQD- and DHQ-derived catalytic system, has already been explained by the pseudo-enantiomeric relation of these two ligands.

Using the trifunctional catalyst in the one-pot reaction for the preparation of diol **2R,3S-27**, the authors completed synthesis of the side chain of paclitaxel according to Scheme 14.12.

The first synthetic process for the paclitaxel side-chain developed by Sharpless et al., using the AD method under homogeneous conditions, led to **30** with 23% overall yield, but the intermediary diol **27** needed to be recrystallized to enrich the e.e [32]. The trifunctional heterogeneous catalyst, instead, afforded this diol with 99% e.e., *without traces of osmium*, and was directly used in the next steps of the synthesis. This technology eliminates leaching of osmium from the solid support, and due to the high toxicity of osmium, offers a considerable advantage over the processes that use osmium salts in solution. Treatment of 2,3-dihydroxy-3-phenyl propionate **27** with HBr/AcOH yields bromo-acetate **28**, which in turn reacts with NaN_3 in DMF, followed by deacylation with NaOAc in MeOH to afford the azido alcohol **29** with overall retention of the configuration at C(3). In the last steps, hydrogenation of the azido alcohol followed by benzoylation gave (2R,3S)-N-benzoyl-3-phenylisoserine methyl ester **30** in 67% overall yield, and nearly 100% optical purity.

Table 14.2 Synthesis of chiral diols using the heterogeneous trifunctional catalyst (LDH-PdOsW)-(DHQD)₂PHAL

Arylhalide	Alkene	Product	Yield (%)	e.e. (%)	Abs. configurations
PhI		 26	85 ^a 82 ^b 89 ^c	99 99 99	<i>R, R</i> <i>R, R</i> <i>R, R</i>
PhI		 <i>2S,3R</i> - 27	93	99	<i>2S, 3R</i>
PhBr		 <i>2R,3S</i> - 27	90 ^d	99	<i>2R, 3S</i>
PhI		 28	92	98	<i>2S, 3R</i>

^aReaction steps are completed in solution^bAfter fifth cycle^cHomogeneous catalyst; Na₂PdCl₄–K₂OsO₄–NaWO₄·H₂O^d(DHQ)₂-PHAL, pseudo enantiomeric ligand is used

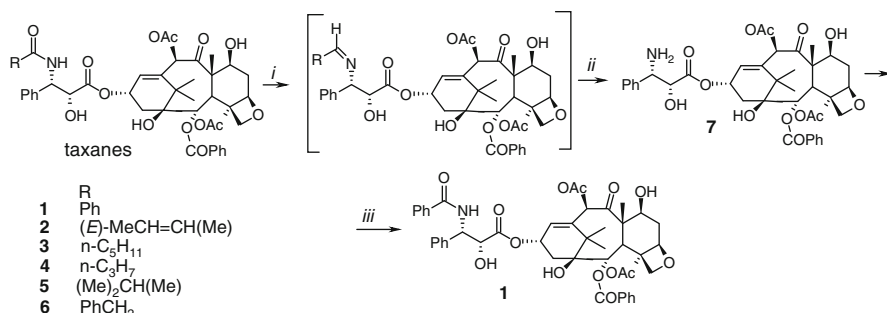
Reagents and conditions: *i.* LDH-PdOsW, TEA, 70 °C, 16h; *ii.* (DHQ)₂PHAL, *t*-BuOH/H₂O, NMM, H₂O₂, r.t., 12h 90% yield, 99% e.e. of **27**; *iii.* HBr-AcOH, 99% yield on **28**; *iv.* NaN₃, DMF; *v.* AcONa, MeOH, 85% on **29**; *vi.* PhCOCl, TEA; *vii.* H₂, Pd-C, 88% on **30**.

Scheme 14.12 Enantioselective route to side chain **30**, based on the LDH-PdOsW catalyzed synthesis of diol **27**

The single-pot biomimetic synthesis of chiral diol **27**, mediated by the recyclable trifunctional catalyst, $\text{Na}_2\text{PdCl}_4\text{--K}_2\text{OsO}_4\text{--Na}_2\text{WO}_4$ embedded in a matrix of layered double hydroxides, resulted in an efficient, low cost process. This protocol provided the desired prochiral olefin from “Heck precursors” and the in situ recycling of NMM to NMO. The whole process starts with cheap precursors and minimizes the number of unit operations. Other similar broad, interdisciplinary studies which led to an extraordinarily selective solution to the splitting of the amide bond in a mixture of compounds from a natural source will be considered in the next section.

14.3.3 Zr-Complex Catalysis in the Reductive N-deacylation of Taxanes to the Primary Amine, the Key Precursor of Paclitaxel

The core structure of paclitaxel is characterized by an α -hydroxy β -benzoylamino carboxylic acid unit, attached to the C13–OH group of the tricyclic diterpenoid skeleton, and by a 4-membered oxetane ring. Two of the five OH groups are free, two are acetylated and one is benzoylated. Such a complex assembly of sensitive functionalities, together with the strained ring, makes any total synthesis of this compound impractical and for large production economically unsustainable. Despite this complexity, it has proved possible to develop an elegant and economically feasible approach from taxanes, as mentioned at the beginning of this chapter. This involved the introduction of key chemical transformations to make more effective use of the extracts of yew biomass in the production of paclitaxel. The biomass consisted of a mixture of six taxanes (**1–6**) in >95% purity and the main challenge in the production of paclitaxel was to convert all the mixed taxanes into paclitaxel with a good yield, by elimination of N-acyl groups, to obtain the key intermediate **7**, followed by its N-benzoylation to **1**, Scheme 14.13 [46].

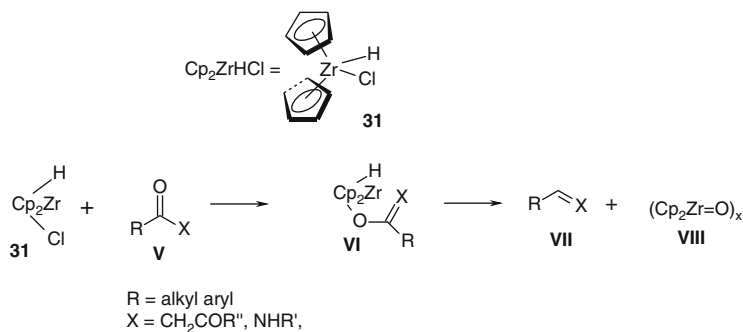


Scheme 14.13 Selective cleavage of the amide bond in taxanes **1–6** on the pathway to paclitaxel **1**

Although taxanes are promising natural precursors of paclitaxel, the formidable task for the chemists was to selectively hydrolyze the amide bond while retaining the four hydrolytically more sensitive ester groups, one at the particularly reactive allylic position, and one highly strained oxepine ring. Obviously, any acid or base catalyzed hydrolysis was too non-specific, whereas enzymatic hydrolysis by peptidases or amidases is known to be rather inefficient with such complex substrates [47].

Creative transformation of primary taxanes to paclitaxel was achieved by the group of B. Ganem at Cornell University. The authors had long experience with reductive deoxygenation of various carbonyl functionalities by the zirconium complex Cp_2ZrHCl (**31**, Scheme 14.14).

Many Zr(IV) complexes are stabilized by cyclopentadienyl (Cp) ligands, and have been used in hydrozirconation and C–C coupling reactions [48]. Complex **31** is characterized by tetrahedral coordination and by the two anionic ligands, hydride and chloride anion. The extreme oxophilic character of Zr(IV) in this complex leads to substitution of the chlorine anion by enolate or enamide oxygen, thus promoting deoxygenation of substrates with an enolizable carbonyl group (Scheme 14.14). By covalently linking the oxygen of substrate **V** directly to the metal centre in Cp_2ZrHCl , hydride addition or hydrozirconation triggers reductive fragmentation of the C–O bond in the intermediate **VI**, driven by the exothermicity of the strong Zr–bonding in the oxo–Zr–polymer **VIII**. As a result, deoxygenation of β -dicarbonyl compounds affords α,β -unsaturated carbonyl compounds **VII** ($\text{X} = \text{CHCOOR}$) [50], while secondary amides are reduced to imines ($\text{X} = \text{NR}'$) [49, 50]. It is this second reaction that proved highly valuable in solving the technical problem of selective cleavage of amide bond in taxanes **1–6**. The critical step in splitting the C–N bond in the amides **1–6** was partial reduction to imines, according to Scheme 14.14. In the absence of reducing agent and despite the generally easier reduction of imines than amides by a number of organometallic hydride complexes [51], imines are stable intermediates. Importantly, the authors envisaged that hydrolytically sensitive imines could be isolated by an efficient non-aqueous work-up, and thus completed a novel approach to this valuable functionality, using easily available amides. Subsequently, it was a relatively easy course to



Scheme 14.14 Hydrozirconation of carbonyl compounds by Cp_2ZrHCl (**31**)

apply aqueous work-up of **1–6**, in order to obtain the *prim*-amine **7**, which is then susceptible to selective N-benzoylation, as a final step, using a commonly available method.

Two-step transformation of the extract mixture of taxanes into paclitaxel was thus based on the chemists' knowledge of organometal-catalyzed, mild deoxygenation of the *sec*-amide group. This reaction is compatible with the presence of ester groups and other sensitive functionalities and represents the final stage of a multi-disciplinary project that has "globalized" manufacturing of paclitaxel. This enterprise is related in his "JOC Perspective" article by B. Ganem [13].

14.4 Conclusion

The transfer of basic research to a commercially valuable process is always a satisfying achievement for chemists in the pharmaceutical industry, and we have discussed some examples in Chaps. 4, 7 and 13. However, the project in which paclitaxel was made available to cancer patients in sufficient quantities and at an acceptable price was a truly heroic endeavour, initiated by scientists from various disciplines and finally completed by synthetic chemists. It would be equally satisfying if this example promotes enthusiasm among synthetic chemists to join collaborative, high quality science projects and, at the same time, to deliver effective pharmaceutical products to the community at large.

References

1. Ojima I, Habuš I, Zhao M, Georg GI, Jayasinghe LR (1991) *J Org Chem* 56:1681–1683
2. Holton RA, Somoza C, Kim HB, Liang F, Biedeger RJ, Boatman D, Shindo M, Smith CC, Kim S, Nadizadeh H, Suzuki Y, Tao C, Vu P, Tang S, Zhang O, Murthi KK, Gentile LS, Liu JH (1994) *J Am Chem Soc* 116:1597–1599
3. Nicolau KC, Zhang Z, Liu JJ, Ueno H, Nantermet PG, Guy RK, Claiborne CF, Renaud J, Coladourous EA, Paulvannan K, Sorensen EJ (1994) *Nature* 367:630–634
4. Nicolau KC, Guy RG (1995) *Angew Chem Int Ed* 34:2079–2090
5. Kingston DGI (2000) *J Natural Products* 63:726–734
6. Ojima I, Lin S, Wang T (1999) *Curr Med Chem* 6:927–954
7. Horwitz SB (2004) *J Nat Prod* 67:136–138
8. Geney R, Sun L, Pera P, Bernacki L, Xia S, Horwitz SB, Simmerling CL, Ojima I (2005) *Chem Biol* 12:339–348
9. Yang Y, Alcaraz AA, Snyder JP (2009) *J Nat Prod* 72:422–429
10. Wani MC, Taylor HL, Wall ME, Coggon P, McPhail AT (1971) *J Am Chem Soc* 93:2325–2327
11. Renner R (2007) *Biotechnol* 2:1207–1209
12. Pandi M, Manikandan RM (2010) *J Biomed Pharmacother* 64:48–53
13. Ganem B, Franke R (2007) *J Org Chem* 72:3981–3987
14. Masters JM, Link JT, Snyder LB, Young WB, Danishefsky SM (1995) *Angew Chem Int Ed* 34:1723–1726
15. Heck RF (1982) *Org Reactions* 27:345–366

16. Geissler H, Beller M, Stark TH (1998) In: Beller M, Bolm C (eds) *Transition metals for organic synthesis*. Wiley-VCH, NY, 166–214
17. Danishefsky SJ, Masters JJ, Young WB et al (1996) *J Am Chem Soc* 118:2843–59
18. Narasaka K, Iwasawa N (1998) *Chemtracts* 11:23–28
19. Choudary BM, Chowdary NS, Madhi S, Kantam ML (2001) *Angew Chem Int Ed* 40: 4619–4623
20. Choudary BM, Yyothi K, Madhi S, Kantam ML (2002) *Adv Synth Catal* 344:503–507
21. Choudary BM, Chowdary NS, Yyothi K, Kantam ML (2002) *J Am Chem Soc* 124:5341–5349
22. Jacobsen EN, Marko I, Mungall WS, Schroder G, Sharpless KB (1988) *J Am Chem Soc* 110:1968–1970
23. Kolb HC, VanNieuwenhze MS, Sharpless KB (1994) *Chem Rev* 94:2483–2457
24. Noe MC, Letavic MA, Snow SL (2005) *Org Reactions* 66:109–625
25. Zaitsev AB, Adolfsson H (2006) *Synthesis*: 1725–1756
26. Galatsis P (2007) In: Li JJ, Corey EJ (eds) *Name reactions for functional group transformations*. Wiley, Hoboken, NJ, 67–83
27. Ager DJ, Allen DR (2006) In: Ager DJ (ed) *Handbook of chiral chemicals*, 2nd edn. CRC Press LLC, Boca Raton, FL, pp 123–146
28. Kobayashi S, Sugiura M (2006) *Adv synth catal* 348:1496–1504, Wiley-VCH Verlag GmbH & Co. KGaA
29. Corey EJ, Noe MC, Grogan MJ (1994) *Tetrahedron Lett* 35:6427–6430
30. Norrby P-O, Kolb HC, Sharpless KB (1994) *J Am Chem Soc* 116:8470–8478
31. Griffith WP, Skapski AC, Woode KA, Wright MJ (1978) *Inorg Chim Acta* 31:L413
32. Sharpless KB, Amberg W, Beller M, Chen H, Hartung J, Kawanami Y, Lubben D, Manoury E, Ogino Y, Shibata T, Ukita T (1991) *J Org Chem* 56:4585–4588
33. Corey EJ, Noe MC, Sarshar S (1994) *Tetrahedron Lett* 35:2861–2864
34. Wai JSM, Marko I, Svendsen JS, Finn MG, Jacobsen EN, Sharpless KB (1989) *J Am Chem Soc* 111:1123–1125
35. Corey EJ, Noe MC, Sarshar S (1993) *J Am Chem Soc* 115:3828–3831
36. Duppau P, Epple R, Thomas AA, Folkin VV, Sharpless KB (2002) *Adv Synth Catal* 344: 421–433
37. Singh MP, Singh HS, Arya BS, Singh AK, Sisodia AK (1975) *Indian J Chem* 13:112–117
38. Minato M, Yamamoto K, Tsuji J (1990) *J Org Chem* 55:766–768
39. Kwong HL, Sorato C, Ogino Y, Chen H, Sharpless KB (1990) *Tetrahedron Lett* 31:2999–3002
40. Lu X, Xu Z, Yang G (2000) *Org Proc Res Dev* 4:575–576
41. Dobler C, Mehlretter G, Sundermeier U, Beller M (2001) *J Organomet Chem* 621:70–76
42. Choudary BM, Chowdary NS, Madhi S, Kantam ML (2003) *J Org Chem* 68:1736–1746
43. Hoegaerts D, Sels BF, DeVos DE, Verpoort F, Jacobs PA (2000) *Catal Today* 60:209–218
44. Trifiro F, Vaccari A (1996) *Comprehensive supramolecular chemistry*, vol 7. Pergamon; Elsevier, Oxford, pp 251–278
45. Choudary BM, Chowdary NS, Madhi S, Kantam ML (2001) *Angew Chem Int Ed* 40: 4620–4623
46. Murray CK, Zhen QY, Cheng X, Peterson SK, for Hauser Inc., US Pat. 5, 679,807
47. Poppe L, Novak L (1992) *Selective biocatalysis*. VCH, Weinheim
48. Rosenthal U, Burlakov V, Arndt P, Baumann W, Spannenberg A (2005) *Organometallics* 24:456–471
49. Godfrey A, Ganem B (1992) *Tetrahedron Lett* 33:7461–6464
50. Schedler DJA, Godfrey A, Ganem B (1993) *Tetrahedron Lett* 34:5035–5038
51. Schedler DJA, Li J, Ganem B (1996) *J Org Chem* 61:4115–4119

Chapter 15

Neoglycoconjugate

Abstract

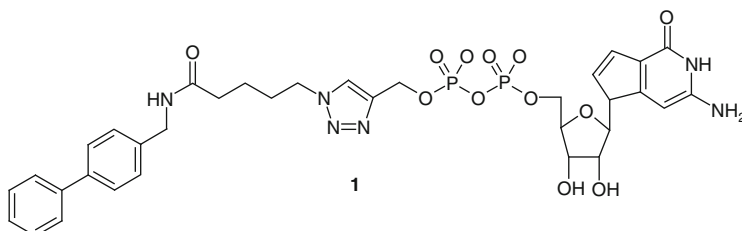
Biological target: The 1,2,3-triazole-linked, diphenyl-substituted neoglycoconjugate **1** is a selective inhibitor of human α -1,3-fucosyltransferase IV (Fuc-T), the enzyme catalysing the final step in the synthesis of oligosaccharides, including the leukocyte and leukaemic cell adhesion molecule, sialyl Lewis X.

Therapeutic profile: The compound has potential for the treatment of inflammation and cancer.

Synthetic highlights: Neoglycoconjugate **1** is a representative of a GDP-triazole screening library produced by the Cu(I)-catalyzed [2 + 3] cycloaddition reaction between azide and acetylene reactants. It is an example of click chemistry, a modular approach using low-energy chemical transformations to generate collections of test compounds. A more recent extension of click chemistry is target-guided synthesis (TGS) or freeze-frame click chemistry in which a biological target itself is used to assemble inhibitors at the binding site. This represents an exciting new strategy for the generation of compound libraries and the effective selection of hits and leads.

15.1 Introduction

Compound **1** (1-(5'-carboxy-(*para*-diphenylmethlyamide)-4-(guanosyldiphospho)methyl-1,2,3-triazole), defined as a neoglycoconjugate [1, 2] was selected as a lead compound from a small library of compounds with potential as modulators of immune responses and cancer metastases [3]. Although this compound is not a marketed drug, there are some exciting aspects of its structure, together with the modern synthetic organic chemistry tools used in the creation of both compound **1** and the library of its analogues, which merit attention.



There are many biological targets that are potentially useful in the therapy of cancer [4, 5]. Among them are adhesion molecules, which mediate the adherence of cells of the immune system, in health and disease, as well as that of leukaemic cancer cells to the endothelium that forms the internal lining of blood vessels. Normally, the vascular endothelium prevents blood cells from sticking to its surface. In lymph nodes and at sites of inflammation or potential tumour growth, however, the endothelium expresses adhesion molecules which trap immune or tumour cells, allowing them to cross the blood vessel wall and enter the tissues. The endothelial adhesion molecules bind to their respective ligands on the cancer cells or leukocytes, which also express the partner molecules in increased amounts.

Leukaemia cells express, among others, sialyl Lewis X, a glycoprotein that binds E-selectin on endothelial cells. The synthesis of sialyl Lewis X is under the rate-limiting control of the enzyme, α -1,3-fucosyltransferase IV (Fuc-T), which has been a target of considerable therapeutic interest. Generally, fucosyltransferases catalyze the final glycosylation step in the biosynthesis and expression of many important oligosaccharides. Fucosylated oligosaccharides are, thus, central to cell-to-cell interactions in connection with many pathological processes, including the immune response and cancer metastasis [5].

15.2 Human α -1,3-Fucosyltransferase IV (Fuc-T)

The most valuable basis for rationale drug design is the availability of the detailed structure of a biological target, often the active site of an enzyme engaged in a pathological process. Such is the case with Fuc-T. The design of various nucleoconjugates, therefore, started with the structure and mechanism of this enzyme.

From the outset, several factors inherent to the enzymatic glycosyl-transfer reaction complicated the rational design of Fuc-T inhibitors [6]. Guanosine diphosphate β -L-fucose (GDP-fucose) is transferred in the terminal step, but this reaction comprises a complex four-partner transition state, which rendered design of GDP-fucose antagonists elusive. GDP-fucose, itself, is a complex molecule. But an important contribution to the design of antagonists came from the finding that most of the binding energy of Fuc-T for this substrate comes from the GDP moiety [7]. Further improvement was possible through the identification of a hydrophobic pocket, adjacent to the binding site, which enhances affinity 70-fold by hydrophobic interaction with acceptor molecules (antagonists, substrates) (Unpublished data, cited in [8]).

Generally, mammalian Fuc-transferases have the typical structure of transmembrane proteins, consisting of a short N-terminal cytoplasmic tail, a transmembrane domain and a stem region followed by a large C-terminal catalytic domain [8, 9]. The substrate, GDP-fucose, binds inside this domain giving the overall structure of Fuc-T-GDP-fucose complex shown in Fig. 15.1 [8].

Interactions between the enzyme and diphosphate are defined by the GDP-fucose complex of Fuc-T in Fig. 15.1. Both side chains of Arg-195 (R195) and Lys-250 (K250) provide the neutralizing positive charges for the diphosphate unit.

Fig. 15.1 Overall structure of the Fuc-T-GDP-fucose complex; stereo view showing the GDP-fucose binding site (reproduced from [8], with the permission of the American Society for Biochemistry and Molecular Biology)

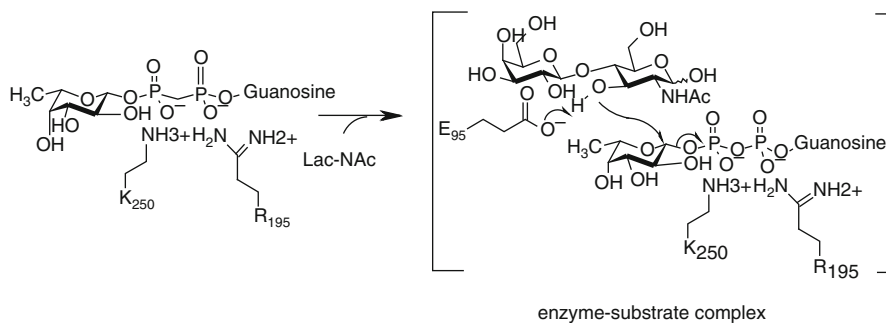
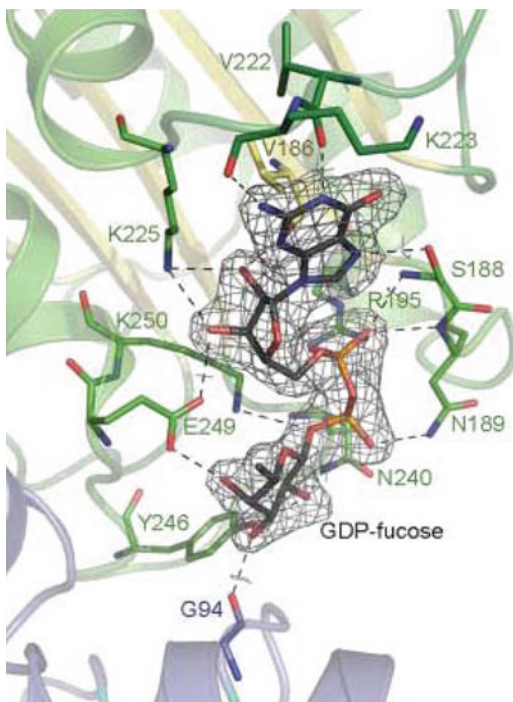


Fig. 15.2 A proposed catalytic mechanism of Fuc-T, whereby Glu-95 (E95) serves as a general base

Eighteen H-bonds are formed with GDP-fucose, seven of them between Fuc-T and the nucleoside moiety, contributing to the highly specific recognition of this substrate. The catalytic mechanism requires binding of *N*-acetylglucosamine (LacNAc) to the pocket in the N-terminal domain of Fuc-T, which has a highly negative electrostatic potential that reduces the pKa of C3-OH group of *N*-acetylglucose unit within LacNAc to favour its nucleophilic attack (Fig. 15.2) [8].

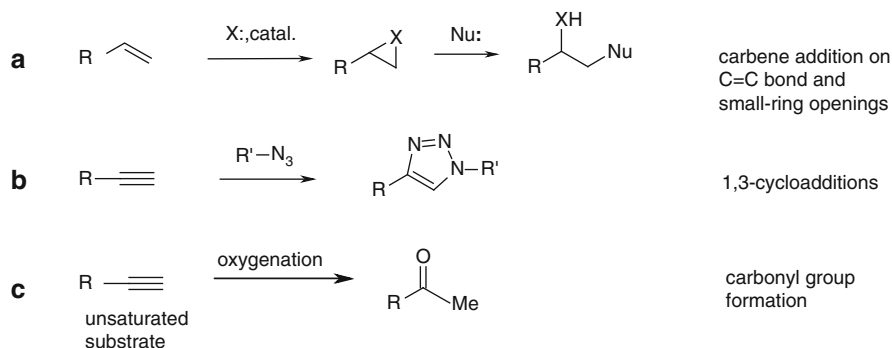
Upon deprotonation of the C3-OH group by Glu-95, the acceptor nucleophile can attack the anomeric position of GDP-fucose to form a glycosidic bond with an inverted configuration [9].

Such detailed understanding of the enzymatic process facilitated design of inhibitors, characterized by the presence of a GDD unit at one end (envisaged to bind to the domain of negative electrostatic potential and the network of H-bonds), and a lipophilic unit at the other. The two units were linked by a conformationally highly flexible linker. Following this general principle, a library of compounds was designed which retained the GDP core, while the attached hydrophobic group and linker length were varied. This library was established using a relatively new methodology, named *click chemistry*, and resulted in the synthesis of the lead compound **1**, a Fuc-T inhibitor [2, 10].

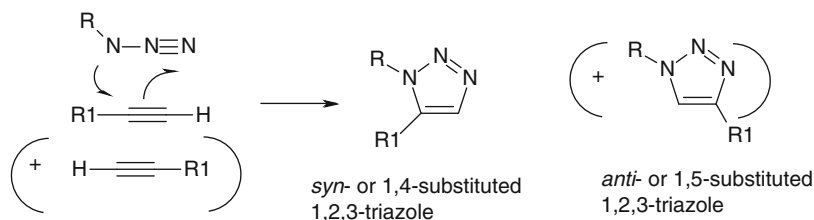
15.3 Click Chemistry: Energetically Preferred Reactions

Before detailed analysis of the discovery process that led to the highly selective Fuc-T inhibitor **1**, click chemistry deserves a more general presentation. Click chemistry is defined by the inventors [1] as a *modular approach that uses only the most practical and reliable chemical transformations to generate collections of test compounds for screening*. In other words, click chemistry uses energetically highly favourable reactions, in which unsaturated units (substrates) provide the carbon framework. Examples are given in Scheme 15.1a–c.

The common characteristics of click chemistry reactions presented in this scheme are their high energetic preference and selective formation of new groups attached via carbon–heteroatom bonds. To achieve this, a highly reactive component, such as the six-electron species X in (a), the azide in (b) or the oxygen carrier in (c) is required. Generally, click chemistry refers to a series of reactions that obey specific criteria, such as being modular, stereoselective, high-yielding and involving simple protocols. Readily available starting materials must be used in this



Scheme 15.1 Representative reactions amenable to click chemistry



Scheme 15.2 Uncontrolled 1,3-dipolar azide-to-alkyne addition leads to isomeric *syn*- and *anti*-triazoles

methodology and should be essentially inert towards most biological and organic conditions, including water and molecular oxygen.

All this applies in particular to the copper (I)-catalyzed coupling of azides and terminal acetylenes to form exclusively 1,4-disubstituted 1,3-triazole linkages, according to example (b) in Scheme 15.1. From the biological standpoint, the topological and electronic features shared by 1,2,3-triazoles and amide bonds are particularly important, since the latter are ubiquitous connectors in Nature. From the synthetic point of view, it is important to note that alkyl azoles can give 1,4- and 1,5-disubstituted, or *syn*- and *anti*-1,2,3-triazoles (Scheme 15.2).

The original reaction, known as Huisgen's 1,3-dipolar cycloaddition, involved thermal treatment of both reagents and afforded 1,2,3-triazoles as approximately 1:1 mixtures of 1,4- and 1,5-disubstituted derivatives [11]. Exclusive formation of 1,4-substituted triazoles succeeded when it was discovered that Cu(I) ions, formed in situ from Cu(0) and Cu(II) salts, completely govern regioselectivity for the addition of alkylazides. Important contributions to the multi-component variant of the copper-catalyzed azide-to-alkyne addition have been reported recently [12, 13]. In this reaction, both reacting partners are generated in situ; azides from the corresponding halides, and copper(I) acetylides from terminal alkynes and Cu(I) ions, whereby the latter are formed by disproportionation of copper(0) and copper (II) species. Carrying out both steps under microwave irradiation (100 W and 125°C) significantly reduces reaction time, affording final products in roughly 90% yield.

Since click chemistry utilizes reactions operating under a large thermodynamic driving force and are largely insensitive to the reaction conditions, they are suitable for computational analysis. K.N. Houk et al. reported a computational study of azide-alkyne 1,3-dipolar cycloaddition in a click-reaction, based on the high-accuracy complete basis set-quantum B3 (CBS-QB3) method [14, 15]. Since they used acetylene as the simplest alkyne, no conclusions about regioselectivity were drawn. However, a surprisingly negligible effect of electron-withdrawing (EWG) or electron-donating (EDG) groups on the activation barrier of 1,3-dipolar cycloaddition was observed. Activation enthalpies for formyl-, mesyl-, methyl- and phenyl-azides were estimated within a narrow range, from 17 to 19 kcal/mol. The activation energies for these azides were also similar, between 27.5 and 30.5 kcal/mol, and all reactions were calculated as being exothermic by 60–70 kcal/mol [15]. The 1,2,3-triazoles were also

30–40 kcal/mol more stable than the 1,2,3-triazolines, formed on addition of azides to ethylenes, thus explaining the irreversibility of the former process.

15.4 Target-Guided Synthesis or Freeze-Frame Click Chemistry

An ingenious variation of click chemistry evolved from *target-guided synthesis* (TGS) or *freeze-frame click chemistry*. It represents a new strategy for generation of compound libraries. By employing biological targets, themselves, to assemble inhibitors within the confines of their binding sites, TGS promises to revolutionize lead discovery in developing new drugs. This method is based on the observation that two reactive species can exert synergistic biological effects as a result of their self-assembly at the active site, usually inside cells. The newly formed inhibitors usually display much higher binding affinities for their biological targets than the individual components, since they simultaneously act through multiple binding interactions [16, 17]. In principle, lead discovery by TGS is independent of the biological function of the target, since it relies solely on its ability to hold the reagents in close proximity until they become connected via the “arranged” chemical reaction. Most approaches to TGS employ highly reactive reagents, strong electrophiles or nucleophiles, metathesis catalysts, etc., which can cause side reactions and even destroy the biological target.

To avoid such complications, Sharpless et al. have developed an extremely reliable approach to *kinetically controlled TGS*, a variant of click chemistry [18, 19], which employs the completely bio-orthogonal [1,3]-dipolar cycloaddition reaction between azides and acetylenes [20]. This process is self-contained, hence no external reagents, catalysts, or side products that might interfere are present, and the “reactants” themselves are largely “invisible” in a biological milieu. Most importantly, despite its high driving force (>50 kcal/mol), the uncatalyzed reaction has a surprisingly high activation barrier ~25 kcal/mol, making it extremely slow at room temperature. Its rate is, therefore, highly dependent on parameters that stabilize the transition state [21]. These authors have shown that acetylcholinesterase (AChE) is able to assemble extremely potent inhibitors, which simultaneously access the enzyme’s active and peripheral binding sites [22–24]. This finding prompted them to combine azide and acetylene reagents, each linked to the known active and peripheral site inhibitors, tacrine and phenylphenanthridinium, respectively [16, 17].

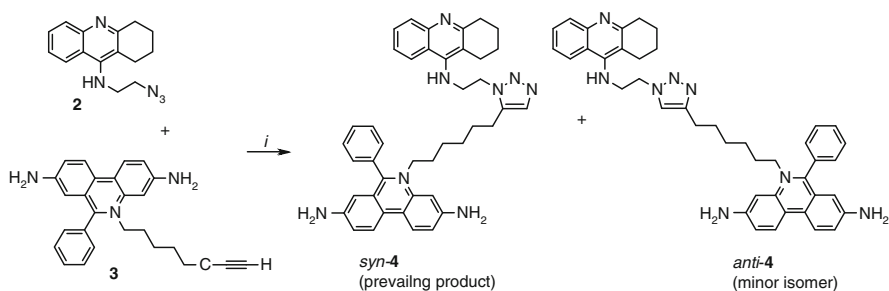
Due to steric restraints imposed by the enzyme active site on the orientation of the reacting partners, this specific approach is also known as *freeze-frame click chemistry*. In recent years, freeze-frame click chemistry has been developed with diverse reactive couples of small molecules [18, 25, 26]. This has opened up a new approach to the in situ design of high affinity ligands for biological targets using bio-orthogonal reactive building blocks within a macromolecular template. Since

the active centre geometry of the macromolecule, usually a protein, is well defined, it controls the stereochemistry of the azide-to-alkyne-addition. In the absence of a macromolecular template or small molecular metal catalysts, two isomeric triazoles, *syn*- or *anti*-, both appear to be likely reaction products, as shown in Scheme 15.2. The influence of binding site geometry also results in the preferential formation of just one of the products. As mentioned, this concept has been successfully developed by K. B. Sharpless et al. for AChE as a “reaction vessel” [24, 27, 28]. The authors selected this enzyme, on the one hand, because of its key role in neurotransmitter hydrolysis in the central and peripheral nervous systems [29, 30]. On the other hand, the structure of the active centre of AChE is well known, and characterized by a narrow gorge lined with aromatic side-chains [31]. Since the active centre is comprised of both acylation and choline-binding sites, it recognizes small-molecule ligands at each site.

As a proof of principle, the authors synthesized by click chemistry the triazole-linked bivalent inhibitor *syn*-4 with site-specific ligands 2 and 3 as building blocks (Scheme 15.3) [27].

This reaction proceeded at the AChE active site with nearly complete *syn*- or 1,5-selectivity, controlled by the topology of the narrow gorge. Strikingly uniform *syn*-selectivity was obtained for enzyme-produced triazoles, independently of the linker length and stereochemistry of the acetylene reagent.

Generally, *syn*-compounds proved highly effective non-covalent inhibitors of AChE, in sharp contrast to their *anti*-isomers. The difference in kinetic parameters for the representative couple of isomers *syn*-4/*anti*-4, as determined for mouse AChE, is impressive (Table 15.1) [28].



Reagents and conditions: *i*. AChE (mouse), active-site concn. 1 mM, r.t.

Scheme 15.3 AChE active site-promoted selective synthesis of *syn*-4

Table 15.1 Kinetic and equilibrium interaction constants for the triazole inhibitors with the highest affinity, generated “in situ” using mouse AChE as the cycloaddition reaction template

	k_{on} ($10^{10} \text{ M}^{-1} \text{ min}^{-1}$)	k_{off} (min^{-1})	K_{d}
<i>syn</i> -4	1.3	0.0011	99 fM
<i>anti</i> -4	2.4	0.30	8,900 fM

These results set the stage for the performance of the first ever *search for AChE inhibitors* through in situ *click chemistry*, based on building blocks that were not previously known to interact with the target. To minimize the number of variables, the authors used the tacrine building block, TZ2, as an “anchor molecule.” In complex with the enzyme, TZ2 recruits and irreversibly links novel peripheral site ligands together to form multivalent AChE inhibitors that simultaneously access multiple binding sites within the enzyme (Fig. 15.3) [26].

On the basis of analogous considerations, these same authors designed a library of complementary acetylene reagents carrying aromatic heterocyclic phenylphenanthridinium mimics, with a spacer of five or six methylene units. To increase the screening throughput, multi-reagent mixtures, containing up to 10 acetylene reagents at a time, were tested. This multi-component in situ *click chemistry* screening approach is conceptually interesting. It addresses the question whether an enzyme complex of one reaction partner, capable of triazole genesis (e.g., the tacrine azide TZ2), can find and select its “best” triazole-forming partner(s) when presented with mixtures of candidates with unknown binding affinities. Thus the enzyme “discovers” its own potent biligand inhibitors.

Another inventive extension of click chemistry is the concept of “click-resins” that promote solid phase supported reactions to work under nearly perfect conditions, fulfilling the requirements of click chemistry [32, 33]. This approach has enabled the assembly of a library of carboxylic arene bioisoeesters, with the general formula **V** [34] as potential dopamine D4 receptor ligands [35]. In essence, the authors completed parallel synthesis of bioactive *tert*-amines **V**, utilizing triazolyl-methylacrylate **7** as a linker. The product was readily generated from the commercial azidomethyl substituted polystyrene **5** and propargyl acrylate **6** via Cu(I) catalyzed 1,3-dipolar cycloaddition (Scheme 15.4).

Solid phase **7** represents a *regenerative Michael receptor* (REM), since on addition of phenylpiperazines **I**, a library of solid-phase derivatives **II** is formed. On benzylation by benzylbromides **III**, quarternary amonium salts **IV** are formed,

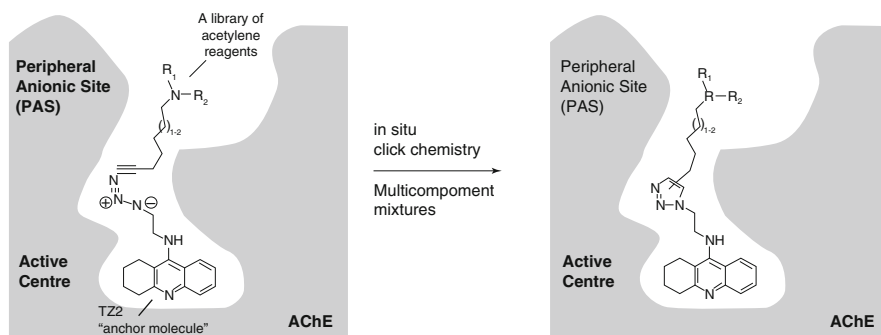
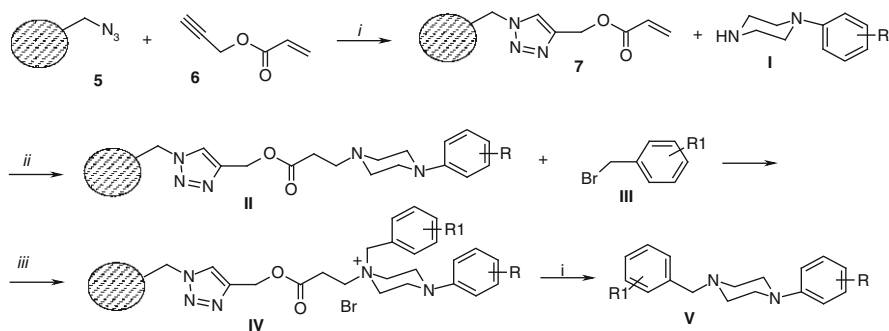


Fig. 15.3 In situ click chemistry screening for AChE inhibitors containing novel peripheral site ligands (reproduced from [26], with the permission of the American Chemical Society)



Reagents and conditions: *i.* Cu(I)I, DMF/THF, DIPEA, 35 °C;
ii. NMP, r.t., 36 h;
iii. DMSO, r.t., 16 h; *iv.* TEA, DMF, r.t., 4 h.

Scheme 15.4 Click chemistry on a resin, applied to the synthesis of bioactive *tert*-amines **V**

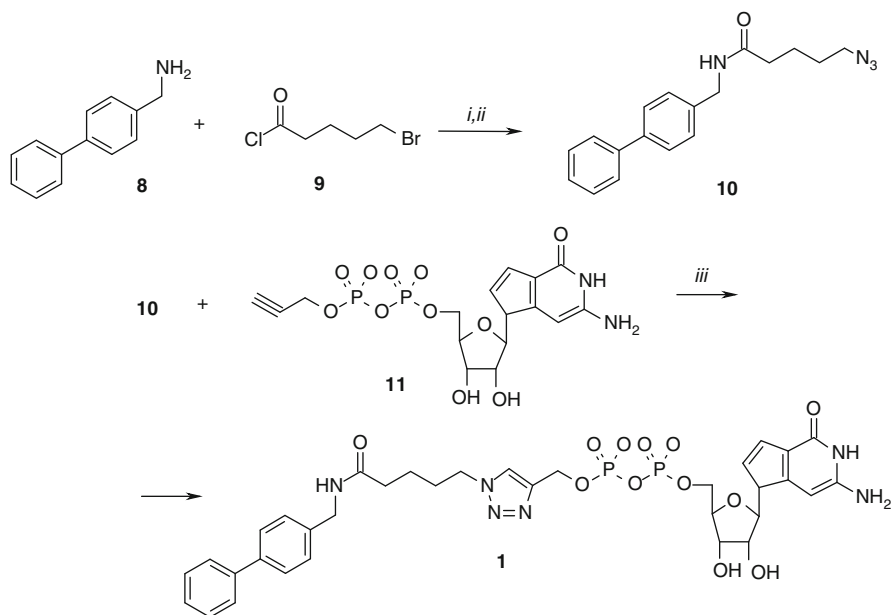
which on Hoffmann elimination, or retro-Michael reaction, afford a library of target compounds **V** and regenerate the Michael receptor **7**.

In conclusion, click chemistry, based on the Cu(I)-catalyzed 1,3-dipolar addition of azides (Huisgen's reaction), has emerged as a tailored transformation pathway either to undertake the structural diversification of privileged scaffolds, or to establish linkages between biologically important molecules. Besides the examples selected for presentation in this chapter, there are many others that are instructive for structural diversification [36–38] and biological linkage applications [39].

15.5 Application of Click Chemistry to the Synthesis of Neoglycoconjugate **1**

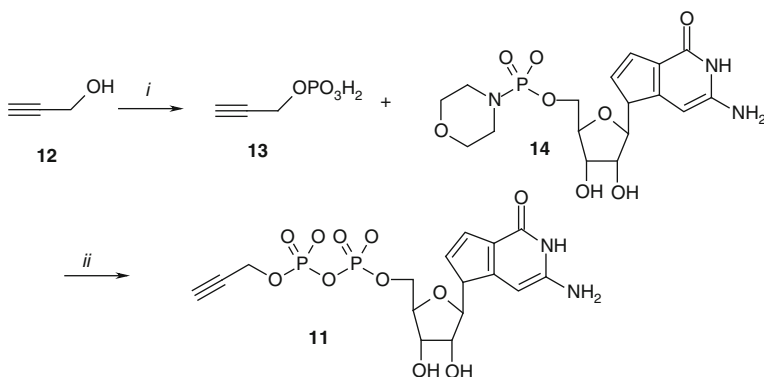
As indicated in Sect. 15.3, in view of the favourable biological properties of triazoles, their chemical stability and compatibility with a plethora of functional groups, click chemistry became an important strategy for the generation of novel compound libraries. The click chemistry concept has also proved highly viable in the search for new drugs. This is illustrated by the finding that SciFinder cites 582 references, up to 2010, in which triazoles have been prepared by click chemistry, most of them (350) published after 2006! Of 127 references that refer to triazole libraries, 43 were created by click chemistry. Preparation of triazole derivatives by click chemistry is claimed in 37 patents, whereas 110 patents claim the click chemistry approach to generate other target structures. Application of this concept to the synthesis of neoglycoconjugate compound **1** is outlined in Scheme 15.5 [40].

For completion of the key click reaction step *iii*, intermediate **11** was crucial. It was prepared by propargylation of **14**, in the presence of lipophilic *tert*-amine, and



Reagents and conditions: *i.* *tert*-amine, solv.; *ii.* NaN_3 , solv.;
iii. Cu(I) , in microplates.

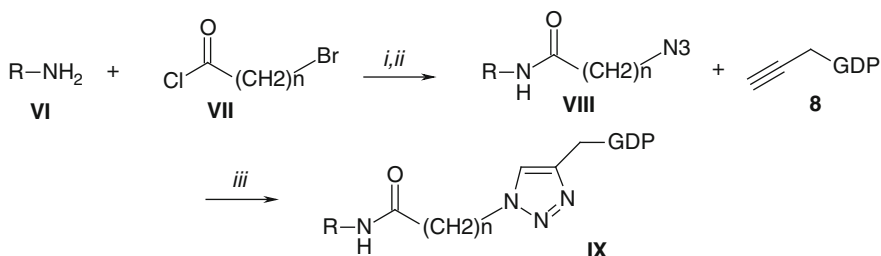
Scheme 15.5 Click reaction on the route to neoglycoconjugate **1**



Reagents and conditions: *i.* H_3PO_4 , I_2 , Et_3N ; *ii.* Oct₃N, 1H-tetrazole.

Scheme 15.6 Synthesis of the click reagent **11**

1H-tetrazole as the basic promoter for the formation of an anhydride P–O–P bond (Scheme 15.6). To this end, guanosine monophosphate (GMP) was activated as the morpholidate **14** and coupled with propargyl phosphate **13**.



Reagents and conditions: *i.* $n = 1-5$, *tert*-amine, solv.; *ii.* NaNO_3 , solv.;
iii. $\text{Cu}(0)/\text{Cu}(\text{II})$, $\text{H}_2\text{O}/\text{EtOH}/\text{tert-BuOH}$, r.t.

Scheme 15.7 Synthesis of the library of triazoles with incorporated GDP

The route in Scheme 15.6 is characterized by the fixed structure of propargyl-GDP **11**, a key intermediate for the synthesis of the library of triazoles (**IX**), available in a one-pot reaction, according to the general Scheme 15.7.

There are some important features of this click reaction; no protecting group on GDP derivative **11** is required; the reaction is completed with ~80–95% yield at room temperature in an aqueous solvent mixture ($\text{H}_2\text{O}/\text{EtOH}/\text{tert-BuOH}$), allowing use of CuSO_4/Cu -wire as an *in situ* source of $\text{Cu}(\text{I})$ ions. According to Scheme 15.7, 86 products with the general formula **IX** were prepared in a 96-well plate and screened for biological activity without further purification. Steady-state kinetic evaluation of purified lead neoglycoconjugate **1** showed that it is a competitive inhibitor against GDP-fucose with $K_i = 62 \text{ nM}$, which made this compound the *first and most potent inhibitor of Fuc-T at the nanomolar level* [3].

15.6 Conclusion

The $\text{Cu}(\text{I})$ -catalyzed stepwise variant of Huisgens's classic 1,3-dipolar cycloaddition seems to be the best example of reliable click chemistry to date. This method may be used widely for the identification of high-affinity inhibitors of other group-transfer targets that are of biological or medicinal interest. Some inventive variants of click chemistry, presented in this chapter, should serve to illustrate its broad application as an elegant synthetic chemistry tool to construct new biologically active compounds.

References

1. Kolb HC, Sharpless KB (2003) *Drug Disc Today* 8:1128–1137
2. Lee LV, Mitchell ML, Huang S-J, Fokin VV, Sharpless KB, Wong C-H (2003) *J Am Chem Soc* 125:9588–9589

3. Sears P, Wong C-H (1998) *Cell Mol Life Sci* 54:223–252
4. Rosa DD, Ismael G, Lago LD, Awada A (2008) *Cancer Treat Rev* 34:61–80
5. Murdoch D, Sager J (2008) *Curr Opin Oncol* 20:104–111
6. Murray BW, Takayama S, Schultz J, Wong C-H (1996) *Biochemistry* 35:11183–11193
7. Mitchel ML, Tian F, Lee LV, Wong C-H (2002) *Angew Chem Int Ed* 41:3041–3044
8. Sun H-Y, Lin S-W, Ko T-P, Pan J-F, Liu C-L, Lin C-N, Wang AH-J, Lin C-H (2007) *J Biol Chem* 282:9973–9982
9. Ihara H, Ikeda Y, Toma S, Wang X, Suzuki T, Gu J, Miyoshi E, Tsukihara T, Honke K, Matsumoto A, Nakagawa A, Taniguchi N (2007) *Glycobiology* 17:455–466
10. Fazio F, Bryan MC, Blixt O, Paulson JC, Wong C-H (2002) *J Am Chem Soc* 124:14397–14402
11. Huisgen R (1984) In: Padwa A (ed) 1, 3-dipolar cycloaddition chemistry, Chap. 1. Wiley, New York, pp 1–176
12. Appukkuttan P, Dehaen W, Fokin VV, Van der Eycken E (2004) *Org Lett* 6:4233–42
13. Gil MV, Arevalo MJ, Lopez O (2007) *Synthesis*: 1589–1620
14. Jones GO, Ess DH, Houk KN (2005) *Helv Chim Acta* 88:1702–1710
15. Jones GO, Houk KN (2008) *J Org Chem* 73:1333–1342
16. Jain A, Huang SG, Whitesides GM (1994) *J Am Chem Soc* 116:5057–5062
17. Mammen M, Chio S-K, Whitesides GM (1998) *Angew Chem Int Ed* 37:2755–2794
18. Lewis WG, Green LG, Grynszpan F, Radić Z, Carlier PR, Taylor P, Finn MG, Sharpless KB (2002) *Angew Chem Int Ed* 41:1053–1057
19. Manetsch R, Krasinski A, Radić Z, Raushel J, Taylor P, Sharpless KB, Kolb HC (2004) *J Am Chem Soc* 126:12809–12818
20. Himo F, Lovell T, Hilgraf R, Rostovtsev VV, Noodleman L, Sharpless KB, Fokin VV (2005) *J Am Chem Soc* 127:210–216
21. Du D-M, Carlier PR (2004) *Curr Pharm Res* 10:3141–3156
22. Carlier PR, Han YF, Chow ES-H, Li CP-L, Wang H, Leu TX, Wong H, Pang Y-P (1999) *Bioorg Med Chem* 7:351–357
23. Han YW, Li CP-L, Chow E, Wang H, Pang Y-P, Carlier PR (1999) *Bioorg Med Chem* 7:2569–2575
24. Mocharla VP, Colasson B, Lee LV, Roper S, Sharpless KB, Wong CH, Kolb HC (2004) *Angew Chem Int Ed* 44:116–120
25. Bourne Y, Radić Z, Kolb HC, Sharpless KB, Taylor P, Marchot P (2005) *Chem Biol Interact* 157/158:159–165
26. Krasinski A, Radić Z, Manetsch R, Raushel J, Taylor P, Sharpless KB, Kolb HC (2005) *J Am Chem Soc* 127:6686–6692
27. Radić Z, Manetsch R, Fournier D, Sharpless KB, Taylor P (2008) *Chem Biol Interact* 175:161–165
28. Quinn DM (1987) *Chem Rev* 87:955–979
29. Taylor P, Radić Z (1994) *Ann Rev Pharmacol Toxicol* 34:281–320
30. Sussman JL, Silman I, Axelsen PH, Hirth C, Goldner M, Bouet F, Ehret-Sabatier L, Schalk I, Harel M (1993) *Proc Natl Acad Sci USA* 90:9031–9035
31. Lober S, Gmeiner P (2004) *Tetrahedron* 60:8699–8702
32. Pilar RL, Loeber S, Huebner H, Gmeiner P (2006) *J Comb Chem* 8:252–261
33. Tietze R, Lober S, Hubner H, Gmeiner P, Kuwert T, Prante O (2008) *Bioorg Med Chem Lett* 18:983–988
34. Klabunde T, Hessler G (2002) *Chem Biol Chem* 3:928–944
35. Sivakumar K, Xie K, Cash BM, Long S, Barnhill HN (2004) *Org Lett* 6:4603–4606
36. Khanatetskyy B, Dallinger D, Kappe CO (2004) *J Comb Chem* 6:884–892
37. Rodriguez-Borges JE, Goncalves S, do Vale ML, Garcia-Mera X, Cuelho A, Sotelo E (2008) *J Comb Chem* 10:372–375
38. Aucagne V, Leigh DA (2006) *Org Lett* 8:4505–4507
39. Pisaneschi F, Cordero FM, Lumini M, Brandi A (2007) *Synlett*: 2882–2884
40. Pedersen LC, Darden TA, Negishi M (2002) *Biol Chem* 277:21869–21973

Chapter 16

12-Aza-Epothilones

Abstract

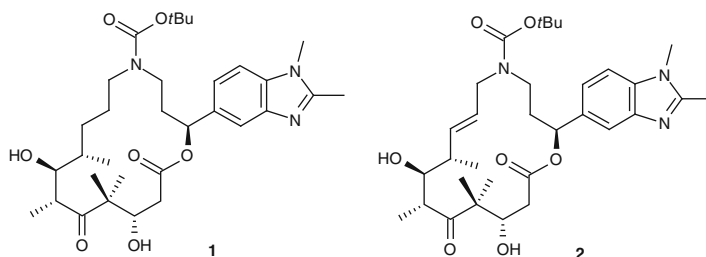
Biological target: 12-Aza-epothilones (azathilones) induce tubulin polymerization, thereby disturbing microtubule function and inhibiting mitosis and cell growth at nM concentrations. They show low susceptibility to P-glycoprotein-mediated efflux and are thus active on multidrug resistant cells.

Therapeutic profile: The compounds are potential anticancer agents.

Synthetic highlights: Natural macrocyclic compounds have been subjected to both extensive and peripheral structural modifications in the search for new lead compounds. An example of the former is the antibiotic azithromycin, whereas 12-aza-epothilones must be approached by total synthesis. This total synthesis of epothilones involves ring closure metathesis using heteroleptic complexes as catalysts and has proved to be an efficient approach to “non-natural, macrocyclic natural products”. In one of the critical steps of this pathway to azathilones, creative site-selective diimide reduction of an allylic C=C bond was applied.

16.1 Introduction

12-Aza-epothilone **1** ((*E*)-(2*S*,9*S*,10*R*,11*R*,14*S*)-10,14-dihydroxy-9,11,13,13-tetramethyl-2-[2-(1,2-dimethyl-benzimidazol-5-yl)]-12,16-dioxo-1-oxa-5-aza-cyclohexadecane-5-carboxylic acid *tert*-butylester) and its 7,8-dehydro analogue **2** are potent inhibitors of human cancer cell growth, and represent a structurally new class of natural product-derived microtubule-stabilizing agents.



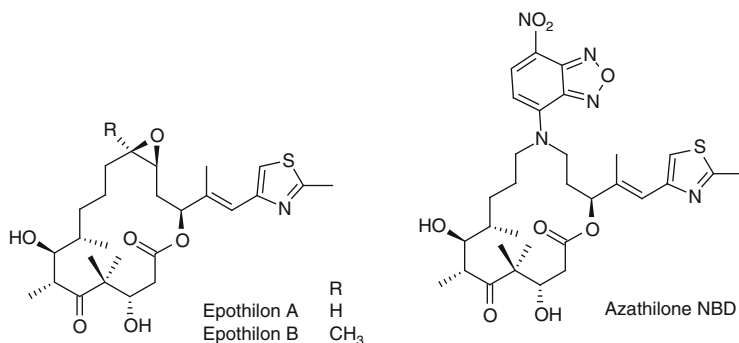


Fig. 16.1 Two representatives of epothilones and azathilone NBD

Leading structures in this field are epothilones A and B (Fig. 16.1), natural macrocyclic bacterial metabolites with potent microtubule-stabilizing and antiproliferative activity [1, 2]. They exhibit almost identical activity and mode of action to that of paclitaxel (Taxol[®]), the chemistry of which is discussed in Chap. 14. Their cytotoxic action is also based on tubulin polymerization with resulting inhibition of mitosis [3].

Many anticancer drugs, including paclitaxel, lose efficacy due to so-called *multi-drug resistance* (MDR). This is mediated by endogenous membrane transporter proteins, such as P-glycoprotein (P-gp), which pump drugs back out of the tumour cells. In marked contrast to paclitaxel, however, epothilones A and B were found to exhibit very low susceptibility to P-gp-mediated drug efflux, thus maintaining virtually equivalent growth inhibitory activity against drug-sensitive and MDR human cells [4].

On the basis of these data, epothilones A, B and some congeners have been widely pursued as lead structures for the development of a new generation of non-taxane-derived microtubule stabilizers for cancer treatment [5]. Five representatives of this class are currently undergoing clinical evaluation in humans. This outcome confirms the view that natural products provide a vast pool of potential lead structures for drug discovery. In a very general sense, the strategy that resulted in 12-aza-epothilones could be viewed as *the synthesis-based equivalent* to the discovery of a new natural product with a specific biological activity.

The rationale behind 12-aza-epothilones as target structures is based on the accumulated knowledge on the biological active site and the mechanism of action of natural epothilones. Some aspects of these studies are briefly discussed in the following sections.

16.2 Epothilones: Mechanism of Action and Structure–Activity Relationships

Epothilones belong to the class of anticancer drugs that target microtubules, along with paclitaxel (Taxol[®]), docetaxel (Taxotere[®]) and some others. All these anticancer drugs function by perturbing the dynamic equilibrium of the

microtubular polymerization of heterodimeric α/β -tubulin subunits. Intracellular microtubules are a crucial part of the skeletal structure of the cell and play a major role in the cell division process that occurs both normally and to an increased extent in cancer cells. Inhibition of tubulin polymerization, thus, reduces cell division. More details on this process are given in Sect. 14.1.

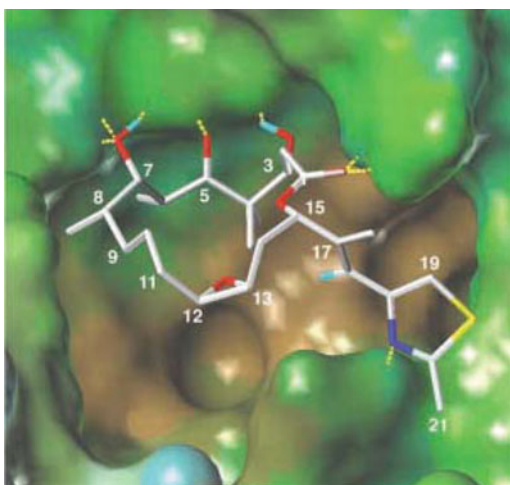
Since the discovery of the epothilones in 1993, an impressive structure–activity relationship (SAR) profile has emerged from the efforts of many synthetic teams [6–8]. This first led to the definition of a common pharmacophore and SAR for the structurally diverse epothilones [9–12], then to the rational design of new structures.

Initially, data were collected on crystal structure and conformation of epothilone B in solution [13], together with information on the binding site of epothilone A on α/β -tubulin, using electron crystallography and molecular modelling (Fig. 16.2) [14]. These facilitated the molecular design of novel, non-natural epothilones.

The most important interactions and conformational properties of the tubulin-bound vs. free epothilones in solution were soon recognized. Thus, the folded conformation of the epoxide in Fig. 16.2 is directed into the underlying hydrophobic basin (brown), which readily accepts the long and bulky hydrophobic group. This observation prompted the replacement of the epoxide with an *N*-tert-butoxycarbonyl unit in some 12-aza-epothilones. A number of thiazole replacements in epothilones A and B also have been shown to retain or improve epothilone activity. Nicolaou et al. found that pyridines, in which the N-atom is *ortho* to the side chain connector, are 10–100 times more active than *meta* and *para* isomers [15]. This finding led to the introduction of other aza-heterocycles, in particular, the benzimidazole ring into the molecule.

Further insight into the complex between β -tubulin and 12-aza-epothilones was obtained by visualization of the binding of fluorescent azathilone NBD (formula given in Fig. 16.1) to cellular microtubules (Fig. 16.3a, b) [16]. Combined with

Fig. 16.2 Epothilone A (white, C; red, O; blue, N; and yellow, S) with hydrogen bonds (yellow dashes) to the associated centres on the tubulin protein (reproduced from [14], with the permission of the American Association for the Advancement of Science)



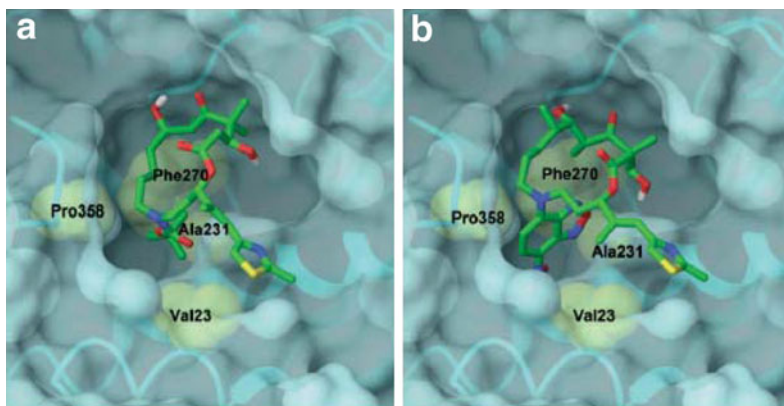


Fig. 16.3 (a) 12-aza-epothilone **1** and (b) azathilone NBD docked to the taxol/epothilone binding site on β -tubulin (reproduced from [16], with the permission of John Wiley and Sons Inc.)

computational studies, a structural model of the complexes between β -tubulin and **1** and azathilone NBD was constructed. The *tert*-butyloxycarbonyl group of **1** and the NBD fluorophore occupy the pocket that includes the hydrophobic side chains of Val23, Ala231, Phe 270 and Pro358, thus specifically contributing to microtubular binding.

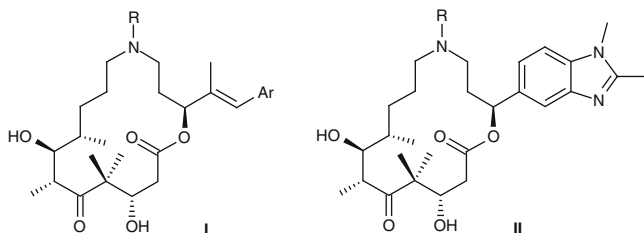
All these data revealed the multiple interactions that epothilones make with β -tubulin. They also explain why modification of the epoxide at the C12–C13 position to form the N12-*tert*-Boc-C13 unit and the introduction of a polycyclic benzimidiazole ring at C15 in 12-aza-epothilone **1** have contributed so much to the improvement of biological activity. Development of 12-aza-epothilones is one of the most impressive successes of the combined structural and molecular biological approach to the design of new lead molecules.

16.3 Extensive vs. Peripheral Structural Modifications of Natural Products

Natural epothilones have been structurally modified by various teams, making use of the broad structural scope of natural product-based drug discovery in this field. Generally, this approach includes the *de novo* construction of libraries of “natural product-like” compounds through *diversity orientated synthesis* (DOS) [17]. A concept for the design of natural product-based libraries, introduced by H. Waldmann [18], has been developed over the last few years [19] (see also Sects. 1.2.1 and 1.2.2 in the introductory chapter).

The synthetic approach to epothilone analogues is an example of *extensive structural modification* of the lead from nature. This approach, rather than simple *peripheral derivatization* of existing leads, is characterized by the replacement of

the backbone carbon C(12) by nitrogen in the macrolactone ring of epothilone A. The resulting analogues, 12-aza-epothilones or azathilones, with the general formulae **I** and **II** are defined as “*non-natural natural products*” [20]. These new leads retain most of the structural features of the natural products, while lying outside the general scope of nature’s biosynthetic machinery. There are no known natural processes for incorporation of a single nitrogen atom into a regular polyketide backbone. Compounds **1** and **2** are members of structural family **II**, characterized by the incorporation of a conformationally constrained benzimidazole unit.



At this point, it should be noted that the concept of *extensive structural modification* is imbedded in the invention of the first aza-macrolide, the antibiotic azithromycin, discovered in 1982 by PLIVA chemists in Zagreb, Croatia [21, 22]. Azithromycin became a multibillion drug on the world market, and represents an early example of therapeutic success with a “non-natural natural compound”, available via extensive structural modification.

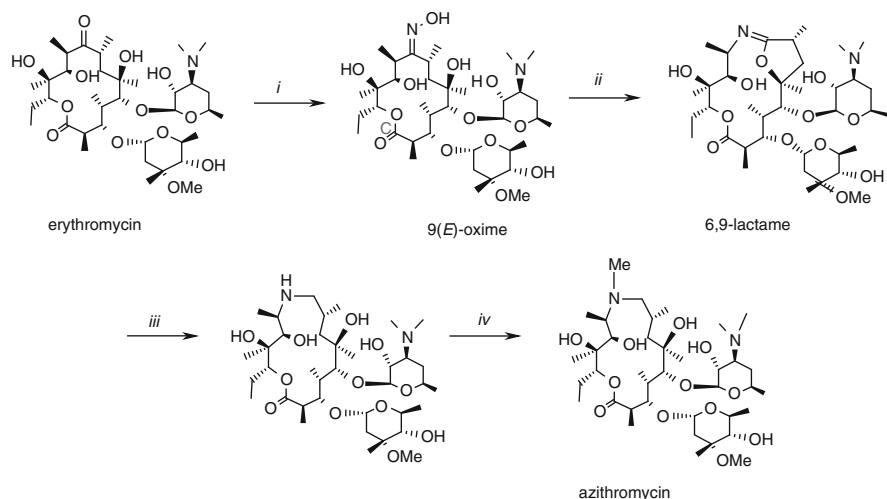
Formally, the N-atom of azithromycin is inserted into the macrolide ring of erythromycin, and the carbonyl group is reduced to methylene. In contrast, in 12-aza-epothilones, the C12 atom in natural epothilones is replaced by an N-atom, and epoxide oxygen is reduced. While the first substantial alteration of the macrolactone ring was achieved in a few steps from erythromycin, the second epothilone modification cannot be made with compounds from the natural pool, and required total synthesis of the target structures.

Azithromycin is derived from the natural product, erythromycin, via Beckmann rearrangement of the intermediary oxime, as outlined in Scheme 16.1.

Ring enlargement of the natural product to its 15-membered aza-congener, followed by *N*-methylation, resulted in an antibiotic that has revolutionized the therapy of many infective diseases, in particular, those caused by highly resistant strains [23].

16.4 Ring Closure Metathesis: An Efficient Approach to Macrocyclic “Non-natural Natural Products”

Contrary to azithromycin, 12-aza-epothilones **1** and **2** are not available from their natural congeners. Therefore, *these target molecules must be approached by total synthesis*, starting from small chiral building blocks. The key issue in their synthesis,



Reagents and conditions: i. $\text{NH}_2\text{OH}/\Delta$, $-\text{H}_2\text{O}$; ii. $\text{ArSO}_2\text{Cl}/\Delta$, then base;
iii. H_2 , catalyst; iv. $\text{HCOOH}/\text{CH}_2\text{O}$.

Scheme 16.1 Synthetic route to the antibiotic azithromycin

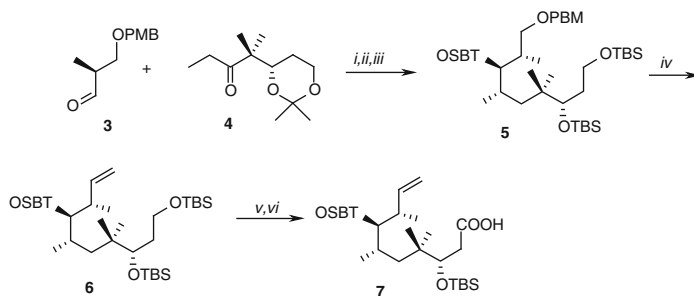
as in the synthesis of most macrocyclic natural and non-natural products is *macrocyclization*. This process is not entropy-favoured, and in its traditional version, requires specific conditions, such as high dilution methods and specific reagents, including activating groups to promote two terminal functionalities for intramolecular reaction. In addition, the macrocyclic ring in epothilones comprises five stereogenic centres of defined absolute configuration. This apparently formidable synthetic task was elegantly solved by the group of Altmann at the ETH Zurich. After taking some inefficient and tedious approaches [24, 25], the authors designed and achieved the synthesis of the target structures **1** and **2**, involving three strategic steps:

1. A stereoselective aldol reaction between aldehyde **3** and ketone **4** creating two stereogenic centres in the correct absolute configuration (Scheme 16.2).
2. Preparation of optically pure *sec*-alcohol **15** (Schemes 16.3 and 16.4).
3. Esterification of carboxylic acid **7** followed by ring closure metathesis (RCM) of *bis*-olefin **16** to unsaturated azathilone **2** (Scheme 16.5) [26–28].

Hydrogenation of **2** to **1** in the last step of Scheme 16.5, as routine as it seems, proved to be extremely sluggish, leading to side reactions and a low yield. This synthetic issue was solved, though not as a practical large-scale approach, as discussed in Sect. 16.5.

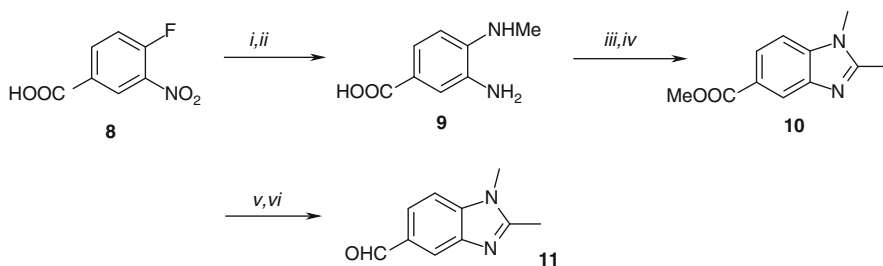
Syntheses of **7** and **15**, the two chiral building blocks with terminal C=C bond are presented in Schemes 16.2, 16.3 and 16.4.

Aldol condensation of *para*-methoxybenzoyl (OPBM), with protected (2*S*)-2-methyl-3-hydroxypropanal **3** and ketone **4** [29], created a 9C atom carbon chain



Reagents and conditions: *i.* LDA, -78°C , then addn. of **3**, 90°C , 76%, d.r. 89:11; *ii.* PPTS, MeOH, r.t.; *iii.* TBSOTf, 2,6-lutidine, -78°C , then r.t.; flash chromatography; *iv.* H_2 , Pd/C, MeOH, r.t.; TPAP, MNO, 4-*A* MS, DCM, r.t. MePh_2Br , LiHDMS, THF, 0°C ; *v.* CSA (1.0 equiv.), DCM/MeOH 1:1, 0°C ; *vi.* PDC (11equiv.), DMF, r.t.

Scheme 16.2 Synthesis of key intermediate **7** on the route to azathilones

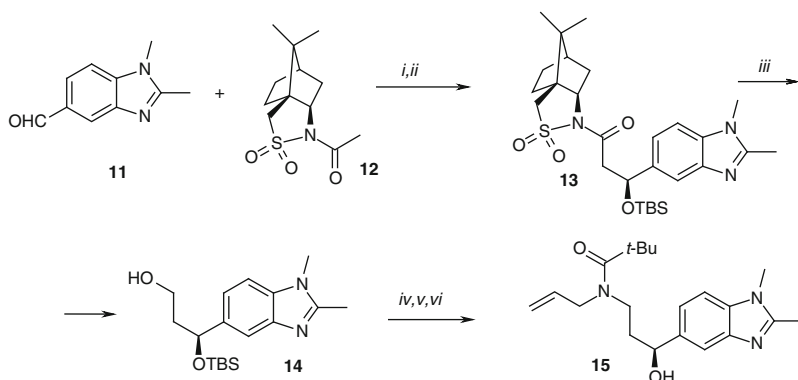


Reagents and conditions: *i.* MeNH_2 , (33% in EtOH), MeOH; *ii.* H_2 , RaNi, THF/MeOH 2:1, 40°C ; *iii.* MeC(OMe)_3 , MeOH, refl.; *iv.* MeOH, H_2SO_4 , refl.; *v.* LiAlH_4 , THF; *vi.* (COCl_2) , DMSO, Et_3N , -78°C to r.t.

Scheme 16.3 Synthetic route to heterocyclic aldehyde **11**

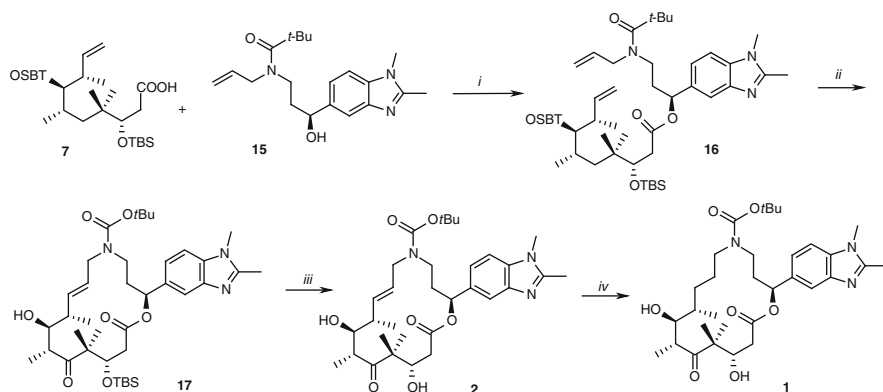
with two new stereogenic centres. Then, three OH groups were protected as *tert*-butyldimethylsilyl (TBS) affording intermediate **5**. Selective hydrogenolytic deprotection of the PMB group in the presence of the other three protecting groups yielded the *prim*-alcohol, which was oxidized to the aldehyde by perruthenate/4-methyl-morpholine-N-oxide (TPAP/MNO) complex and submitted to chain elongation in **6** via the Wittig reaction. Site-selective hydrolysis of the TBS protecting group on the *prim*-carbon atom was completed at 0°C in the presence of *camphor-sulphonic acid* (CSA), and in the final step, alcohol was oxidized to carboxylic acid **7** by pyridinium dichromate. It is worth emphasizing that the five-step synthesis of **7** required stereoselective formation of two stereogenic centres and two site-selective transformations of the *prim*-hydroxy groups.

Synthesis of the second building block, *sec*-alcohol **15**, is outlined in Schemes 16.3 and 16.4. The key step is represented by stereoselective addition of chiral auxiliary, *N*-acyl-sultam **12**, to the aldehyde **11**. However, preparation of an achiral building block is often not straightforward and **11** serves as a good example



Reagents and conditions: *i.* Et_3B , $\text{CF}_3\text{SO}_3\text{H}$, hexane, r.t., then Hunig's base, 0°C , then **11** at -5°C , then **12** at -78°C ; *ii.* TBSCl-imidazole, DMF, 40°C ; *iii.* DIBAL-H, DCM, -78°C ; *iv.* Ph_3P , imidazol, I_2/MeCN ; *v.* $\text{CH}_2=\text{CHCH}_2\text{NH}_2$, reflux; *vi.* $(\text{tert-BuO})_2\text{CO}/\text{THF}$, aq. $\text{NaHCO}_3/\text{EtOAc}$.

Scheme 16.4 Synthetic route to the second key intermediate, allylamine **15**



Reagents and conditions: *i.* DCC, DMAP/DCM, $^\circ\text{C}$; *ii.* 2nd generation Grubbs catalyst (0.15 equiv., incremental addition), DCM, reflux; *iii.* HF-Py complex, pyridine/THF, r.t.; *iv.* $\text{KO}_2\text{C-N-CO}_2\text{K}$ (excess), AcOH, DCM.

Scheme 16.5 Final steps in the synthesis of epothilones **1** and **2**

of the fact that even the “two-dimensional life” of a synthetic organic chemist is not easy. On the route to **11** from commercially available trisubstituted aromatic compound, six steps are needed, all completed with a high to very high yield (Scheme 16.3).

Starting from **11** and **12**, the aldol reaction was completed in the presence of *N,N*-diisopropylethylamine (Hunig's base) with 91% d.e. and the resulting *sec*-alcohol protected as TBS ether **13**. In the next steps, the sulphonamide-amide unit

was reductively split and the resulting 1,3-diol transformed in two steps into the selectively protected **14** (Scheme 16.4).

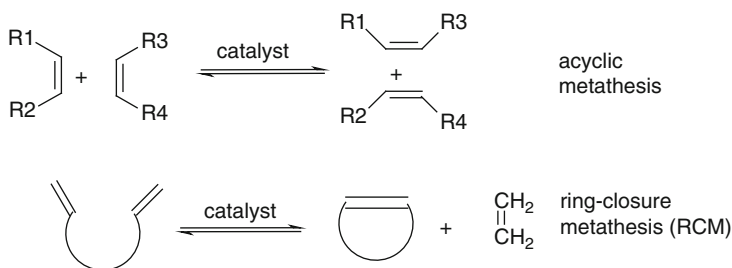
This intermediate was transformed into allylamine **15** via the 3-iodo derivative, which was reacted with allylamine. Then N-Boc was protected by di-*tert*-butyl dicarbonate, and finally OTBS protection removed by the aqueous work-up to obtain **15**. The detailed protocol for the final steps *iv*–*vi* is reported in the patent, which does not state the yields [30]. The final steps of the synthesis of **1** are given in Scheme 16.5 [27].

Successful completion of step *ii* in Scheme 16.5 was crucial for the whole synthetic project. The interaction of the two terminal double bonds to form the macrocyclic ring, a process clearly against entropic requirements, is fascinating. Known as the Grubbs reaction [31, 32], according to one of its inventors (although many outstanding synthetic chemists substantially contributed to its development and broad application [33, 34]), this cyclization deserves detailed analysis. It is the cyclic variant of an acyclic *alkene metathesis*; both are presented in Scheme 16.6.

RCM is an entropy-driven process as it cuts one substrate molecule into two products; one is volatile (ethene, propene, etc.) so the desired cycloalkene accumulates in the reaction solution. The basic catalytic cycle of RCM is given in Scheme 16.7.

Although not specifically shown in the Scheme, all individual steps in the catalytic cycle are reversible, and consequently so is the overall transformation. This generally accepted mechanism, known as the *Chauvin mechanism* [35], involves a sequence of formal [2 + 2] cycloadditions/cycloreversions involving alkene, carbene and metallacyclobutane intermediates. Since all these steps run within the coordination sphere of the central metal, the demands on the electronic properties of the metal and the stereoelectronic properties of the ligands to form an effective catalytic complex are very stringent. Although the first effective complexes included Mo as the central atom, those developed later were based on the “late” transition metals, W, Ru and Ta, in particular. Examples of the “first” and “second” generation complexes **18**–**22** are given in Fig. 16.4.

Their development remains the basis for progress in the field of RCM reactions, since the experience accumulated enabled the design of more effective, versatile and robust catalysts. To understand the requirements that these catalytic species



Scheme 16.6 Two principles of alkene metathesis

Scheme 16.7 Schematic presentation of the catalytic cycle in the RCM reaction

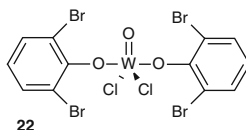
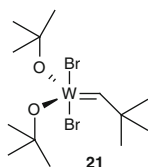
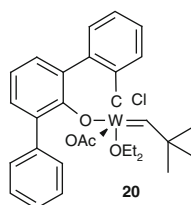
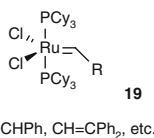
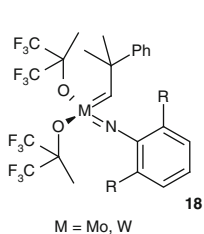
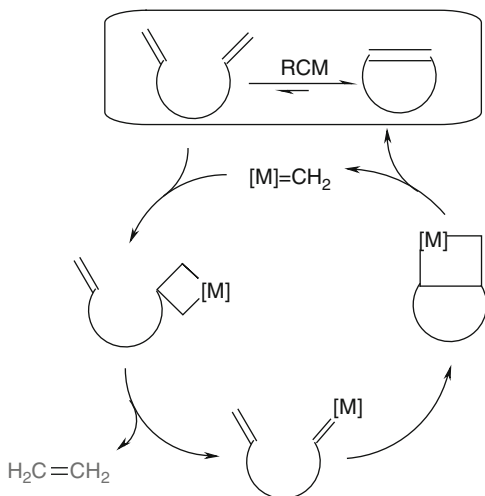
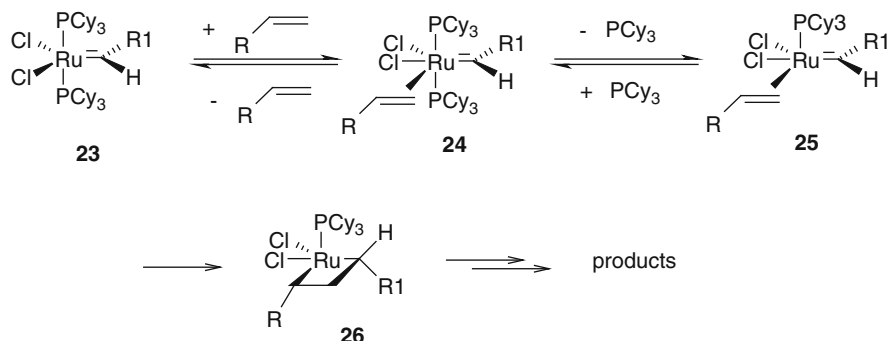


Fig. 16.4 Structures of representative catalytic complexes **18–22** for the RCM reaction

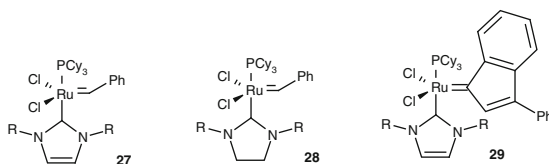
were able to satisfy, let us consider the mechanism of the metathetic process in Scheme 16.8 [36].

In the initial five-coordinated 16-electron ruthenium complex **23**, two neutral ligands, two anionic ligands and one carbene-type ligand are present. This complex first introduces alkene into the highly labile species **24** that then dissociates with the loss of one trialkylphosphine ligand. To allow this process, the effect of the anionic chlorides (which are electron-withdrawing groups) must be counterbalanced by the electron-donating phosphines, such as *tricyclohexylphosphine* (PCy_3), with a large cone angle. The bulky and electron-donating character of the residual phosphine is decisive for stabilizing the reactive intermediate **24**. The proposed “dissociative



Scheme 16.8 The mechanism of the metathetic process

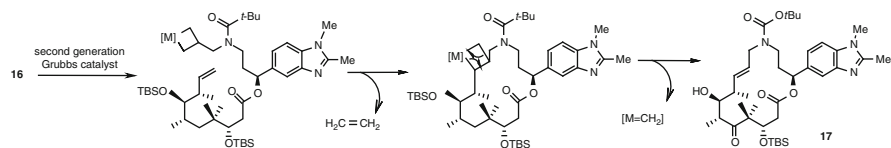
Fig. 16.5 Structure of representative heteroleptic catalytic complexes for RCM reaction



mechanism” that leads to **25** and **26** is the result of detailed physico-chemical studies [36], corroborated by synthetic results with a number of specifically designed ligands [37]. This mechanistic scheme tells us that the *cis* alkene binding site to carbene and *trans* to that of the chlorides, determines metathesis, and together with the subsequent formation of the metallacycle these represent the rate-determining steps.

Mechanistic and synthetic data encouraged the “second” generation of the alkene metathesis catalysts. It was concluded that the steric and electronic properties of the residual neutral ligand in the catalytically relevant intermediate **26** are decisive for the performance of the catalyst. It was self-evident to introduce into the catalytic complex an even more basic and sterically demanding ligand than trialkyl phosphines to increase the life-time and reactivity of this species. The solution was found in “stable” *N*-heterocyclic carbenes, represented by the complexes **27–29** (Fig. 16.5). Soon, it was observed that double substitution of PCy_3 by carbene-type ligands led to complexes with excessively high stability and limited catalytic activity. This observation led to the idea that a kinetically inert, electron-donating carbene ligand, in combination with a coordinatively labile phosphine ligand, should result in synergism. Representatives of such *heteroleptic* complexes are presented in Fig. 16.5.

They differ, both in the imidazoline or imidazolidine-derived *N*-heterocyclic carbene and in the substituents R on the N-atoms, as well as in the alkylidene fragment. Most importantly, the activity of the catalysts **27–29** is significantly higher than that of the parent Grubbs carbene **19** and comes close to that of Schrock’s Mo alkylidene complex **18**. In combination with exceptional thermal stability and resistance towards oxygen and moisture, together with compatibility with many



Scheme 16.9 Detailed mechanism of RCM step 16–17

functional groups, these complexes proved exceedingly useful tools in synthetic organic chemistry, in particular, RCM reactions used to synthesize natural products and their structural congeners [34].

According to our present knowledge, the RCM step 16–17 in Scheme 16.6, on the route to **1**, may be presented as shown in Scheme 16.9.

Effective ring closure to form **17** resulted in an 85% yield of the isolated product with exclusive *E*-selectivity. No trace of the corresponding *Z*-isomer could be detected. This is an important feature of the RCM process, in view of the defined conformational properties of the unsaturated macrolactone ring that are required for SAR studies of azathilones [38].

Recently, this reaction was improved for the preparation of “hypermodified” epothilone analogues; when completed with Grubbs catalysts of the second generation in refluxing toluene, 94% yield and *E/Z* ratio >10:1 of the target products were achieved [39].

The key step on any synthetic route is of strategic importance, its successful completion allowing detours and modifications of protocols in some less critical steps. In the case of 12-aza-epothilones, it is the RCM reaction, which is why it is important to understand its mechanistic and practical aspects.

16.5 Diimide Reduction of the Allylic C=C Bond

As mentioned in the previous section, conversion of 12-aza-epothilone **2** to **1**, in the last step of Scheme 16.5, was hampered by the allylic character of the C9=C10 double bond. Catalytic hydrogenations of **2** mostly afforded a mixture of hydrogenated product and products of the reductive ester hydrogenolysis, or hydrogenolysis of the allylic C11–N12 bond, without reduction of the double bond. The use of H₂/Ra-Ni in EtOH did not result in any conversion of **2**. Interestingly, hydrogenation of 9,10-unsaturated precursors of azathilones with the general formulae **I**, in the presence of Wilkinson’s catalyst, Rh(I)(PPh₃)Cl, resulted in selective hydrogenation of the more substituted, sterically hindered side-chain double bond.

In view of the well-known preference of complex hydrides for reduction of the C=X over the C=C double bond, by delivery of hydride ion to the positively polarized C atom in the former, a mild reagent that delivers two H atoms *in the absence of a metal catalyst* seemed preferable for reduction of 12-aza-epothilone **2** to **1**. An early report by Fischer et al. [40, 41], that hydrazine reduces selectively

the vinylic C=C bond in chlorines and porphyrines, hardly produced a stir in the organic synthetic community for 20 years. It was Corey who reported that diimide, or 1,2-diazine, is a reactive hydrogenating agent in the hydrazine–alkene system, confirming the coincidence of the factors that accelerate the oxidation of hydrazine to nitrogen via diimide with accelerated reduction [42]. The whole process is outlined in Scheme 16.10.

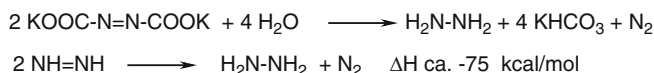
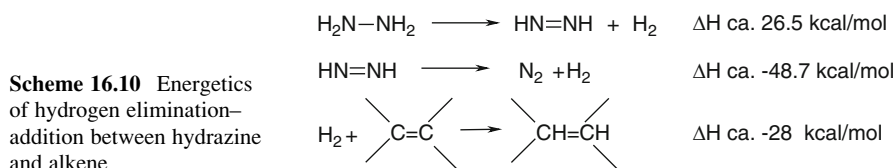
The thermochemical data in Scheme 16.10 reveal that direct transfer from hydrazine to an alkene is at most only slightly exothermic, and therefore slow, whereas the corresponding transformation of diimide is energetically favoured by almost 70 kcal/mol [43].

The coincidence of these factors, which accelerate the oxidation of hydrazine to nitrogen via diimide and those which accelerate reduction, prompted the use of *dipotassium diazodicarboxylate* (PADA), or azidoformate, as a reducing agent. This substance undergoes acid-catalyzed, rapid and irreversible decomposition in water, with the obligatory intermediacy of diimide (Scheme 16.11).

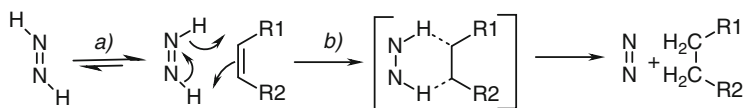
The ultimate fate of diimide is sealed by its capacity to function both as a hydrogen acceptor and a powerful hydrogen donor. This latter property allows for the concerted, pericyclic hydrogen transfer from the *cis*-diimide isomer, a less stable isomer in solution, as presented in Scheme 16.12.

This scheme is based on experimental and calculated data of the rate constants, and activation parameters, which are all in agreement with the following scenario [43]:

- trans*-diimide is in solvent-catalyzed equilibrium with its high-energy *cis* isomer
- The *cis* isomer donates both hydrogen atoms in a concerted manner with virtually no activation enthalpy, the transition state being highly entropy controlled.



Scheme 16.11 Decomposition scheme of dipotassium diazodicarboxylate



Scheme 16.12 Concerted mechanism of hydrogenation of C=C bond by diimide

The synthetic viability of the process, as outlined in Schemes 16.11 and 16.12, using in situ generated diimide, was demonstrated by reduction of a number of terminal, internal, conjugated and cyclic alkenes [42, 44, 45]. Diimide reduction was successfully used in the reduction of *E*-9,10-epothilones [46] and the *trans*-cyclopropane-based epothilone **A** analogue [38].

Reduction of azathilone **2** to **1** with PADA/AcOH (Scheme 16.5), proceeded sluggishly, and only after 8 days could the total yield be increased to 52% after HPLC purification.

16.6 Conclusion

Synthetic success in completion of either a critical step or any single step on the designed route to chiral drugs requires profound knowledge of the mechanism and finely tuned experimental details. The highlights of the synthetic efforts to azathilones and other “hypermethylated” epothilones, presented in this chapter, give a general impression of the many versatile synthetic steps required on such a complex route.

The example of diimide reduction of the allylic C=C bond also demonstrates that once a specific synthetic reaction has been performed on a laboratory scale, with acceptable yield, additional optimization work is usually required to establish a truly practical approach to the transformation. Such technological improvements facilitate progress in research towards new drug entities by supplying the needed quantities, returning again to the point we made in Fig. 1.2 in the introductory chapter of this book.

References

1. Bollag DM, McQueney PA, Zhu J, Hensens O (1995) *Cancer Res* 55:2325–2333
2. Girth K, Bedorf N, Hofle G, Irschik H, Reichenbach H (1996) *J Antibiot* 49:560–566
3. Hofle G, Reichenbach H (2005) Epothilone, a Myxobacterial Metabolite with Promising Antitumor Activity. In: Cragg GM, Kingston DGI, Newman DG (eds) *Anticancer agents from natural products*. Taylor & Francis, Boca Raton, FL, pp 413–450
4. Kowalsk RJ, Giannakakou P, Hamel E (1997) *J Biol Chem* 272:2534–2541
5. Nikolau KC, Ritzen A, Namoto K (2001) *JCS Chem Commun*: 1523–1535
6. Bertinato P, Sorensen EJ, Meng D, Danishefsky SJ (1996) *J Org Chem* 61:8000–8001
7. Nikolau KC, Winssinger N, Pastor J, Ninkovic S, Sarabia F, He Y, Vourloumis D, Tang Z, Li T, Giannakakou P, Hamel E (1997) *Nature* 387:268–272
8. Wartmann M, Altmann K-H (2002) *Curr Med Chem Anticancer Agents* 2:123–128
9. Altmann K-H, Bold G, Caravatti G, Florsheimer A, Guignano V, Wartmann M (2000) *Biorg Med Chem* 10:2675–2678
10. Carlomagno T, Blommers MJJ, Meiler J, Jahnke W, Schupp TT, Peterson F, Schinzer D, Altmann K-H, Griesinger C (2003) *Angew Chem Int Ed* 42:2511–2515
11. Goodin S, Kane MP, Rubin EH (2004) *J Clin Oncol* 22:2015–2025
12. Forli S, Manetti F, Altmann K-H, Botta M (2010) *ChemMedChem* 5:35–40
13. Hofle G, Bedorf M, Steinmetz H, Schomburg D, Gerth K, Reichenbach H (1996) *Angew Chem Int Ed* 35:1567–1569

14. Nettles JH, Li H, Cornett B, Krahn JM, Smyder JP, Downing KH (2004) *Science* 305:866–869
15. Nikolaou KC, Scarpelli R, Bollbuck B, Werschkun B, Pereira MMA, Wartmann M, Altmann K-H, D Zaharevitz, Gussio R, Giannakakou P (2000) *Chem Biol* 7:593–599
16. Gertsch J, Feyen F, Butzberger A, Gerber B, Pfeiffer B, Altmann K-H (2009) *Chembiochem* 10:2513–2521
17. Burke MD, Schreiber SL (2004) *Angew Chem Int Ed* 43:46–58
18. Breinbauer R, Vetter IR, Waldmann H (2002) *Angew Chem Int Ed* 41:2878–2890
19. Koch MA, Waldmann H (2005) *Drug Discov Today* 10:471–483
20. Tietze LF, Bell HP, Chandrasekar S (2003) *Angew Chem Int Ed* 42:3996–4028
21. Kobrehel G, Radobolja G, Tamburašev Z, Đokic S, (PLIVA) (1982). 11-Aza-10-deoxo-10-dihydroerythromycin A and derivatives thereof as well a process for their preparation. US 4 328 334
22. Đokic S, Kobrehel G, Lazarevski G, Lopotar N, Tamburašev Z, Kamenar B, Nagl A, Vicković I (1986) *J Chem Soc Perkin Trans I*: 1881–1990
23. Retsema J, Girard A, Schelkly W, Manousos M, Anderson M, Bright G, Borovoy R, Brenan L, Mason R (1987) *Antimicrob Agent Chemother* 31:1939–1947
24. Altmann K-H, Florsheimer A, Bold G, Caravatti G, Wartmann M (2004) *Chimia* 58:686–690
25. Cachoux F, Scgaal F, Teichert A, Wagner T, Altmann K-H (2004) *Synlett*; 2709–2712
26. Feyen F, Gertsch J, Wartmann M, Altmann K-H (2006) *Angew Chem Int Ed* 52:5880–5885
27. Feyen F, Cachoux F, Gertsch J, Wartmann M, Altmann K-H (2008) *Acc Chem Res* 41:21–31
28. Feyen F, Jantsch A, Hauenstein K, Pfeiffer B, Altmann K-H (2008) *Tetrahedron* 64: 7920–7928
29. Altmann K-H, Bold G, Caravatti G, Denni D, Florsheimer A, Schmidt A, Rihs G, Wartmann M (2002) *Helv Chim Acta* 85:4086–4110
30. Altmann K-H, Feyen F, Gertsch J (ETH, Zurich), WO 2007/110214 A1.
31. Nguyen ST, Johnson LK, Grubbs RH, Ziller JW (1992) *J Am Chem Soc* 114:3974–3975
32. Nguyen ST, Grubbs RH, Ziller JW (1993) *J Am Chem Soc* 115:9858–9859
33. Furstner A (ed) (1998) *Alkene metathesis in organic synthesis*. Springer, Berlin
34. Furstner A (2000) *Angew Chem Int Ed* 39:3912–3043
35. Herrison J-L, Chauvin Y (1970) *Macromol Chem* 141:161–176
36. Dias EL, Nguyen ST, Grubbs RH (1997) *J Am Chem Soc* 119:3887–3897
37. Cucculu ME, Li C, Nolan SP, Nguyen ST, Grubbs RH (1998) *Organometallics* 17:5565–5568
38. Kuzniwesky CN, Gertsch J, Wartmann M, Altmann K-H (2008) *Org Lett* 10:1183–1186
39. Altmann K-H (2005) *Curr Pharm Des* 11:1595–1613
40. Fischer H, Gibian H (1941) *Liebigs Ann Chem* 548:183–194
41. Fischer H, Gibian H (1942) *Liebigs Ann Chem* 550:208–251
42. Corey EJ, Mock WL, Pasto DJ (1961) *Tetrahedron Lett*: 347–352
43. Balu EJ, Hochheimer EF, Unger HJ (1961) *J Chem Phys* 34:1060–1068
44. Tang HR, McKee ML, Stanbury DM (1995) *J Am Chem Soc* 117:8967–8973
45. Pasto DJ, Taylor TT (1991) *Org React* 40:91–155
46. Rivkin A, Yoshimura F, Gabarda AE, Cho YS, Chou T-C, Dog H, Danishefsky SJ (2004) *J Am Chem Soc* 126:10913–10922

Synthetic Methods and Concepts Discussed in the Chapters

Chapter 2: Aliskiren Fumarate

- (a) Strategy based on visual-imagery, starting from Nature's chiral pool; Dali-like presentation of objects that can be viewed in more than one way.
- (b) *trans*-Diastereoselectivity of the Grignard reaction of phenyl-magnesiocuprate controlled by anchoring of the second mole of reagent to the proximal *tert*-hydroxy group.
- (c) Fine-tuning of the chiral ligand for the Rh complex, which catalyses hydrogenation of the selected substrate with extreme enantioselectivities.
- (d) Extremely high enantioselectivities in the hydrogenation of the "hard" internal C=C bond in α , β -unsaturated carboxylic acids with the Rh(TriFer)-complex; the dimethylamino moiety in the ligand, TriFer, serves as the second interaction centre via electrostatic interaction with the carboxylate unit.

Chapter 3: (R)-K-13675

- (a) Non-hydrolytic, anomalous lactone ring-opening by Me₃SiI/EtOH
- (b) The Mitsunobu reaction in ether bond formation
- (c) Optimization of the Mitsunobu reaction without loss of enantiomeric purity
- (d) Large-scale production of (S)-2-hydroxybutyrolactone
- (e) Williamson-type ether bond formation in aryl-alkyl ethers with inversion of configuration at the stereogenic centre

Chapter 4: Sitagliptin Phosphate

- (a) C-Acyl mevalonate as an N-acylating agent and its mechanism of reaction
- (b) Ferrocenyl-based chiral phosphines, Josiphos-ligands; highly enantioselective hydrogenation of unprotected β -enamino amides
- (c) Ammonium chloride as a stabilizer of the imine form; an effective promoter of catalytic enantioselective hydrogenation

Chapter 5: Valsartan

- (a) Cu-promoted catalytic decarboxylative biaryl synthesis, biomimetic type aerobic decarboxylation and the Goossen reaction
- (b) Coupling to biaryls with the Suzuki–Miyaura reaction, a stereoselective approach to the axially chiral biaryl system; the case of vancomycin

Chapter 6: Amino-1,4-benzodiazepines

- (a) Crystallization induced asymmetric transformation
- (b) Configurational stability, racemization and enantiomerization
- (c) Asymmetric Ireland–Claisen rearrangement
- (d) Hydroboration of the terminal C=C bond; anti-Markovnikov hydration

Chapter 7: Sertraline

- (a) Stereoselective reduction of ketones and imines under kinetic and thermodynamic control
 - $\text{MeNH}_2/\text{EtOH-H}_2/\text{Pd}/\text{CaCO}_3$ in “telescoped process”
 - Hydrosilylation by the (*R,R*)-(EBTHI)TiF₂/PhSiH₃ catalytic system
 - Chiral diphenyloxazaborolidine in the reduction of *racemic* ketones
- (b) SCRAM complex in the catalytic epimerization of the *trans*- to *cis*-isomer of sertraline
- (c) Desymmetrization of oxabenzonorbornadiene; Suzuki coupling of arylboronic acids and vinyl halides
- (d) The Horner–Wadsworth–Emmons reaction; synthesis of sertraline from L-ascorbic acid
- (e) Pd-catalysed (Tsuji–Trost) coupling of arylboronic acids and allylic esters
- (f) Simulated moving bed (SMB), general concept and production of sertraline

Chapter 8: 1,2-Dihydroquinolines

- (a) Asymmetric organocatalysis
 - L-Proline as a pioneering organocatalyst
 - The chiral thiourea organocatalyst for the catalytic enantioselective Pétasis reaction
 - The diastereoselective Pétasis reaction
 - One-pot, four-component Pétasis borono–Mannich reaction
- (b) Multicomponent reactions (MCRs); general concept and examples

Chapter 9: (–)-Menthol

- (a) Enantioselective allylic amine–enamine–imine rearrangement; catalysis by the Rh(I)-(–)-BINAP complex
- (b) High diastereoselectivity of the hydrogenation of 2-isopropyl-5-methylphenol by H₂/Cu-chromate catalyst to *all-trans* 2-isopropyl-5-methyl cyclohexanol, one of the three possible racemic diastereomers
- (c) Unsaturated aldehyde undergoes intramolecular ene-reaction mediated by zinc dibromide, which is completely controlled by the first chiral centre.

Chapter 10: Fexofenadine Hydrochloride

- (a) Retrosynthetic analysis of fexofenadine, synthone approach
- (b) Alkynes as synthetic equivalents for ketones, Hg(II) and Pt(II) promoted hydration
- (c) ZnBr₂-catalysed transposition of α -haloketones to terminal carboxylic acids mechanism
- (d) Oxazaborolidine-based catalysts for enantioselective reduction of ketones
- (e) Microbial oxidation of non-activated C–H bond; biotransformation of terfenadine to fexofenadine with *Cunninghamella blakesleeana* and *Absidia corymbifera*
- (f) Bioisosteres; silicon switch of fexofenadine to sila-fexofenadine

Chapter 11: Montelukast Sodium

- (a) Asymmetric hydrogenation of ketones with α -pinenes
- (b) Non-linear effect (NLE) in asymmetric reactions
- (c) Chiral Ru(II) complexes, catalysts for enantioselective hydrogen transfer
- (d) Biocatalytic reduction of ketones; ketoreductase KRED (KetoREDuctase) scaled-up to a production batch of >200 kg
- (e) Remarkable effect of Ce(III) chloride on the Grignard reaction; structure and mechanism
- (f) Replacement of the hydroxyl group for a thiol group; high nucleophilicity of the soft Cs-salts of thioacids; selective split of the C(O)–S bond in thioesters by hydrazine under mild conditions

Chapter 12: Thiolactone Peptides and Peptidomimetics

- (a) Development of chemical ligation (CL) in peptide synthesis
 - *Chaotropes*, polar salts that increase the concentration of the reacting partners in peptide synthesis

- (b) Development of native chemical ligation (NCL) in peptide synthesis
 - SPPS, Rink-PEGA resin
- (c) Development of NCL in thiolactone peptide synthesis
 - Reducing agent tris-(2-carboxy)ethyl phosphine (TCEP); formation of thiol group; its intramolecular attack on the activated ester group

Chapter 13: Efavirenz

- (a) Asymmetric addition of an alkyne anion to a C=O bond
 - Ephedrines as chiral modifiers
 - Chiral Li^+ aggregates as the initiators of NLE
- (b) Scale-up of Grignard-type alkynylation promoted by the use of Et_2Zn as a weak Lewis acid

Chapter 14: Paclitaxel

- (a) Intramolecular Heck reaction on the pathway to baccatine III
- (b) Heterogeneous trifunctional catalyst (LDH-PdOsW) for biomimetic synthesis of chiral diols; synthesis of the paclitaxel side-chain
- (c) The catalytic Cp_2ZrHCl complex for reductive, non-hydrolytic N-deacylation of taxanes to *primary* amine, the key precursor of paclitaxel

Chapter 15: Neoglycoconjugates

- (a) Click chemistry, energetically preferred reactions
- (b) Target-guided synthesis (TGS or freeze-frame click chemistry); a new strategy for the generation of compound libraries
- (c) Application of click chemistry in the synthesis of neoglycoconjugates
- (d) 1,3-Dipolar cycloaddition of azides to alkenes (Huisgen reaction)

Chapter 16: 12-Aza-Epothilones

- (a) Ring closure metathesis (RCM), the shortest approach to “non-natural natural-product” lead compounds
- (b) Selective oxidation of *primary*-alcohols to aldehydes with the perruthenate/4-methyl-morpholine-N-oxide (TPAP/NMO) complex
- (c) Diimide (PADA) reduction of the allylic C=C bond

Index

A

absorption-distribution-metabolism-excretion (ADME), 5
 AChE inhibitors, 204
 acquired immunodeficiency syndrome (AIDS), 169
 aliskiren fumarate, 13
 α -alkoxy- β -arylpropionic acids, 31
Allegra[®], 125, 126
 3-amino-1,4-benzodiazepines, 69
 ammonium chloride, promoter of enantioselective hydrogenation, 52
 angiotensin-converting enzyme (ACE), 15, 56
 anomalous lactone ring-opening, 35, 41
 anti-Markovnikov hydration, 76, 77
 area under the curve (AUC), 127
 arylboronic acids, 60
 α -aryloxy- β -phenylpropionic acids, 33
 asymmetric addition of alkyne anion, 169, 173
 asymmetric dihydroxylation (AD), 185
 asymmetric hydrogenation, 22
 asymmetric Ireland-Claisen rearrangement, 74, 75
 asymmetric organocatalysis, 105
 atropisomerism, 63
 attrition of potential NDE, 4
 auto-inducing peptides (AIPs), 156, 158
 axially chiral biaryls, 63
 12-aza-epothilones, 209
 azithromycin, 213, 214

B

baccatin III, 182
 Beckmann rearrangement, 213
 bidentate phosphines, 51

(*R*) and (*S*)-BINAP, 122
 biologically orientated synthesis, 8
 blockbuster drug, 1, 9
 bond dissociation energy (BDE), 36, 37
tert-butyldimethylsilyl (TBS), 215
 (*S*)-*n*-butyl-2-hydroxybutanoate, 41

C

C-acyl Meldrum's acid, 47, 49
 Cahn-Ingold-Prelog (CIP) rules, 33
 camphorsulphonic acid (CSA), 215
 candidate drug (CD), 3
 catalytic epimerization, 90
 CeCl₃-THF solvate, 150, 151
 central nervous system (CNS), 6
 Chauvin mechanism, 217
 chaotrope, 160
 chemical ligation, 156, 158, 161
 chemoselective reactivity, 162
 chiral auxiliary, 22
 chiral diphenyloxazaborolidine, 91
 chiral drugs, 5
 (–)-chloro-diisopinocampheyl borane ((Ipc)₂BCl), 145, 147
 click chemistry, 200
 click resins, 204
 clinical candidate (CC), 3
 compound libraries, 202
 configurational stability, 71
 Cp (cyclopentadienyl), 193
 Cp₂ZrHCl complex, 193
 crystallization induced asymmetric transformation, 73, 74, 79
 C/Si bioisosterism, 137
 cyclooctadiene (COD), 23
 cytochrome P450 (CYP), 4

D

Daliesque synthetic plan, 19
 decarboxylative biaryl synthesis, 62
 diastereoselective hydrogenation, 87
 (DHQ)₂-PHAL, 186
 (DHQD)₂-PHAL, 186
 dihydroquinidine (DHQD), 186
 dihydroquinine (DHQ), 186
 1,2-dihydroquinolones, 103
 diimide reduction, 220
 diisobutyl aluminium hydride
 (DIBAL-H), 19
 diisopropyl azidodicarboxylate (DIAD), 40
 DNA-templated synthesis, 9, 10
Diovan[®], 55
 dipeptidyl peptidase 4 (DPP4) inhibitor, 45
 diphenylphosphorylazide (dppa), 94
 dipotassium diazodicarboxylate
 (PADA), 221
 diversity oriented synthesis (DOS), 212

E

efavirenz, 169
 electron-donating group (EDG), 201
 electron-withdrawing group (EWG), 201
 β-enamino amides, 50
 enantiomerization, 72
 enantioselective enamine-imine
 rearrangement, 119
 enantioselective hydrogenation, 22
 enantioselective hydrogen transfer, 148
 ephedrine-derived chiral auxiliaries, 174
 equilibration of chiral aggregates, 175
 ESR spectroscopy, 36
 ethylenebis(η⁵-tetrahydroindenyl)titanium
 difluoride (EBTHI)TiF₂, 88, 89
 Et₂Zn, weak Lewis acid as promoter, 176

F

ferrocene-based chiral ligands, 23
 fexofenadine hydrochloride, 125
 N-Fmoc, 164, 165
 Food and Drug Administration (FDA), 2
 freeze-frame click chemistry, 202
 α-1,3-fucosyltransferase, 198
 Fuc-T-GDP-fucose complex, 199

G

GDP-fucose, 198
 glucocorticoid receptor (GCR), 104
 Goossen's synthesis of biaryls, 60, 61
 G-protein-coupled receptors (GPCRs), 56
 Grignard reagent, 20, 134, 144, 150, 176

H

halogen binding pocket (HBP), 85
 HBTU/DIEA coupling reagent, 162, 163
 heteroleptic catalytic complexes, 219
 heterolytic bond splitting, 37
 high-density lipoprotein (HDL), 30
 histamine receptors, 126
 homolytic bond splitting, 37
 homo- vs. heterochiral complexes in NLE, 147
 Horner-Wadsworth-Emmons reaction, 96, 97
 Huisgen's 1,3-dipolar cycloaddition, 201
 human immunodeficiency viruses 1 and 2 (HIV 1
 and 2), 169
 Hunig's base, 216
 hydroboration of alkenes, 78
 hydroboration of ketones, 144, 147
 hydrogen bond interactions, 171, 172, 181
 hydrazirone, 193

I

incorporation of genomics, 9
 intramolecular Heck reaction, 182, 184
 inversion of configuration, 40
 iodotrimethylsilane, 40
 isocyanide-based multi-component
 reactions, 113

J

Januvia[®], 45
 Josephos ligands, 50

K

ketoreductase KRED, 150
 kinetic resolution, 89
 K₃[Fe(CN)₆], oxidant, 187, 188
 K₂OsO₂(OH)₄, oxidant, 187

L

layered double hydroxides (LDH), 189, 190
 lead compound, 35
 lead generation, optimization, 4
 leukotriene C₄, D₄, E₄ antagonists, 142
 leukotriene D₄ (LTD₄) antagonists, 143
 Li-aminoalkoxides, 174
 Li-chiral aggregates, 175
 ligand binding domain (LBD), 30
 Lipinski's "rule of five", 8
 liquid-phase peptide synthesis (LPPS), 156
 Log P, 7

M

macrocyclization, 214
 Meerwein-Verley-Ponndorf reaction, 148

- membrane reactor system, 135, 136
(-)-menthol, 117
metal-mediated double bond migration, 120
N-methylmorpholine N-oxide (NMO), 187
Michael receptor, 205
Michael-type addition, 53, 205
microbial oxidation, 135
mifepristone, 104
Mitsunobu reaction, azides, 93, 94
Mitsunobu reaction,
 ether-bond forming, 38
 mechanism, 40
montelukast sodium, 141
multi-component reactions (MCR), 112
- N**
native chemical ligation, 156, 160
natural products, 6
neoglycoconjugate, 197, 205, 206
new drug entity (NDE), 1
new medical entity (NME), 11
non-linear effect (NLE) or asymmetric
 amplification, 146, 174
- O**
oxybenzoylglycine derivatives, 34
O-*tert*-butyldimethylsilyl (OTBS), 164
- P**
paclitaxel, 179
peptide inhibitor CGP 38560A, 15
peroxisome proliferator-activated receptor α
 (PPAR α), 29, 31
Petasis reaction, 106, 108, 111
phase transfer catalysis (PCT), 150, 152
planar chiral complexes, 60
polar surface area (PSA), 8
polyethylene glycol (PEG-600), 152
privileged structures, 69, 92
proof of concept (PoC), 4, 46
- Q**
quantitative structure-activity relationship
 (QSAR), 57
quorum sensing system, 157
- R**
racemic switch, 127, 128
racemisation, 71
reductive N-deacylation, 192
regioselectivity, 201, 207
renin, 14
renin-angiotensin-aldosterone system
 (RAAS), 14, 56
retrosynthetic analysis, 129
reverse transcriptase inhibitors (RTIs), 170
ring-closure metathesis (RCM), 213, 214, 217
Rink-amide resin, 162, 163
Risalez[®], 13
- S**
sartans, 56, 59
SCRAM catalyst, 90, 91
selective serotonin reuptake inhibitors (SSRIs),
 84, 85
sertraline, 83
 γ -secretase, 71
 γ -secretase inhibitors, 70
Sharpless asymmetric dihydroxylation, 185
sila-fexofenadine, 137, 138
simulated moving bed (SMB)
 process, 98, 101
Singular[®], 141
sitagliptin binding to the active site, X-ray, 47
sitagliptin phosphate monohydrate, 45
site-selective oxidation, 134
slow reacting substance of anaphylaxis
 (SRS-A), 142
solid-phase peptide synthesis
 (SPSP), 156, 159
Stocrin[®], 169
structure-activity relationship (SAR), 5, 211
Sustava[®], 169
Suzuki coupling, 92, 93
Suzuki-Miyaura reaction, 60, 64
syn/anti selectivity, 203
synthon, 129, 131
- T**
target-guided synthesis (TGS), 202
target molecule (TM), 129
taxanes, 181, 182
Taxol[®], 179
Tekturna[®], 13
Telfast[®]
 thiolactone peptides, 155
thiourea-type organocatalysts, 110
(1*R*,2*R*)-*N*-(*para*-tolylsulfonyl)-1,2-
 diphenylethylenediamine (TsDPEN), 149
tricyclic antidepressants (TACs), 84
TriFer, ferrocene-based ligand, 23
triflate ester, 41, 42
trifluoroacetic acid (TFA), 38
trifunctional catalyst system (PdOsW),
 185, 191
tris-(2-carboxy)ethyl phosphine (TCEP), 166
Tsuji-Trost coupling, 94

β -tubulin, 180, 181, 211, 212
turn over number (TON), 26, 123

U

Uemura's route to biaryl unit in vancomycin,
65, 66

V

valsartan, 55, 57
vancomycin, 55

W

Wieland-Miescher ketone, 105
Williamson-type ether synthesis, 42

Z

ZnBr₂-catalyzed rearrangement, 131, 133
Zolofit[®], 83
Zr-complex catalysis, 192